Multimodality imaging for myocardial injury in acute myocardial infarction and the assessment of valvular heart disease

Podlesnikar, T.

Multimodality Imaging for Myocardial Injury in Acute Myocardial Infarction and the Assessment of Valvular Heart Disease

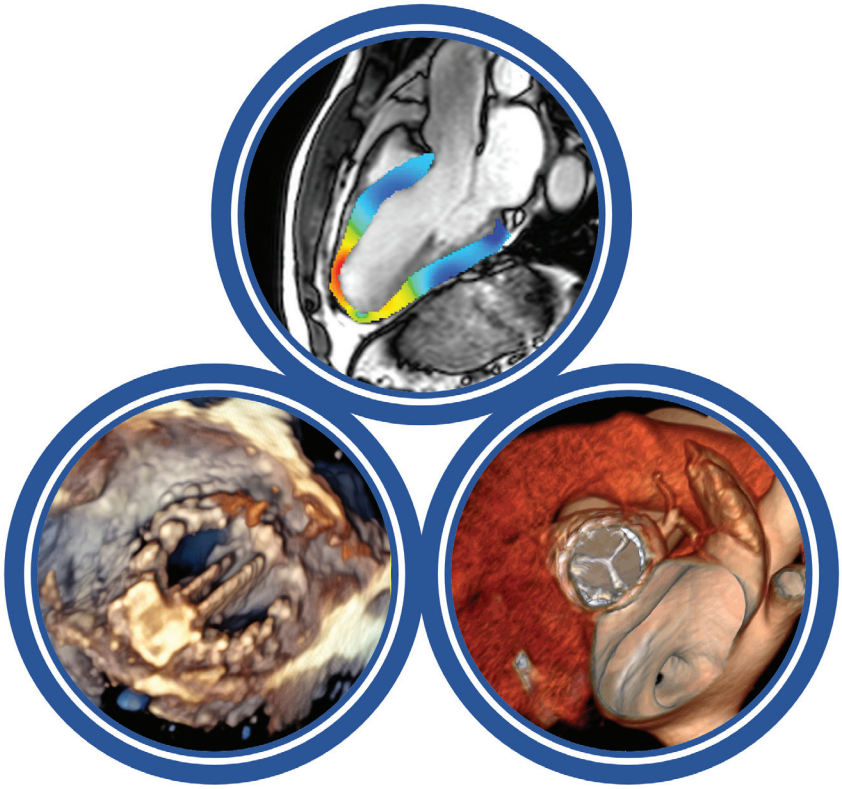

Tomaž Podlesnikar

Multimodality Imaging for Myocardial Injury in Acute Myocardial Infarction and the Assessment of Valvular Heart Disease

Tomaž Podlesnikar

Multimodality Imaging for Myocardial Injury in Acute Myocardial Infarction and the Assessment of Valvular Heart Disease

The studies described in this thesis were performed at the Department of Cardiology of the Leiden University Medical Center, Leiden, The Netherlands

Cover: T. Podlesnikar

Layout: T. Podlesnikar, T. Pogorevc

Edition: 1st edition

Place: Leiden, The Netherlands

Self-published by T. Podlesnikar

Year of publishing: 2022

Printrun: 50 copies

Printing: Design Sudio

CIP - Kataložni zapis o publikaciji

Univerzitetna knjižnica Maribor

616.127-005.8-073(043.3)

PODLESNIKAR, Tomaž

Multimodality imaging for myocardial injury in acute myocardial infarction and the assessment of valvular heart disease : [the studies described in this thesis were performed at the Department of Cardiology of the Leiden University Medical Center, Leiden, The Netherlands] / Tomaž Podlesnikar. - 1st ed. - Maribor : [samozal.] T. Podlesnikar, 2022

ISBN 978-961-07-1172-8

COBISS.SI-ID 111722755

Multimodality Imaging for Myocardial Injury in Acute Myocardial Infarction and the Assessment of Valvular Heart Disease

Proefschrift

ter verkrijging van

de graad van doctor aan de Universiteit Leiden,

op gezag van rector magnificus prof.dr.ir. H. Bijl,

volgens besluit van het college voor promoties

te verdedigen op dinsdag 28 juni 2022

klokke 13.30 uur

door

Tomaž Podlesnikar

geboren te Maribor, Slovenië

in 1981

Promotor:

Prof. dr. J.J. Bax

Co-promotor:

Dr. V. Delgado

Leiden Promotiecommissie:

Prof. dr. J. Braun

Dr. N. Ajmone Marsan

Dr. M. Bootsma

Prof. dr. B. Ibáñez	Centro Nacional de Investigaciones Cardiovasculares (CNIC), Madrid, Spain; IIS-Fundación Jiménez Díaz University Hospital, Madrid, Spain
Dr. C. Bucciarelli-Ducci	Royal Brompton & Harefield Hospitals, London, United Kingdom
Prof. dr. Z. Fras	Univerzitetni klinični center Ljubljana, Ljubljana, Slovenia

Financial support by the Dutch Heart Foundation for the publication of this thesis is gratefully acknowledged

To Blanka and Tibor,
to my mum and dad

TABLE OF CONTENTS

1

General introduction and outline of the thesis

GENERAL INTRODUCTION

The outcome of patients with ST-segment elevation myocardial infarction (STEMI) has significantly improved over the last decades.[1,2] Timely reperfusion with primary percutaneous coronary intervention (PCI) and implementation of evidence-based and guideline-recommended treatments have contributed significantly to these improved outcomes.[3,4] However, STEMI survivors are still at high risk of recurrent cardiovascular events such as congestive heart failure, arrhythmia, and sudden death.[5,6] Thus, the search continues for novel effective therapies that can be administered as an adjunct to primary PCI in STEMI to reduce myocardial infarct size and prevent heart failure.[7,8] In order to demonstrate a clear clinical benefit of any such intervention advanced cardiac imaging plays an important role. Although electrocardiogram, echocardiography, single photon emission computed tomography and cardiac biomarker release have been widely used, cardiovascular magnetic resonance (CMR) is currently the recommended technique for the assessment of myocardial injury in STEMI trials.[8,9] CMR is the gold standard to assess left ventricular ejection fraction (LVEF), the widely implemented functional parameter, and infarct size, the structural surrogate of myocardial infarction.[10] Both parameters have been associated with long-term mortality and morbidity after STEMI.[11,12] However, CMR also allows for the assessment of myocardial edema, microvascular damage and left ventricular (LV) strain, which can serve as powerful complementary tools to evaluate the benefits of cardioprotective therapies (Figure 1).

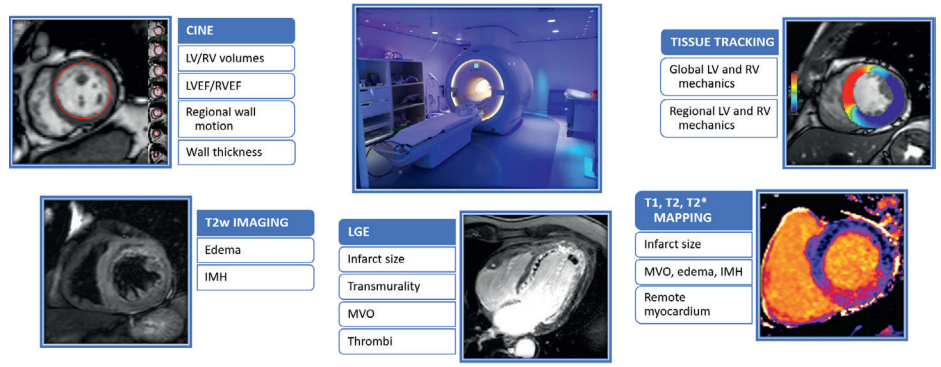

Figure 1: Cardiovascular magnetic resonance after acute myocardial infarction. Within a single scan, the assessment of left and right ventricular volumes and function, myocardial edema, infarct extent and transmurality, and microvascular damage can be performed. IMH, intramyocardial hemorrhage; LGE, late gadolinium enhancement; LV, left ventricular; LVEF, left ventricular ejection fraction; MVO, microvascular obstruction; RV, right ventricular; RVEF, right ventricular ejection fraction; T2w, T2-weighted.

Multimodality cardiac imaging plays a central role in management of patients with valvular heart disease (VHD). Whenever VHD and heart failure coexist, advanced imaging may help answering the dilemma whether the LV dysfunction is due the disease of the valve or the ventricle.[13,14] In patients with transcatheter aortic valve replacement (TAVR) multiple imaging modalities define procedural planning, periprocedural guidance and long-term follow-up.[15,16] Furthermore, novel biomarkers of myocardial injury, like focal replacement and diffuse interstitial myocardial fibrosis with CMR, hold promise to redefine the optimal timing for intervention in asymptomatic patients with severe VHD.[17]

Cardiovascular magnetic resonance-derived left ventricular strain after acute myocardial infarction

Acute myocardial infarction results in myocardial cell necrosis and changes in extracellular collagen matrix that portend adverse consequences on LV structure and function.[18] While early intravenous beta-blocker administration offers physiological rationale for lowering the myocardial infarction burden,[19] their routine use has been disputed over the last decades due to conflicting data on patients outcome.[20] The Effect of Metoprolol in Cardioprotection During an Acute Myocardial Infarction (METOCARD-CNIC) trial was the first randomized control clinical trial in the modern era of primary PCI, that showed a clear clinical benefit of early administration of intravenous beta blockade in STEMI patients.[21,22] Early intravenous metoprolol resulted in a significant reduction of LV end-systolic volumes, an increase in LVEF and a smaller infarct size, assessed with late gadolinium enhancement (LGE), 1 week after anterior STEMI, as evaluated with CMR imaging.[21] In addition, early metoprolol administration was associated with an improved LVEF after 6 months.[22]

While LVEF and infarct size are the cornerstones to evaluate myocardial injury after acute myocardial infarction, LV strain assessment can provide additional important information. It detects subtle systolic dysfunction in patients with preserved LVEF and allows excellent intra- and inter-observer reproducibility.[23,24] Moreover, LV strain with speckle tracking echocardiography has shown incremental prognostic value to predict adverse LV remodeling and outcome after STEMI.[25,26] On the other hand, LV strain with CMR has been much less extensively evaluated, mainly due to the complex acquisition and postprocessing techniques. Until recently, LV strain with CMR could only be investigated with tissue tracking technologies, such as myocardial tagging, strain encoded (SENC) imaging, displacement encoding with stimulated echoes (DENSE) imaging, which rely on specialized pulse sequences and additional scanning

time.[27] However, recent development of feature-tracking CMR, a post-processing software platform that allows multidirectional LV strain assessment from routinely acquired functional cine images (in a similar fashion to speckle-tracking echocardiography), has opened a gateway to wider implementation of LV strain assessment with CMR in the research and clinical practice.[28,29] Time course of global LV longitudinal (GLS) and circumferential (GCS) strain after acute myocardial infarction has not yet been evaluated with feature-tracking CMR. In addition, the impact of early intravenous metoprolol on global LV myocardial strain in the acute and chronic stage of STEMI remain to be elucidated.

The tissue healing process after reperfused myocardial infarction is complex and affects the infarcted area as well as the distant myocardium.[30,31] Several studies have described the evolution of regional LV strain with CMR after myocardial infarction, mostly showing gradual improvement of LV strain in the infarct zone and no significant changes in the remote zone.[32-36] However, none of them employed the novel feature-tracking algorithm to investigate regional LV strain. Furthermore, it remains to be elucidated whether the cardioprotective effects of early intravenous metoprolol are confined to the infarct zone strain, remote zone strain or both. There is as well conflicting evidence on the impact of microvascular obstruction (MVO) and intramyocardial hemorrhage (IMH), both surrogates of microvascular damage in acute myocardial infarction, on regional strain recovery.[34-36] Finally, the effect of adverse LV remodeling (commonly defined as ≥20% increase in LV end-diastolic volume) on the infarct and remote zone myocardial strain has not yet been evaluated.

While the results of the METOCARD-CNIC clinical trial have shown a clear clinical benefit among patients receiving early intravenous metoprolol in terms of smaller LV infarct size[21] and more preserved long-term LV systolic function[22] this has not been fully translated into improved patient prognosis. Namely, early intravenous metoprolol administration was associated with a nonsignificant trend towards reduced occurrence of pre-specified MACE (10.8% in the metoprolol group versus 18.3% in the control group; P=0.065) at a median follow-up of 2 years.[22] However, the prognostic value of early intravenous metoprolol has not yet been explored with longer follow-up data. In addition, the prognostic value of global LV strain with feature tracking CMR over traditional markers of myocardial injury, such as LVEF and infarct size with LGE should be evaluated, especially in the view of the recent studies showing conflicting results.[37-40] Finally, it remains to be elucidated whether the association between global LV strain and prognosis is modulated by the early intravenous metoprolol treatment.

Multimodality cardiac imaging in valvular heart disease

VHD and heart failure are major health issues that are steadily increasing in prevalence in Western populations.[41-44] VHD and heart failure frequently co-exist, which can complicate accurate diagnosis of the severity of valve stenosis or regurgitation and affect therapy.[45,46] Cardiac imaging plays a central role in determining the mechanism and the severity of VHD as well as the degree of accompanying LV remodeling and systolic dysfunction. Furthermore, the decision upon the optimal treatment strategy (e.g., surgical valve repair versus replacement, feasibility of percutaneous valve interventions) rely heavily on accurate and detailed cardiac imaging.[41,42] Echocardiography is the primary imaging modality and may be complemented by cardiac computed tomography (CT) and CMR when additional anatomical or functional information is needed.

Over the last decades, TAVR has emerged as an effective alternative to surgical aortic valve replacement for patients with symptomatic severe aortic stenosis.[41,42] Patient selection, accurate sizing of the prosthesis, choice of the procedural approach requires the use of several imaging modalities to optimize the results and minimize complications such as paravalvular regurgitation, aortic annulus rupture, pacemaker implantation or vascular injury.[15,47] Multidetector row computed tomography (MDCT) has become the key imaging modality for pre-procedural evaluation of TAVR candidates in most centers due to its low invasiveness and comprehensive evaluation. Procedural guidance is mainly performed with fluoroscopy assistance, however, in high-risk situations transthoracic echocardiography or transesophageal echocardiography (TEE) can be employed. Prosthesis durability, indices of valve stenosis and regurgitation, thrombosis, infective endocarditis and LV function and remodeling are the key imaging parameters during the follow-up of TAVR patients.

Selection of appropriate TAVR prosthesis size relies on accurate measurement of the aortic annulus, which is a virtual ring at the hinge points of the aortic valve leaflets and as such difficult to characterize with 2-dimensional imaging techniques.[48] Although MDCT is currently considered the reference standard to measure the aortic valve annulus, it requires the use of nephrotoxic contrast and data acquisition during the systolic phase may lead to motion artifacts that reduce the accuracy of the aortic annulus measurements. In contrast, 3-dimensional (3D) TEE permits the acquisition of 3D data along the entire cardiac cycle with adequate temporal and spatial resolution, allowing for accurate measurements of the aortic annulus.[49,50] Recently, automated software for post-processing of 3D TEE datasets have been developed. However, a head-to-head comparison between MDCT and dedicated automated 3D TEE software for aortic annulus assessment and TAVR prosthesis size selection has not yet been performed. Furthermore, the effect of the aortic valve calcification burden on the accuracy of the 3D TEE measurements has not yet been studied.

The decision to operate in patients with severe VHD is frequently complex and relies on an individual risk-benefit analysis. Current guidelines recommend to intervene in patients with symptomatic severe VHD and in asymptomatic patients with reduced LVEF, LV dilatation, pulmonary hypertension, right ventricular dilatation and dysfunction and presence of atrial fibrillation.[41,42] However, most of these adverse consequences of severe VHD are observed in advanced stages of the disease and are partially irreversible after intervention, leading to suboptimal long-term clinical outcomes.[51] Therefore, additional markers that identify early structural and functional consequences of severe VHD would help to redefine the optimal timing for intervention. CMR imaging with T1 mapping and LGE assessment permit myocardial tissue characterization and provide measures of focal replacement and diffuse myocardial fibrosis, whereas CMR tagging and feature-tracking CMR allow for the assessment of myocardial deformation (strain), a functional parameter that indirectly reflects myocardial fibrosis. Accumulating evidence on the deleterious impact of LV myocardial fibrosis on clinical outcomes after surgical treatment of left-sided VHD has raised interest on tissue characterization with CMR techniques.[52-55]

Recent investigations demonstrated an association between mitral valve prolapse (MVP) and malignant ventricular arrhythmias.[56-58] Various imaging parameters have been proposed to predict the risk for developing malignant ventricular arrythmias and sudden cardiac death in patients with MVP, among which fibrosis of the papillary muscles and of the inferolateral LV wall has gained prominence.[59-62] However, it remains to be elucidated whether MVP also associates with diffuse myocardial fibrosis, detected with novel CMR techniques such as extracellular volume (ECV). Moreover, the interplay between patient characteristics, mitral regurgitation grade and markers of LV fibrosis needs to be explored in order to translate this information into clinical practice.

OUTLINE OF THE THESIS

The objective of this thesis was twofold: i) to evaluate myocardial injury and cardioprotective effects of early intravenous metoprolol after STEMI with feature-tracking CMR, and ii) to explore the role of multimodality cardiac imaging in patients with VHD.

In **Part I** the role of LV strain with feature-tracking CMR among patients included in the METOCARD-CNIC randomized clinical trial is investigated. **Chapter 2** focuses on the changes in GLS and GCS from the first week to 6 months after STEMI and explores the impact of early intravenous metoprolol on global LV strain. In **Chapter 3** the effects of early intravenous metoprolol treatment, MVO, IMH and adverse LV remodeling on the evolution of infarct and remote zone circumferential strain over 6 months after STEMI are evaluated. In **Chapter 4** long-term 5-year follow-up results of the patients included in the METOCARD-CNIC trial are presented. The prognostic value of early intravenous metoprolol, GCS, GLS and the association between global LV strain and early intravenous metoprolol treatment on patient prognosis are analyzed.

Part II provides a perspective on the use of multimodality cardiac imaging in VHD. In **Chapter 5**, the role of echocardiography, cardiac CT and CMR in patients with VHD and heart failure is discussed. **Chapter 6** provides an overview of the advantages and limitations of different cardiac imaging techniques in the evaluation of patients undergoing TAVR. In **Chapter 7**, novel automated 3D TEE software is compared to the gold-standard MDCT for the aortic annulus sizing and prosthesis selection in TAVR patients. In addition, the influence of the quantity of aortic valve calcium on the accuracy of the 3D TEE algorithm and the selection of TAVR prosthesis size is explored. **Chapter 8** summarizes the current status of CMR techniques to assess myocardial fibrosis and appraises the current evidence on the use of these techniques for the risk stratification of patients with severe VHD. In **Chapter 9** the role of myocardial fibrosis is further explored in patients with MVP.

REFERENCES

1. Puymirat E, Simon T, Cayla G, Cottin Y, Elbaz M, Coste P *et al.* Acute Myocardial Infarction: Changes in Patient Characteristics, Management, and 6-Month Outcomes Over a Period of 20 Years in the FAST-MI Program (French Registry of Acute ST-Elevation or Non-ST-Elevation Myocardial Infarction) 1995 to 2015. *Circulation* 2017;136(20):1908-19.
2. Szummer K, Wallentin L, Lindhagen L, Alfredsson J, Erlinge D, Held C *et al.* Improved outcomes in patients with ST-elevation myocardial infarction during the last 20 years are related to implementation of evidence-based treatments: experiences from the SWEDEHEART registry 1995-2014. *Eur Heart J* 2017;38(41):3056-65.
3. Yeh RW, Sidney S, Chandra M, Sorel M, Selby JV, Go AS. Population trends in the incidence and outcomes of acute myocardial infarction. *N Engl J Med* 2010;362(23):2155-65.
4. Jernberg T, Johanson P, Held C, Svennblad B, Lindback J, Wallentin L. Association between adoption of evidence-based treatment and survival for patients with ST-elevation myocardial infarction. *Jama* 2011;305(16):1677-84.
5. Ibanez B, James S, Agewall S, Antunes MJ, Bucciarelli-Ducci C, Bueno H *et al.* 2017 ESC Guidelines for the management of acute myocardial infarction in patients presenting with ST-segment elevation: The Task Force for the management of acute myocardial infarction in patients presenting with ST-segment elevation of the European Society of Cardiology (ESC). *Eur Heart J* 2018;39(2):119-77.
6. O'Gara PT, Kushner FG, Ascheim DD, Casey DE, Jr., Chung MK, de Lemos JA *et al.* 2013 ACCF/AHA guideline for the management of ST-elevation myocardial infarction: executive summary: a report of the American College of Cardiology Foundation/American Heart Association Task Force on Practice Guidelines. *J Am Coll Cardiol* 2013;61(4):485-510.
7. Yellon DM, Hausenloy DJ. Myocardial reperfusion injury. *N Engl J Med* 2007;357(11):1121-35.
8. Ibanez B, Heusch G, Ovize M, Van de Werf F. Evolving therapies for myocardial ischemia/reperfusion injury. *J Am Coll Cardiol* 2015;65(14):1454-71.
9. Bulluck H, Dharmakumar R, Arai AE, Berry C, Hausenloy DJ. Cardiovascular Magnetic Resonance in Acute ST-Segment-Elevation Myocardial Infarction: Recent Advances, Controversies, and Future Directions. *Circulation* 2018;137(18):1949-64.
10. Schulz-Menger J, Bluemke DA, Bremerich J, Flamm SD, Fogel MA, Friedrich MG *et al.* Standardized image interpretation and post processing in cardiovascular magnetic resonance: Society for Cardiovascular Magnetic Resonance (SCMR) board of trustees task force on standardized post processing. *J Cardiovasc Magn Reson* 2013;15(1):35.

11. Sutton NR, Li S, Thomas L, Wang TY, de Lemos JA, Enriquez JR *et al.* The association of left ventricular ejection fraction with clinical outcomes after myocardial infarction: Findings from the Acute Coronary Treatment and Intervention Outcomes Network (ACTION) Registry-Get With the Guidelines (GWTG) Medicare-linked database. *Am Heart J* 2016;178:65-73.
12. Stone GW, Selker HP, Thiele H, Patel MR, Udelson JE, Ohman EM *et al.* Relationship Between Infarct Size and Outcomes Following Primary PCI: Patient-Level Analysis From 10 Randomized Trials. *J Am Coll Cardiol* 2016;67(14):1674-83.
13. Clavel MA, Magne J, Pibarot P. Low-gradient aortic stenosis. *Eur Heart J* 2016;37(34):2645-57.
14. Podlesnikar T, Delgado V, Bax JJ. Imaging of Valvular Heart Disease in Heart Failure. *Card Fail Rev* 2018;4(2):78-86.
15. Bax JJ, Delgado V, Bapat V, Baumgartner H, Collet JP, Erbel R *et al.* Open issues in transcatheter aortic valve implantation. Part 1: patient selection and treatment strategy for transcatheter aortic valve implantation. *European Heart Journal* 2014;35(38):2627-38.
16. Bax JJ, Delgado V, Bapat V, Baumgartner H, Collet JP, Erbel R *et al.* Open issues in transcatheter aortic valve implantation. Part 2: procedural issues and outcomes after transcatheter aortic valve implantation. *Eur Heart J* 2014;35(38):2639-54.
17. Podlesnikar T, Delgado V, Bax JJ. Cardiovascular magnetic resonance imaging to assess myocardial fibrosis in valvular heart disease. *Int J Cardiovasc Imaging* 2018;34(1):97-112.
18. Jugdutt BI. Ventricular remodeling after infarction and the extracellular collagen matrix: when is enough enough? *Circulation* 2003;108(11):1395-403.
19. Lopez-Sendon J, Swedberg K, McMurray J, Tamargo J, Maggioni AP, Dargie H *et al.* Expert consensus document on beta-adrenergic receptor blockers. *Eur Heart J* 2004;25(15):1341-62.
20. Chen ZM, Pan HC, Chen YP, Peto R, Collins R, Jiang LX *et al.* Early intravenous then oral metoprolol in 45,852 patients with acute myocardial infarction: randomised placebo-controlled trial. *Lancet* 2005;366(9497):1622-32.
21. Ibanez B, Macaya C, Sanchez-Brunete V, Pizarro G, Fernandez-Friera L, Mateos A *et al.* Effect of early metoprolol on infarct size in ST-segment-elevation myocardial infarction patients undergoing primary percutaneous coronary intervention: the Effect of Metoprolol in Cardioprotection During an Acute Myocardial Infarction (METOCARD-CNIC) trial. *Circulation* 2013;128(14):1495-503.
22. Pizarro G, Fernandez-Friera L, Fuster V, Fernandez-Jimenez R, Garcia-Ruiz JM, Garcia-Alvarez A *et al.* Long-term benefit of early pre-reperfusion metoprolol administration in patients with acute myocardial infarction: results from the METOCARD-CNIC trial (Effect of Metoprolol in Cardioprotection During an Acute Myocardial Infarction). *J Am Coll Cardiol* 2014;63(22):2356-62.

23. Stanton T, Leano R, Marwick TH. Prediction of all-cause mortality from global longitudinal speckle strain: comparison with ejection fraction and wall motion scoring. *Circ Cardiovasc Imaging* 2009;2(5):356-64.
24. Kraigher-Krainer E, Shah AM, Gupta DK, Santos A, Claggett B, Pieske B *et al.* Impaired systolic function by strain imaging in heart failure with preserved ejection fraction. *J Am Coll Cardiol* 2014;63(5):447-56.
25. Joyce E, Hoogslag GE, Leong DP, Debonnaire P, Katsanos S, Boden H *et al.* Association between left ventricular global longitudinal strain and adverse left ventricular dilatation after ST-segment-elevation myocardial infarction. *Circ Cardiovasc Imaging* 2014;7(1):74-81.
26. Antoni ML, Mollema SA, Delgado V, Atary JZ, Borleffs CJ, Boersma E *et al.* Prognostic importance of strain and strain rate after acute myocardial infarction. *Eur Heart J* 2010;31(13):1640-7.
27. Ibrahim el SH. Myocardial tagging by cardiovascular magnetic resonance: evolution of techniques--pulse sequences, analysis algorithms, and applications. *J Cardiovasc Magn Reson* 2011;13:36.
28. Claus P, Omar AM, Pedrizzetti G, Sengupta PP, Nagel E. Tissue Tracking Technology for Assessing Cardiac Mechanics: Principles, Normal Values, and Clinical Applications. *JACC Cardiovasc Imaging* 2015;8(12):1444-60.
29. Pedrizzetti G, Claus P, Kilner PJ, Nagel E. Principles of cardiovascular magnetic resonance feature tracking and echocardiographic speckle tracking for informed clinical use. *J Cardiovasc Magn Reson* 2016;18(1):51.
30. Reimer KA, Jennings RB. The changing anatomic reference base of evolving myocardial infarction. Underestimation of myocardial collateral blood flow and overestimation of experimental anatomic infarct size due to tissue edema, hemorrhage and acute inflammation. *Circulation* 1979;60(4):866-76.
31. Fernandez-Jimenez R, Sanchez-Gonzalez J, Aguero J, Garcia-Prieto J, Lopez-Martin GJ, Garcia-Ruiz JM *et al.* Myocardial edema after ischemia/reperfusion is not stable and follows a bimodal pattern: imaging and histological tissue characterization. *J Am Coll Cardiol* 2015;65(4):315-23.
32. Kidambi A, Mather AN, Swoboda P, Motwani M, Fairbairn TA, Greenwood JP *et al.* Relationship between myocardial edema and regional myocardial function after reperfused acute myocardial infarction: an MR imaging study. *Radiology* 2013;267(3):701-8.
33. Gerber BL, Garot J, Bluemke DA, Wu KC, Lima JA. Accuracy of contrast-enhanced magnetic resonance imaging in predicting improvement of regional myocardial function in patients after acute myocardial infarction. *Circulation* 2002;106(9):1083-9.
34. Neizel M, Korosoglou G, Lossnitzer D, Kuhl H, Hoffmann R, Ocklenburg C *et al.* Impact of systolic and diastolic deformation indexes assessed by strain-encoded imaging to predict persistent severe myocardial dysfunction in patients after acute myocardial infarction at follow-up. *J Am Coll Cardiol* 2010;56(13):1056-62.

35. O'Regan DP, Ariff B, Baksi AJ, Gordon F, Durighel G, Cook SA. Salvage assessment with cardiac MRI following acute myocardial infarction underestimates potential for recovery of systolic strain. *Eur Radiol* 2013;23(5):1210-7.
36. Kidambi A, Mather AN, Motwani M, Swoboda P, Uddin A, Greenwood JP *et al.* The effect of microvascular obstruction and intramyocardial hemorrhage on contractile recovery in reperfused myocardial infarction: insights from cardiovascular magnetic resonance. *J Cardiovasc Magn Reson* 2013;15:58.
37. Eitel I, Stiermaier T, Lange T, Rommel KP, Koschalka A, Kowallick JT *et al.* Cardiac Magnetic Resonance Myocardial Feature Tracking for Optimized Prediction of Cardiovascular Events Following Myocardial Infarction. *JACC Cardiovasc Imaging* 2018;11(10):1433-44.
38. Gavara J, Rodriguez-Palomares JF, Valente F, Monmeneu JV, Lopez-Lereu MP, Bonanad C *et al.* Prognostic Value of Strain by Tissue Tracking Cardiac Magnetic Resonance After ST-Segment Elevation Myocardial Infarction. *JACC Cardiovasc Imaging* 2018;11(10):1448-57.
39. Yoon YE, Kang SH, Choi HM, Jeong S, Sung JM, Lee SE *et al.* Prediction of infarct size and adverse cardiac outcomes by tissue tracking-cardiac magnetic resonance imaging in ST-segment elevation myocardial infarction. *Eur Radiol* 2018;28(8):3454-63.
40. Reindl M, Tiller C, Holzknecht M, Lechner I, Beck A, Plappert D *et al.* Prognostic Implications of Global Longitudinal Strain by Feature-Tracking Cardiac Magnetic Resonance in ST-Elevation Myocardial Infarction. *Circ Cardiovasc Imaging* 2019;12(11):e009404.
41. Baumgartner H, Falk V, Bax JJ, De Bonis M, Hamm C, Holm PJ *et al.* 2017 ESC/EACTS Guidelines for the management of valvular heart disease. *Eur Heart J* 2017;38(36):2739-91.
42. Otto CM, Nishimura RA, Bonow RO, Carabello BA, Erwin JP, 3rd, Gentile F *et al.* 2020 ACC/AHA Guideline for the Management of Patients With Valvular Heart Disease: A Report of the American College of Cardiology/American Heart Association Joint Committee on Clinical Practice Guidelines. *Circulation* 2021;143(5):e72-e227.
43. Ponikowski P, Voors AA, Anker SD, Bueno H, Cleland JG, Coats AJ *et al.* 2016 ESC Guidelines for the diagnosis and treatment of acute and chronic heart failure: The Task Force for the diagnosis and treatment of acute and chronic heart failure of the European Society of Cardiology (ESC)Developed with the special contribution of the Heart Failure Association (HFA) of the ESC. *Eur Heart J* 2016;37(27):2129-200.
44. Yancy CW, Jessup M, Bozkurt B, Butler J, Casey DE, Jr., Drazner MH *et al.* 2013 ACCF/AHA guideline for the management of heart failure: executive summary: a report of the American College of Cardiology Foundation/American Heart Association Task Force on practice guidelines. *Circulation* 2013;128(16):1810-52.

45. Marciniak A, Glover K, Sharma R. Cohort profile: prevalence of valvular heart disease in community patients with suspected heart failure in UK. *BMJ Open* 2017;7(1):e012240.
46. Iung B, Delgado V, Rosenhek R, Price S, Prendergast B, Wendler O *et al.* Contemporary Presentation and Management of Valvular Heart Disease: The EURObservational Research Programme Valvular Heart Disease II Survey. *Circulation* 2019.
47. Podlesnikar T, Delgado V. Update: Cardiac Imaging (II). Transcatheter Aortic Valve Replacement: Advantages and Limitations of Different Cardiac Imaging Techniques. *Rev Esp Cardiol (Engl Ed)* 2016;69(3):310-21.
48. Piazza N, de Jaegere P, Schultz C, Becker AE, Serruys PW, Anderson RH. Anatomy of the aortic valvar complex and its implications for transcatheter implantation of the aortic valve. *Circ Cardiovasc Interv* 2008;1(1):74-81.
49. Ng AC, Delgado V, van der Kley F, Shanks M, van de Veire NR, Bertini M *et al.* Comparison of aortic root dimensions and geometries before and after transcatheter aortic valve implantation by 2- and 3-dimensional transesophageal echocardiography and multislice computed tomography. *Circ Cardiovasc Imaging* 2010;3(1):94-102.
50. Khalique OK, Kodali SK, Paradis JM, Nazif TM, Williams MR, Einstein AJ *et al.* Aortic annular sizing using a novel 3-dimensional echocardiographic method: use and comparison with cardiac computed tomography. *Circ Cardiovasc Imaging* 2014;7(1):155-63.
51. Enriquez-Sarano M, Sundt TM, 3rd. Early surgery is recommended for mitral regurgitation. *Circulation* 2010;121(6):804-11; discussion 12.
52. Dweck MR, Joshi S, Murigu T, Alpendurada F, Jabbour A, Melina G *et al.* Midwall fibrosis is an independent predictor of mortality in patients with aortic stenosis. *J Am Coll Cardiol* 2011;58(12):1271-9.
53. Barone-Rochette G, Pierard S, De Meester de Ravenstein C, Seldrum S, Melchior J, Maes F *et al.* Prognostic significance of LGE by CMR in aortic stenosis patients undergoing valve replacement. *J Am Coll Cardiol* 2014;64(2):144-54.
54. Chin CW, Everett RJ, Kwiecinski J, Vesey AT, Yeung E, Esson G *et al.* Myocardial Fibrosis and Cardiac Decompensation in Aortic Stenosis. *JACC Cardiovasc Imaging* 2016.
55. Chaikriangkrai K, Lopez-Mattei JC, Lawrie G, Ibrahim H, Quinones MA, Zoghbi W *et al.* Prognostic value of delayed enhancement cardiac magnetic resonance imaging in mitral valve repair. *Ann Thorac Surg* 2014;98(5):1557-63.
56. Basso C, Perazzolo Marra M, Rizzo S, De Lazzari M, Giorgi B, Cipriani A *et al.* Arrhythmic Mitral Valve Prolapse and Sudden Cardiac Death. *Circulation* 2015;132(7):556-66.

57. Hourdain J, Clavel MA, Deharo JC, Asirvatham S, Avierinos JF, Habib G *et al.* Common Phenotype in Patients With Mitral Valve Prolapse Who Experienced Sudden Cardiac Death. *Circulation* 2018;138(10):1067-9.

58. Essayagh B, Sabbag A, Antoine C, Benfari G, Yang LT, Maalouf J *et al.* Presentation and Outcome of Arrhythmic Mitral Valve Prolapse. *J Am Coll Cardiol* 2020;76(6):637-49.

59. Han Y, Peters DC, Salton CJ, Bzymek D, Nezafat R, Goddu B *et al.* Cardiovascular magnetic resonance characterization of mitral valve prolapse. *JACC Cardiovasc Imaging* 2008;1(3):294-303.

60. Perazzolo Marra M, Basso C, De Lazzari M, Rizzo S, Cipriani A, Giorgi B *et al.* Morphofunctional Abnormalities of Mitral Annulus and Arrhythmic Mitral Valve Prolapse. *Circ Cardiovasc Imaging* 2016;9(8):e005030.

61. Muthukumar L, Rahman F, Jan MF, Shaikh A, Kalvin L, Dhala A *et al.* The Pickelhaube Sign: Novel Echocardiographic Risk Marker for Malignant Mitral Valve Prolapse Syndrome. *JACC Cardiovasc Imaging* 2017;10(9):1078-80.

62. Ermakov S, Gulhar R, Lim L, Bibby D, Fang Q, Nah G *et al.* Left ventricular mechanical dispersion predicts arrhythmic risk in mitral valve prolapse. *Heart* 2019;105(14):1063-9.

Part I

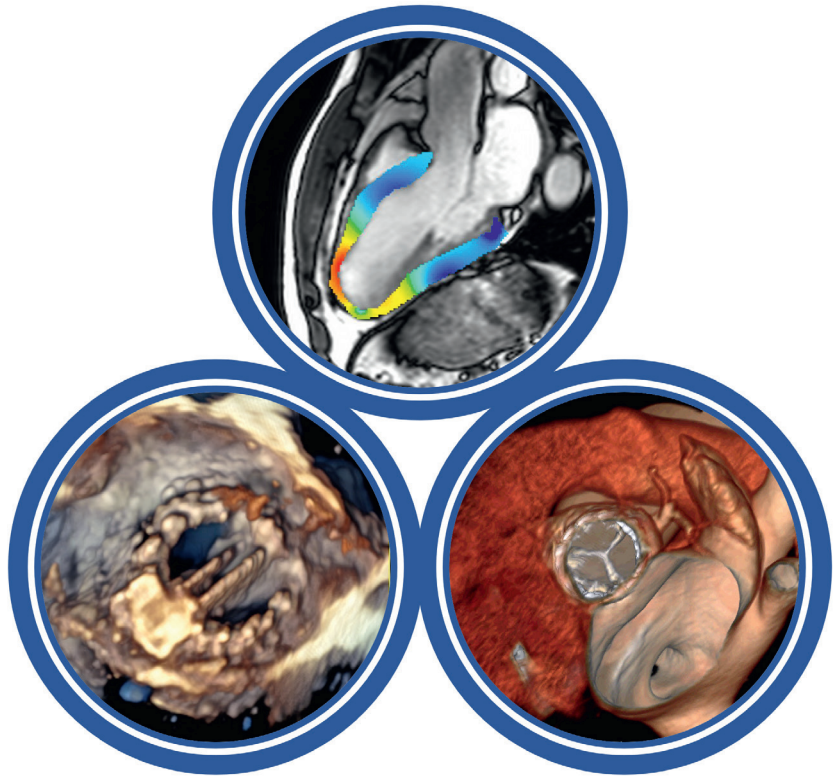

Cardiovascular Magnetic Resonance-derived Left Ventricular Strain in Acute Myocardial Infarction

2

Effect of early metoprolol during ST-segment elevation myocardial infarction on left ventricular strain: feature-tracking cardiovascular magnetic resonance substudy from the METOCARD-CNIC trial

Tomaž Podlesnikar, Gonzalo Pizarro, Rodrigo Fernández-Jiménez, Jose M Montero-Cabezas, Javier Sánchez-González, Chiara Bucciarelli-Ducci, Nina Ajmone Marsan, Zlatko Fras, Jeroen J Bax, Valentin Fuster, Borja Ibáñez, Victoria Delgado

JACC Cardiovasc Imaging 2019;12(7 Pt 1):1188-98

ABSTRACT

Background: Early intravenous metoprolol before primary percutaneous coronary intervention (PCI) in ST-segment elevation myocardial infarction (STEMI) portends better outcomes in the METOCARD-CNIC trial. The aim of the present study was to evaluate the effect of early intravenous metoprolol on left ventricular (LV) strain assessed with feature-tracking cardiovascular magnetic resonance (CMR).

Methods: A total of 197 patients with acute anterior STEMI who were enrolled in the METOCARD-CNIC trial (100 allocated to intravenous metoprolol before primary PCI and 97 control patients) were evaluated. LV global circumferential strain (GCS) and global longitudinal strain (GLS) were measured with feature-tracking CMR at 1 week and 6 months after STEMI and compared between randomization groups.

Results: Patients who received early intravenous metoprolol had significantly more preserved LV strain compared to the control patients at 1 week after STEMI (GCS: -13.9±3.8% versus -12.6±3.9%, respectively; P=0.013; GLS: -11.9±2.8% versus -10.9±3.2%, respectively; P=0.032). In both groups, LV strain significantly improved during follow-up (mean difference between 6-month and 1-week strain for the metoprolol group: GCS: -2.9%, 95% CI: -3.5% to -2.4; GLS: -2.9%, 95% CI: -3.4 to -2.4; both P<0.001; the control group: GCS: -3.4%, 95% CI: -3.9% to -2.8%; GLS: -3.4%, 95% CI: -3.9% to -3.0%; both P<0.001). When dividing the overall cohort of patients in quartiles of GCS and GLS, there were significantly less patients in the first quartile (i.e. the worst LV systolic function) who received early intravenous metoprolol compared to control patients at 1 week and 6 months (P<0.05 for GCS and GLS at both time points).

Conclusions: In patients with anterior STEMI, early administration of intravenous metoprolol before primary PCI was associated with significantly less patients with severely depressed LV GCS and GLS, both at 1 week and 6 months. Feature-tracking CMR represents a complementary tool to evaluate the benefits of cardioprotective therapies.

INTRODUCTION

The long-term treatment with beta-blockers after ST-segment elevation myocardial infarction (STEMI) is well established and the benefit appears to be greatest for patients with myocardial infarction complicated by heart failure, left ventricular (LV) systolic dysfunction, or ventricular arrhythmias.[1,2] Current European and American guidelines recommend initiating oral beta-blockers in the first 24 hours after STEMI.[1,2] The role of routine early, intravenous beta-blockers administration prior to primary percutaneous coronary intervention (PCI) is less firmly established. In the context of reduced oxygen supply during myocardial infarction, beta-blockers have the potential to reduce ischemic injury when administered prior to PCI, through their effect on slowing of heart rate, decreasing myocardial contractility, and lowering systemic blood pressure. In addition, some beta-blockers have shown to be able to reduce reperfusion-injury by inhibiting neutrophils function.[3] The Effect of Metoprolol in Cardioprotection During an Acute Myocardial Infarction (METOCARD-CNIC) trial showed that early administration of intravenous metoprolol before primary PCI significantly reduced infarct size 1 week post-STEMI as evaluated by cardiovascular magnetic resonance (CMR) imaging.[4] In addition, early metoprolol administration was associated with improved long-term LV ejection fraction (LVEF), fewer indications for cardioverter-defibrillator implantation, and fewer heart failure readmissions.[5] Accordingly, current European guidelines indicate that intravenous beta-blockers should be considered at the time of presentation in STEMI patients undergoing primary PCI provided that there are no contraindications, no signs of acute heart failure, and the systolic blood pressure is >120 mmHg.[1]

The impact of early intravenous metoprolol on LV myocardial strain has not yet been evaluated. In contrast to LVEF, LV strain does not rely on geometrical assumptions, shows superior intra- and inter-observer reproducibility and can detect subtle systolic dysfunction in patients with preserved LVEF.[6,7] Recent development of feature-tracking CMR allows multidirectional myocardial strain assessment from standard cine images without the need for specialized pulse sequences or additional scanning time.[8] In the METOCARD-CNIC trial population, we evaluated LV global circumferential (GCS) and longitudinal (GLS) strain measured with feature-tracking CMR both at 1 week and 6 months after primary PCI.

METHODS

Patient population

The present study included patients who were enrolled in the METOCARD-CNIC trial and completed 1-week and 6-month CMR study. Briefly, the multicenter randomized METOCARD-CNIC clinical trial recruited patients with first anterior STEMI undergoing primary PCI.[9] A total of 270 patients were randomized to receive up to 15 mg intravenous metoprolol before reperfusion versus conventional therapy. All patients received oral metoprolol, first dose 12-24 hours after STEMI. Exclusion criteria were Killip class III to IV acute heart failure, systolic blood pressure persistently <120 mmHg, PR interval >240 milliseconds (or type II–III atrioventricular block), heart rate persistently <60 beats/min, or active treatment with any beta-blocker agent. Of the initial population, 202 patients underwent 2 CMR studies, at 1 week (5 to 7 days) and 6 months after STEMI. Conventional CMR parameters of LV dimensions, function and myocardial scar and LV GCS and GLS measured with feature-tracking analysis were evaluated at both time points for the overall population as a single group, and for each randomization treatment arm individually.

The study was approved by the ethical committees and institutional review boards at each participating center. All eligible patients gave written informed consent.

Cardiovascular magnetic resonance

The CMR protocol has been described in detail elsewhere.[9] Data acquisition was performed with 1.5 and 3.0 T CMR scanners. LV 2-, 3- and 4-chamber views and a stack of contiguous short-axis slices covering the whole LV were acquired with steady-state free precession functional cine imaging. Typical acquisition parameters were: voxel size 1.6×2 mm, slice thickness 8 mm, gap 0 mm, cardiac phases 25-30, TR 3.5, TE 1.7, flip angle 40, SENSE 1.5, averages 1, FOV 360 × 360 mm. Subsequently, segmented inversion recovery gradient echo sequence acquired 10-15 minutes after a cumulative dose of 0.2 mmol/kg intravenous gadolinium contrast agent (Magnevist, Schering AG, Berlin, Germany) was employed for myocardial necrosis/fibrosis imaging. LV volumes, LV mass, LVEF and late gadolinium enhancement (LGE) data were analyzed with dedicated software (QMass MR 7.5; Medis, Leiden, the Netherlands) as described previously.[9]

Feature-tracking CMR analysis

Feature-tracking CMR analysis was performed on steady-state free precession cine images with dedicated software (CVI[42] v5.3, Circle Cardiovascular Imaging, Calgary, Canada) (Figure 1, Videos

1 and 2). First, the LV endo- and epicardium were delineated at end-diastole in the LV 2-, 3- and 4-chamber views and contiguous short-axis slices and the LV reference points were defined: the mitral annulus and the LV apex in long-axis views and the anterior right ventricular insertion point in the short-axis slices. The most basal short-axis slices, in which the image plane showed LV myocardium only at end-diastole but not at end-systole were excluded. The outlined myocardium borders were automatically tracked throughout the cardiac cycle with fully automated feature-tracking analysis. The quality of the myocardium tracking was visually evaluated. Global time-strain curves were obtained and peak LV GCS and GLS values were recorded.

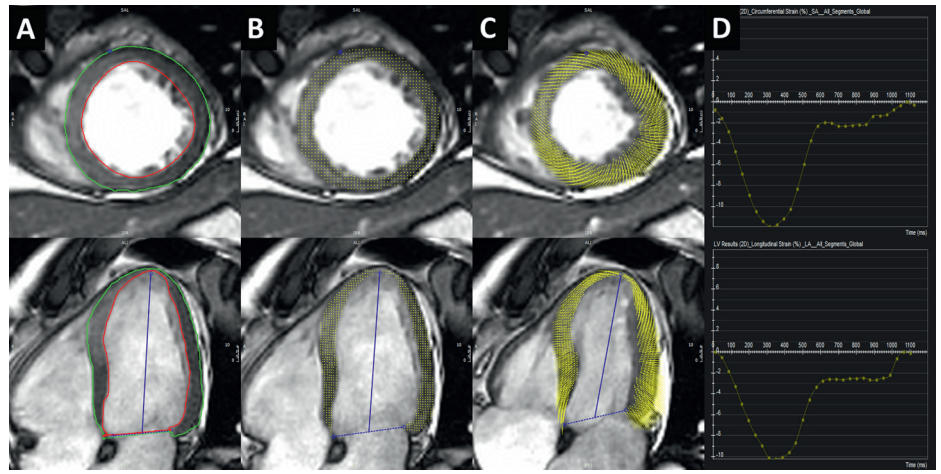

Figure 1: Feature tracking cardiovascular magnetic resonance. (A) Left ventricular (LV) mid-cavity short-axis and 4-chamber long-axis end-diastolic steady-state free precession images. LV endo- and epicardium (red and green lines) were delineated and LV reference points were defined: the anterior right ventricular insertion point in the short-axis view and the mitral annulus and LV apex in the 4-chamber view. The same method was repeated in the remaining long- and short-axis slices. **(B and C)** Visual evaluation of myocardium tracking (Video 1 and 2 in supplementary material). The interventricular septum and LV anterior wall in the short-axis view and the mid-to-apical septum and apex in 4-chamber view (infarcted area) show impaired deformation compared to the other myocardial segments (B = end-diastole, C = end-systole). **(D)** Global time-strain curves were obtained and peak global circumferential strain (-11.9%, top image) and peak global longitudinal strain (-10.2%, bottom image) values were recorded.

A single observer (TP) performed feature-tracking analysis of CMR data. The same observer repeated the analysis of 20 randomly selected CMR scans after 4 weeks to assess the intra-observer variability. A second observer (JMMC), blinded to the results of the first observer, re-measured a different subset of 20 randomly selected CMR scans for the assessment of inter-observer variability.

Statistical analysis

Continuous variables are presented as mean ± standard deviation and categorical variables as frequencies (percentages). Patients were divided into 2 groups according to the treatment received. Comparisons between the early metoprolol group and the control group were performed using independent samples t-test for continuous variables and Pearson's Chi square test or Fischer's exact test for categorical variables. Fischer's exact test was used when the expected value of a categorical variable was <5. Comparisons between 1-week and 6-month CMR data were performed using paired samples t-test. In addition, the study population was divided in quartiles of LV GCS and GLS. The number of patients within the first quartile of LV GCS and GLS (worst LV systolic function) at each randomization treatment arm (early intravenous metoprolol vs control patients) was compared with Pearson's Chi square test at 1 week and 6 months of follow-up. In addition, logistic regression analysis was performed to assess the value of LV GCS and GLS 1 week after STEMI to predict LVEF normalization (≥50%) at 6 months. Odds ratios and 95% confidence intervals (CI) were calculated and adjusted for infarct size (LGE extent) at 1-week CMR, demographic and clinical variables (age, sex, body mass index, presence of hypertension, diabetes, dyslipidemia, smoking status) and treatment randomization arm (early intravenous metoprolol vs. control patients).

The intra- and inter-observer agreement for GCS and GLS measurements were assessed with intraclass correlation coefficients. A two-sided P-value of <0.05 was statistically significant and excellent agreement was defined as an intraclass correlation coefficient >0.9. All statistical analyses were performed using IBM SPSS Statistics 23 (IBM, Armonk, New York).

RESULTS

Of the initial 202 patients who underwent 2 CMR studies, feature-tracking CMR analysis was feasible in 197 patients (early metoprolol group: N=100; control group: N=97) and they formed the population of the present analysis. LV GLS analysis at 6 months was feasible in 195 patients (early metoprolol group: N=99; control group: N=96).

Patients demographics, cardiovascular risk factors, clinical characteristics at recruitment and procedural characteristics of the overall population (mean age 58.1 years, 88% male) and the patients divided according to received randomization treatment (metoprolol vs control) are presented in Table 1. There were no statistically significant differences between both groups. Conventional and feature-tracking CMR parameters of LV structure and function, evaluated at 1 week and 6 months after STEMI for the overall population and for each randomization treatment arm individually, are presented in Table 2.

Table 1: Patients demographics, cardiovascular risk factors, clinical status at recruitment and procedural characteristics.

	Total (N=197)	Metoprolol (N=100)	Control (N=97)	P-value
Demographics				
Age (years)	58.1±11.3	57.8±12.3	58.4±10.1	0.698
Sex (male)	173 (88)	87 (87)	86 (89)	0.865
BMI (kg/m²)	27.6±3.5	27.6±3.5	27.6±3.5	0.900
Cardiovascular risk factors				
Hypertension	74 (38)	37 (37)	37 (38)	0.955
Diabetes mellitus	39 (20)	21 (21)	18 (19)	0.616
Dyslipidemia	85 (43)	43 (43)	42 (43)	0.935
Smoking*	126 (64)	64 (64)	62 (64)	0.839
Clinical status at recruitment				
Killip class II†	19 (10)	8 (8)	11 (11)	0.441
Systolic BP (mmHg)	142±19	142±18	142±19	0.949
Diastolic BP (mmHg)	88±16	89±16	87±15	0.266
Heart rate (bpm)	82±13	82±14	81±13	0.539
Procedural characteristics				
Ischemia duration (min)	194±65	197±62	191±68	0.488
TIMI grade 0-1 flow before primary PCI	163 (83)	80 (80)	83 (86)	0.373
Successful PCI (TIMI grade 2-3 flow)	194 (99)	100 (100)	94 (97)	0.117

BMI = body mass index; BP = blood pressure; PCI = percutaneous coronary intervention; TIMI = Thrombolysis in Myocardial Infarction. Values are mean ± SD or n (%).
*smoking was defined as current or quitted <10 years ago.
†all other patients were Killip class I (Killip class III to IV were study's exclusion criteria).

Table 2: Effect of treatment randomization on conventional and feature tracking CMR parameters.

	1 week					6 months				
	Overall (N=197)	Metoprolol (N=100)	Control (N=97)	Mean difference [95% CI]	P-value	Overall (N=197)	Metoprolol (N=100)	Control (N=97)	Mean difference [95% CI]	P-value
LVEDV (mL)	172.6±36.2	169.8±33.4	175.5±38.8	-5.6 [-15.8 to 4.5]	0.276	191.6±42.6	187.0±38.8	196.5±45.9	-9.5 [-21.5 to 2.5]	0.119
LVESV (mL)	97.8±31.3	92.9±26.6	102.8±34.9	-9.8 [-18.6 to -1.1]	**0.028**	104.4±40.8	98.2±36.1	110.8±44.5	-12.6 [-24.1 to -1.2]	**0.031**
LVEF (%)	44.2±9.4	45.8±9.1	42.6±9.6	3.2 [0.6 to 5.8]	**0.017**	47.0±10.8	48.7±10.0	45.3±11.4	3.4 [0.4 to 6.4]	**0.028**
LV mass (g)	111.5±25.4	109.1±25.2	113.9±25.5	-4.7 [-11.9 to 2.4]	0.192	85.7±17.6	84.6±17.4	86.8±17.7	-2.3 [-7.2 to 2.7]	0.371
LGE (%)	22.7±12.8	20.9±11.6	24.7±13.8	-3.8 [-7.4 to -0.2]	**0.039**	16.9±9.7	15.7±9.5	18.0±9.7	-2.3 [-5.1 to 0.5]	0.104
LV GCS (%)	-13.3±3.9	-13.9±3.8	-12.6±3.9	-1.4 [-2.4 to -0.3]	**0.013**	-16.4±4.2	-16.9±4.0	-15.9±4.4	-0.9 [-2.1 to 0.3]	0.122
LV GLS (%)	-11.4±3.0	-11.9±2.8	-10.9±3.2	-0.9 [-1.8 to -0.1]	**0.032**	-14.6±3.0	-14.8±2.9	-14.4±3.0	-0.4 [-1.2 to 0.5]	0.379

CI = confidence interval; CMR = cardiovascular magnetic resonance; GCS = global circumferential strain; GLS = global longitudinal strain; LGE = late gadolinium enhancement; LV = left ventricular; LVEDV = left ventricular end-diastolic volume; LVEF = left ventricular ejection fraction; LVESV = left ventricular end-systolic volume.
Values are mean ± SD unless otherwise indicated.

LV conventional and feature-tracking CMR parameters 1 week after STEMI

One week after intervention (metoprolol or control), patients who received early intravenous metoprolol showed significantly smaller LV end-systolic volumes, higher LVEF and smaller infarct sizes assessed by LGE (Table 2, Figure 2). In addition, patients who received early intravenous metoprolol had more preserved LV GCS and GLS than patients in the control group (GCS: -13.9±3.8% versus -12.6±3.9%, respectively; P=0.013; GLS: -11.9±2.8% versus -10.9±3.2%, respectively; P=0.032).

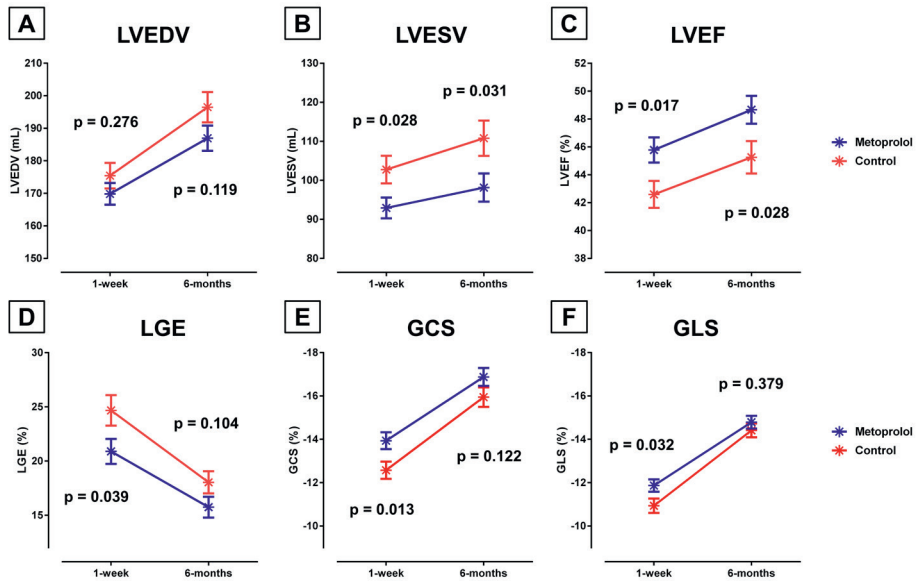

Figure 2: Time course and effect of treatment randomization on conventional and feature tracking cardiovascular magnetic resonance parameters after ST-segment elevation myocardial infarction. Left ventricular end-diastolic volume (LVEDV) **(A)**, left ventricular end-systolic volume (LVESV) **(B)**, left ventricular ejection fraction (LVEF) **(C)**, late gadolinium enhancement (LGE) **(D)**, peak global circumferential strain (GCS) **(E)** and peak global longitudinal strain (GLS) **(F)** in the early intravenous metoprolol and the control group, at 1 week and at 6 months after the acute event. The asterisks represent the mean values and the error bars represent the standard errors of the mean. P-values describe the statistical significance between both treatment arms at each time point.

Changes in LV conventional and feature-tracking CMR parameters between 1-week and 6-month follow-up after STEMI

There were significant changes in conventional CMR parameters and LV strain between 1-week and 6-month follow-up in the overall population and in both study treatment arms (Table 3, Figure 2 and 3). LV end-diastolic and end-systolic volumes significantly increased over time. However, LV dilation was more pronounced for LV end-diastolic volumes than for LV end-systolic volumes, partly explaining the significant improvement of LVEF over time. The percentage of LV myocardium with LGE significantly decreased over the 6 months of follow-up. In addition, LV GCS and GLS significantly improved over the 6-month follow-up (mean difference between 6-month and 1-week strain for the metoprolol group: GCS: -2.9%, 95% CI: -3.5% to -2.4; GLS: -2.9%, 95% CI: -3.4 to -2.4; both P<0.001; the control group: GCS: -3.4%, 95% CI: -3.9% to -2.8%; GLS: -3.4%, 95% CI: -3.9% to -3.0%; both P<0.001).

Table 3: Time course of LV conventional and feature tracking CMR parameters after STEMI.

	Overall (N=197)			Metoprolol (N=100)			Control (N=97)		
	Mean difference	95% CI	P-value	Mean difference	95% CI	P-value	Mean difference	95% CI	P-value
LVEDV (mL)	18.9	15.3 to 22.5	**<0.001**	16.4	11.6 to 21.2	**<0.001**	21.5	16.2 to 26.8	**<0.001**
LVESV (mL)	6.7	3.4 to 9.9	**<0.001**	4.9	0.4 to 9.3	**0.032**	8.5	3.6 to 13.4	**0.001**
LVEF (%)	2.7	1.8 to 3.6	**<0.001**	2.9	1.5 to 4.2	**<0.001**	2.6	1.3 to 3.9	**<0.001**
LV mass (g)	-25.8	-28.5 to -23.2	**<0.001**	-24.6	-28.3 to -20.9	**<0.001**	-27.0	-30.9 to -23.1	**<0.001**
LGE (%)	-5.8	-6.7 to -4.8	**<0.001**	-5.1	-6.5 to -3.8	**<0.001**	-6.5	-7.8 to -5.1	**<0.001**
LV GCS (%)	-3.2	-3.5 to -2.8	**<0.001**	-2.9	-3.5 to -2.4	**<0.001**	-3.4	-3.9 to -2.8	**<0.001**
LV GLS (%)	-3.2	-3.5 to -2.8	**<0.001**	-2.9	-3.4 to -2.4	**<0.001**	-3.4	-3.9 to -3.0	**<0.001**

STEMI = ST-segment elevation myocardial infarction; other abbreviations as in Table 2.

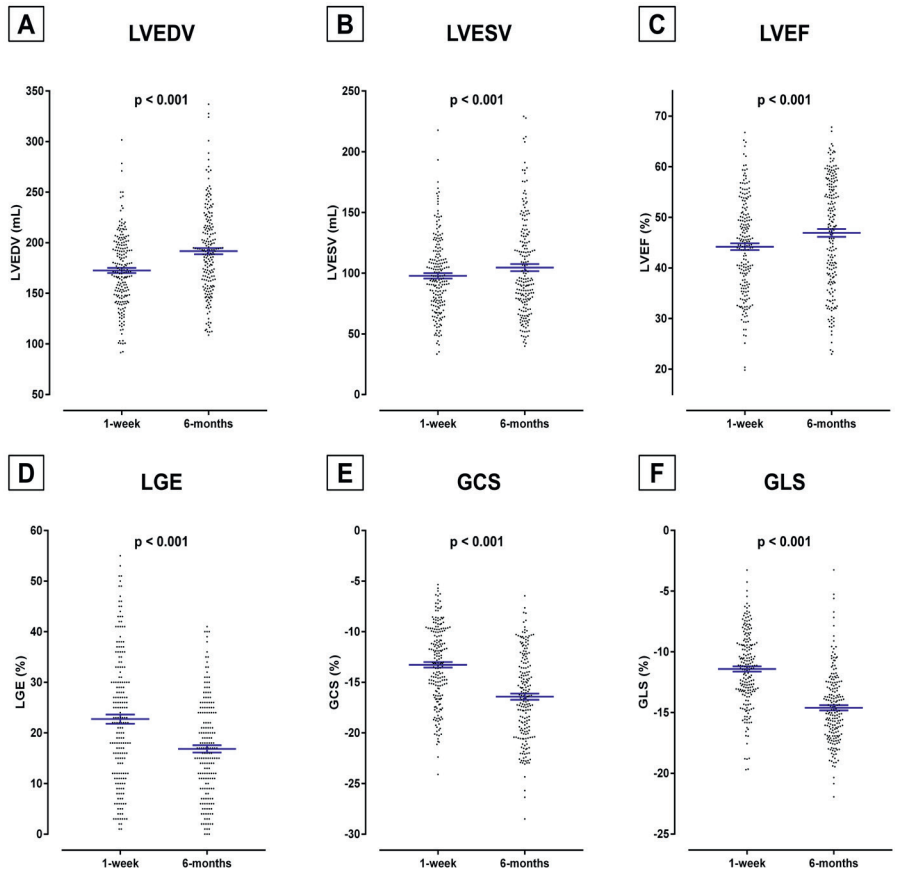

Figure 3: Time course of conventional and feature tracking cardiovascular magnetic resonance parameters after ST-segment elevation myocardial infarction in the overall population. Left ventricular end-diastolic volume (LVEDV) **(A)**, left ventricular end-systolic volume (LVESV) **(B)**, left ventricular ejection fraction (LVEF) **(C)**, late gadolinium enhancement (LGE) **(D)**, peak global circumferential strain (GCS) **(E)** and peak global longitudinal strain (GLS) **(F)** in the overall population at 1 week and at 6 months after the acute event. Dots are individual patient data. Blue lines represent the mean ± standard error of the mean. P-values describe the statistical significance between the two time points.

LV GCS and GLS at 1 week after STEMI were significant predictors of LVEF normalization (LVEF ≥50%) at 6-month follow-up (Table 4). Each 1 percent increase in LV GCS was associated with 40.8% higher likelihood of LVEF normalization (P<0.001) and each 1% of increase in LV GLS was associated with 40.9% higher likelihood of LVEF normalization at 6 months after STEMI (P<0.001). Both, LV GCS and GLS, remained significant predictors of LVEF normalization after adjusting for the extent of LGE on 1-week CMR, demographic and clinical variables and treatment randomization arm (P<0.001 for both).

Table 4: Left ventricular ejection fraction (LVEF), left ventricular global circumferential (GCS) and longitudinal (GLS) strain at 1 week after myocardial infarction as predictors of LVEF normalization (LVEF ≥50%) at 6 months after the acute event.

	Univariate analysis			Multivariate analysis 1*			Multivariate analysis 2†		
	Odds ratio	95% CI	P-value	Odds ratio	95% CI	P-value	Odds ratio	95% CI	P-value
LVEF (%)	1.289	1.203-1.382	**<0.001**	1.190	1.100-1.286	**<0.001**	1.231	1.129-1.342	**<0.001**
GCS (%)	0.592	0.513-0.682	**<0.001**	0.723	0.619-0.843	**<0.001**	0.715	0.610-0.839	**<0.001**
GLS (%)	0.591	0.505-0.692	**<0.001**	0.718	0.600-0.860	**<0.001**	0.666	0.542-0.819	**<0.001**

CI = confidence interval.
*adjusted for the extent of late gadolinium enhancement (LGE) on 1-week cardiovascular magnetic resonance (CMR).
†adjusted for the extent of LGE on 1-week CMR, age, sex, body mass index, presence of hypertension, diabetes, dyslipidemia, smoking status and treatment randomization arm (early intravenous metoprolol vs control).

LV conventional and feature-tracking CMR parameters 6 months after STEMI

The improvements in LV conventional and feature-tracking CMR parameters resulted in non-significant differences in LV end-diastolic volumes, LV mass and LGE between both treatment arms at 6 months (Table 2, Figure 2). However, patients who received early intravenous metoprolol still had significantly smaller LV end-systolic volumes and higher LVEF. In addition, patients who received early intravenous metoprolol showed a non-significant trend for more preserved LV strain compared to patients in the control group (GCS: -16.9±4.0% versus -15.9±4.4%, respectively; P=0.122; GLS: -14.8±2.9% versus -14.4±3.0%, respectively; P=0.379).

The effect of early metoprolol on severe LV systolic dysfunction

When dividing the overall cohort of patients in quartiles of GCS and GLS, there were significantly less number of patients receiving early intravenous metoprolol in the first GCS and GLS quartile (i.e. the worst LV systolic function), both at 1 week and at 6 months (Table 5, Figure 4). At 1 week after STEMI, there were 18 patients who received early intravenous metoprolol versus 31 patients with the conventional treatment in the first GCS quartile group (≥-10.0%) (P=0.023) and 13 patients who received early metoprolol versus 36 control patients in the first GLS quartile group (≥-9.3%) (P<0.001). At 6 months after STEMI, there were 17 patients who received early intravenous metoprolol versus 32 patients with the conventional treatment in the first GCS quartile group (≥-13.1%) (P=0.009) and 18 patients who received early metoprolol versus 31 control patients in the first GLS quartile group (≥-12.8%) (P=0.023).

Table 5: Number of patients in GCS and GLS quartiles at 1 week and 6 months after STEMI.

LV GCS 1 week				
	1st quartile (≥-10.0%)	2nd quartile (-10.0% to -13.1%)	3rd quartile (-13.1% to -16.3%)	4th quartile (<-16.3%)
Metoprolol	18	22	34	26
Control	31	28	15	23
LV GLS 1 week				
	1st quartile (≥-9.3%)	2nd quartile (-9.3% to -11.3%)	3rd quartile (-11.3% to -13.2%)	4th quartile (<-13.2%)
Metoprolol	13	34	25	28
Control	36	16	25	20
LV GCS 6 months				
	1st quartile (≥-13.1%)	2nd quartile (-13.1% to -16.4%)	3rd quartile (-16.4% to -19.8%)	4th quartile (<-19.8%)
Metoprolol	17	30	27	26
Control	32	20	22	23
LV GLS 6 months				
	1st quartile (≥-12.8%)	2nd quartile (-12.8% to -15.0%)	3rd quartile (-15.0% to -16.8%)	4th quartile (<-16.8%)
Metoprolol	18	26	29	26
Control	31	23	20	22

Abbreviations as in Table 2.

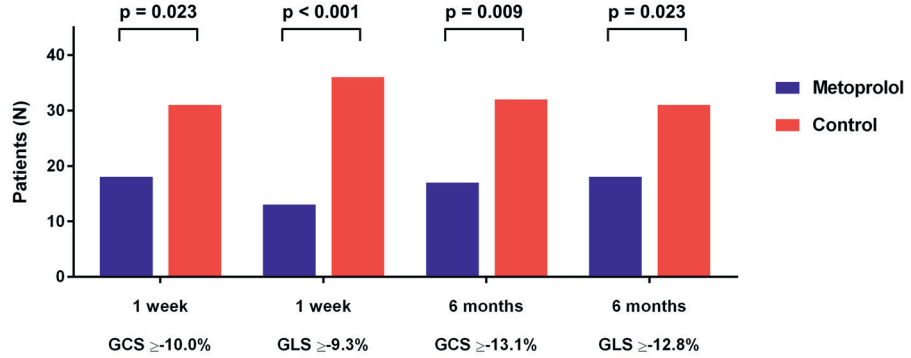

Figure 4: Number of patients within the first quartile of LV GCS and GLS (worst LV systolic function) in the early metoprolol group versus controls at 1-week and 6-month follow-up. Patients in the first global circumferential strain (GCS) and global longitudinal strain (GLS) quartile (worst LV systolic function) were compared according to the treatment received (early intravenous metoprolol vs conventional therapy) at 1 week and at 6 months after acute ST-segment elevation myocardial infarction.

Reproducibility of global left ventricular strain measurements

Excellent intra- and inter-observer variabilities for the feature-tracking CMR analysis of GCS and GLS were obtained. The intra-observer intraclass correlation coefficients (95% CI) for the measurement of LV GCS and GLS were 0.990 (0.975-0.996) and 0.982 (0.955-0.993), respectively. Furthermore, the inter-observer intraclass correlation coefficients (95% CI) for the measurement of LV GCS and GLS were 0.995 (0.987-0.998) and 0.990 (0.976-0.996), respectively.

DISCUSSION

The present study demonstrates that in patients with anterior STEMI treated with primary PCI, early administration of intravenous metoprolol was associated with more preserved LV GCS and GLS at 1 week after myocardial infarction as compared to control patients. In addition, early administration of intravenous metoprolol before primary PCI was associated with significantly less patients with severely depressed GCS and GLS both at 1 week and 6 months. Altogether, these data indicate that early intravenous metoprolol before reperfusion improves short and long-term LV systolic dysfunction as evaluated with feature-tracking CMR.

LV conventional and feature-tracking CMR parameters 1 week after STEMI

Acute myocardial infarction results in myocardial cell necrosis and changes in extracellular collagen matrix that portend adverse consequences on LV structure and function.[10] While early intravenous beta-blocker administration offers physiological rationale for lowering the myocardial infarction burden, their routine use has been disputed over the last decades due to the conflicting data on patients outcome.[11] The METOCARD-CNIC trial was the first randomized control trial in the modern era of primary PCI in STEMI patients, showing that early administration of intravenous metoprolol resulted in significant reduction of LV end-systolic volumes, increase in LVEF and smaller LGE-assessed infarct size 1 week after anterior STEMI, as evaluated by CMR imaging.[4] The present study provides additional information on the effect of early intravenous metoprolol on LV systolic function by means of circumferential and longitudinal shortening, assessed with novel feature-tracking CMR algorithm. This is important since LV strain with speckle tracking echocardiography has been shown to be a more sensitive marker of LV dysfunction[7] and to provide incremental prognostic information over LVEF in the STEMI population.[12] Recently, clinical implications of feature-tracking CMR in STEMI have been demonstrated.[13,14] Our results show that GCS and GLS were more preserved in patients who received early intravenous metoprolol, supporting the rationale to use beta-blocker intravenously in clinically stable STEMI patients before primary PCI.[1]

Time course of LV structural and functional changes after STEMI

In the healing process of acute myocardial infarction important structural and functional changes take place in both the infarct area and the remote zone.[10] Several studies have focused on LV remodeling after acute myocardial infarction.[15-17] In a large prospective STEMI registry including 507 patients treated with primary PCI and imaged with CMR at 1 week and 6 months, LV end-diastolic volume increased (from 79±21 mL/m^2 to 81±23 mL/m^2; P=0.06) and LV end-systolic volume decreased (from 41±19 mL/m^2 to 39±21 mL/m^2; P=0.02) over time.[16] This resulted in a significant increase in LVEF (from 50±12% to 54±13%, respectively; P<0.001). In the present study including a homogenous population with anterior STEMI patients treated with primary PCI, LV end-diastolic and LV end-systolic volumes both increased significantly over time in patients receiving early intravenous metoprolol as well as in control patients (Table 3, Figure 2 and 3). However, the increase was proportionally larger for LV end-diastolic volume than for LV end-systolic volume, resulting in an increase in LVEF. Furthermore, several authors have reported a reduction in infarct size, assessed with LGE CMR in STEMI patients treated with primary PCI.[16,18] Engblom *et al.*[18] showed a progressive decrease of LGE, expressed as the percentage of total LV mass, from days 1, 7, 42 to 182; however, there was no significant additional reduction of hyperenhanced myocardium at 1 year. The LGE reduction occurred predominantly during the first week after infarction (63% of the total 1-year reduction). In addition, Bodi *et al.*[16] reported significant reduction of LGE from 1 week to 6 months after STEMI (21±14% and 17±12%, respectively; P<0.001). This is in line with the results of the present study, which also demonstrated a decrease in LV hyperenhancement from 1 week to 6 months post-infarction.

In addition, the present study evaluated LV strain with feature-tracking CMR. LV strain has been extensively studied with speckle tracking echocardiography after acute myocardial infarction.[19] On the other hand, global LV strain with CMR after myocardial infarction has been less extensively evaluated, but a few studies investigated the time changes of regional LV strain, using different myocardial tagging techniques.[20,21] Kidambi *et al.*[20] showed an improvement of infarct zone peak systolic circumferential strain from day 2 to day 90 in 39 patients after STEMI treated with primary PCI, using complementary spatial modulation of magnetization myocardial tagging technique. Neizel *et al.*[21] demonstrated an improvement in peak systolic circumferential strain in the myocardial segments with >50% transmural LGE (P<0.05) with strain-encoded imaging. The present study is, however, the first to assess the time course of GCS and GLS in a large anterior STEMI population with feature-tracking CMR. We demonstrated an overall improvement of 3.2% of GCS and GLS between 1-week and 6-month follow-up (P<0.001 for both).

The effect of metoprolol on long-term results

The results of the METOCARD-CNIC trial have shown long-term benefit of early intravenous metoprolol after acute anterior STEMI.[5] Patients who received early intravenous metoprolol had smaller LV end-systolic volumes and more preserved LVEF at 6 months after STEMI, however there were no statistically significant differences in LGE-assessed infarct size between both treatment arms. In the present analysis, GCS and GLS showed a tendency towards more preserved values in the metoprolol group, but the differences did not reach the level of statistical significance. These results suggest that GCS and GLS are more closely related to myocardial infarct size, assessed with LGE CMR, than to changes in LV volumes, described by LVEF. This is in line with the published reports, showing that GLS with echocardiography is a better predictor of LGE-assessed infarct size compared to LVEF, whether measured in the acute phase after revascularization or at follow-up.[22,23]

The different effects of metoprolol on GCS and GLS between 1-week and 6-month follow-up might be explained by the kinetics of the healing process of myocardial infarction. Edema is a very dynamic process during the first week after myocardial infarction,[24] and strain closely associates with its intensity and volume.[20] Moreover, cardioprotective therapies may affect the extent and intensity of post-myocardial infarction edema.[25] We may reasonably assume that the differences in LV GCS and GLS between both treatment arms were more pronounced in the acute phase because of a blunted edematous reaction in metoprolol treated patients as compared to control patients and have diluted at 6-month follow-up due an overall large resorption of edema and necrotic tissue.[26,27]

Importantly however, when dividing the overall cohort of patients in quartiles of GCS and GLS, there was a significantly fewer number of patients receiving early intravenous metoprolol in the first GCS and GLS quartile (i.e. the worst LV systolic function), both at 1 week and at 6 months after STEMI (Figure 4). This shows that early metoprolol administration has a long-term beneficial effect on the healing process of STEMI and prevents severe LV systolic dysfunction. Our results support the use of early intravenous metoprolol in STEMI patients without contraindications to beta-blockers undergoing primary PCI.

Study limitations

Feature-tracking is a novel technique to assess LV strain with CMR. Recommendations on how to perform feature-tracking analysis are lacking, there are no accepted standard reference values for LV strain and the agreement between different vendors of feature-tracking software is

largely unknown.[28] However, LV strain with feature-tracking CMR has shown to closely correlate with myocardial tagging and speckle tracking echocardiography and demonstrated superior intra- and inter-observer variability compared to both methods.[29,30] Furthermore, evaluation of LV strain was not a predefined study endpoint of the METOCARD-CNIC trial. Of the initial 202 patients who underwent 2 CMR studies in the METOCARD-CNIC trial, 5 patients were excluded from the LV strain analysis (7 patients from the analysis of GLS at 6 months) due to poor CMR cine image quality, which may have influenced our results. However, 98% (97%) feasibility of strain assessment with feature-tracking CMR is similar to what has been described before.[29,30]

CONCLUSION

Early intravenous metoprolol is associated with improved LV strain at 1 week after the acute anterior STEMI. Furthermore, early intravenous metoprolol is associated with less patients having worst LV systolic function at 1-week and at 6-month follow-up, compared with control patients. In conclusion, early metoprolol administration before primary PCI reduces the incidence of severe LV systolic dysfunction, both at short- and long-term follow-up as evaluated by feature-tracking CMR.

REFERENCES

1. Ibanez B, James S, Agewall S, Antunes MJ, Bucciarelli-Ducci C, Bueno H *et al.* 2017 ESC Guidelines for the management of acute myocardial infarction in patients presenting with ST-segment elevation: The Task Force for the management of acute myocardial infarction in patients presenting with ST-segment elevation of the European Society of Cardiology (ESC). *Eur Heart J* 2018;39(2):119-77.
2. O'Gara PT, Kushner FG, Ascheim DD, Casey DE, Jr., Chung MK, de Lemos JA *et al.* 2013 ACCF/AHA guideline for the management of ST-elevation myocardial infarction: executive summary: a report of the American College of Cardiology Foundation/American Heart Association Task Force on Practice Guidelines. *J Am Coll Cardiol* 2013;61(4):485-510.
3. Garcia-Prieto J, Villena-Gutierrez R, Gomez M, Bernardo E, Pun-Garcia A, Garcia-Lunar I *et al.* Neutrophil stunning by metoprolol reduces infarct size. *Nat Commun* 2017;8:14780.
4. Ibanez B, Macaya C, Sanchez-Brunete V, Pizarro G, Fernandez-Friera L, Mateos A *et al.* Effect of early metoprolol on infarct size in ST-segment-elevation myocardial infarction patients undergoing primary percutaneous coronary intervention: the Effect of Metoprolol in Cardioprotection During an Acute Myocardial Infarction (METOCARD-CNIC) trial. *Circulation* 2013;128(14):1495-503.
5. Pizarro G, Fernandez-Friera L, Fuster V, Fernandez-Jimenez R, Garcia-Ruiz JM, Garcia-Alvarez A *et al.* Long-term benefit of early pre-reperfusion metoprolol administration in patients with acute myocardial infarction: results from the METOCARD-CNIC trial (Effect of Metoprolol in Cardioprotection During an Acute Myocardial Infarction). *J Am Coll Cardiol* 2014;63(22):2356-62.
6. Stanton T, Leano R, Marwick TH. Prediction of all-cause mortality from global longitudinal speckle strain: comparison with ejection fraction and wall motion scoring. *Circ Cardiovasc Imaging* 2009;2(5):356-64.
7. Kraigher-Krainer E, Shah AM, Gupta DK, Santos A, Claggett B, Pieske B *et al.* Impaired systolic function by strain imaging in heart failure with preserved ejection fraction. *J Am Coll Cardiol* 2014;63(5):447-56.
8. Schuster A, Hor KN, Kowallick JT, Beerbaum P, Kutty S. Cardiovascular Magnetic Resonance Myocardial Feature Tracking: Concepts and Clinical Applications. *Circ Cardiovasc Imaging* 2016;9(4):e004077.
9. Ibanez B, Fuster V, Macaya C, Sanchez-Brunete V, Pizarro G, Lopez-Romero P *et al.* Study design for the "effect of METOprolol in CARDioproteCtioN during an acute myocardial InfarCtion" (METOCARD-CNIC): a randomized, controlled parallel-group, observer-blinded clinical trial of early pre-reperfusion metoprolol administration in ST-segment elevation myocardial infarction. *Am Heart J* 2012;164(4):473-80.e5.
10. Jugdutt BI. Ventricular remodeling after infarction and the extracellular collagen matrix: when is enough enough? *Circulation* 2003;108(11):1395-403.

11. Chen ZM, Pan HC, Chen YP, Peto R, Collins R, Jiang LX *et al.* Early intravenous then oral metoprolol in 45,852 patients with acute myocardial infarction: randomised placebo-controlled trial. *Lancet* 2005;366(9497):1622-32.
12. Antoni ML, Mollema SA, Delgado V, Atary JZ, Borleffs CJ, Boersma E *et al.* Prognostic importance of strain and strain rate after acute myocardial infarction. *Eur Heart J* 2010;31(13):1640-7.
13. Gavara J, Rodriguez-Palomares JF, Valente F, Monmeneu JV, Lopez-Lereu MP, Bonanad C *et al.* Prognostic Value of Strain by Tissue Tracking Cardiac Magnetic Resonance After ST-Segment Elevation Myocardial Infarction. *JACC Cardiovasc Imaging* 2018;11(10):1448-57.
14. Eitel I, Stiermaier T, Lange T, Rommel KP, Koschalka A, Kowallick JT *et al.* Cardiac Magnetic Resonance Myocardial Feature Tracking for Optimized Prediction of Cardiovascular Events Following Myocardial Infarction. *JACC Cardiovasc Imaging* 2018;11(10):1433-44.
15. Joyce E, Hoogslag GE, Leong DP, Debonnaire P, Katsanos S, Boden H *et al.* Association between left ventricular global longitudinal strain and adverse left ventricular dilatation after ST-segment-elevation myocardial infarction. *Circ Cardiovasc Imaging* 2014;7(1):74-81.
16. Bodi V, Monmeneu JV, Ortiz-Perez JT, Lopez-Lereu MP, Bonanad C, Husser O *et al.* Prediction of Reverse Remodeling at Cardiac MR Imaging Soon after First ST-Segment-Elevation Myocardial Infarction: Results of a Large Prospective Registry. *Radiology* 2016;278(1):54-63.
17. Ganame J, Messalli G, Masci PG, Dymarkowski S, Abbasi K, Van de Werf F *et al.* Time course of infarct healing and left ventricular remodelling in patients with reperfused ST segment elevation myocardial infarction using comprehensive magnetic resonance imaging. *Eur Radiol* 2011;21(4):693-701.
18. Engblom H, Hedstrom E, Heiberg E, Wagner GS, Pahlm O, Arheden H. Rapid initial reduction of hyperenhanced myocardium after reperfused first myocardial infarction suggests recovery of the peri-infarction zone: one-year follow-up by MRI. *Circ Cardiovasc Imaging* 2009;2(1):47-55.
19. Antoni ML, Mollema SA, Atary JZ, Borleffs CJ, Boersma E, van de Veire NR *et al.* Time course of global left ventricular strain after acute myocardial infarction. *Eur Heart J* 2010;31(16):2006-13.
20. Kidambi A, Mather AN, Swoboda P, Motwani M, Fairbairn TA, Greenwood JP *et al.* Relationship between myocardial edema and regional myocardial function after reperfused acute myocardial infarction: an MR imaging study. *Radiology* 2013;267(3):701-8.
21. Neizel M, Korosoglou G, Lossnitzer D, Kuhl H, Hoffmann R, Ocklenburg C *et al.* Impact of systolic and diastolic deformation indexes assessed by strain-encoded imaging to predict persistent severe myocardial dysfunction in patients after acute myocardial infarction at follow-up. *J Am Coll Cardiol* 2010;56(13):1056-62.

22. Vartdal T, Brunvand H, Pettersen E, Smith HJ, Lyseggen E, Helle-Valle T *et al.* Early prediction of infarct size by strain Doppler echocardiography after coronary reperfusion. *J Am Coll Cardiol* 2007;49(16):1715-21.
23. Gjesdal O, Helle-Valle T, Hopp E, Lunde K, Vartdal T, Aakhus S *et al.* Noninvasive separation of large, medium, and small myocardial infarcts in survivors of reperfused ST-elevation myocardial infarction: a comprehensive tissue Doppler and speckle-tracking echocardiography study. *Circ Cardiovasc Imaging* 2008;1(3):189-96.
24. Fernandez-Jimenez R, Barreiro-Perez M, Martin-Garcia A, Sanchez-Gonzalez J, Aguero J, Galan-Arriola C *et al.* Dynamic Edematous Response of the Human Heart to Myocardial Infarction: Implications for Assessing Myocardial Area at Risk and Salvage. *Circulation* 2017;136(14):1288-300.
25. Fernandez-Jimenez R, Galan-Arriola C, Sanchez-Gonzalez J, Aguero J, Lopez-Martin GJ, Gomez-Talavera S *et al.* Effect of Ischemia Duration and Protective Interventions on the Temporal Dynamics of Tissue Composition After Myocardial Infarction. *Circ Res* 2017;121(4):439-50.
26. Dall'Armellina E, Karia N, Lindsay AC, Karamitsos TD, Ferreira V, Robson MD *et al.* Dynamic changes of edema and late gadolinium enhancement after acute myocardial infarction and their relationship to functional recovery and salvage index. *Circ Cardiovasc Imaging* 2011;4(3):228-36.
27. Fieno DS, Hillenbrand HB, Rehwald WG, Harris KR, Decker RS, Parker MA *et al.* Infarct resorption, compensatory hypertrophy, and differing patterns of ventricular remodeling following myocardial infarctions of varying size. *J Am Coll Cardiol* 2004;43(11):2124-31.
28. Claus P, Omar AM, Pedrizzetti G, Sengupta PP, Nagel E. Tissue Tracking Technology for Assessing Cardiac Mechanics: Principles, Normal Values, and Clinical Applications. *JACC Cardiovasc Imaging* 2015;8(12):1444-60.
29. Khan JN, Singh A, Nazir SA, Kanagala P, Gershlick AH, McCann GP. Comparison of cardiovascular magnetic resonance feature tracking and tagging for the assessment of left ventricular systolic strain in acute myocardial infarction. *Eur J Radiol* 2015;84(5):840-8.
30. Obokata M, Nagata Y, Wu VC, Kado Y, Kurabayashi M, Otsuji Y *et al.* Direct comparison of cardiac magnetic resonance feature tracking and 2D/3D echocardiography speckle tracking for evaluation of global left ventricular strain. *Eur Heart J Cardiovasc Imaging* 2016;17(5):525-32.

3

Left ventricular functional recovery of infarcted and remote myocardium after ST-segment elevation myocardial infarction (METOCARD-CNIC randomized clinical trial substudy)

Tomaž Podlesnikar, Gonzalo Pizarro, Rodrigo Fernández-Jiménez, Jose M Montero-Cabezas, Nina Greif, Javier Sánchez-González, Chiara Bucciarelli-Ducci, Nina Ajmone Marsan, Zlatko Fras, Jeroen J Bax, Valentin Fuster, Borja Ibáñez, Victoria Delgado

J Cardiovasc Magn Reson 2020;22(1):44

ABSTRACT

Background: We aimed to evaluate the effect of early intravenous metoprolol treatment, microvascular obstruction (MVO), intramyocardial hemorrhage (IMH) and adverse left ventricular (LV) remodeling on the evolution of infarct and remote zone circumferential strain after acute anterior ST-segment elevation myocardial infarction (STEMI) with feature-tracking cardiovascular magnetic resonance (CMR).

Methods: A total of 191 patients with acute anterior STEMI enrolled in the METOCARD-CNIC randomized clinical trial were evaluated. LV infarct zone and remote zone circumferential strain were measured with feature-tracking CMR at 1 week and 6 months after STEMI.

Results: In the overall population, the infarct zone circumferential strain significantly improved from 1 week to 6 months after STEMI (-8.6±9.0% to -14.5±8.0%; P<0.001), while no changes in the remote zone strain were observed (-19.5±5.9% to -19.2±3.9%; P=0.466). Patients who received early intravenous metoprolol had significantly more preserved infarct zone circumferential strain compared to the controls at 1 week (P=0.038) and at 6 months (P=0.033) after STEMI, while no differences in remote zone strain were observed. The infarct zone circumferential strain was significantly impaired in patients with MVO and IMH compared to those without (P<0.001 at 1 week and 6 months), however it improved between both time points regardless of the presence of MVO or IMH (P<0.001). In patients who developed adverse LV remodeling (defined as ≥20% increase in LV end-diastolic volume) remote zone circumferential strain worsened between 1 week and 6 months after STEMI (P=0.036), while in the absence of adverse LV remodeling no significant changes in remote zone strain were observed.

Conclusions: Regional LV circumferential strain with feature-tracking CMR allowed comprehensive evaluation of the sequelae of an acute STEMI treated with primary percutaneous coronary intervention and demonstrated long-lasting cardioprotective effects of early intravenous metoprolol.

INTRODUCTION

Cardiovascular magnetic resonance (CMR) is a powerful noninvasive clinical and research imaging tool for the assessment of the sequelae of an acute myocardial infarction.[1] Within a single scan, assessment of left ventricular (LV) volumes and function, myocardial edema, infarct extent and transmurality, and microvascular damage can be performed. Traditional parameters such as LV volumes and LV ejection fraction and CMR-specific parameters, such as infarct size with late gadolinium enhancement (LGE), presence of microvascular obstruction (MVO) and intramyocardial hemorrhage (IMH) have demonstrated to predict post-infarction LV remodeling and clinical outcome.[2-4] Recently, feature-tracking CMR has been shown to allow for multidirectional myocardial strain assessment from standard CMR cine images without the need for specialized pulse sequences and additional scanning time.[5,6] Global LV longitudinal strain and circumferential strain with feature-tracking CMR have provided important prognostic information after myocardial infarction.[7,8] On the other hand, regional LV deformation has been mostly studied in small single-center studies with different CMR tissue tracking techniques, such as myocardial tagging, strain encoded (SENC) imaging, displacement encoding with stimulated echoes (DENSE) imaging or feature-tracking.[9-15] However, the evolution of LV strain after a ST-segment elevation myocardial infarction (STEMI) within infarcted and remote myocardium has not yet been investigated with feature-tracking CMR.

Accordingly, the present sub-analysis of the Effect of Metoprolol in Cardioprotection During an Acute Myocardial Infarction (METOCARD-CNIC) trial[16] evaluated the changes in regional LV peak circumferential strain after ST-segment elevation myocardial infarction (STEMI) using feature-tracking CMR. The infarct zone and the remote zone circumferential strain were assessed at 1 week and 6 months after STEMI and the effects of the treatment arm (metoprolol versus control), MVO, IMH and adverse LV remodeling on the evolution of infarct and remote zone strain were investigated.

METHODS

Patient population

The present study included patients who were enrolled in the METOCARD-CNIC trial.[16] Briefly, the multicenter randomized METOCARD-CNIC clinical trial recruited patients with first anterior STEMI undergoing primary percutaneous coronary intervention (PCI). A total of 270 patients were randomized to receive up to 15 mg intravenous metoprolol before reperfusion

versus conventional therapy. Of the initial population, 202 patients underwent CMR at 1 week (5 to 7 days) and at 6 months after STEMI. Patients receiving intravenous metoprolol and controls were comparable in terms of demographic characteristics, cardiovascular risk profile, procedural characteristics and discharge medication, as previously described.[16-18] Infarct zone and remote zone circumferential strain were evaluated with feature-tracking CMR at 1 week and 6 months after STEMI. Moreover, the effects of the treatment arm (metoprolol versus control), MVO, IMH and adverse LV remodeling on infarct and remote zone strain were investigated.

The study was approved by the ethical committees and institutional review boards at each participating center. All eligible patients gave written informed consent.

Cardiovascular magnetic resonance

The CMR protocol has been described in detail elsewhere.[19] Data acquisition was performed with 1.5 and 3T CMR scanners at 1 week and 6 months after STEMI. LV long-axis views and a stack of contiguous short-axis slices to cover the whole LV were acquired with balanced steady-state free precession (bSSFP) functional cine imaging. Data acquisition parameters were: voxel size 1.6×2 mm, slice thickness 8 mm, gap 0 mm, cardiac phases 25-30, TR 3.5, TE 1.7, flip angle 40, SENSE 1.5, averages 1, FOV 360×360 mm. Subsequently, edema imaging was performed using a T2-weighted short tau inversion recovery (STIR) sequence, followed by LGE imaging with segmented inversion recovery gradient echo sequence, acquired 10-15 minutes after intravenous gadolinium contrast agent.

CMR parameters were analyzed with dedicated software (QMass MR 7.5; Medis, Leiden, the Netherlands). LV volumes and function were determined from bSSFP cine short-axis image dataset. Infarct size was defined as the percent of LGE with full-width-half-maximum technique on delayed enhancement images. The presence of MVO, defined as hypointense areas within the hyperenhanced infarct zone, was evaluated by visual assessment on 1-week CMR. Areas with MVO were included in the infarct size. The presence of IMH, defined as hypointense areas within the brighter edematous zone on T2-STIR images, was evaluated by visual assessment on 1-week CMR.

Feature-tracking cardiovascular magnetic resonance analysis

Feature-tracking CMR analysis was performed with dedicated software (cvi[42] v5.3, Circle Cardiovascular Imaging, Calgary, Canada). First, the LV endo- and epicardium were delineated in contiguous short-axis slices and the anterior right ventricular insertion point was defined. The most basal slice(s), if the aortic valve plane was present in systolic frames, and most apical slices(s), if myocardial borders were unclear, were excluded. In addition, the mitral annulus and the LV apex were defined in long-axis slices to allow for automated LV segmentation. The outlined myocardium borders were automatically tracked throughout the cardiac cycle with fully automated feature-tracking analysis. The quality of the myocardium tracking was visually evaluated with manual adjustments of the contours if necessary (<5% of cases). Segmental peak circumferential strain values were obtained according to the 16-segment model of LV.[20] Twenty randomly selected CMR scans were chosen (>4 weeks after the primary analysis) for the assessment of intra- and inter-observer reproducibility of the segmental circumferential strain measurements.

Definition of infarct zone and remote zone myocardium

The LV myocardium was divided into the infarct zone and the remote zone regions. Taking into consideration that the METOCARD-CNIC trial included a homogeneous population of patients with anterior STEMI and that in >98% of patients undergoing CMR the culprit lesion was in the left anterior descending coronary artery (LAD),[16] the infarct zone was defined as the LAD perfusion territory. The segmental coronary artery distribution model from the American Society of Echocardiography and the European Association of Cardiovascular Imaging guidelines was used.[20] In addition, according to previous studies with CMR and single-photon emission computed tomography showing that the apical segments most commonly correspond to the LAD perfusion territory, all apical segments were included in the infarct zone.[21,22] Importantly, the proximal and the mid-distal LAD infarctions were defined differently.[23] When the culprit coronary artery lesion was in the proximal LAD, the infarct zone included the segments 1-2, 7-8 and 13-16 and the rest of LV myocardium was defined as the remote zone (Figure 1A). If the culprit lesion was in the mid or distal LAD, the infarct zone included the segments 7-8 and 13-16 (the basal anterior and anteroseptal segments were not included), while the rest of LV myocardium was defined as the remote zone (Figure 1B).

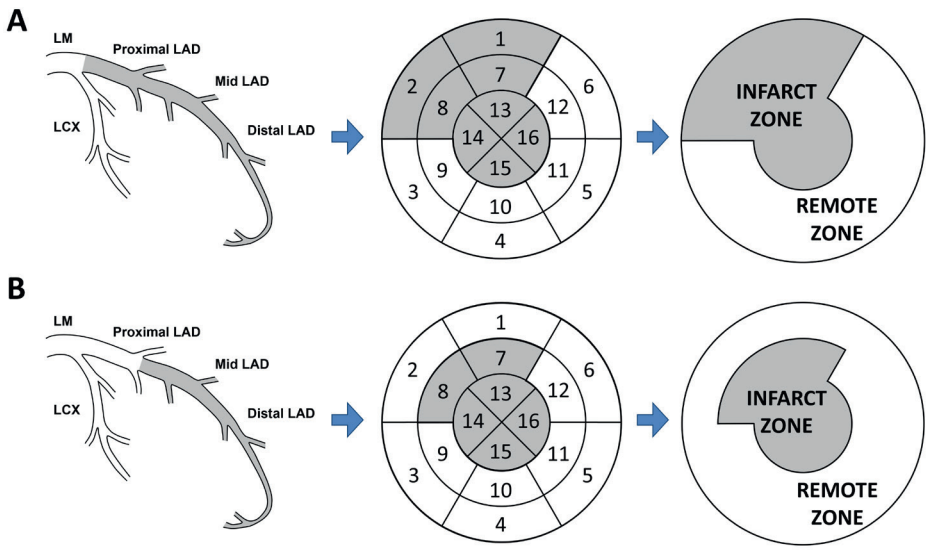

Figure 1: Definition of the infarct and remote zone myocardium. (A) In case the culprit coronary artery lesion was in the proximal left anterior descending coronary artery (LAD), the infarct zone was defined according to the 16-segment model of the left ventricle (LV) with the segments 1-2, 7-8 and 13-16 and the rest of the LV myocardium was defined as the remote zone. **(B)** If the culprit lesion was found in mid or distal LAD, the infarct zone included segments 7-8 and 13-16 and the rest of LV myocardium was defined as the remote zone. LAD = left anterior descending; LCX = left circumflex; LM = left main.

Study endpoints

The objective of the present analysis was to study the evolution of LV circumferential strain within the infarct zone and the remote zone myocardium in patients with anterior STEMI treated with primary PCI and receiving early intravenous metoprolol versus patients treated with standard of care. Furthermore, the impact of MVO and IMH on infarct and remote zone circumferential strain was investigated. Finally, regional circumferential strain was investigated in patients who developed adverse LV remodeling. Adverse LV remodeling was defined as ≥20% increase in LV end-diastolic volume at 6 months compared to the LV end-diastolic volume at 1 week after STEMI.[24] For each patient population (metoprolol vs. control treatment; presence vs. absence of MVO and IMH; presence vs. absence of adverse LV remodeling) the infarct and remote zone strain values were compared at 1 week and at 6 months after STEMI.

Statistical analysis

Continuous variables are presented as mean ± standard deviation. Comparisons between 1-week and 6-month infarct and remote zone circumferential strain were performed using paired samples t-test. Comparisons between infarct and remote zone circumferential strain among different groups of patients (with respect to the randomization treatment, the presence of MVO, IMH and adverse LV remodeling) were performed using independent samples t-test. The intra- and inter-observer agreement for the segmental circumferential LV strain measurements were assessed with intraclass correlation coefficients. A two-sided P-value of <0.05 was statistically significant and excellent agreement was defined as an intraclass correlation coefficient >0.9. All statistical analyses were performed with SPSS (v 23, Statistical Package for the Social Sciences, International Business Machines, Inc., Armonk, New York, USA).

RESULTS

Of 202 patients with 1-week and 6-month CMR scans, 6 patients were excluded due to a non-LAD infarction (3 patients in the metoprolol group and 3 patients in the control group).[16] In addition, feature-tracking could not be performed in 5 patients (1 in the early metoprolol group and 4 in the control group) due to CMR image acquisition artefacts. Finally, LV circumferential strain analysis was feasible in 191 patients (early metoprolol group: N=97; control group: N=94) and they formed the population of the present analysis. A proximal LAD infarct was present in 60 patients and a mid-distal LAD infarct was present in 131 patients, with no statistically significant differences between both treatment arms. Patients demographics, cardiovascular risk factors, clinical status at recruitment, procedural characteristics and CMR parameters at 1 week and 6 months after STEMI of the overall population and of the randomization treatment (metoprolol vs control) groups are presented in the Table 1 and do not differ from those previously published.[16-18]

Table 1: Patients demographics, cardiovascular risk factors, clinical status at recruitment, procedural characteristics and CMR parameters at 1 week and 6 months after STEMI.

	Total (N=191)	Metoprolol (N=97)	Control (N=94)	P-value
Demographics				
Age (years)	57.9±11.2	57.4±12.2	58.4±10.2	0.539
Sex (male)	168 (88)	83 (88)	85 (88)	0.887
BMI (kg/m²)	27.6±3.5	27.6±3.5	27.6±3.6	0.964
Cardiovascular risk factors				
Hypertension	72 (38)	35 (36)	37 (39)	0.680
Diabetes mellitus	39 (20)	21 (22)	18 (19)	0.642
Dyslipidemia	83 (44)	42 (43)	41 (44)	0.985
Smoking*	124 (65)	64 (66)	60 (64)	0.681
Clinical status at recruitment				
Killip class II†	19 (10)	8 (8)	11 (12)	0.425
Systolic BP (mmHg)	142±19	142±18	143±20	0.892
Diastolic BP (mmHg)	88±16	90±16	87±16	0.246
Heart rate (bpm)	82±13	82±14	81±13	0.777
Procedural characteristics				
Ischemia duration (min)	194±65	198±63	190±67	0.354
TIMI grade 0-1 flow before primary PCI	158 (83)	77 (79)	81 (86)	0.272
Successful PCI (TIMI grade 2-3 flow)	188 (98)	97 (100)	91 (97)	0.117
CMR parameters at 1 week				
LVEDV (mL)	173.1±36.2	170.8±33.4	175.4±38.9	0.378
LVESV (mL)	98.4±31.4	93.6±26.8	103.3±35.1	**0.032**
LVEF (%)	44.0±25.5	45.7±9.2	42.3±9.5	**0.012**
LV mass (g)	111.8±25.5	109.9±25.2	113.8±25.8	0.287
LGE (%)	23.0±12.9	21.1±11.7	25.0±13.8	**0.036**
MVO	117 (61)	52 (54)	65 (69)	**0.034**
IMH	81 (42)	36 (37)	45 (48)	0.133
LV GCS (%)	-13.2±3.9	13.9±3.8	12.5±3.9	**0.011**
CMR parameters at 6 months				
LVEDV (mL)	192.3±43.2	187.4±39.0	197.4±46.8	0.112
LVESV (mL)	105.4±41.3	98.5±36.3	112.5±45.1	**0.020**
LVEF (%)	46.7±10.9	48.6±10.1	44.7±11.4	**0.013**
LV mass (g)	85.8±17.8	84.8±17.6	86.9±18.0	0.426
LGE (%)	17.0±9.8	15.8±9.7	18.2±9.8	0.099
Adverse LV remodeling‡	52 (27)	21 (22)	31 (33)	0.079
LV GCS (%)	-16.4±4.3	16.9±4.1	15.8±4.4	0.087

BMI = body mass index; BP = blood pressure; CMR = cardiovascular magnetic resonance; GCS = global circumferential strain; IMH = intramyocardial hemorrhage; LGE = late gadolinium enhancement; LV = left ventricular; LVEDV = left ventricular end-diastolic volume; LVEF = left ventricular ejection fraction; LVESV = left ventricular end-systolic volume; MVO = microvascular obstruction; PCI = percutaneous coronary intervention; STEMI = ST-segment elevation myocardial infarction; TIMI = Thrombolysis in Myocardial Infarction.

Continuous variables are presented as mean ± standard deviation and categorical variables as frequencies (percentages). Comparisons between the early metoprolol group and the control group were performed using independent samples t-test for continuous variables and Pearson's Chi square test or Fischer's exact test for categorical variables. Fischer's exact test was used when the expected value of a categorical variable was <5.

*smoking was defined as current or quitted <10 years ago.

†all other patients were Killip class I (Killip class III to IV were study's exclusion criteria).

‡adverse LV remodeling was defined as ≥20% increase in LVEDV at 6 months.

Evolution of infarct and remote zone circumferential strain

In the overall population the infarct zone strain significantly improved from 1 week to 6 months after STEMI (from -8.6% to -14.5%, mean difference (MD) -5.9%; 95% confidence interval (CI) -6.9 to -4.8; P<0.001), while no significant changes in the remote zone strain were observed (from -19.5% to -19.2%, MD 0.3%; 95% CI -0.5 to 1.1; P=0.466).

The effect of early intravenous metoprolol on infarct and remote zone circumferential strain

One week after STEMI, patients who received early intravenous metoprolol had more preserved infarct zone strain (P=0.038) compared to the control group, while no significant differences in the remote zone strain were observed (P=0.589). The infarct zone strain significantly improved from 1 week to 6 months after STEMI in both groups of patients (P<0.001), while the remote zone strain remained stable (P>0.05). At 6 months after STEMI, the infarct zone strain remained significantly more preserved among patients receiving early intravenous metoprolol compared to the controls (P=0.033), while no significant differences in the remote zone strain between both treatment arms were observed (P=0.879). The effects of early intravenous metoprolol on infarct and remote zone strain are summarized in Table 2 and Figure 2. In addition, two patient examples, one receiving early intravenous metoprolol and one receiving standard care, are shown in Figures 3 and 4.

Table 2: The effect of early intravenous metoprolol on infarct and remote zone strain.

	Infarct zone circumferential strain (%)				Remote zone circumferential strain (%)			
	1 week	6 months	MD [95% CI]	P-value*	1 week	6 months	MD [95% CI]	P-value*
Metoprolol (N=97)	-9.9±7.6	-15.7±7.5	-5.7 [-6.8 to -4.6]	**<0.001**	-19.7±3.6	-19.2±4.1	0.6 [-0.2 to 1.3]	0.153
Control (N=94)	-7.2±10.1	-13.2±8.3	-6.0 [-7.7 to -4.2]	**<0.001**	-19.3±7.5	-19.3±3.7	0.0 [-1.4 to 1.4]	0.984
MD [95% CI]	-2.7 [-5.3 to -0.1]	-2.5 [-4.7 to -0.2]			-0.5 [-2.1 to 1.2]	0.1 [-1.0 to 1.2]		
P-value†	**0.038**	**0.033**			0.589	0.876		

CI = confidence interval; MD = mean difference.

*the P-values for the strain difference between 6 months and 1 week.

†the P-values for the strain difference between the groups.

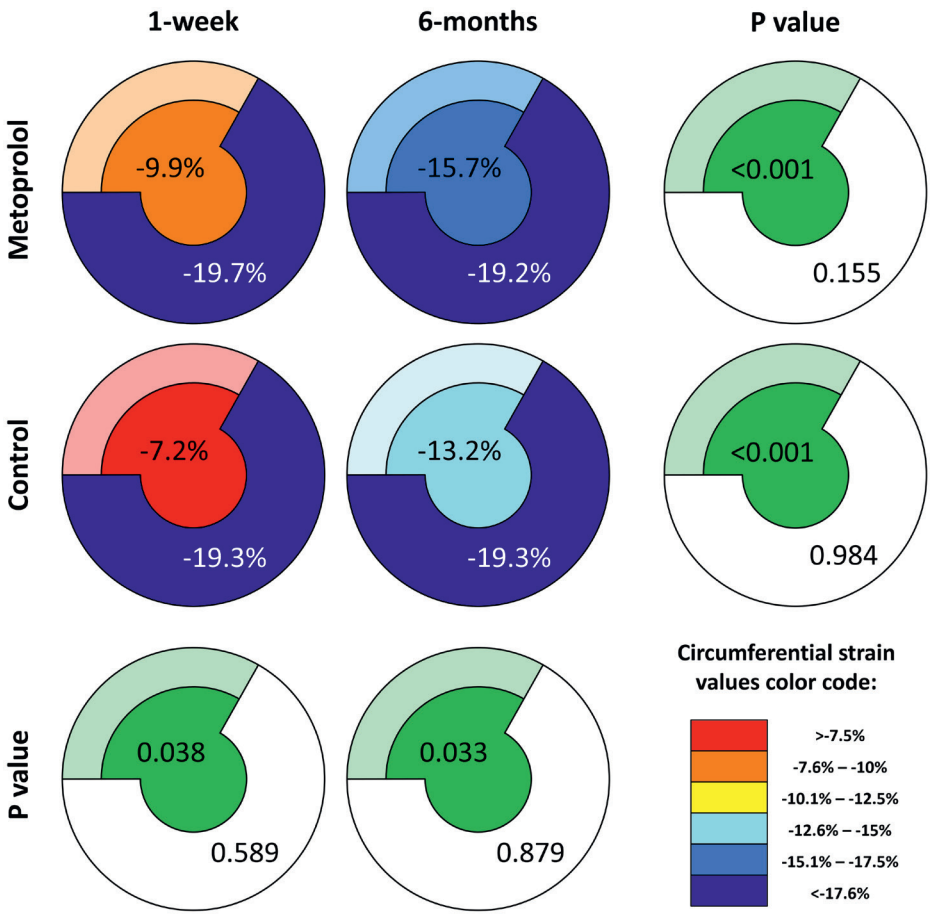

Figure 2: The infarct zone and the remote zone strain after ST-segment elevation myocardial infarction (STEMI) in patients receiving early intravenous metoprolol versus controls. Left ventricular (LV) infarct zone and remote zone strains are schematically presented with the mean values in patients receiving early intravenous metoprolol and in patients receiving conventional treatment at 1 week and at 6 months after STEMI. LV was split into the infarct and the remote zone as explained in Figure 1. In order to schematically present different infarct territories in patients with proximal left anterior descending coronary artery (LAD) coronary artery infarcts and mid-distal LAD infarcts, fainter colors were used to paint the basal anterior and anteroseptal segments, signifying that these segments were either included in the infarct zone (proximal LAD infarcts) or remote zone (mid-distal LAD infarcts) strain analysis. Comparisons between 1-week and 6-month strains are graphically represented on the right-hand side using the same model, with corresponding P-values shown separately for the infarct and remote zone strain analysis. In addition, comparisons between the metoprolol and the control group are shown in the bottom row.

The effect of MVO and IMH on infarct and remote zone circumferential strain

The infarct zone strain was significantly more impaired in patients with MVO or IMH, both at 1 week and at 6 months after STEMI (P<0.001). In contrast, there were no differences in remote zone strain between the 2 groups at both time points (P>0.05). Importantly, the infarct zone strain improved from 1 week to 6 months regardless of the presence of MVO and IMH (P<0.001) and remote zone strain remained stable in all groups of patients (P>0.05). The effects of MVO and IMH on infarct and remote zone strain are summarized in Table 3 and 4. In addition, two patient examples, one with MVO and IMH and one without, are shown in Figures 3 and 4.

Table 3: The effect of microvascular obstruction (MVO) on infarct and remote zone strain.

	Infarct zone circumferential strain (%)				Remote zone circumferential strain (%)			
	1 week	6 months	MD [95% CI]	P-value*	1 week	6 months	MD [95% CI]	P-value*
MVO (N=117)	-5.1±8.8	-11.2±7.8	-6.2 [-7.7 to -4.7]	**<0.001**	-19.3±7.0	-19.2±3.8	0.1 [-1.0 to 1.3]	0.828
No MVO (N=73)	-14.2±6.1	-19.5±5.1	-5.3 [-6.5 to -4.1]	**<0.001**	-19.7±3.4	-19.2±4.2	0.5 [-0.5 to 1.5]	0.313
MD [95% CI]	9.2 [6.9 to 11.5]	8.3 [6.5 to 10.2]			0.4 [-1.4 to 2.1]	0.0 [-1.2 to 1.1]		
P-value†	**<0.001**	**<0.001**			0.677	0.981		

MVO = microvascular obstruction; other abbreviations as in Table 2.
*the P-values for the strain difference between 6 months and 1 week.
†the P-values for the strain difference between the groups.

Table 4: The effect of intramyocardial hemorrhage (IMH) on infarct and remote zone strain.

	Infarct zone circumferential strain (%)				Remote zone circumferential strain (%)			
	1 week	6 months	MD [95% CI]	P-value*	1 week	6 months	MD [95% CI]	P-value*
IMH (N=81)	-4.1±9.4	-10.5±7.8	-6.4 [-8.3 to -4.4]	**<0.001**	-19.2±7.7	-19.3±3.7	-0.2 [-1.7 to 1.4]	0.852
No IMH (N=110)	-11.9±7.1	-17.4±6.8	-5.5 [-6.5 to -4.4]	**<0.001**	-19.8±4.0	-19.1±4.1	0.6 [-0.1 to 1.4]	0.102
MD [95% CI]	7.8 [5.5 to 10.2]	6.9 [4.8 to 9.0]			0.6 [-1.1 to 2.3]	-0.2 [-1.3 to 0.9]		
P-value†	**<0.001**	**<0.001**			0.504	0.736		

IMH = intramyocardial hemorrhage; other abbreviations as in Table 2.
*the P-values for the strain difference between 6 months and 1 week.
†the P-values for the strain difference between the groups.

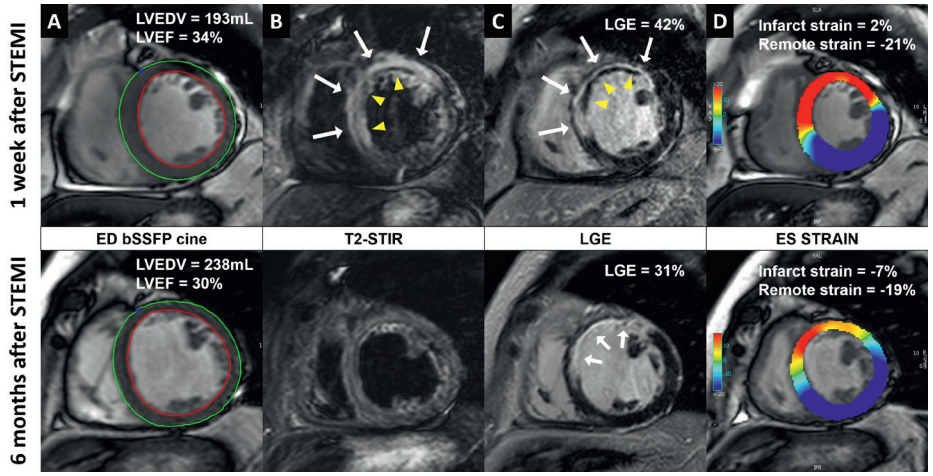

Figure 3: A patient with a proximal LAD infarct receiving standard STEMI treatment. (A) Balanced steady state free precession (bSSFP) end-diastolic images with endo- and epi-cardial contours. The patient developed adverse left ventricular (LV) remodeling (defined as ≥20% increase in LV end-diastolic volume (LVEDV) and had a slight reduction in LV ejection fraction (LVEF) at 6 months after STEMI. **(B)** T2-weighted short tau inversion recovery (STIR) images, showing the presence of edema (white arrows) and intramyocardial hemorrhage (IMH) (yellow arrowheads) at 1-week after STEMI. **(C)** Late gadolinium enhancement (LGE) images, showing the presence of acute ischemic injury (white arrows) with microvascular obstruction (MVO, yellow arrowheads) at 1 week after STEMI and infarct scar (white arrows) at 6-months. **(D)** End-systolic bSSFP images with feature-tracking circumferential LV strain overlay. At 6 months the infarct zone circumferential strain improved despite the presence of a huge infarct with IMH and MVO in the acute phase, while the remote zone strain slightly declined. bSSFP = balanced steady state free precession; ED = end-diastolic; ES = end-systolic; IMH = intramyocardial hemorrhage; LAD = left anterior descending coronary artery = LGE = late gadolinium enhancement; LV = left ventricular; LVEDV = left ventricular end-diastolic volume; LVEF = left ventricular ejection fraction; MVO = microvascular obstruction; SSFP = steady-state free precession; STEMI = ST-segment elevation myocardial infarction; STIR = short tau inversion recovery.

The effect of adverse LV remodeling on infarct and remote zone circumferential strain

There were no statistically significant differences in the infarct zone strain and remote zone strain between patients who did and those who did not develop adverse LV remodeling, both at 1 week and at 6 months after STEMI (P>0.05). Furthermore, in both patient populations the infarct zone strain improved between 1 week and 6 months after STEMI (P<0.001). However, in patients who developed adverse LV remodeling remote zone strain worsened between 1 week and 6 months after STEMI (P=0.036), while in the absence of adverse LV remodeling no significant changes in remote zone strain were observed (P=0.991). The effects of adverse LV remodeling on infarct and remote zone strain are summarized in Table 5. In addition, two patient examples, one with adverse LV remodeling and one without, are shown in Figures 3 and 4.

Table 5: The effect of left ventricular (LV) remodeling on infarct and remote zone strain.

	Infarct zone circumferential strain (%)				Remote zone circumferential strain (%)			
	1 week	6 months	MD [95% CI]	P-value*	1 week	6 months	MD [95% CI]	P-value*
LV remodeling (N=52)	-7.6±8.2	-12.6±9.4	-5.0 [-6.6 to -3.4]	**<0.001**	-20.2±3.7	-19.1±3.7	1.1 [0.1 to 2.1]	**0.036**
No LV remodeling (N=139)	-9.0±9.3	-15.1±7.3	-6.2 [-7.4 to -4.9]	**<0.001**	-19.2±6.5	-19.3±4.0	0.0 [-1.0 to 1.0]	0.991
MD [95% CI]	1.3 [-1.6 to 4.2]	2.5 [-0.4 to 5.4]			-1.0 [-2.8 to 0.9]	0.1 [-1.1 to 1.4]		
P-value†	0.366	0.087			0.317	0.822		

LV = left ventricular; other abbreviations as in Table 2.

*the P-values for the strain difference between 6 months and 1 week.

†the P-values for the strain difference between the groups.

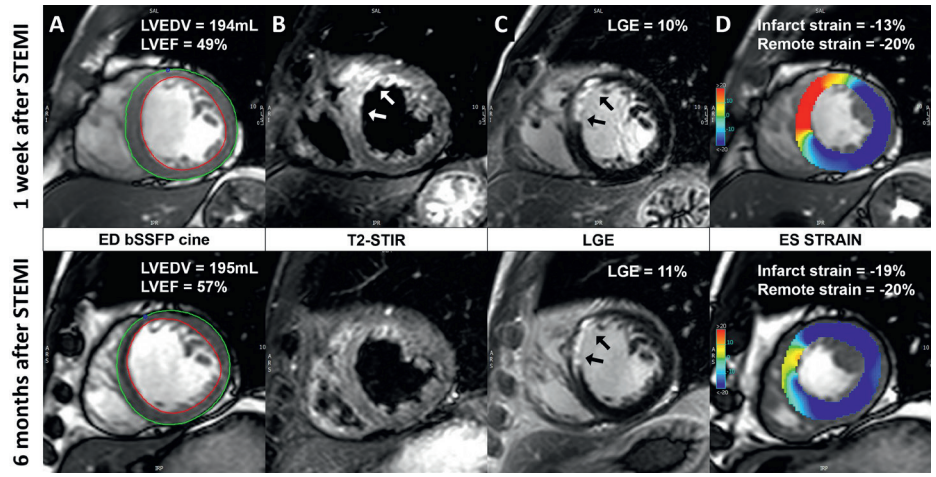

Figure 4: A patient with a mid-LAD infarct receiving early intravenous metoprolol. (A) bSSFP end-diastolic images with endo- and epi-cardial contours. The LV volumes remained stable and the LVEF increased at 6 months after STEMI. **(B)** T2-STIR images showing the presence of edema (white arrows) at 1-week after STEMI. **(C)** LGE images showing the presence of acute ischemic injury/infarct scar (black arrows) at 1 week/6-months after STEMI. **(D)** End-systolic bSSFP images with feature-tracking circumferential LV strain overlay. At 6 months the infarct zone circumferential strain improved while the remote zone strain remained stable. Abbreviations as in Figure 3.

Reproducibility of segmental circumferential left ventricular strain measurements

Excellent intra- and inter-observer variabilities for the feature-tracking CMR analysis of the segmental circumferential strain were obtained. The intra-observer intraclass correlation coefficient (95% CI) was 0.925 (0.906-0.940) and the inter-observer intraclass correlation coefficient (95% CI) was 0.907 (0.884-0.926).

DISCUSSION

The present study shows that the infarct zone circumferential strain improved while the remote zone circumferential strain remained stable between 1 week and 6 months after STEMI. Early intravenous metoprolol had a long-lasting cardioprotective effect on the infarct zone circumferential strain and no significant effect on the remote zone circumferential strain. The infarct zone circumferential strain was significantly impaired in patients with MVO and IMH, but it improved between 1 week and 6 months after STEMI regardless of the presence of MVO or IMH. In patients with adverse LV remodeling, defined as ≥20% increase in LV end-diastolic volume, the infarct zone circumferential strain improved but the remote zone circumferential strain worsened between 1 week and 6 months after STEMI.

Evolution of the infarct and remote zone circumferential strain

Several studies have used CMR to monitor the evolution of regional LV strain after reperfused myocardial infarction.[9-13] Kidambi *et al.*[9] compared changes in circumferential strain with myocardial tagging in the infarct and remote myocardium in 39 patients who underwent CMR at 2, 30 and 90 days after STEMI. A gradual improvement of the infarct zone circumferential strain was observed (-10.2%, -16.0% and -18.6% at days 2, 30 and 90, respectively, P<0.001 for 30-day versus 2-day strain and P=0.04 for 90-day versus 30-day strain) while no significant dynamics in the remote myocardium circumferential strain was observed (-22.6%, -24.0%, -24.1% at days 2, 30 and 90, P=0.17 for 90-day versus 2-day strain). Moreover, Gerber *et al.*[11] studied regional circumferential strain with myocardial tagging in 20 patients after myocardial infarction. Myocardial strain improved between day 4 and 7 months in infarcted segments, with no changes observed in the remote myocardium.

Similar to the reported literature, our results demonstrate an improvement in the infarct zone circumferential strain and no significant changes in the remote zone circumferential strain between the acute (1 week) and chronic stage (6 months) of STEMI. However, the present study included a much larger, homogeneous group of patients with anterior STEMI prospectively included in the multi-center randomized controlled clinical METOCARD-CNIC trial.[16] In addition, while other authors have employed different CMR tissue tracking techniques like myocardial tagging, SENC or DENSE imaging, in the present analysis LV circumferential strain was evaluated with feature-tracking CMR.

The effect of early intravenous metoprolol on infarct and remote zone circumferential strain

Early intravenous metoprolol has been associated with improved short-term and long-term outcomes in the METOCARD-CNIC trial.[16,17] Patients who received intravenous metoprolol prior to primary PCI had significantly reduced infarct size 1 week after STEMI and had more preserved LVEF at 1 week and at 6 months after STEMI. In addition, we have previously shown that patients pre-treated with intravenous metoprolol had more preserved global circumferential strain at 1 week after STEMI, while at 6 months the differences were not significant.[18] However, the present study demonstrates that the infarct zone circumferential strain was more preserved among patients receiving early intravenous metoprolol, both at 1 week and at 6 months after STEMI. This is a very important finding, especially in the view that the differences between the treatment arms in global circumferential strain at 6 months were nonsignificant, underscoring the long-lasting cardioprotective effects of early intravenous metoprolol.

Interestingly, no differences in remote zone circumferential strain were found between patients receiving early intravenous metoprolol and controls. Recently, a slight progressive increase in T2 relaxation time of the remote myocardium has been reported in patients during the first week after STEMI, implying a mild degree of edema of the remote myocardium.[25] Since LV strain is closely associated with post-myocardial infarction edema,[9] we may have expected to observe more preserved remote LV circumferential strain in the early intravenous metoprolol group 1 week after STEMI. However, our results imply that the beneficial cardioprotective effects of early intravenous metoprolol were largely confined to the infarct zone myocardium.

The effect of microvascular obstruction and intramyocardial hemorrhage on infarct zone circumferential strain

MVO and IMH are independent predictors of adverse LV remodeling and clinical outcome after STEMI.[3,4] However, there is a conflicting evidence on the impact of MVO and IMH on regional strain recovery.[10,12,13] Kidambi *et al.*[10] demonstrated an improvement in infarct zone circumferential strain with myocardial tagging between day 2 and day 90 after STEMI in the presence of MVO or IMH. The changes were largely driven by the recovery of epicardial strain (P=0.03 in the presence of MVO and IMH, P<0.01 in the presence of MVO alone), while mid-myocardial and endocardial strain recovery was attenuated (P≥0.05). Moreover, O'Regan *et al.*[12] demonstrated a modest improvement of circumferential strain with myocardial tagging in segments with MVO between day 3 and 1 year after STEMI (-8.1±0.8% and -14.1±1.0%, respectively; P=0.003).

On the other hand, Neizel *et al.*[13] have demonstrated no segmental circumferential strain recovery in the presence of MVO between 3 days and 6 months after STEMI (P=0.2). In our study, the infarct zone circumferential strain was significantly more impaired in patients with MVO or IMH, both at 1 week and 6 months after STEMI, however, it improved between the two time points regardless of the presence of MVO or IMH.

These data indicate the complexity of the healing processes in the infarcted myocardium. Histopathological studies have shown that early infarct tissue consists of a necrotic core, hemorrhage, acute inflammation and islands of tissue repair.[26] These zones often have irregular and patchy distributions and are not confined to the radial location (inner, middle, or outer third) within the infarct.[26] We may reasonably assume that the improvement of infarct zone circumferential strain in patients with MVO and IMH was due to the resorption of edema and necrotic tissue, suggesting a preserved healing capacity of the infarcted myocardium even in the presence of adverse CMR findings.

The effect of adverse LV remodeling on remote zone circumferential strain

Similar to the majority of previous studies[9,11] we have shown no differences in the evolution of remote zone circumferential strain in the overall population, as well as in patients divided according to the randomization treatment, patients with MVO and IMH. However, patients with adverse LV remodeling presented with a small, but statistically significant worsening of the remote zone circumferential strain. Bulluck *et al.*[27] demonstrated increased extracellular volume fraction of the remote myocardium acutely and at 5±2 months after STEMI in patients who developed adverse LV remodeling (defined as ≥20% increase in LV end-diastolic volume). Moreover, remote zone noncontrast T1 mapping provided independent and incremental prognostic information above the clinical risk factors and traditional CMR outcome markers in STEMI patients treated by primary PCI.[28] These findings indicate that LV remodeling after myocardial infarction is a complex and multifactorial process that may involve excessive inflammation/fibrosis of the remote myocardium and may result in impaired circumferential strain.

Limitations

Feature-tracking is a novel CMR technique to assess LV strain. Reference values for LV strain and the agreement between different vendors of feature-tracking software are largely unknown.[29] Furthermore, evaluation of LV strain was not a predefined study endpoint of the METOCARD-CNIC trial. Of the initial 196 patients with a LAD infarct who underwent 2 CMR studies in the METOCARD-CNIC trial, 5 patients were excluded from the LV strain analysis due to poor CMR cine image quality, which may have influenced our results. However, 97% feasibility of strain assessment with feature-tracking CMR is similar to what has been described previously,[30,31] and excellent intra- and inter-observer reproducibility of the segmental feature-tracking strain analysis were observed, similar or slightly better to what has been reported in the literature.[32,33] In the present analysis we did not analyze regional radial and longitudinal strain since previous studies have shown that, on the segmental level, feature-tracking-derived circumferential strain is the most robust and has the lowest intra- and inter-observer variability.[30,31]

CONCLUSION

Regional LV circumferential strain analysis with feature-tracking CMR has revealed several important insights on the impact of MVO, IMH and adverse LV remodeling on the evolution of the infarct zone and remote zone circumferential strain. Furthermore, in patients with first anterior STEMI treated with primary PCI long-lasting cardioprotective effects of early intravenous metoprolol treatment on the infarct zone strain were demonstrated.

REFERENCES

1. Bulluck H, Dharmakumar R, Arai AE, Berry C, Hausenloy DJ. Cardiovascular Magnetic Resonance in Acute ST-Segment-Elevation Myocardial Infarction: Recent Advances, Controversies, and Future Directions. *Circulation* 2018;137(18):1949-64.
2. Hombach V, Grebe O, Merkle N, Waldenmaier S, Hoher M, Kochs M *et al.* Sequelae of acute myocardial infarction regarding cardiac structure and function and their prognostic significance as assessed by magnetic resonance imaging. *Eur Heart J* 2005;26(6):549-57.
3. Eitel I, de Waha S, Wohrle J, Fuernau G, Lurz P, Pauschinger M *et al.* Comprehensive prognosis assessment by CMR imaging after ST-segment elevation myocardial infarction. *J Am Coll Cardiol* 2014;64(12):1217-26.
4. Ganame J, Messalli G, Dymarkowski S, Rademakers FE, Desmet W, Van de Werf F *et al.* Impact of myocardial haemorrhage on left ventricular function and remodelling in patients with reperfused acute myocardial infarction. *Eur Heart J* 2009;30(12):1440-9.
5. Pedrizzetti G, Claus P, Kilner PJ, Nagel E. Principles of cardiovascular magnetic resonance feature tracking and echocardiographic speckle tracking for informed clinical use. *J Cardiovasc Magn Reson* 2016;18(1):51.
6. Schuster A, Hor KN, Kowallick JT, Beerbaum P, Kutty S. Cardiovascular Magnetic Resonance Myocardial Feature Tracking: Concepts and Clinical Applications. *Circ Cardiovasc Imaging* 2016;9(4):e004077.
7. Eitel I, Stiermaier T, Lange T, Rommel KP, Koschalka A, Kowallick JT *et al.* Cardiac Magnetic Resonance Myocardial Feature Tracking for Optimized Prediction of Cardiovascular Events Following Myocardial Infarction. *JACC Cardiovasc Imaging* 2018;11(10):1433-44.
8. Gavara J, Rodriguez-Palomares JF, Valente F, Monmeneu JV, Lopez-Lereu MP, Bonanad C *et al.* Prognostic Value of Strain by Tissue Tracking Cardiac Magnetic Resonance After ST-Segment Elevation Myocardial Infarction. *JACC Cardiovasc Imaging* 2018;11(10):1448-57.
9. Kidambi A, Mather AN, Swoboda P, Motwani M, Fairbairn TA, Greenwood JP *et al.* Relationship between myocardial edema and regional myocardial function after reperfused acute myocardial infarction: an MR imaging study. *Radiology* 2013;267(3):701-8.
10. Kidambi A, Mather AN, Motwani M, Swoboda P, Uddin A, Greenwood JP *et al.* The effect of microvascular obstruction and intramyocardial hemorrhage on contractile recovery in reperfused myocardial infarction: insights from cardiovascular magnetic resonance. *J Cardiovasc Magn Reson* 2013;15:58.
11. Gerber BL, Garot J, Bluemke DA, Wu KC, Lima JA. Accuracy of contrast-enhanced magnetic resonance imaging in predicting improvement of regional myocardial function in patients after acute myocardial infarction. *Circulation* 2002;106(9):1083-9.

12. O'Regan DP, Ariff B, Baksi AJ, Gordon F, Durighel G, Cook SA. Salvage assessment with cardiac MRI following acute myocardial infarction underestimates potential for recovery of systolic strain. *Eur Radiol* 2013;23(5):1210-7.
13. Neizel M, Korosoglou G, Lossnitzer D, Kuhl H, Hoffmann R, Ocklenburg C *et al.* Impact of systolic and diastolic deformation indexes assessed by strain-encoded imaging to predict persistent severe myocardial dysfunction in patients after acute myocardial infarction at follow-up. *J Am Coll Cardiol* 2010;56(13):1056-62.
14. Mangion K, Carrick D, Clerfond G, Rush C, McComb C, Oldroyd KG *et al.* Predictors of segmental myocardial functional recovery in patients after an acute ST-Elevation myocardial infarction. *Eur J Radiol* 2019;112:121-9.
15. Khan JN, Nazir SA, Singh A, Shetye A, Lai FY, Peebles C *et al.* Relationship of Myocardial Strain and Markers of Myocardial Injury to Predict Segmental Recovery After Acute ST-Segment-Elevation Myocardial Infarction. *Circ Cardiovasc Imaging* 2016;9(6).
16. Ibanez B, Macaya C, Sanchez-Brunete V, Pizarro G, Fernandez-Friera L, Mateos A *et al.* Effect of early metoprolol on infarct size in ST-segment-elevation myocardial infarction patients undergoing primary percutaneous coronary intervention: the Effect of Metoprolol in Cardioprotection During an Acute Myocardial Infarction (METOCARD-CNIC) trial. *Circulation* 2013;128(14):1495-503.
17. Pizarro G, Fernandez-Friera L, Fuster V, Fernandez-Jimenez R, Garcia-Ruiz JM, Garcia-Alvarez A *et al.* Long-term benefit of early pre-reperfusion metoprolol administration in patients with acute myocardial infarction: results from the METOCARD-CNIC trial (Effect of Metoprolol in Cardioprotection During an Acute Myocardial Infarction). *J Am Coll Cardiol* 2014;63(22):2356-62.
18. Podlesnikar T, Pizarro G, Fernandez-Jimenez R, Montero-Cabezas JM, Sanchez-Gonzalez J, Bucciarelli-Ducci C *et al.* Effect of Early Metoprolol During ST-Segment Elevation Myocardial Infarction on Left Ventricular Strain: Feature-Tracking Cardiovascular Magnetic Resonance Substudy From the METOCARD-CNIC Trial. *JACC Cardiovasc Imaging* 2019;12(7 Pt 1):1188-98.
19. Ibanez B, Fuster V, Macaya C, Sanchez-Brunete V, Pizarro G, Lopez-Romero P *et al.* Study design for the "effect of METOprolol in CARDioproteCtioN during an acute myocardial InfarCtion" (METOCARD-CNIC): a randomized, controlled parallel-group, observer-blinded clinical trial of early pre-reperfusion metoprolol administration in ST-segment elevation myocardial infarction. *Am Heart J* 2012;164(4):473-80.e5.
20. Lang RM, Badano LP, Mor-Avi V, Afilalo J, Armstrong A, Ernande L *et al.* Recommendations for cardiac chamber quantification by echocardiography in adults: an update from the American Society of Echocardiography and the European Association of Cardiovascular Imaging. *Eur Heart J Cardiovasc Imaging* 2015;16(3):233-70.

21. Ortiz-Perez JT, Rodriguez J, Meyers SN, Lee DC, Davidson C, Wu E. Correspondence between the 17-segment model and coronary arterial anatomy using contrast-enhanced cardiac magnetic resonance imaging. *JACC Cardiovasc Imaging* 2008;1(3):282-93.
22. Pereztol-Valdes O, Candell-Riera J, Santana-Boado C, Angel J, Aguade-Bruix S, Castell-Conesa J *et al.* Correspondence between left ventricular 17 myocardial segments and coronary arteries. *Eur Heart J* 2005;26(24):2637-43.
23. Cerci RJ, Arbab-Zadeh A, George RT, Miller JM, Vavere AL, Mehra V *et al.* Aligning coronary anatomy and myocardial perfusion territories: an algorithm for the CORE320 multicenter study. *Circ Cardiovasc Imaging* 2012;5(5):587-95.
24. Joyce E, Hoogslag GE, Leong DP, Debonnaire P, Katsanos S, Boden H *et al.* Association between left ventricular global longitudinal strain and adverse left ventricular dilatation after ST-segment-elevation myocardial infarction. *Circ Cardiovasc Imaging* 2014;7(1):74-81.
25. Fernandez-Jimenez R, Barreiro-Perez M, Martin-Garcia A, Sanchez-Gonzalez J, Aguero J, Galan-Arriola C *et al.* Dynamic Edematous Response of the Human Heart to Myocardial Infarction: Implications for Assessing Myocardial Area at Risk and Salvage. *Circulation* 2017;136(14):1288-300.
26. Reimer KA, Jennings RB. The changing anatomic reference base of evolving myocardial infarction. Underestimation of myocardial collateral blood flow and overestimation of experimental anatomic infarct size due to tissue edema, hemorrhage and acute inflammation. *Circulation* 1979;60(4):866-76.
27. Bulluck H, Rosmini S, Abdel-Gadir A, White SK, Bhuva AN, Treibel TA *et al.* Automated Extracellular Volume Fraction Mapping Provides Insights Into the Pathophysiology of Left Ventricular Remodeling Post-Reperfused ST-Elevation Myocardial Infarction. *J Am Heart Assoc* 2016;5(7).
28. Reinstadler SJ, Stiermaier T, Liebetrau J, Fuernau G, Eitel C, de Waha S *et al.* Prognostic Significance of Remote Myocardium Alterations Assessed by Quantitative Noncontrast T1 Mapping in ST-Segment Elevation Myocardial Infarction. *JACC Cardiovasc Imaging* 2018;11(3):411-9.
29. Claus P, Omar AM, Pedrizzetti G, Sengupta PP, Nagel E. Tissue Tracking Technology for Assessing Cardiac Mechanics: Principles, Normal Values, and Clinical Applications. *JACC Cardiovasc Imaging* 2015;8(12):1444-60.
30. Augustine D, Lewandowski AJ, Lazdam M, Rai A, Francis J, Myerson S *et al.* Global and regional left ventricular myocardial deformation measures by magnetic resonance feature tracking in healthy volunteers: comparison with tagging and relevance of gender. *J Cardiovasc Magn Reson* 2013;15:8.
31. Andre F, Steen H, Matheis P, Westkott M, Breuninger K, Sander Y *et al.* Age- and gender-related normal left ventricular deformation assessed by cardiovascular magnetic resonance feature tracking. *J Cardiovasc Magn Reson* 2015;17:25.

32. Wu L, Germans T, Guclu A, Heymans MW, Allaart CP, van Rossum AC. Feature tracking compared with tissue tagging measurements of segmental strain by cardiovascular magnetic resonance. *J Cardiovasc Magn Reson* 2014;16:10.
33. Mangion K, Burke NMM, McComb C, Carrick D, Woodward R, Berry C. Feature-tracking myocardial strain in healthy adults- a magnetic resonance study at 3.0 tesla. *Scientific Reports* 2019;9(1):3239.

4

Five-year outcomes and prognostic value of feature-tracking cardiovascular magnetic resonance in patients receiving early prereperfusion metoprolol in acute myocardial infarction

Tomaž Podlesnikar, Gonzalo Pizarro, Rodrigo Fernández-Jiménez, Jose M Montero-Cabezas, Javier Sánchez-González, Chiara Bucciarelli-Ducci, Nina Ajmone Marsan, Zlatko Fras, Jeroen J Bax, Valentin Fuster, Borja Ibáñez, Victoria Delgado

Am J Cardiol 2020;133:39-47

ABSTRACT

Background: The aim of the present study was to investigate the long-term impact of early intravenous metoprolol in ST-segment elevation myocardial infarction (STEMI) patients in terms of left ventricular (LV) strain with feature-tracking cardiovascular magnetic resonance (CMR) and its association with prognosis.

Methods: A total of 270 patients with first anterior STEMI enrolled in the randomized METOCARD-CNIC clinical trial, assigned to receive up to 15 mg intravenous metoprolol before primary percutaneous coronary intervention (PCI) versus conventional STEMI therapy, were included. LV global circumferential (GCS) and longitudinal (GLS) strain were assessed with feature-tracking CMR at 1 week after STEMI in 215 patients. The occurrence of major adverse cardiac events (MACE) at 5-year follow-up was the primary endpoint.

Results: Among 270 patients enrolled, 17 of 139 patients assigned to metoprolol arm and 31 of 131 patients assigned to control arm experienced MACE (HR:0.500, 95%CI:0.277-0.903; P=0.022). Impaired LV GCS and GLS strain were significantly associated with increased occurrence of MACE (GCS: HR:1.208, 95%CI:1.076-1.356, P=0.001; GLS: HR:1.362, 95%CI:1.180-1.573, P<0.001). On multivariable analysis, LV GLS provided incremental prognostic value over late gadolinium enhancement (LGE) and LV ejection fraction (LVEF) (LGE+LVEF chi-square=12.865, LGE+LVEF+GLS chi-square=18.459; P=0.012). Patients with GLS ≥-11.5% (above median value) who received early intravenous metoprolol were 64% less likely to experience MACE than their counterparts with same degree of GLS impairment (HR:0.356, 95%CI:0.129-0.979; P=0.045).

Conclusions: Early intravenous metoprolol has a long-term beneficial prognostic effect, particularly in patients with severely impaired LV systolic function. LV GLS with feature-tracking CMR early after PCI offers incremental prognostic value over conventional CMR parameters in risk stratification of STEMI patients.

INTRODUCTION

The outcome of patients with ST-segment elevation myocardial infarction (STEMI) has significantly improved over the last decades.[1,2] However, STEMI survivors are still at high risk of recurrent cardiovascular events such as congestive heart failure, arrhythmia, and sudden death.[3,4] In the acute phase of STEMI, novel therapeutic approaches aiming at reducing the ischemia-reperfusion injury are being tested.[5,6] The beneficial effect of early intravenous beta-blockade in STEMI population was demonstrated in the Effect of Metoprolol in Cardioprotection During an Acute Myocardial Infarction (METOCARD-CNIC) trial[7,8] and was adopted by current guidelines.[3] Recently, the impact of multidirectional left ventricular (LV) strain with feature-tracking cardiovascular magnetic resonance (CMR) has been studied in STEMI patients.[9-14] Conflicting results with respect to the incremental value of feature-tracking CMR over traditional markers of infarct injury, such as LV ejection fraction (LVEF) and infarct size with late gadolinium enhancement (LGE), have been observed.[9-14] The current analysis aims at addressing three questions: (1) whether early intravenous metoprolol offers a long-term beneficial effect in STEMI patients over a 5-year follow-up, (2) whether LV global circumferential (GCS) and longitudinal (GLS) strain with feature-tracking CMR show incremental prognostic value over conventional CMR parameters in STEMI patients and (3) whether the association between global LV strain and prognosis is modulated by early intravenous metoprolol treatment.

METHODS

Patient population

The METOCARD-CNIC trial was a multicenter, randomized, parallel-group, single-blinded (to outcome evaluators) clinical trial (ClinicalTrials.gov identifier: NCT01311700). The study design and protocol have been previously described.[15] Briefly, a total of 270 patients with first anterior STEMI were randomized to receive up to 15 mg intravenous metoprolol before primary percutaneous coronary intervention versus conventional therapy. Patients presenting with Killip class III to IV acute heart failure, systolic blood pressure persistently <120 mmHg, PR interval >240 milliseconds (or type II–III atrioventricular block), heart rate persistently <60 bpm, or active treatment with any beta-blocker agent were excluded from the trial. All patients, including those in control arm, received oral metoprolol (first dose 12-24 hours after reperfusion). CMR was performed in 220 patients at 1 week (5 to 7 days) after STEMI. There were no differences in demographic variables, cardiovascular risk profile and procedural character-

istics between patients receiving early intravenous metoprolol and the controls.[7] The study was approved by the ethical committees and institutional review boards at each participating center. All eligible patients gave written informed consent.

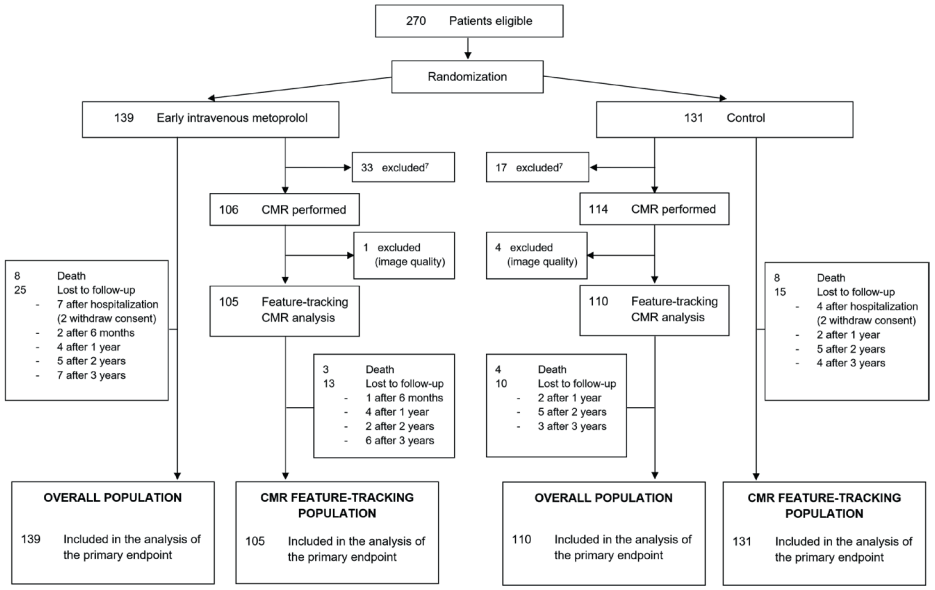

Figure 1: Study flow diagram. CMR = cardiovascular magnetic resonance.

Cardiovascular magnetic resonance data acquisition and conventional analysis

The CMR data acquisition was performed with 1.5 and 3.0 T CMR scanners. The 2-, 3- and 4-chamber views and a stack of contiguous short-axis slices to cover the whole LV were acquired with steady-state free precession functional cine imaging. Data acquisition parameters were: voxel size 1.6×2 mm, slice thickness 8 mm, gap 0 mm, cardiac phases 25-30, TR 3.5, TE 1.7, flip angle 40, SENSE 1.5, averages 1, FOV 360×360 mm. Segmented inversion recovery gradient echo sequence, acquired 10-15 minutes after a cumulative dose of 0.2 mmol/kg intravenous gadolinium contrast agent was employed for myocardial necrosis/fibrosis imaging. CMR data were analyzed with dedicated software (QMass MR 7.5; Medis, Leiden, the Netherlands) as described before.[15] LVEF was determined from the short-axis cine images with LV trabeculations included within the blood pool. LGE was quantified according to full-width-half-maximum method from short-axis delayed enhancement images and expressed as the percent of LV mass. The presence of microvascular obstruction (MVO), defined as hypointense areas within the hyperenhanced zone on LGE images, was evaluated.

Feature-tracking cardiovascular magnetic resonance analysis

Feature-tracking CMR analysis was performed with dedicated software (cvi[42] v5.3, Circle Cardiovascular Imaging, Calgary, Canada). First, the LV endo- and epicardium were manually delineated at end-diastole in short-axis and 2-, 3- and 4-chamber long-axis views. In addition, the anterior right ventricular insertion point, the mitral annulus and the LV apex were defined. Short-axis slices covering the whole LV were included in GCS analysis. Subsequently, the outlined myocardium borders were automatically tracked throughout the cardiac cycle with fully automated feature-tracking analysis. The quality of the myocardium tracking was visually evaluated with manual adjustments of the contours if necessary. Global time-strain curves were obtained and peak GCS and GLS values were recorded.

Clinical endpoints

The primary endpoint of the present analysis was the occurrence of major adverse cardiac events (MACE) at 5-year follow-up after STEMI. MACE was defined as the composite of death, rehospitalization for heart failure, reinfarction and malignant ventricular arrhythmias (ventricular fibrillation, sustained ventricular tachycardia), as in the pre-specified METOCARD-CNIC trial endpoint.[15] Readmissions because of the heart failure were due to heart failure decompensation or due to the indication for implantable cardioverter defibrillator therapy. Clinical follow-up was performed by telephone interview and access to hospital reports. Clinical events for the 2-year follow-up[8] were blindly adjudicated by a committee but the extended follow up events were not adjudicated. Some events were self-reported by the patient and in other cases a discharge report was available. To evaluate the prognostic influence of LV strain on outcomes, only the events occurring after the first CMR scan, i.e. 1 week after STEMI, were included. In particular, all malignant ventricular arrhythmias occurred earlier and were not included in the analysis.

Statistical analysis

Normally distributed continuous variables are presented as mean and standard deviation and compared using independent samples t-tests. Non-normal data are reported as medians, first and third quartiles and were compared with Mann-Whitney U test. Categorical variables are presented as counts and percentages and compared using the Pearson's Chi-square test. For the primary endpoint analysis, patients were censored at the occurrence of the first event. The impact of early intravenous metoprolol in the overall METOCARD-CNIC trial population

was evaluated with Kaplan-Meier method and with Cox proportional hazards regression model. Subsequently, Cox regression analysis was performed in the cohort with available 1-week CMR scan to identify the conventional and feature-tracking CMR variables associated with the primary endpoint. Hazard ratios (HR) and 95% confidence intervals (CI) were calculated and adjusted for demographic and clinical variables. To evaluate the incremental prognostic value of LV GCS and GLS over the conventional CMR parameters, nested regression models were created and the global Chi-square values were compared. To investigate if patient prognosis was modulated by the interaction between global LV strain and early intravenous metoprolol treatment, patients were divided according to the median GCS and GLS values and the randomization status (early intravenous metoprolol vs. control group). The cumulative event rates were estimated using Kaplan-Meier survival curves. In addition, exploratory Cox regression analysis was performed to compare the HR for the occurrence of primary endpoint between individual groups. A two-sided P-value of <0.05 was statistically significant. All statistical analyses were performed using IBM SPSS Statistics 23 (IBM, Armonk, New York).

RESULTS

Impact of early intravenous metoprolol on long-term patient outcome

In the overall METOCARD-CNIC trial population of 270 patients (139 treated with early intravenous metoprolol and 131 with conventional STEMI therapy) 214 patients (79.3%) completed the 5-year follow-up and 48 patients (17.8%) presented with MACE (Figure 1). Patients who received early intravenous metoprolol had fewer cumulative MACE (HR 0.500, 95%CI: 0.277-0.903; P=0.022) and fewer heart failure admissions (HR 0.298, 95%CI: 0.096-0.924; P=0.036) (Table 1). The Kaplan-Meier curves for the occurrence of MACE in both treatment arms are shown in Figure 2.

Table 1: The occurrence of MACE in patients according to the randomization status in the overall METOCARD-CNIC trial population.

	Metoprolol (N=139)	Control (N=131)	HR (95% CI)	P-value
MACE*	17 (12.2%)	31 (23.7%)	0.500 (0.277-0.903)	**0.022**
Death	8 (5.8%)	8 (6.1%)	0.903 (0.339-2.405)	0.838
Cardiac death	3 (2.2%)	6 (4.6%)		
Non-cardiac death†	5 (3.6%)	2 (1.5%)		
HF admission	4 (2.9%)	12 (9.2%)	0.298 (0.096-0.924)	**0.036**
Re-infarction	1 (0.7%)	5 (3.8%)	0.179 (0.021-1.536)	0.117
Malignant ventricular arrhythmia	5 (3.6%)	10 (7.6%)	0.477 (0.163-1.397)	0.177

CI = confidence interval; HF = heart failure; HR = hazard ratio; MACE = major adverse cardiac events.
*A few patients experienced more than 1 event, however in MACE only the first event was included.
†Among non-cardiac deaths 6 were due to cancer and 1 due to hemoptysis (metoprolol group).

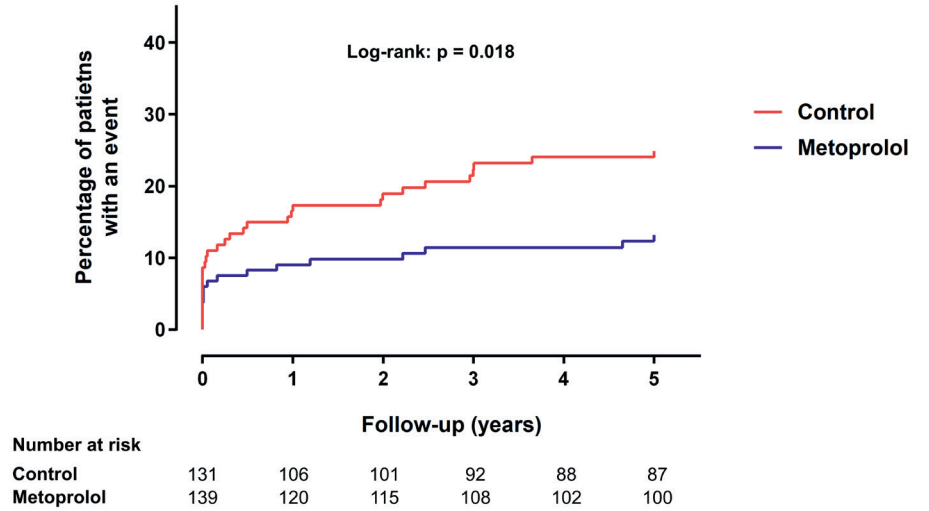

Figure 2: Kaplan Meier estimates for cumulative major adverse cardiac event rates in the overall METOCARD-CNIC trial population.

Prognostic value of LV GCS and GLS with feature-tracking CMR

Among 220 patients who underwent 1-week CMR scan, feature-tracking analysis was feasible in 215 patients (early metoprolol group: N=105 of 106; control group: N=110 of 114) and they formed the population for the LV strain analysis (Figure 1). A total of 185 patients (86.0%) completed the 5-year follow-up and 25 patients (11.6%) presented with MACE. Patients experiencing MACE had higher body mass index, were more often diabetic and had more pronounced LV systolic dysfunction (demonstrated by impaired LVEF, GCS and GLS) and greater infarct size 1

week after STEMI compared to patients without MACE (Table 2). On univariable Cox regression analysis, LV CMR imaging parameters (except for MVO) were significantly associated with the occurrence of the primary endpoint (Table 3). Each 1% increase in LV GCS was associated with 21% increased risk of MACE whereas each 1% increase in LV GLS was associated with 36% increased risk of MACE. After adjusting for demographic and clinical variables, the association between LV GCS and GLS with the occurrence of MACE remained statistically significant (Table 3). Moreover, after adjusting for demographic and clinical variables also MVO was significantly associated with the occurrence of the primary endpoint. To assess the incremental prognostic value of GCS and GLS over conventional CMR parameters, nested regression models were created and global chi-square values were calculated (Figure 3). Adding GLS to a model including LGE and LVEF significantly increased the chi-square value (LGE+LVEF chi-square = 12.865, LGE+LVEF+GLS chi-square = 18.459; P=0.012). In contrast, the addition of LV GCS or MVO to the model including LGE and LVEF did not have statistically significant incremental prognostic value.

Table 2: Clinical and CMR characteristics of patients with feature-tracking CMR analysis.

	Overall (N=215)	MACE (N=25)	No MACE (N=190)	P-value
Age (years)	58.4±11.5	61.8±9.1	57.9±11.7	0.059
Men	187 (87%)	23 (92%)	164 (86%)	0.748
BMI (kg/m²)	27.3 (25.4-29.4)	28.1 (27.5-30.9)	26.7 (25.2-29.3)	**0.006**
Hypertension	84 (39%)	14 (56%)	70 (37%)	0.071
Diabetes mellitus	42 (20%)	9 (36%)	33 (17%)	**0.029**
Smoker*	136 (63%)	15 (60%)	121 (64%)	0.670
LGE (%)	22.0±13.3	28.4±14.1	21.1±13.0	**0.009**
Presence of MVO	126 (59%)	19 (76%)	107 (56%)	0.068
LVEF (%)	44.9±9.8	38.6±9.3	45.8±9.5	**0.001**
LV GCS (%)	-13.5±4.0	-11.2±4.3	-13.8±3.9	**0.002**
LV GLS (%)	-11.6±3.2	-9.1±3.0	-11.9±3.1	**<0.001**

BMI = body mass index; GCS = global circumferential strain; GLS = global longitudinal strain; LGE = late gadolinium enhancement; LVEF = left ventricular ejection fraction; MACE = major adverse cardiac event; MVO = microvascular obstruction.
Values are mean±SD, median (interquartile range) or n (%).
*Smoker was defined as current or quitted <10 years ago.

Table 3: Clinical and CMR variables as predictors of the primary endpoint in patients with feature-tracking CMR analysis.

	Univariable analysis			Multivariable analysis*		
	HR	95%CI	P-value	HR	95%CI	P-value
Age (years)	1.026	0.991-1.063	0.140			
Men	1.696	0.400-7.195	0.473			
BMI (kg/m²)	1.118	1.023-1.222	**0.014**			
Hypertension	2.088	0.948-4.599	0.068			
Diabetes mellitus	2.537	1.121-5.743	**0.025**			
Smoker†	0.831	0.373-1.850	0.650			
LGE (%)	1.040	1.009-1.071	**0.010**	1.046	1.014-1.078	**0.004**
Presence of MVO	2.261	0.903-5.662	0.081	2.801	1.081-7.257	**0.034**
LVEF (%)	0.922	0.882-0.965	**<0.001**	0.908	0.868-0.951	**<0.001**
GCS (%)	1.208	1.076-1.356	**0.001**	1.228	1.094-1.378	**<0.001**
GLS (%)	1.362	1.180-1.573	**<0.001**	1.372	1.184-1.589	**<0.001**

BMI = body mass index; CI = confidence interval; GCS = global circumferential strain; GLS = global longitudinal strain; HR = hazard ratio; LGE = late gadolinium enhancement; LVEF = left ventricular ejection fraction; MVO = microvascular obstruction.
*CMR variables were adjusted for demographic and clinical parameters (age, sex, BMI, hypertension, diabetes mellitus, smoking status).
†Smoker was defined as current or quitted <10 years ago.

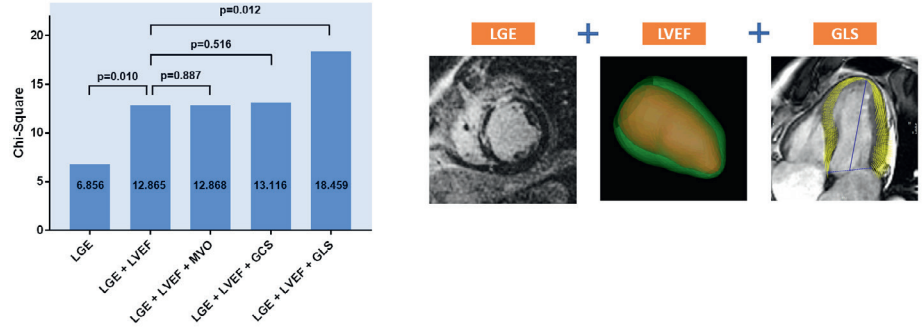

Figure 3: Incremental prognostic value of left ventricular strain with feature-tracking CMR. Bar graphs illustrate the prognostic value of cardiovascular magnetic resonance (CMR) imaging parameters for the assessment of the occurrence of major adverse cardiac events, displayed by chi-square values on the y-axis. GCS = global circumferential strain; GLS = left ventricular global longitudinal strain; LGE = late gadolinium enhancement; LVEF = left ventricular ejection fraction; MVO = microvascular obstruction.

Impact of early intravenous metoprolol on the prognostic value of LV GCS and GLS

To explore the interaction between LV GCS and GLS and the effect of early intravenous metoprolol, 215 patients with 1-week CMR feasible for feature-tracking analysis (the LV strain population) were divided into 4 groups according to the median LV GCS (-13.1%; interquartile

range -10.0 to -16.5%) and GLS values (-11.5%; interquartile range -9.4 to -13.4%) and the randomization status (early intravenous metoprolol vs conventional therapy). The crude event rates in each patient group are presented in Table 4. The Kaplan–Meier curves show significant differences between groups for the cumulative MACE (Figure 4). Patients with more impaired strain who were treated with conventional STEMI therapy had the highest event rates while the differences between other 3 groups were less pronounced. In the exploratory subgroup analysis, patients with more impaired GLS (≥-11.5%) who received early intravenous metoprolol were 64% less likely to experience MACE (HR 0.356, 95%CI: 0.129-0.979; P=0.045) than their counterparts with same degree of GLS impairment but receiving conventional STEMI therapy. A similar, but not statistically significant trend was observed for patients with more impaired GCS (≥-13.1%) (HR for early metoprolol treatment 0.400, 95%CI: 0.132-1.216; P=0.106).

Table 4: The occurrence of MACE in patients according to the median GCS and GLS and the randomization status.

	GCS ≥ -13.1%		GCS < -13.1%	
	Control (N=65)	Metoprolol (N=42)	Control (N=45)	Metoprolol (N=63)
MACE*	14 (21.5%)	4 (9.5%)	4 (8.9%)	3 (4.8%)
Death	3 (4.6%)	1 (2.4%)	1 (2.2%)	2 (3.2%)
Cardiac death	3 (4.6%)	0	0	0
Non-cardiac death†	0	1 (2.4%)	1 (2.2%)	2 (3.2%)
HF admission	9 (13.8%)	3 (7.1%)	1 (2.2%)	1 (1.6%)
Re-infarction	3 (4.6%)	0	2 (4.4%)	0
	GLS ≥ -11.5%		**GLS < -11.5%**	
	Control (N=58)	**Metoprolol (N=49)**	**Control (N=52)**	**Metoprolol (N=56)**
MACE*	15 (25.9%)	5 (10.2%)	3 (5.8%)	2 (3.6%)
Death	3 (5.2%)	1 (2.0%)	1 (1.9%)	2 (3.6%)
Cardiac death	3 (5.2%)	0	0	0
Non-cardiac death†	0	1 (2.0%)	1 (1.9%)	2 (3.6%)
HF admission	10 (17.2%)	4 (8.2%)	0	0
Re-infarction	3 (5.2%)	0	2 (3.8%)	0

GCS = global circumferential strain; GLS = global longitudinal strain; HF = heart failure; MACE = major adverse cardiac event.
*One patient in the impaired GCS/GLS group treated with conventional therapy experienced 2 events, however in MACE only the first event was included.
†All 4 non-cardiac deaths were due to cancer.

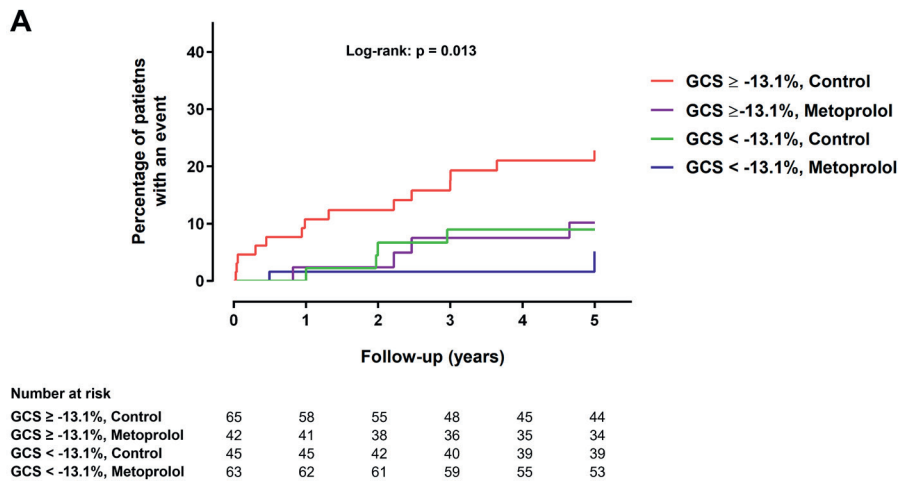

Figure 4: Kaplan Meier estimates for cumulative major adverse cardiac event rates according to the global left ventricular strain and the randomization status. (A) Patients were divided according to the global left ventricular circumferential strain (GCS) ≥-13.1% (more impaired) vs. <-13.1% (more preserved) and the treatment group (early intravenous metoprolol vs. control group). **(B)** Patients were divided according to the global left ventricular longitudinal strain (GLS) ≥-11.5% (more impaired) vs. <-11.5% (more preserved) and the treatment group.

DISCUSSION

The present study demonstrated that: (1) early intravenous metoprolol has a long-term beneficial prognostic value in STEMI patients, (2) LV GLS measured with feature-tracking CMR early after STEMI provides incremental prognostic value over LVEF and infarct size assessed with

LGE and (3) the association between GCS, GLS and prognosis is modulated by early intravenous metoprolol treatment with the majority of MACE occurring in patients with impaired LV strain treated with conventional STEMI therapy.

Long-term prognostic value of early intravenous metoprolol in STEMI

The METOCARD-CNIC trial was the first randomized control trial in the modern era of primary PCI in STEMI that evaluated the cardioprotective effect of intravenous beta-blockers.[7] Early intravenous administration of metoprolol (prior to primary PCI) was associated with significant reduction of primary endpoint, the infarct size measured with LGE CMR 1 week after STEMI.[7] In addition, early intravenous metoprolol administration was associated with a non-significant trend towards reduced occurrence of pre-specified MACE (10.8% in the metoprolol group versus 18.3% in the control group; P=0.065) and a significant reduction in heart failure readmissions (2.2% in the metoprolol group versus 6.9% in the control group; P=0.046) at a median follow-up of 2 years.[8] In the present article the impact of early intravenous metoprolol treatment in the METOCARD-CNIC trial population was re-investigated with extended 5-year follow-up data and significant reduction in both, MACE as well as heart failure readmissions, was demonstrated. In addition, we have previously shown that patients who received early intravenous metoprolol had more preserved global LV strain and infarct zone circumferential strain after STEMI.[16,17] However, in the present analysis we have demonstrated that patients with impaired LV strain, particularly those with impaired GLS, who were treated with early intravenous metoprolol had lower adverse event rates than their counterparts with same degree of LV strain impairment but receiving conventional STEMI therapy. These results strengthen our current evidence of the beneficial long-term prognostic effect of early intravenous metoprolol in STEMI patients with primary PCI and without contraindications to beta-blockers.

Prognostic value of LV GCS and GLS with feature-tracking CMR

In recent years, several CMR techniques have emerged to assess regional and global LV systolic function in patients with acute myocardial infarction.[18] Among these techniques, feature-tracking CMR has gained prominence as a fast and accurate modality for the assessment of LV strain using standard cine images. Recently, the association between multidirectional LV strain with feature-tracking CMR after myocardial infarction and patients outcome has been explored in 4 large patient cohorts.[9-12] Eitel *et al.*[9] included 1107 patients after myocardial infarction and demonstrated an incremental prognostic value of LV GLS for all-cause mortality

but not for the occurrence of MACE, over LVEF and infarct size. Gavara *et al.*[10] studied 323 patients after STEMI and showed that LV GLS rather than GCS or global radial strain was an independent predictor of MACE. However, in the multivariable models including clinical and CMR variables GLS did not significantly improve patients risk reclassification. Yoon *et al.*[11] and Reindl *et al.*[12] demonstrated incremental prognostic value of GLS with feature-tracking CMR over LVEF and CMR markers of infarct severity for the occurrence of MACE in in 247 STEMI and 451 STEMI patients, respectively. Similarly, our results show that both impaired LV GCS and GLS were strong predictors of adverse cardiac events after myocardial infarction and LV GLS analysis provided incremental prognostic value over conventional CMR parameters. Compared to the other studies, the patient population in our study was homogenous, consisting of anterior STEMI patients without signs of acute heart failure, prospectively included in the multi-center randomized controlled clinical trial.[7]

Why LV GLS provides incremental prognostic value over conventional CMR parameters of myocardial damage after STEMI and LV GCS does not?

The different prognostic value of LV GLS and GCS might be the explained by the difference in LV mechanics described by both indices. During acute myocardial infarction myocardial cell injury spreads from the endocardium to the epicardium with increasing duration of coronary occlusion and severity of ischemia; the so-called 'wavefront phenomenon of myocardial death'.[19] Since the majority of longitudinally-oriented myocardial fibers are located in the subendocardium[20] the LV longitudinal systolic function becomes impaired first. On the other hand, the circumferential myocardial fibers that are found in the LV midwall[20] require a greater degree of transmural myocardial injury to impact on circumferential shortening. We may reasonably assume that impaired LV GCS reflects more severe myocardial injury and as such provides similar prognostic information to other CMR parameters. On the other hand, the ability of LV GLS to account for the subendocardial infarct injury suggests that this parameter is a more sensitive marker of LV systolic dysfunction that adds additional prognostic information above other CMR parameters.

Study limitations

Feature-tracking is a novel technique to assess LV strain with CMR. Standardization of feature-tracking analysis as well as the reference values for LV strain and the agreement across various vendors of feature-tracking software are not established.[21] Furthermore, the evalua-

tion of LV strain was not a predefined study endpoint of the METOCARD-CNIC trial. A limited number of events occurred during 5-year follow-up of patients included in the METOCARD clinical trial, which makes multivariable testing challenging, especially in the subgroup analysis. Of the initial 220 patients who underwent 1-week CMR study in the METOCARD-CNIC trial, 5 patients were excluded from the LV strain analysis due to poor CMR cine image quality (arrhythmias, metallic artefacts) which may have influenced our results. However, 98% feasibility of strain assessment with feature-tracking CMR is similar to what has been described before.[22,23] In addition, excellent intra- and inter-observer reproducibility of feature-tracking analysis in our institution have been reported.[16]

CONCLUSION

Early intravenous metoprolol has a long-term beneficial prognostic effect, particularly in patients who were at a greater risk for the occurrence of MACE due to severely impaired LV systolic function. Moreover, global LV strain assessment with feature-tracking CMR early after primary PCI provides important information in risk stratification of STEMI patients. LV GLS offers incremental prognostic value over traditional markers of LV injury, such as LVEF and infarct size with LGE.

REFERENCES

1. Puymirat E, Simon T, Cayla G, Cottin Y, Elbaz M, Coste P *et al.* Acute Myocardial Infarction: Changes in Patient Characteristics, Management, and 6-Month Outcomes Over a Period of 20 Years in the FAST-MI Program (French Registry of Acute ST-Elevation or Non-ST-Elevation Myocardial Infarction) 1995 to 2015. *Circulation* 2017;136(20):1908-19.
2. Szummer K, Wallentin L, Lindhagen L, Alfredsson J, Erlinge D, Held C *et al.* Improved outcomes in patients with ST-elevation myocardial infarction during the last 20 years are related to implementation of evidence-based treatments: experiences from the SWEDEHEART registry 1995-2014. *Eur Heart J* 2017;38(41):3056-65.
3. Ibanez B, James S, Agewall S, Antunes MJ, Bucciarelli-Ducci C, Bueno H *et al.* 2017 ESC Guidelines for the management of acute myocardial infarction in patients presenting with ST-segment elevation: The Task Force for the management of acute myocardial infarction in patients presenting with ST-segment elevation of the European Society of Cardiology (ESC). *Eur Heart J* 2018;39(2):119-77.
4. O'Gara PT, Kushner FG, Ascheim DD, Casey DE, Jr., Chung MK, de Lemos JA *et al.* 2013 ACCF/AHA guideline for the management of ST-elevation myocardial infarction: executive summary: a report of the American College of Cardiology Foundation/American Heart Association Task Force on Practice Guidelines. *J Am Coll Cardiol* 2013;61(4):485-510.
5. Yellon DM, Hausenloy DJ. Myocardial reperfusion injury. *N Engl J Med* 2007;357(11):1121-35.
6. Ibanez B, Heusch G, Ovize M, Van de Werf F. Evolving therapies for myocardial ischemia/reperfusion injury. *J Am Coll Cardiol* 2015;65(14):1454-71.
7. Ibanez B, Macaya C, Sanchez-Brunete V, Pizarro G, Fernandez-Friera L, Mateos A *et al.* Effect of early metoprolol on infarct size in ST-segment-elevation myocardial infarction patients undergoing primary percutaneous coronary intervention: the Effect of Metoprolol in Cardioprotection During an Acute Myocardial Infarction (METOCARD-CNIC) trial. *Circulation* 2013;128(14):1495-503.
8. Pizarro G, Fernandez-Friera L, Fuster V, Fernandez-Jimenez R, Garcia-Ruiz JM, Garcia-Alvarez A *et al.* Long-term benefit of early pre-reperfusion metoprolol administration in patients with acute myocardial infarction: results from the METOCARD-CNIC trial (Effect of Metoprolol in Cardioprotection During an Acute Myocardial Infarction). *J Am Coll Cardiol* 2014;63(22):2356-62.
9. Eitel I, Stiermaier T, Lange T, Rommel KP, Koschalka A, Kowallick JT *et al.* Cardiac Magnetic Resonance Myocardial Feature Tracking for Optimized Prediction of Cardiovascular Events Following Myocardial Infarction. *JACC Cardiovasc Imaging* 2018;11(10):1433-44.

10. Gavara J, Rodriguez-Palomares JF, Valente F, Monmeneu JV, Lopez-Lereu MP, Bonanad C *et al.* Prognostic Value of Strain by Tissue Tracking Cardiac Magnetic Resonance After ST-Segment Elevation Myocardial Infarction. *JACC Cardiovasc Imaging* 2018;11(10):1448-57.
11. Yoon YE, Kang SH, Choi HM, Jeong S, Sung JM, Lee SE *et al.* Prediction of infarct size and adverse cardiac outcomes by tissue tracking-cardiac magnetic resonance imaging in ST-segment elevation myocardial infarction. *Eur Radiol* 2018;28(8):3454-63.
12. Reindl M, Tiller C, Holzknecht M, Lechner I, Beck A, Plappert D *et al.* Prognostic Implications of Global Longitudinal Strain by Feature-Tracking Cardiac Magnetic Resonance in ST-Elevation Myocardial Infarction. *Circ Cardiovasc Imaging* 2019;12(11):e009404.
13. Mangion K, Carrick D, Clerfond G, Rush C, McComb C, Oldroyd KG *et al.* Predictors of segmental myocardial functional recovery in patients after an acute ST-Elevation myocardial infarction. *Eur J Radiol* 2019;112:121-9.
14. Nucifora G, Muser D, Tioni C, Shah R, Selvanayagam JB. Prognostic value of myocardial deformation imaging by cardiac magnetic resonance feature-tracking in patients with a first ST-segment elevation myocardial infarction. *Int J Cardiol* 2018;271:387-91.
15. Ibanez B, Fuster V, Macaya C, Sanchez-Brunete V, Pizarro G, Lopez-Romero P *et al.* Study design for the "effect of METOprolol in CARDioproteCtioN during an acute myocardial InfarCtion" (METOCARD-CNIC): a randomized, controlled parallel-group, observer-blinded clinical trial of early pre-reperfusion metoprolol administration in ST-segment elevation myocardial infarction. *Am Heart J* 2012;164(4):473-80.e5.
16. Podlesnikar T, Pizarro G, Fernandez-Jimenez R, Montero-Cabezas JM, Sanchez-Gonzalez J, Bucciarelli-Ducci C *et al.* Effect of Early Metoprolol During ST-Segment Elevation Myocardial Infarction on Left Ventricular Strain: Feature-Tracking Cardiovascular Magnetic Resonance Substudy From the METOCARD-CNIC Trial. *JACC Cardiovasc Imaging* 2019;12(7 Pt 1):1188-98.
17. Podlesnikar T, Pizarro G, Fernández-Jiménez R, Montero-Cabezas JM, Greif N, Sánchez-González J *et al.* Left ventricular functional recovery of infarcted and remote myocardium after ST-segment elevation myocardial infarction (METOCARD-CNIC randomized clinical trial substudy). *J Cardiovasc Magn Reson* 2020;22(1):44.
18. Mangion K, McComb C, Auger DA, Epstein FH, Berry C. Magnetic Resonance Imaging of Myocardial Strain After Acute ST-Segment-Elevation Myocardial Infarction: A Systematic Review. *Circ Cardiovasc Imaging* 2017;10(8).
19. Reimer KA, Lowe JE, Rasmussen MM, Jennings RB. The wavefront phenomenon of ischemic cell death. 1. Myocardial infarct size vs duration of coronary occlusion in dogs. *Circulation* 1977;56(5):786-94.

20. Greenbaum RA, Ho SY, Gibson DG, Becker AE, Anderson RH. Left ventricular fibre architecture in man. *Br Heart J* 1981;45(3):248-63.
21. Amzulescu MS, De Craene M, Langet H, Pasquet A, Vancraeynest D, Pouleur AC *et al.* Myocardial strain imaging: review of general principles, validation, and sources of discrepancies. *European heart journal cardiovascular Imaging* 2019;20(6):605-19.
22. Augustine D, Lewandowski AJ, Lazdam M, Rai A, Francis J, Myerson S *et al.* Global and regional left ventricular myocardial deformation measures by magnetic resonance feature tracking in healthy volunteers: comparison with tagging and relevance of gender. *J Cardiovasc Magn Reson* 2013;15:8.
23. Andre F, Steen H, Matheis P, Westkott M, Breuninger K, Sander Y *et al.* Age- and gender-related normal left ventricular deformation assessed by cardiovascular magnetic resonance feature tracking. *J Cardiovasc Magn Reson* 2015;17:25.

Part II

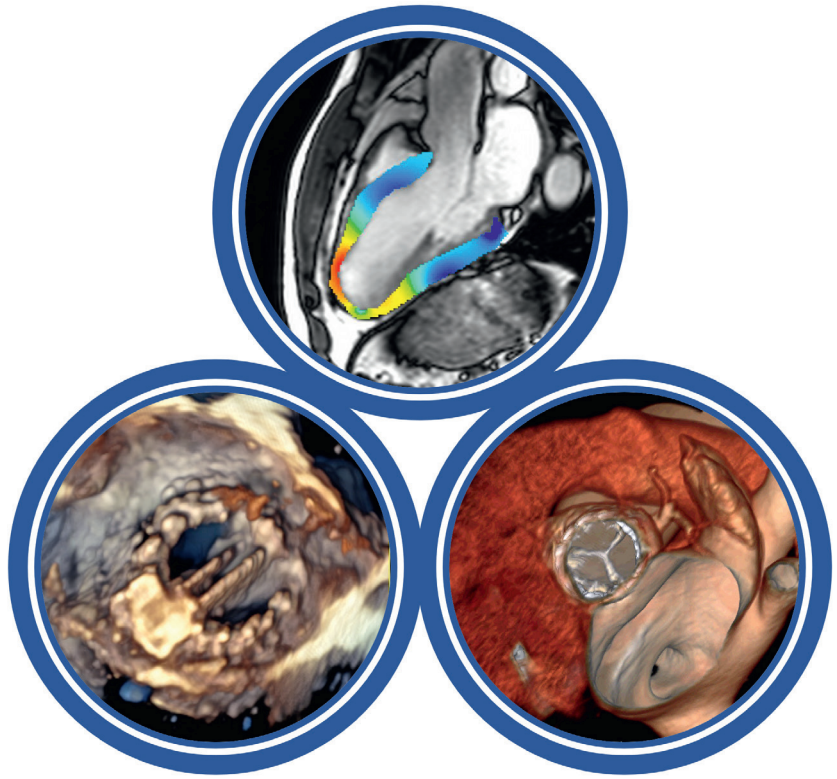

Multimodality Cardiac Imaging in Valvular Heart Disease

5

Imaging of valvular heart disease in heart failure

Tomaž Podlesnikar, Victoria Delgado, Jeroen J Bax

Card Fail Rev 2018;4(2):78-86

ABSTRACT

Valvular heart disease (VHD) and heart failure (HF) are major health issues that are steadily increasing in prevalence in Western populations. VHD and HF frequently co-exist, which can complicate the accurate diagnosis of the severity of valve stenosis or regurgitation and affect decisions about therapeutic options. Transthoracic echocardiography is the first-line imaging modality to determine left ventricular (LV) systolic function, to grade valvular stenosis or regurgitation and to characterize the mechanism underlying valvular dysfunction. 3D transesophageal echocardiography, cardiovascular magnetic resonance and cardiac computed tomography are alternative imaging modalities that help in the diagnosis of patients with HF and VHD. The integration of multimodality cardiovascular imaging is important when deciding whether the patient should receive transcatheter valve repair and replacement therapies. In this article, the use of multimodality imaging to diagnose and treat patients with VHD and HF is reviewed.

INTRODUCTION

Heart failure (HF) is a rapidly growing public health problem with an estimated prevalence of more than 26 million people worldwide.[1] In developed countries the prevalence is 1–2% peaking at ≥10% among people aged over 70 years.[2] In the United States, the lifetime risk of developing HF is 20% among individuals aged 40 years old or older.[3] Diagnosing the underlying cause of HF is central to the choice of appropriate treatment. Significant valvular heart disease (VHD; moderate and severe) was found in 14% of patients who were referred for echocardiography due to suspected HF.[4] Among patients with moderate and severe native VHD included in the Euro Heart Survey, 69.8% presented with HF symptoms and the most frequent valvular lesions were aortic stenosis (AS) and mitral regurgitation (MR).[5]

Cardiac imaging plays a central role in determining the mechanism and the severity of VHD as well as the degree of accompanying left ventricular (LV) remodeling and systolic dysfunction. The primary dilemma in patients with VHD and HF is to determine whether the LV dysfunction is due to the disease of the valve or the ventricle. In patients with AS and HF symptoms, LV systolic dysfunction is usually secondary to the valve disease, while in patients with HF and functional MR, LV systolic dysfunction and remodeling are primary and are responsible for mitral valve malcoaptation. Furthermore, LV dimensions and ejection fraction (LVEF) are key parameters to indicate the need for valve surgery.[6-8] With advances in percutaneous valve interventions – transcatheter aortic valve replacement (TAVR) and percutaneous transcatheter mitral valve repair, several other imaging parameters need to be evaluated to assess feasibility and predict therapeutic success. Echocardiography is the primary imaging modality and may be complemented by cardiac computed tomography (CT) and cardiovascular magnetic resonance (CMR) when additional anatomical or functional information is needed. This review article focuses on the use multimodality imaging to evaluate patients with HF and most frequent VHD – MR and AS – and how to decide the optimal intervention.

MITRAL REGURGITATION IN HEART FAILURE

Significant (moderate and severe) MR is among the most common VHD, with an estimated prevalence of 1.7% in the United States peaking at 9.3% in people older than 75 years of age.[9] In a study involving 70,043 patients with suspected HF referred for echocardiography, MR of any severity was found in 12.5% and moderate or severe MR in 3.1% of patients.[4] MR is classified as primary (organic) if there is primary structural abnormality of any component of the

mitral valve apparatus (leaflets, chordae tendineae, papillary muscles or mitral annulus). The most common etiologies include degenerative disease, rheumatic disease and endocarditis.[10,11] In contrast, secondary (functional) MR results from LV dilation and dysfunction whereas the components of the mitral valve were originally normal. The main causes of secondary MR are ischemic heart disease and dilated cardiomyopathy.[10,11]

Patients with severe primary MR commonly present with no or minimal symptoms.[12] In contrast, HF is always present in secondary MR.[13] In a large retrospective study including 1,256 patients with ischemic and non-ischemic cardiomyopathy, any grade of secondary MR was present in 73% and 24% had severe MR.[13]

Patients with HF and significant MR are usually evaluated using transthoracic and transesophageal echocardiography. The underlying mechanism (primary versus secondary) and the severity of MR are systematically analyzed. Grading of MR is based on a multiparametric approach which includes qualitative, semiquantitative and quantitative parameters (Table 1).[6,10] It is important to note that the evaluation of MR severity is significantly influenced by the LV loading conditions and the systemic blood pressure.[14] In patients with HF, decreased transmitral pressure gradients – due to lower systemic blood pressure and high left atrial (LA) pressures – result in lower velocity regurgitant jets, which appear small on Doppler color flow images. Furthermore, vena contracta and flow convergence assume circular geometry at the regurgitant jet orifice. In secondary MR, the regurgitant orifice is frequently crescent in shape, and vena contracta, regurgitant volume and effective regurgitant orifice area (EROA) calculated using the proximal isovelocity surface area (PISA) method may therefore significantly underestimate the severity of MR.[10,11]

Table 1: Echocardiographic criteria for the definition of severe mitral regurgitation.

	Signs of severe MR		Strengths	Limitations
	Primary	Secondary		
QUALITATIVE				
Valve morphology	Flail leaflet, ruptured papillary muscle, severe retraction, large perforation	Severe tenting, poor leaflet coaptation	• 3D echocardiography provides detailed views of the MV, including surgical view	• Absence of specific signs does not exclude severe MR
LV and LA size	Dilated		• Normal size almost excludes severe chronic primary MR	• Nonspecific in secondary MR • Can be within the normal range in acute severe MR or in smaller people
Color flow regurgitant jet*	Large central jet or eccentric wall-impinging jet of variable size		• Rapid qualitative assessment • Good for screening for MR • Evaluates the spatial orientation of the regurgitant jet	• Dependent on hemodynamic and technical variables • May underestimate the severity in eccentric jets
Continuous wave Doppler signal of regurgitant jet	Holosystolic, dense, triangular		• Easy to use	• Triangular signal is insensitive • Signal density is gain dependent
Flow convergence	Large throughout systole (≥1 cm at a Nyquist limit of 30-40 cm/sec)		• Rapid qualitative assessment • Can be used in eccentric jets • Absence of PISA is usually a sign of mild MR	• PISA size is affected by • Multiple jets • Non-circular regurgitant orifices (common in secondary MR) • non-holosystolic MR
SEMIQUANTITATIVE				
Vena contracta width (mm)*	≥7 (>8 for average between apical two- and four-chamber views)		• Less dependent on hemodynamic and technical factors (e.g. pulse repetition frequency) • Can be applied in eccentric jets	• Challenging in • Multiple jets • Non-circular regurgitant orifices (common in secondary MR) • Non-holosystolic MR
Pulmonary vein flow	Minimal to no systolic flow/systolic flow reversal		• Systolic flow reversal in ≥1 pulmonary vein is specific for severe MR	• Insensitive • Not accurate if MR jet is directed into the sampled vein • Blunting of the systolic wave in AF, elevated LA pressure
Mitral inflow	E-wave dominant (≥1.5 m/s[6]; ≥1.2 m/s[10])		• Easy to use • Dominant A-wave inflow pattern virtually excludes severe MR	• Non-specific (high E waves in secondary MR, AF and MS)
QUANTITATIVE				
2D EROA (mm2)†	≥40	≥20[6]	• PISA method • Main method of MR quantification • Practical calculation • Can be used in eccentric jets • Volumetric method • Valid with multiple and eccentric jets • Valid in non-holosystolic MR	• PISA method • PISA size affected by several factors (see flow convergence) • Error in PISA radius is squared • Volumetric method • Not valid for in concomitant AR • Cumbersome, training needed • Errors in measurements can combine in the final results
Regurgitant volume (mL)†	≥60	≥30[6]		
Regurgitant fraction (%)[10]	≥50		• Accounts for low-flow conditions (common in secondary MR)	• Errors in measurements of each parameter (regurgitant volume, LV end-diastolic volume) can magnify in the final results

2D = 2-dimensional; 3D = 3-dimensional; AF = atrial fibrillation; AR = aortic regurgitation; CW = continuous wave; EROA = effective regurgitant orifice area; LA = left atrium; LV = left ventricle; MR = mitral stenosis; MR = mitral regurgitation; MV = mitral valve; PISA = proximal isovelocity surface area.

*At a Nyquist limit 50-70 cm/sec.

†European guidelines recommend lower thresholds values for severe secondary MR compared with the American guidelines.

Source: Baumgartner *et al.*[6]; Zoghbi *et al.*[10]

With the development of 3-dimensional (3D) echocardiography, the vena contracta area can be directly visualized using multiplanar reformation planes across the regurgitant orifice and measured by planimetry (Figure 1). Zeng *et al.*[15] proposed definition of severe MR to have

a cut-off value of 3D vena contracta area ≥0.41 cm^2. In patients with functional MR, the 3D vena contracta area has been shown to be significantly larger than the 2-dimensional PISA-derived EROA (0.39±0.17 cm^2 versus 0.27±0.11 cm^2, respectively; P<0.001), resulting in an average 27% underestimation of the EROA by the PISA method compared with the 3D vena contracta area.[15]

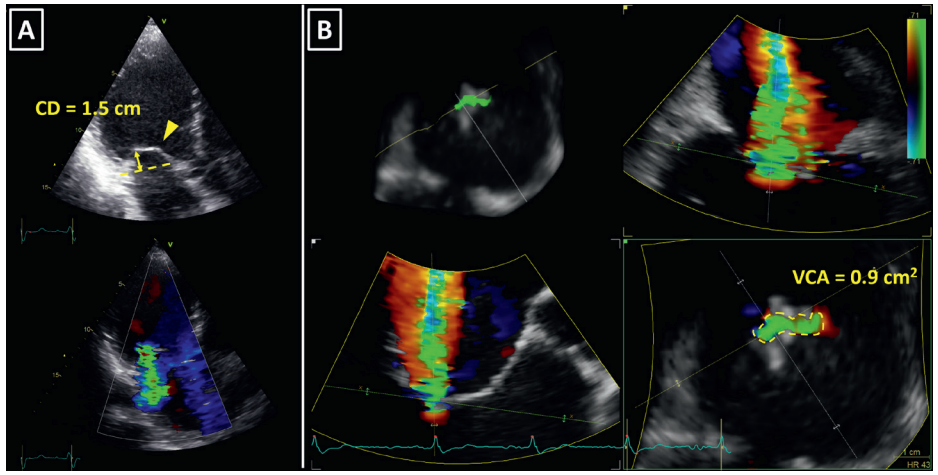

Figure 1: 3-dimensional vena contracta area in secondary mitral regurgitation. (A) Apical left ventricular long axis view, showing restriction and severe tenting of both mitral valve leaflets (upper image); the coaptation depth (CD, yellow arrow) was 1.5 cm and the bend in the body of the anterior mitral leaflet (yellow arrowhead) demonstrated tethering by the secondary chordae (known as the ''seagull'' or ''hockey stick'' sign). Bottom image shows prominent color flow Doppler regurgitant jet. **(B)** Multi-planar reconstruction of the 3-dimensional color flow Doppler dataset across the regurgitant orifice. Note the highly crescentic shape of the vena contracta (bottom right image), which involved the whole coaptation line from the anterolateral to the posteromedial mitral valve commissure. 3-dimensional vena contracta area (VCA) of 0.9 cm^2 (yellow dotted line) was in the range of severe mitral regurgitation.[15]

The assessment of the severity of MR with color flow Doppler echocardiography is based on instantaneous peak flow rates and is therefore reliable only when there is little temporal variation of MR during the cardiac cycle. However, secondary MR is often dynamic, peaking in early and late systole and improves during mid systole when LV pressures are at their maximum.[16] In such circumstances, MR should be quantified with volumetric methods, which account for the whole systole. In the absence of aortic regurgitation or intracardiac shunt, the difference between stroke volume measured at the mitral annulus (LV inflow) and the LV outflow tract (LV outflow) equals MR volume. Volumetric method is frequently used with CMR.[6,7] The preferred method to quantify MR with CMR is to use phase contrast CMR to subtract the aortic forward flow from the LV stroke volume, assessed by planimetry of the LV short-axis cine images (Figure 2).[10]

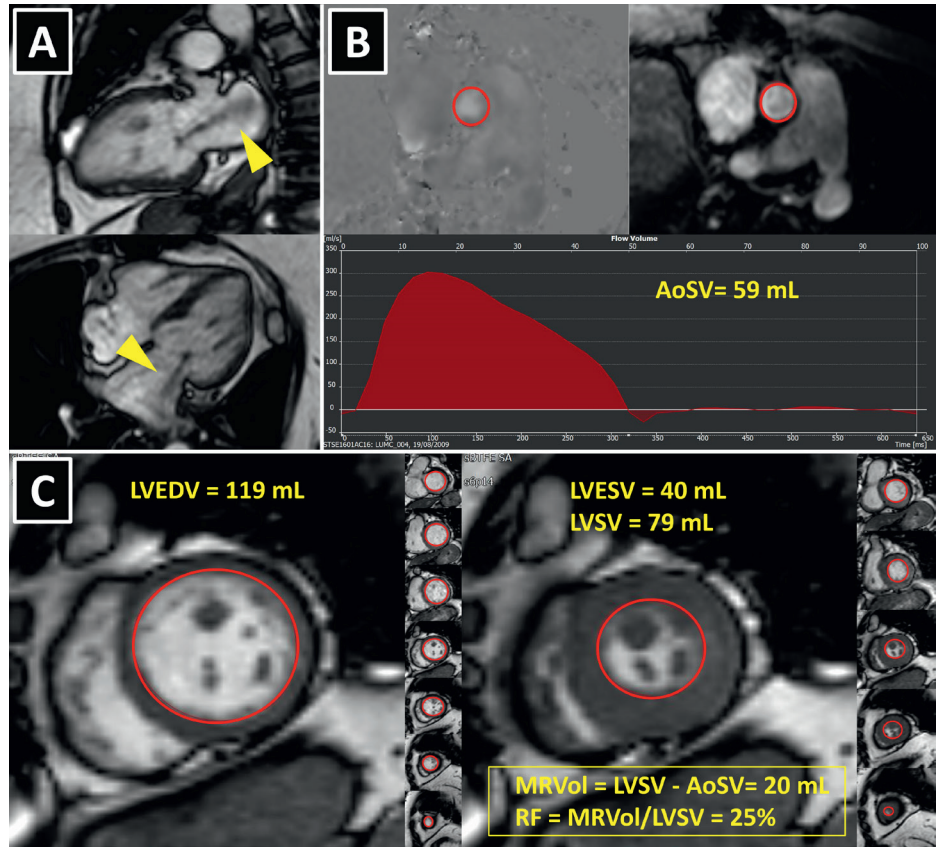

Figure 2: Cardiovascular magnetic resonance to quantify mitral regurgitation. A 74-year-old patient with heart failure symptoms had inconsistent grading of the severity of mitral regurgitation (MR) with echocardiography and was referred for cardiovascular magnetic resonance (CMR). **(A)** Left ventricular systolic cine images show prominent MR jet (yellow arrowheads). MR was caused by mitral annular dilatation, secondary to severe left atrial dilatation. The patient had a long-lasting history of paroxysmal atrial fibrillation. **(B)** Left ventricular *forward* stroke volume (AoSV) was measured with phase contrast CMR in the ascending aorta, just above the aortic valve. **(C)** *Total* left ventricular stroke volume (LVSV) was obtained using planimetry of the short-axis cine images as the difference between left ventricular end-diastolic volume (LVEDV; left image) and left ventricular end-systolic volume (LVESV; right image). Since the patient had no aortic regurgitation the difference between the LVSV and AoSV was equal to mitral regurgitant volume (MRVol). The regurgitant fraction (RF) was calculated by dividing MRvol by LVSV. The results (MRVol 20 mL, RF 25%) clearly ruled out severe MR, which was further supported by normal left ventricular volumes.

SELECTING INTERVENTIONS FOR MITRAL REGURGITATION

After establishing the diagnosis of symptomatic severe secondary MR, the type of valve intervention is based upon the degree of LV functional impairment, evidence of myocardial

viability and the ability to perform revascularization. When revascularization is indicated, surgical intervention should be considered.[6,8] However, the preferred type of surgical treatment, i.e. mitral valve repair by means of restrictive annuloplasty or chordal-sparing valve replacement, is not agreed upon. European guidelines recommend mitral valve repair as the preferred method, while mitral valve replacement may be considered in patients with echocardiographic risk factors for residual or recurrent MR (Table 2).[6,17] In contrast, American guidelines recommend chordal-sparing mitral valve replacement for severely symptomatic patients (New York Heart Association Class III to IV) with chronic severe ischemic MR.[8] This recommendation is based on the results of a randomized control trial that showed a higher rate of moderate or severe MR recurrence at 2 years follow-up in patients who underwent mitral valve repair compared with patients who underwent chordal-sparing mitral valve replacement (58.8% versus 3.8%, P<0.001), leading to higher incidence of HF and repeat hospitalizations in the mitral valve repair group.[18] When revascularization is not indicated, the decision between surgery and percutaneous edge-to-edge repair is made based on the degree of LV dysfunction and the surgical risk. When the surgical risk is low and LVEF >30%, surgery may be considered, while percutaneous edge-to-edge repair is preferred for patients presenting with high surgical risk or LVEF <30% despite optimal medical management (including pharmacological treatment and cardiac resynchronization therapy).[6] In the United States, percutaneous edge-to-edge repair is currently not approved for clinical use in secondary MR.[8]

For successful surgical and percutaneous mitral valve repair in secondary MR, accurate LV assessment, including LV volumes, LVEF and sphericity index, is mandatory, accompanied by geometric assessment of the MV apparatus (tenting area, coaptation depth, leaflet angles, and inter-papillary muscle distance). Transthoracic and transesophageal echocardiography are the primary modalities; however, detailed information can also be obtained with cardiac CT and CMR. Table 2 summarizes the echocardiographic criteria that suggest increased risk of MR recurrence after mitral valve repair as well as unfavorable anatomical conditions for percutaneous edge-to-edge repair with a MitraClip device (Abbott Vascular, Menlo Park, CA, US).[17] In patients with secondary MR who are undergoing surgery, successful repair is less likely in the presence of severe mitral valve tethering with coaptation depth >1 cm, systolic tenting area >2.5 cm^2, posterior mitral leaflet angle >45° and distal anterior mitral leaflet angle >25°.[17,19] Furthermore, global and regional LV remodeling, indicated by LV end-diastolic dimension >65 mm, end-systolic dimension >51 mm, systolic sphericity index >0.7 and interpapillary muscle distance >20 mm predict a lower likelihood of successful mitral valve repair.[17,20] A leaflet coaptation depth >11 mm and coaptation length <2 mm challenge the percutaneous edge-to-edge mitral valve repair since these parameters indicate advanced LV remodeling with excessive tethering of the mitral leaflets.[17] Large regurgitant orifices often require implantation of >1 MitraClip to reduce MR. Short posterior leaflet, cleft, severe annular calcification and calcification in the grasping area are other anatomical conditions that challenge percutaneous edge-to-edge repair.[17] Peri-procedural transesophageal echocardiography is crucial to perform successful percutaneous implantation of a MitraClip device (Figure 3).

Table 2: Unfavorable anatomical conditions for successful surgical and percutaneous edge-to-edge repair in secondary mitral regurgitation.

SURGICAL REPAIR	PERCUTANEOUS REPAIR
Parameters related to mitral valve tethering	
Coaptation depth >1 cm	Coaptation depth >11 mm
Systolic tenting area >2.5 cm^2	Coaptation length <2 mm
Posterior mitral leaflet angle >45°	Severe asymmetric tethering
Distal anterior mitral leaflet angle >25°	Large (>50%) inter-commissural extension of regurgitant jet
Parameters related to left ventricular remodeling	
LV end-diastolic diameter >65 mm	Severe annular dilatation
LV end-systolic diameter >51 mm	Severe LV remodeling
End-systolic inter-papillary muscle distance >20 mm	
Systolic sphericity index >0.7	
Unfavorable anatomical conditions specific for percutaneous edge-to-edge repair	
	Short posterior leaflet
	Calcification in the grasping area
	Severe annular calcification
	Cleft

LV = left ventricular. Source: De Bonis *et al.*[17]

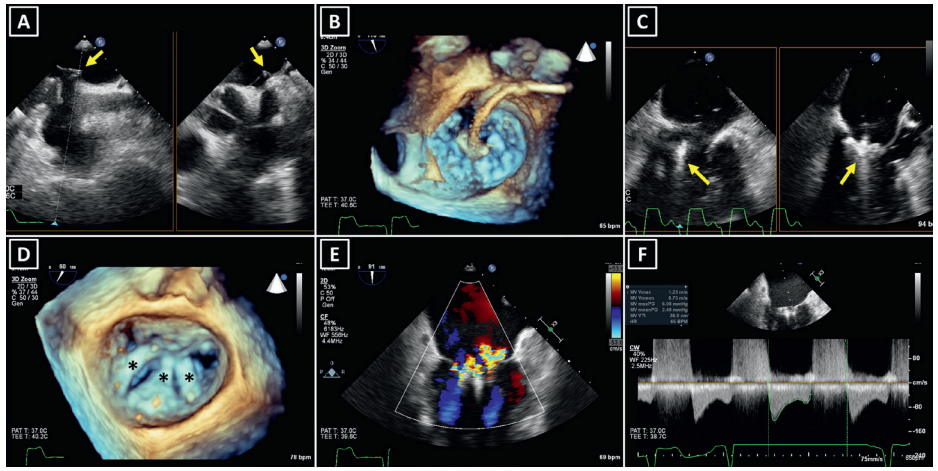

Figure 3: Transesophageal echocardiography during MitraClip implantation: guiding the intervention (A-C) and the assessment of procedural results (D-E). (A) Transseptal puncture. Arrows point at the tenting of the interatrial septum before the puncture in two simultaneous perpendicular image planes. **(B)** Opening of the Mitraclip device in the left atrium. **(C)** The MitraClip implantation – orienting the device arms perpendicular to the leaflets (arrows) is essential for successful grasping of the mitral valve. **(D)** Three MitraClips were implanted (asterisks) in a patient with severe secondary mitral regurgitation. **(E)** Assessment of residual mitral regurgitation. **(F)** Transmitral gradient measurement for the evaluation of post-implant mitral valve stenosis.

AORTIC STENOSIS IN HEART FAILURE

The LV pressure overload caused by AS increases LV wall stress and as a consequence the LV responds with myocyte hypertrophy to maintain a normal LVEF. However, this response is counterproductive in the long-term and causes LV diastolic dysfunction, myocardial ischemia in the subendocardium, increased myocardial fibrosis (reactive and replacement) and eventually LV systolic dysfunction.[21] Clinically, patients with severe AS may present with dyspnea, chest pain and syncope.

The prevalence of HF among patients with severe AS varies largely based on the definition of HF (e.g. reduced LVEF, presence of symptoms) and the characteristics of patients included in the studies. In a large cohort study (n=79,043) involving people with HF symptoms referred for echocardiography, at least mild AS was found in 10.1% and moderate or severe AS in 3.2%.[4] Furthermore, in the Euro Heart Survey 19.3% of patients with severe AS undergoing surgical aortic valve replacement (SAVR) had LVEF <50%.[5] In a more contemporary series of 42,776 patients with AS undergoing SAVR included in the German Aortic Valve Registry, LVEF <50% was present

in 26.6% of the patients.[22] Data from the American Transcatheter Valve Therapy (TVT) Registry showed a 25.6% prevalence of reduced LVEF (<45%) among 42,988 patients undergoing TAVR.[23]

Doppler echocardiography is the preferred technique for the assessment of the severity of AS. The primary hemodynamic parameters defining severe AS with echocardiography are the peak jet velocity ≥4 m/s, mean transvalvular pressure gradient ≥40 mmHg and aortic valve area (AVA) by continuity equation <1.0 cm² (Table 3).[24] In the majority of patients, these criteria coincide. However, up to 30% of patients may show low peak jet velocity and transaortic valve gradient with an AVA <1 cm².[25] This is frequently observed among patients with LVEF <50%, the so-called classical low-flow low-gradient severe AS.

Table 3: Echocardiographic criteria for the definition of severe AS.

	Severe AS	Common mistakes in the assessment of LFLG AS	Recommendations to avoid mistakes in the assessment of LFLG AS
Peak velocity (m/s)	≥4.0	• Underestimation of peak velocity and mean gradient: • misalignment of the ultrasound beam with the AS jet • high blood pressure	• Multiple acoustic windows to determine the highest velocity • Parallel ultrasound beam alignment with the direction of flow • Measurements when patient has normal blood pressure
Mean gradient (mmHg)	≥40		
AVA (cm²) by continuity equation (LVOT area × LVOT VTI)	<1.0	• Underestimation of LVOT area: • Elliptical shape of LVOT • Calcifications • Sigmoid septum • Diastolic measurements • Underestimation of LVOT VTI: • PW Doppler sample volume placed too apically	• Systolic LVOT diameter in ≥3 beats (sinus rhythm) and in ≥5 beats (irregular rhythm) • 3D planimetric measurement of the LVOT area (3D TEE, CT) • PW Doppler sample volume should be in the middle of LVOT just below the flow convergence where smooth velocity curve is obtained
AVAi (cm²/m²)	<0.6	• Underestimation in obese patients	• Important measure in children, adolescents, small adults
Velocity ratio (LVOT velocity / peak velocity)	<0.25	• Underestimation of LVOT velocity or peak velocity	• Multiple acoustic windows to determine the highest peak velocity • Parallel ultrasound beam alignment with the direction of flow • Measurements when patient has normal blood pressure • PW Doppler sample volume in the middle of LVOT just below the flow convergence where smooth velocity curve is obtained

3D = 3-dimensional; AS = aortic stenosis; AVA = aortic valve area; AVAi = indexed aortic valve area; CT = computed tomography; LFLG = low-flow low-gradient; LVOT = left ventricular outflow tract; PW = pulsed wave; TEE = transesophageal echocardiography; VTI = velocity time integral.
Source: Baumgartner *et al.*[24]

Low-dose dobutamine stress echocardiography is the primary diagnostic method to differentiate between true severe AS and pseudo-severe AS in patients with reduced LVEF.[24] In patients with true severe AS, intravenous infusion of low-dose dobutamine will increase the LV contractility and stroke volume leading to an increase in mean transvalvular gradient while the AVA will remain narrow (Figure 4). In contrast, pseudo-severe AS is diagnosed when the

increase in LV contractility and stroke volume is accompanied by an increase in AVA >1.0 cm^2 (Figure 5). While patients with true severe low-flow low-gradient AS should undergo prompt aortic valve intervention, the course of action for patients with pseudo-severe AS is less clear. Fougeres *et al.*[26] demonstrated comparable survival of patients with pseudo-severe AS to that of propensity-matched patients with systolic HF and no evidence of VHD. However, this has recently been challenged by another study that demonstrated a very high risk for clinical events (defined as the composite of all-cause death, aortic valve replacement and HF hospitalization) among patients with HF and moderate AS.[27] Furthermore, in a retrospective analysis of 1,090 patients with moderate AS and LVEF ≤50% aortic valve surgery was associated with a higher 5-year survival compared to medical therapy.[28] While current guidelines do not recommend aortic valve intervention in HF patients with moderate AS, this view might change after the results of the ongoing international, multicenter, randomized, clinical trial TAVR UNLOAD (NCT02661451), which has been designed to compare the efficacy and safety of transfemoral TAVR in addition to optimal HF therapy vs HF therapy alone in HF patients with moderate AS.[29]

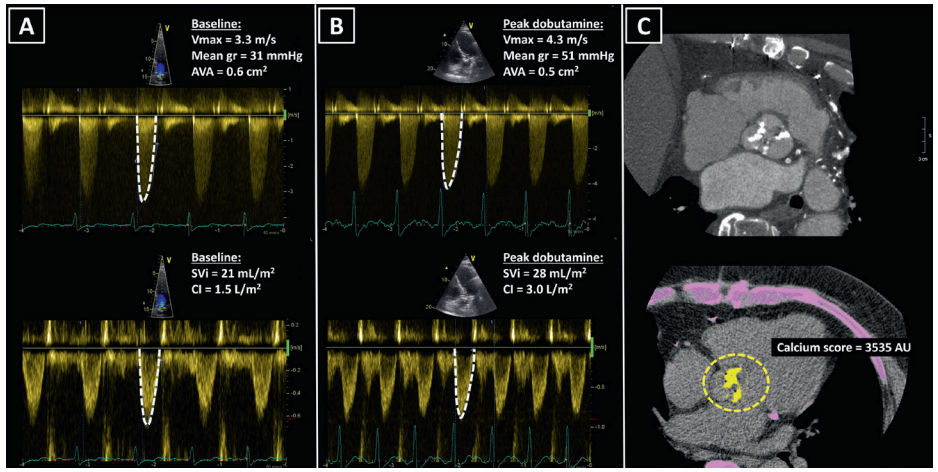

Figure 4: Classical low-flow low-gradient severe aortic stenosis. (A) A 75-year old male with ischemic cardiomyopathy, reduced left ventricular ejection fraction (32%) and low cardiac output. At rest, echocardiography showed calcified aortic valve with severely narrowed valve area <1.0 cm2, while peak velocity and mean gradient were in the range of moderate aortic stenosis. **(B)** During low-dose dobutamine stress echocardiography peak jet velocity and mean gradient increased ≥4.0 m/s and ≥40 mmHg respectively, and the aortic valve area remained <1.0 cm2, revealing true severe aortic stenosis. Furthermore, an increase in cardiac output demonstrated left ventricular contractile reserve. **(C)** Computed tomography showed a tricuspid aortic valve with high calcium score, suggesting high likelihood of severe aortic stenosis. AU = arbitrary units; AVA = aortic valve area; CI = cardiac index; Mean gr = mean gradient; SVi = stroke volume index; Vmax = peak velocity.

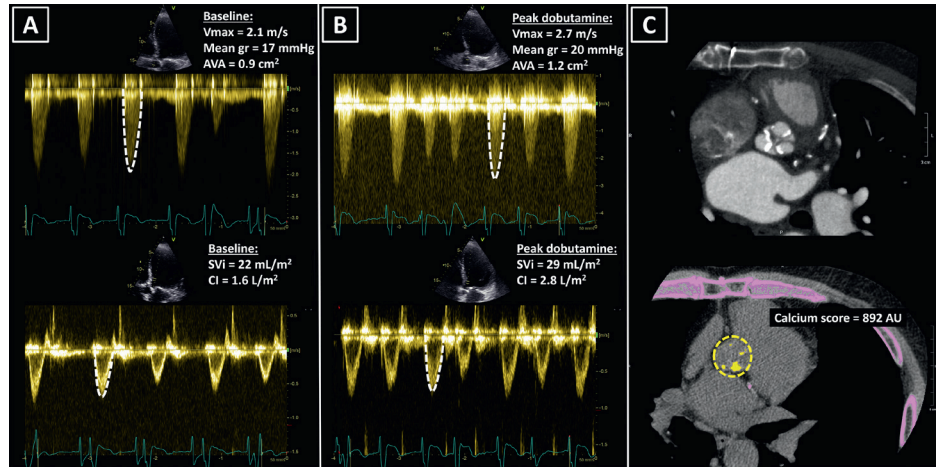

Figure 5: Pseudo-severe low-flow low-gradient aortic stenosis. (A) An 80-year old male with dilated cardiomyopathy, reduced left ventricular ejection fraction (21%) and low cardiac output. At rest, echocardiography showed calcified aortic valve with an area <1.0 cm2 (suggesting severe aortic stenosis), while peak velocity and mean gradient were representative of mild aortic stenosis. **(B)** During low-dose dobutamine stress echocardiography, the peak jet velocity and mean gradient marginally increased and the aortic valve area increased >1.0 cm2, revealing pseudo-severe aortic stenosis. **(C)** Computed tomography showed tricuspid aortic valve with low calcium score, suggesting non-severe aortic stenosis. AU = arbitrary units; AVA = aortic valve area; CI = cardiac index; Mean gr = mean gradient; SVi = stroke volume index; Vmax = peak velocity.

In patients without contractile reserve, defined as failure to increase stroke volume >20% during dobutamine stress echocardiography, the assessment of aortic valve calcification burden with cardiac CT may help to estimate the severity of AS (Figure 4 and 5).[24] Aortic valve calcium score is quantified using the Agatston method and expressed in arbitrary units (AU).[30] Cueff *et al.*[31] demonstrated a good overall correlation between the degree of aortic valve calcification and hemodynamic parameters of AS severity assessed by the AVA (r=-0.63, P<0.001), indexed AVA (r=-0.67, P<0.001), mean gradient (r=0.78, P<0.001) and peak velocity (r=0.79, P<0.001). The proposed cut-off value of 1,651 AU yielded a 93% sensitivity and 75% specificity in grading AS severity in patients with classical low-flow low-gradient AS. Clavel *et al.*[32] proposed different cut-off values to define severe AS for men and women, 2,065 AU and 1,274 AU, respectively. The joint European and American recommendations for the assessment of AS consider the aortic valve calcium score as a continuum – a very high calcium score suggests severe AS and low calcium score suggests severe AS is unlikely (Table 4).[24]

Table 4: Calcium score by computed tomography in grading of aortic stenosis.

	Men	Women
Severe aortic stenosis very likely	≥3,000	≥1,600
Severe aortic stenosis likely	≥2,000	≥1,200
Sever aortic stenosis unlikely	<1,600	<800

Source: Baumgartner *et al.*[24]

TREATMENT OPTIONS FOR AORTIC STENOSIS

Current therapeutic options for patients with severe AS and HF are conservative medical therapy, SAVR and TAVR. For patients with symptomatic high-gradient severe AS there is no lower LVEF limit for aortic valve intervention (Class I recommendation), since LV function will likely improve after relief of stenosis.[6,7] Asymptomatic severe AS patients with an LVEF <50% should undergo aortic valve replacement (Class I recommendation).[6,7] In patients with classical low-flow low-gradient severe AS (with reduced LVEF) aortic valve intervention is indicated when dobutamine stress echocardiography shows evidence of LV contractile reserve (Class I recommendation in European guidelines and Class IIa in American guidelines).[6,7] An intervention should also be considered in patients without LV contractile reserve, particularly when CT calcium score is high (Class IIa recommendation in European guidelines, while the American guidelines stress the importance of individualized decisions in these high-risk patients).[6,7] Tribouilloy *et al.*[33] demonstrated that patients with low-flow low-gradient severe AS without contractile reserve experience high operative mortality, but SAVR was associated with better outcomes compared with patients who were treated conservatively. Only symptomatic patients with severe comorbidities, in whom aortic valve intervention is unlikely to improve survival or quality of life, should be treated with medical therapy.[6]

The choice of the intervention in patients with symptomatic severe AS and HF should be made by the specialist heart team and should take into account patient's cardiac and extracardiac characteristics, the individual risk of surgery, the feasibility of TAVR, as well as the local experience and outcome data.[6,8] Table 5 lists the imaging-derived characteristics that guide the decision to choose TAVR or SAVR. Multi-slice CT has become the imaging modality of choice for pre-procedural evaluation of TAVR candidates in most centers due to its low invasiveness and comprehensive evaluation.[6] It allows assessment of the size and the shape of the aortic annulus, its distance to the coronary ostia, the distribution of calcifications and the dimensions of the aortic root, which is of paramount importance to determine feasibility of TAVR and to choose appropriate prosthesis size (Figure 6). However, if CT is contraindicated (e.g., if the patient has severely impaired renal function), 3D transesophageal echocardiography can be used to determine the aortic annulus size. It is important to remember that the obtained annulus dimensions with 3D transesophageal echocardiography are smaller than those measured with cardiac CT and the echocardiographic accuracy can be reduced in heavily calcified aortic valves.[34,35] Cardiac CT also allows assessment of the peripheral arteries to determine feasibility of transfemoral access, which is the least invasive TAVR approach, used in the majority of patients.[23,36] Cardiac CT allows detailed visualization of iliofemoral arteries and aorta with the assessment of size, tortuosity, degree of calcification and plaque burden (Figure 6). For currently available TAVR delivery catheters, a 6.0-6.5 mm minimal luminal vessel diameter of femoral arteries is considered acceptable.[37] In case of contraindications to CT, invasive angiography or, less commonly, CMR angiography might be employed.

Table 5: Imaging-derived characteristics that guide the decision between TAVR and SAVR in patient at increased surgical risk.

	Favours TAVR	Favours SAVR
Peripheral arteries anatomy favorable for transfemoral TAVR	+	
Unfavorable access (any) for TAVR		+
Porcelain aorta	+	
Expected patient-prosthesis mismatch	+	
Short distance between coronary ostia and aortic valve annulus		+
Size of aortic valve annulus out of range for TAVR		+
Aortic root morphology unfavorable for TAVR		+
Valve morphology (bicuspid, degree of calcification, calcification pattern) unfavorable for TAVR		+
Presence of thrombi in aorta or left ventricle		+

SAVR = surgical aortic valve replacement; TAVR = transcatheter aortic valve replacement.

Source: Baumgartner *et al.*[6]

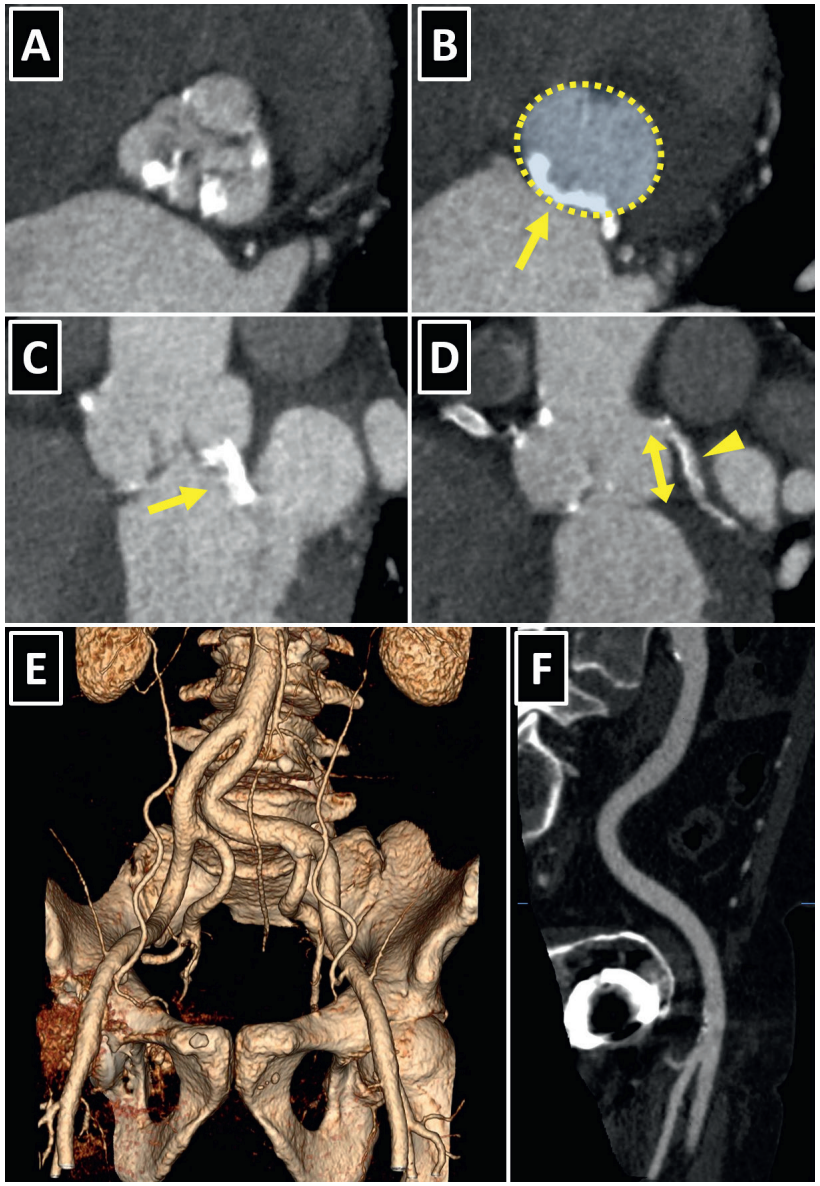

Figure 6: Computed tomography (CT) in pre-procedural assessment for transcatheter aortic valve replacement (TAVR). (A) Double oblique transverse view of a calcified tricuspid aortic valve. **(B)** Planimetry of the aortic annulus. The posterior part of the annulus was severely calcified (arrow), increasing the likelihood of aortic rupture in case of an oversized TAVR prosthesis implantation or post-dilatation with an oversized balloon. **(C)** The calcification extended form the aortic annulus into the left ventricular outflow tract towards the anterior mitral valve leaflet (arrow). **(D)** Measurement of the distance between left main coronary artery and the aortic annulus (arrow). A calcified plaque in the left coronary artery is visible (arrowhead). **(E)** Tortuous bilateral iliofemoral arteries. **(F)** Multi-planar reconstruction revealed only mildly calcified right iliofemoral artery with adequate lumen diameter to allow for transfemoral TAVR.

CONCLUSION

Accurate grading of valvular lesion and reliable assessment of LV dysfunction is of paramount importance when deciding the most appropriate therapy for patients with VHD and HF. Transthoracic echocardiography is the first-line imaging modality to quantify LV systolic function and grade of valvular stenosis and regurgitation, as well as characterizing the mechanism of valvular dysfunction. However, in HF patients, quantification of valvular dysfunction remains challenging and the use of other imaging techniques such as 3D transesophageal echocardiography, CMR and CT is needed to determine whether the valve stenosis and regurgitation are severe. The integration of multimodality cardiovascular imaging is even more important when assessing suitability for transcatheter valve repair and replacement therapies. CT has become the key imaging modality for pre-procedural evaluation of patients undergoing TAVR, and 3D transesophageal echocardiography is crucial to guide percutaneous edge-to-edge mitral valve repair.

REFERENCES

1. Savarese G, Lund LH. Global Public Health Burden of Heart Failure. *Card Fail Rev* 2017;3(1):7-11.
2. Ponikowski P, Voors AA, Anker SD, Bueno H, Cleland JG, Coats AJ *et al.* 2016 ESC Guidelines for the diagnosis and treatment of acute and chronic heart failure: The Task Force for the diagnosis and treatment of acute and chronic heart failure of the European Society of Cardiology (ESC)Developed with the special contribution of the Heart Failure Association (HFA) of the ESC. *Eur Heart J* 2016;37(27):2129-200.
3. Yancy CW, Jessup M, Bozkurt B, Butler J, Casey DE, Jr., Drazner MH *et al.* 2013 ACCF/AHA guideline for the management of heart failure: executive summary: a report of the American College of Cardiology Foundation/American Heart Association Task Force on practice guidelines. *Circulation* 2013;128(16):1810-52.
4. Marciniak A, Glover K, Sharma R. Cohort profile: prevalence of valvular heart disease in community patients with suspected heart failure in UK. *BMJ Open* 2017;7(1):e012240.
5. Iung B, Baron G, Butchart EG, Delahaye F, Gohlke-Barwolf C, Levang OW *et al.* A prospective survey of patients with valvular heart disease in Europe: The Euro Heart Survey on Valvular Heart Disease. *Eur Heart J* 2003;24(13):1231-43.
6. Baumgartner H, Falk V, Bax JJ, De Bonis M, Hamm C, Holm PJ *et al.* 2017 ESC/EACTS Guidelines for the management of valvular heart disease. *Eur Heart J* 2017;38(36):2739-91.
7. Nishimura RA, Otto CM, Bonow RO, Carabello BA, Erwin JP, 3rd, Guyton RA *et al.* 2014 AHA/ACC Guideline for the Management of Patients With Valvular Heart Disease: executive summary: a report of the American College of Cardiology/American Heart Association Task Force on Practice Guidelines. *Circulation* 2014;129(23):2440-92.
8. Nishimura RA, Otto CM, Bonow RO, Carabello BA, Erwin JP, 3rd, Fleisher LA *et al.* 2017 AHA/ACC Focused Update of the 2014 AHA/ACC Guideline for the Management of Patients With Valvular Heart Disease: A Report of the American College of Cardiology/American Heart Association Task Force on Clinical Practice Guidelines. *Circulation* 2017;135(25):e1159-e95.
9. Nkomo VT, Gardin JM, Skelton TN, Gottdiener JS, Scott CG, Enriquez-Sarano M. Burden of valvular heart diseases: a population-based study. *Lancet* 2006;368(9540):1005-11.
10. Zoghbi WA, Adams D, Bonow RO, Enriquez-Sarano M, Foster E, Grayburn PA *et al.* Recommendations for Noninvasive Evaluation of Native Valvular Regurgitation: A Report from the American Society of Echocardiography Developed in Collaboration with the Society for Cardiovascular Magnetic Resonance. *J Am Soc Echocardiogr* 2017;30(4):303-71.

11. Lancellotti P, Tribouilloy C, Hagendorff A, Popescu BA, Edvardsen T, Pierard LA *et al.* Recommendations for the echocardiographic assessment of native valvular regurgitation: an executive summary from the European Association of Cardiovascular Imaging. *Eur Heart J Cardiovasc Imaging* 2013;14(7):611-44.
12. Avierinos JF, Tribouilloy C, Grigioni F, Suri R, Barbieri A, Michelena HI *et al.* Impact of ageing on presentation and outcome of mitral regurgitation due to flail leaflet: a multicentre international study. *Eur Heart J* 2013;34(33):2600-9.
13. Rossi A, Dini FL, Faggiano P, Agricola E, Cicoira M, Frattini S *et al.* Independent prognostic value of functional mitral regurgitation in patients with heart failure. A quantitative analysis of 1256 patients with ischaemic and non-ischaemic dilated cardiomyopathy. *Heart* 2011;97(20):1675-80.
14. Yoran C, Yellin EL, Becker RM, Gabbay S, Frater RW, Sonnenblick EH. Dynamic aspects of acute mitral regurgitation: effects of ventricular volume, pressure and contractility on the effective regurgitant orifice area. *Circulation* 1979;60(1):170-6.
15. Zeng X, Levine RA, Hua L, Morris EL, Kang Y, Flaherty M *et al.* Diagnostic value of vena contracta area in the quantification of mitral regurgitation severity by color Doppler 3D echocardiography. *Circ Cardiovasc Imaging* 2011;4(5):506-13.
16. Hung J, Otsuji Y, Handschumacher MD, Schwammenthal E, Levine RA. Mechanism of dynamic regurgitant orifice area variation in functional mitral regurgitation: physiologic insights from the proximal flow convergence technique. *J Am Coll Cardiol* 1999;33(2):538-45.
17. De Bonis M, Al-Attar N, Antunes M, Borger M, Casselman F, Falk V *et al.* Surgical and interventional management of mitral valve regurgitation: a position statement from the European Society of Cardiology Working Groups on Cardiovascular Surgery and Valvular Heart Disease. *Eur Heart J* 2016;37(2):133-9.
18. Goldstein D, Moskowitz AJ, Gelijns AC, Ailawadi G, Parides MK, Perrault LP *et al.* Two-Year Outcomes of Surgical Treatment of Severe Ischemic Mitral Regurgitation. *N Engl J Med* 2016;374(4):344-53.
19. Kongsaerepong V, Shiota M, Gillinov AM, Song JM, Fukuda S, McCarthy PM *et al.* Echocardiographic predictors of successful versus unsuccessful mitral valve repair in ischemic mitral regurgitation. *Am J Cardiol* 2006;98(4):504-8.
20. Braun J, Bax JJ, Versteegh MI, Voigt PG, Holman ER, Klautz RJ *et al.* Preoperative left ventricular dimensions predict reverse remodeling following restrictive mitral annuloplasty in ischemic mitral regurgitation. *Eur J Cardiothorac Surg* 2005;27(5):847-53.
21. Carabello BA, Paulus WJ. Aortic stenosis. *Lancet* 2009;373(9667):956-66.
22. Fujita B, Ensminger S, Bauer T, Mollmann H, Beckmann A, Bekeredjian R *et al.* Trends in practice and outcomes from 2011 to 2015 for surgical aortic valve replacement: an update from the German Aortic Valve Registry on 42 776 patients. *Eur J Cardiothorac Surg* 2018;53(3):552-9.

23. Carroll JD, Vemulapalli S, Dai D, Matsouaka R, Blackstone E, Edwards F *et al.* Procedural Experience for Transcatheter Aortic Valve Replacement and Relation to Outcomes: The STS/ACC TVT Registry. *J Am Coll Cardiol* 2017;70(1):29-41.
24. Baumgartner HC, Hung JC-C, Bermejo J, Chambers JB, Edvardsen T, Goldstein S *et al.* Recommendations on the echocardiographic assessment of aortic valve stenosis: a focused update from the European Association of Cardiovascular Imaging and the American Society of Echocardiography. *Eur Heart J Cardiovasc Imaging* 2017;18(3):254-75.
25. Minners J, Allgeier M, Gohlke-Baerwolf C, Kienzle RP, Neumann FJ, Jander N. Inconsistencies of echocardiographic criteria for the grading of aortic valve stenosis. *Eur Heart J* 2008;29(8):1043-8.
26. Fougeres E, Tribouilloy C, Monchi M, Petit-Eisenmann H, Baleynaud S, Pasquet A *et al.* Outcomes of pseudo-severe aortic stenosis under conservative treatment. *European Heart Journal* 2012;33(19):2426-33.
27. van Gils L, Clavel MA, Vollema EM, Hahn RT, Spitzer E, Delgado V *et al.* Prognostic Implications of Moderate Aortic Stenosis in Patients With Left Ventricular Systolic Dysfunction. *J Am Coll Cardiol* 2017;69(19):2383-92.
28. Samad Z, Vora AN, Dunning A, Schulte PJ, Shaw LK, Al-Enezi F *et al.* Aortic valve surgery and survival in patients with moderate or severe aortic stenosis and left ventricular dysfunction. *Eur Heart J* 2016;37(28):2276-86.
29. Spitzer E, Van Mieghem NM, Pibarot P, Hahn RT, Kodali S, Maurer MS *et al.* Rationale and design of the Transcatheter Aortic Valve Replacement to UNload the Left ventricle in patients with ADvanced heart failure (TAVR UNLOAD) trial. *Am Heart J* 2016;182:80-8.
30. Agatston AS, Janowitz WR, Hildner FJ, Zusmer NR, Viamonte M, Jr., Detrano R. Quantification of coronary artery calcium using ultrafast computed tomography. *J Am Coll Cardiol* 1990;15(4):827-32.
31. Cueff C, Serfaty JM, Cimadevilla C, Laissy JP, Himbert D, Tubach F *et al.* Measurement of aortic valve calcification using multislice computed tomography: correlation with haemodynamic severity of aortic stenosis and clinical implication for patients with low ejection fraction. *Heart* 2011;97(9):721-6.
32. Clavel MA, Messika-Zeitoun D, Pibarot P, Aggarwal SR, Malouf J, Araoz PA *et al.* The complex nature of discordant severe calcified aortic valve disease grading: new insights from combined Doppler echocardiographic and computed tomographic study. *J Am Coll Cardiol* 2013;62(24):2329-38.
33. Tribouilloy C, Levy F, Rusinaru D, Gueret P, Petit-Eisenmann H, Baleynaud S *et al.* Outcome after aortic valve replacement for low-flow/low-gradient aortic stenosis without contractile reserve on dobutamine stress echocardiography. *J Am Coll Cardiol* 2009;53(20):1865-73.

34. Ng AC, Delgado V, van der Kley F, Shanks M, van de Veire NR, Bertini M *et al.* Comparison of aortic root dimensions and geometries before and after transcatheter aortic valve implantation by 2- and 3-dimensional transesophageal echocardiography and multislice computed tomography. *Circ Cardiovasc Imaging* 2010;3(1):94-102.
35. Podlesnikar T, Prihadi EA, van Rosendael PJ, Vollema EM, van der Kley F, de Weger A *et al.* Influence of the Quantity of Aortic Valve Calcium on the Agreement Between Automated 3-Dimensional Transesophageal Echocardiography and Multidetector Row Computed Tomography for Aortic Annulus Sizing. *Am J Cardiol* 2018;121(1):86-93.
36. Walther T, Hamm CW, Schuler G, Berkowitsch A, Kotting J, Mangner N *et al.* Perioperative Results and Complications in 15,964 Transcatheter Aortic Valve Replacements: Prospective Data From the GARY Registry. *J Am Coll Cardiol* 2015;65(20):2173-80.
37. Bax JJ, Delgado V, Bapat V, Baumgartner H, Collet JP, Erbel R *et al.* Open issues in transcatheter aortic valve implantation. Part 2: procedural issues and outcomes after transcatheter aortic valve implantation. *Eur Heart J* 2014;35(38):2639-54.

6

Transcatheter aortic valve replacement: advantages and limitations of different cardiac imaging techniques

Tomaž Podlesnikar, Victoria Delgado

Rev Esp Cardiol (Engl Ed) 2016;69(3):310-21

ABSTRACT

Transcatheter aortic valve replacement is an established therapy for patients with symptomatic severe aortic stenosis and contraindications or high risk for surgery. Advances in prosthesis and delivery systems designs and continuous advances in multimodality imaging, particularly the 3-dimensional techniques, have led to improved outcomes with significant reductions in the incidence of frequent complications such as paravalvular aortic regurgitation. In addition, data on prosthesis durability are accumulating. Multimodality imaging plays a central role in the selection of patients who are candidates for transcatheter aortic valve replacement, procedure planning and guidance, and follow-up of prosthesis function. The strengths and limitations of each imaging technique for transcatheter aortic valve replacement will be discussed in this review article.

INTRODUCTION

Transcatheter aortic valve replacement (TAVR) has become a safe and feasible alternative treatment for patients with severe aortic stenosis (AS) who have contraindications or are at high risk for surgical aortic valve (AV) replacement. In terms of survival and improvement in clinical symptoms, large randomized clinical trials have proven TAVR to be superior to medical therapy (and balloon valvuloplasty) in patients deemed inoperable[1,2] and non-inferior to surgical AV replacement in patients with high operative risk.[3,4] These results encouraged the rapid implementation of TAVR in current practice with more than 200.000 patients treated worldwide.[5] Patient selection, accurate sizing of the prosthesis and procedural planning require the use of several imaging modalities to optimize results and minimize the complications such as paravalvular regurgitation (PVAR), pacemaker implantation, vascular injury or annulus rupture. Procedural guidance is mainly performed under fluoroscopy assistance and, still, in many laboratories, with the help of transthoracic echocardiography (TTE) or transesophageal echocardiography (TEE). The steep learning curve of the procedure and the low number of periprocedural complications in high-volume centers have allowed less invasive TAVR by implanting the device under conscious sedation. Therefore, the need for TEE during the procedure has recently been questioned. In addition, prosthesis durability is an important factor to eventually expand this procedure to patients with low-intermediate operative risk. Five years follow-up data from the Placement of AoRTic TraNscathetER valves (PARTNER) trial showed no structural degeneration of the balloon expandable prosthesis with stable transvalvular gradients and aortic valve areas (AVA).[6,7] However, the use of high spatial resolution imaging techniques such as multidetector row computed tomography (MDCT) have raised concern due to the presence of thickening and restriction of the prosthetic leaflets suggesting subclinical thrombosis that could not be appreciated with echocardiography.[8] The present review article summarizes the role of multimodality imaging for preprocedural planning (patient selection, device sizing and procedural access), procedural guidance and follow-up, highlighting the pros and cons of each imaging modality.

PREPROCEDURAL PLANNING

Accurate assessment of AS severity, aortic valve and root anatomy and geometry and evaluation of feasibility of peripheral vascular access are three key steps during planning of TAVR.

Aortic stenosis severity

Doppler TTE is the imaging technique of choice to assess AS severity.[9,10] It provides key insights into AV anatomy, degree of calcification, hemodynamic consequences of AS (left ventricular [LV] size, wall thickness and function, pulmonary arterial pressure), concomitant valve disease and aortic pathology. Aortic jet velocity >4 m/s, mean transvalvular pressure gradient >40 mmHg and calculated aortic valve area (AVA) <1.0 cm^2 define severe AS.[9,10] There are situations however where these parameters are not congruent, challenging the diagnosis of severe AS and the management of the patients.

When severe AS coexists with reduced LV systolic function, the flow derived indices may underestimate the degree of AS. Such condition is termed classical low-flow low-gradient AS and is characterized by reduced LV ejection fraction (LVEF), an AVA <1.0 cm^2, aortic velocity <4 m/s, mean gradient <40 mmHg and stroke volume index <35 mL/m^2.[10,11] In this subgroup of patients differentiation between true severe AS and pseudosevere AS has important therapeutic implications.[12,13] Using low dose dobutamine stress echocardiography (DSE), the contractile reserve of the left ventricle is increased leading to an increase in LV stroke volume (flow).[11] In a true severe AS the increase in flow is associated with an increase in transvalvular gradients while the AVA remains <1.0 cm^2 (Figure 1). In contrast, in pseudosevere AS the increase in LV contractility and flow results in an increase in AVA >1.0 cm^2 while the transvalvular gradients remain low. However, 30-40% of patients with classical low-flow low-gradient severe AS do not show contractile reserve during low dose DSE.[13] In this specific group of patients, the use of computed tomography and the assessment of aortic valve calcification burden may help to estimate the severity of AS (Figure 1).[14,15] A cut-off value of aortic valve calcification of ≥1,274 AU in women and ≥2,065 AU in men were more frequently associated with severe AS.[14]

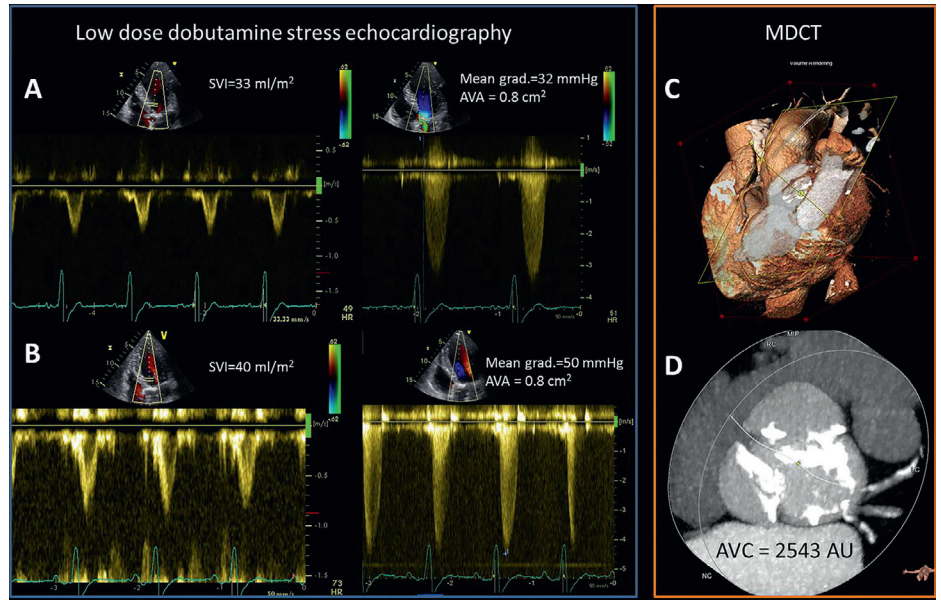

Figure 1: **Low-dose dobutamine stress echocardiography (DSE) and aortic valve calcification (AVC) assessment with multidetector row computed tomography (MDCT) in a patient with low-flow low-gradient severe aortic stenosis (AS) with reduced left ventricular systolic function. (A)** Baseline echocardiographic assessment revealed discrepant indices of AS severity. The mean gradient was 32 mm Hg and aortic valve area (AVA) was 0.8 cm^2. Stroke volume index (SVI) of 33 ml/m^2. **(B)** Low-dose DSE resulted in an increase of the mean gradient to 50 mm Hg, the AVA remained unchanged and the SVI increased by 21%. This indicates that the patient had classical low-flow low-gradient severe AS and a presence of flow reserve (SVI increased >20%). **(C)** Volume rendered cardiac MDCT with a plane across the aortic annulus. **(D)** AVC load, using the Agatston method, was measured 2543 arbitrary units (AU), indicating severe aortic stenosis (cut-offs for severe AS ≥2,065 AU in men and ≥1,274 AU in women[14]).

Patients with paradoxical low-flow low-gradient severe AS present with preserved LVEF, AVA <1.0 cm^2, mean gradient <40 mmHg and LV stroke volume index <35 mL/m^2.[9,10] In this subgroup of patients, the low-flow condition is determined by the small LV cavity due to severe LV hypertrophy. The management of these patients remains challenging. Clavel *et al.*[16] compared the outcome of 187 patients with paradoxical low-flow low-gradient severe AS with 187 patients with severe AS and high gradient (matched according to AVA) and with 187 patients with moderate AS (matched according to mean transvalvular gradient) and showed that patients with paradoxical low-flow low-gradient severe AS have reduced overall survival (1-year 89±2%; 5-year 64±4%) compared with patients with high gradient severe AS (1-year 96±1%; 5-year 82±3%) or moderate AS (1-year 96±1%; 5-year 81±3%). Moreover, AV replacement was significantly associated with improved survival in patients with paradoxical low-flow low-gra-

dient severe AS, but not in the moderate AS group.[16] Of note, the study population was relatively heterogeneous with a significant proportion of patients being asymptomatic and with heterogeneous management (80% of patients with severe AS and high gradient underwent AV replacement compared with 56% in the group of paradoxical low-flow low-gradient and 40% in moderate AS). In contrast, Jander *et al.*[17] demonstrated that patients with asymptomatic severe AS, low gradient and preserved LVEF (low stroke volume index <35 mL/m2 was present in 51%) had comparable outcome to that of patients with moderate AS (major cardiovascular events 14.8±1.0% versus 14.1±1.5%, respectively; P=0.59).

According to current guidelines the finding of paradoxical low-flow low-gradient AS has to be approached stepwise.[9] Any source of error in measured parameters of the continuity equation used for AVA calculation has to be addressed first. Left ventricular outflow tract (LVOT) cross-sectional area (CSA) is one of the key parameters. With 2-dimensional (2D) echocardiography, LVOT CSA is traditionally derived by measuring mid-systolic sagittal LVOT diameter in the parasternal long-axis view assuming a circular geometry. However, a sigmoid septal basal hypertrophy characteristic of elderly patients may challenge the accuracy of this method since the LVOT may become elliptical (Figure 2).[18,19] By measuring the planimetric area of the LVOT with a 3-dimensional (3D) imaging technique such as MDCT and introducing the value into the continuity equation it has been demonstrated that 33% of the low-gradient severe AS patients with preserved LVEF could be reclassified into moderate AS.[20] In case of small body surface area (BSA) the correction for BSA is necessary, with an AVA index <0.6 cm^2/m^2 indicating severe AS. A severely increased global hemodynamic afterload (i.e. valvulo-arterial impedance) should be also excluded. Furthermore, particular attention has to be paid to accurately determine the LV stroke volume, preferably by confronting measurements from other independent methods (2D or 3D volumetric methods by means of echocardiography, cardiac magnetic resonance imaging [CMR] or MDCT). Low dose DSE can provide additional information about the actual severity of the AS and can predict the risk of adverse events, but safety of DSE in patients with pronounced LV concentric remodeling and small LV cavities has yet to be established.[21] In addition, evaluation of the degree of AV calcification by computed tomography may be of help in this group of patients.[14,15]

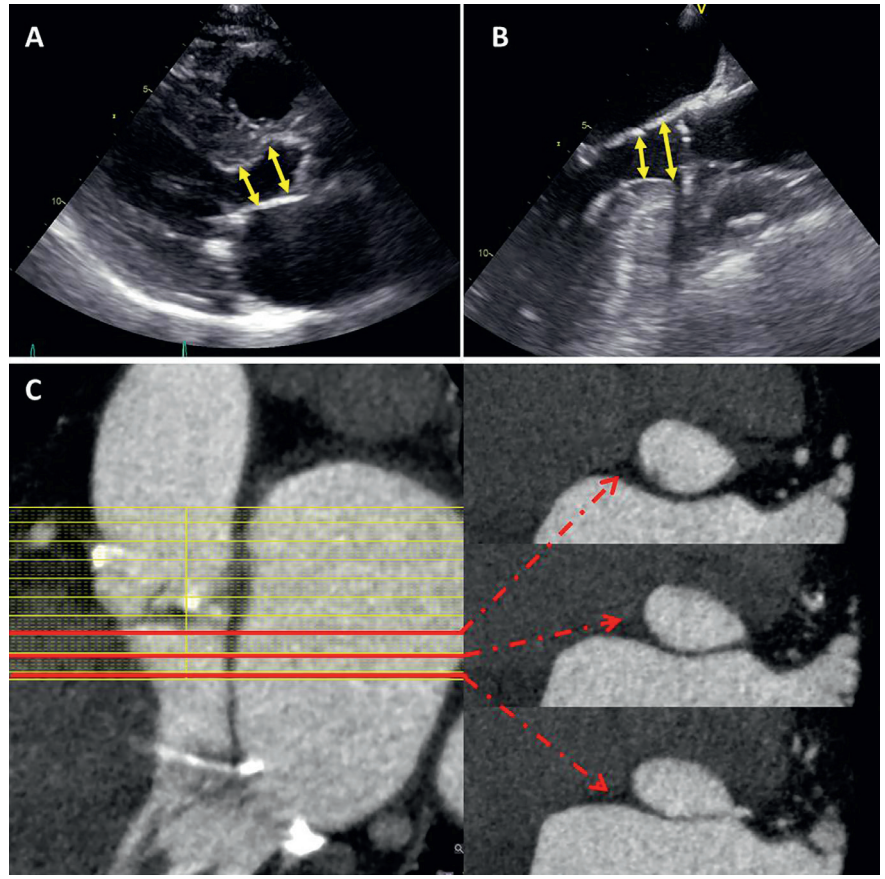

Figure 2: Assessment of left ventricular outflow tract (LVOT) with transthoracic (A) and transesophageal (B) echocardiography and multidetector row computed tomography (C). On 2-dimensional transthoracic and transesophageal echocardiography the measurement of the LVOT may vary significantly (arrows), particularly in patients with sigmoid septum, having important implications on aortic valve area calculation. On MDCT, the cross-sectional area of the LVOT at each level shows the increase of the elliptical shape for the aortic annulus toward the left ventricle. Red lines depict LVOT areas at 3 different levels showing the change in area and ellipticity of the LVOT.

Aortic annulus size

In contrast to surgical AV replacement, where surgeons can directly determine the optimal prosthesis size and visualize the adaptation of the prosthesis to the aortic root, in TAVR appropriate prosthesis selection rely mostly on preprocedural imaging. Too small prosthesis increases the risk of significant paravalvular regurgitation (PVAR) and prosthesis migration, while oversized prostheses may lead to incomplete deployment, potentially resulting in both, valvular and paravalvular regurgitation, or even catastrophic aortic annulus rupture.[22,23]

3D imaging techniques (3D echocardiography, MDCT, CMR) are currently the preferred tools to assess the aortic annulus size. Sagittal aortic annulus diameter, normally measured with 2D echocardiography tends to underestimate the true aortic annulus size.[24] In contrast, studies using 3D TEE or MDCT have shown that selection of prosthesis size based on these imaging modalities is associated with lower incidence of significant PVAR.[25] [26,27] These 3D imaging techniques permit the measurement of the aortic annulus area and perimeter using direct planimetry and diameters derived from the area and the perimeter. The majority of manufacturers have also included these measurements into the prosthesis size charts allowing the standardization of the prosthesis selection.

The MDCT provides high spatial resolution images of the aortic annulus and aortic root. This imaging technique has become key in TAVR due to its low invasiveness and comprehensive evaluation of candidates for TAVR, including assessment of aortic annulus, burden of aortic valve and root calcification and peripheral arteries anatomy (Figure 3). In addition, MDCT permits planning of the C-arm projections needed for AV balloon dilation and prosthesis deployment, reducing the need of repeated angiographies during the procedure.[28,29] However, in patients with associated impaired renal function, the use of MDCT should be tailored in order to reduce the risk of periprocedural acute kidney injury. 3D TEE has also shown to be of value to size the aortic annulus, aortic root dimensions, aortic valve calcification burden and height of coronary ostia relative to the aortic annulus (Figure 4).[30] This imaging modality is however relatively uncomfortable for patients and the acoustic shadowing caused by the aortic cusp calcifications may impact on the spatial resolution of the images and on the accuracy of the measurements. CMR permits 3D analysis of the aortic annulus and root anatomy similarly to MDCT. However, this imaging technique is less available and not feasible in patients with non-MRI compatible implanted devices. These 3D imaging modalities have been compared in several studies showing similar accuracy to size the aortic annulus.[24,31,32] Of note, the data acquisition should be preferably performed with electrocardiogram (ECG) gating to obtain the systolic and diastolic dimensions of the aortic annulus. A recent study by Murphy and co-workers including 507 patients with severe AS who underwent ECG-gated MDCT showed significant changes in aortic annulus area and perimeter between systole and diastole (8.23% and 3.36%, respectively).[33] The implications of these findings are relevant since the use of the diastolic measure would have resulted in change of the prosthesis size (undersizing) in 50% of the patients. Therefore, assessment of systolic and diastolic measurements is recommended.[34]

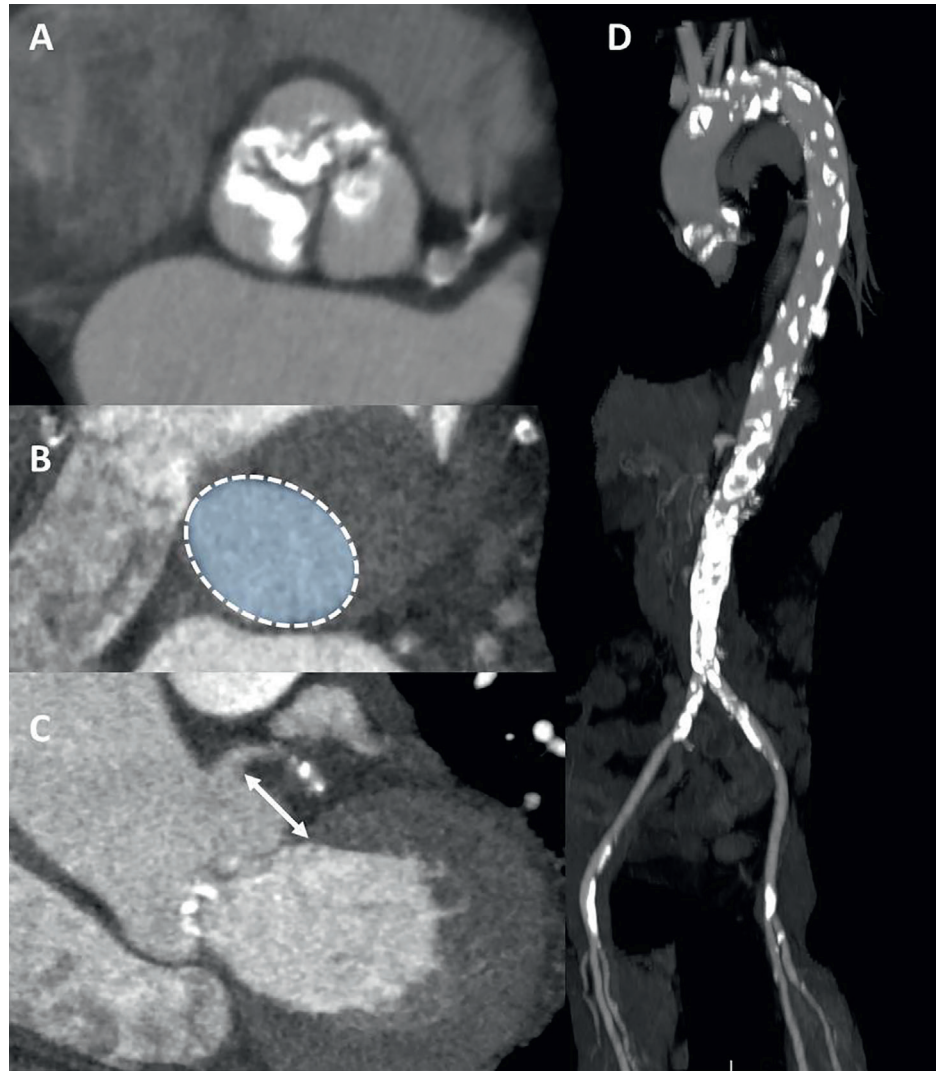

Figure 3: The role of multidetector row computed tomography (MDCT) in preprocedural assessment. **(A)** Double oblique transverse view of severely calcified tricuspid aortic valve. **(B)** Planimetry of the aortic annulus. **(C)** Measurement of the distance between the left main coronary artery and the aortic annulus (white arrow). **(D)** CT aortography reveals severely calcified aorta, particularly in the aortic arch and in the descendent part. Calcifications are present in both iliofemoral arteries as well.

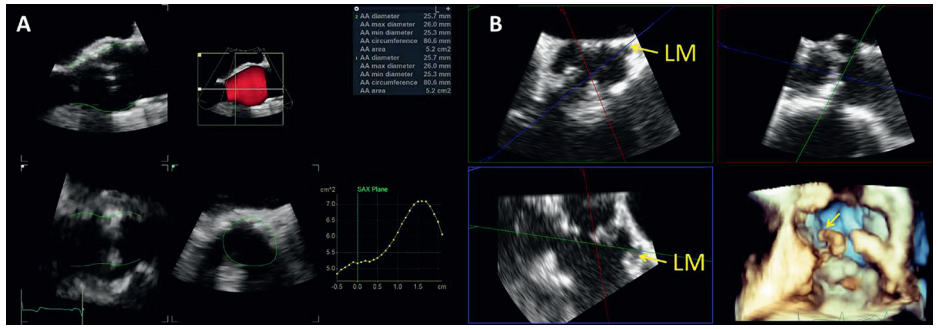

Figure 4: 3-dimensional transesophageal echocardiography (3D-TEE) in TAVR planning. (A) Automated analysis of the aortic root (AVQ software, GE, Horten, Norway) allows quick alignment of the orthogonal planes across the aortic annulus (AA) and accurate sizing. **(B)** Multiplanar 3D reconstruction of the aortic root to measure the distance between the main (LM) coronary artery from the aortic annulus (yellow arrows). At the same time the presence of bulky calcified cusps that may obstruct the coronary ostia can be appreciated, particularly in the 3D reconstruction.

During the procedure, aortic annulus can be also measured with supraaortic angiography during balloon aortic valvuloplasty (Figure 5). Several studies have shown the accuracy of this methodology to size the prosthesis.[35,36] During the balloon valvuloplasty, the presence of residual PVAR on angiography indicates undersized balloon.[36] Other authors have proposed the measurement of the balloon with sterile calipers during inflation at 2 atms and during full volume balloon inflation at the level of the valve any additional increase in the intraballoon pressure >2 atms will indicate that the diameter of the balloon is equal or larger than the aortic annulus.[35]

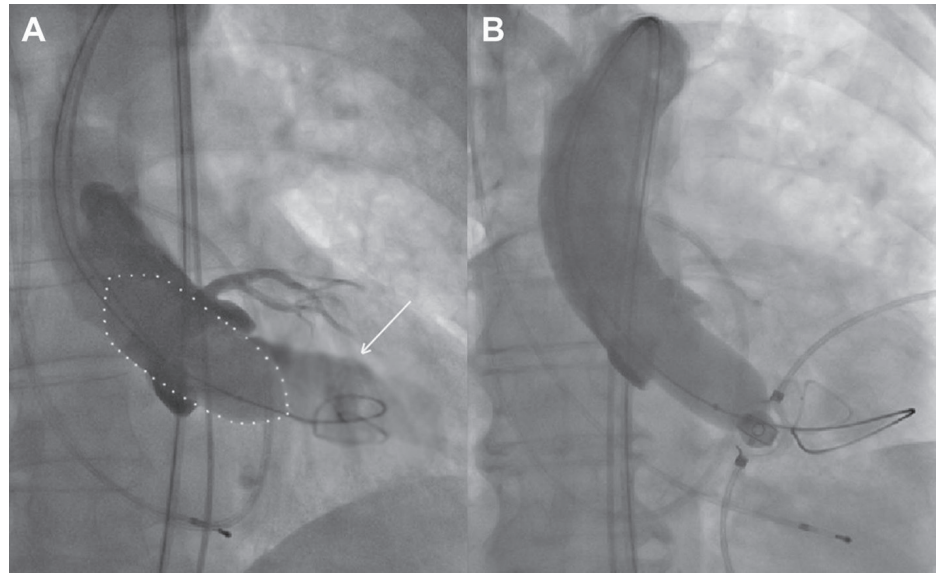

Figure 5: Supra-aortic angiography during balloon aortic valvuloplasty (BAV) for prosthesis size selection. (A) A 23-mm balloon (white dotted line) was chosen for a preparatory BAV according to the 2-dimensional transesophageal echocardiography (2D TEE) data on the aortic annulus size. Concurrent supra-aortic angiography, showing contrast regurgitation into the left ventricle (white arrow), indicated annulus size underestimation by 2D TEE and resulted in the selection of a bigger prosthesis. **(B)** Absence of contrast regurgitation into the left ventricle during BAV with a 23-mm balloon confirmed correct annular sizing based on pre-interventional 2D TEE. Reproduced with permission from Patsalis *et al*.[36]

Procedural access

One of the key aspects of preprocedural planning in TAVR is to choose the optimal access route. Potential TAVR access sites are transfemoral (TF), transapical (TA), transaortic (TAo), transsubclavian, transaxillary and transcarotid. The predominant approach worldwide is TF, since it is the least invasive and the most familiar to interventional cardiologists. According to the data from TAVR registries TF approach is chosen in Europe in 71-75%[37,38], while in USA in 56%.[39] Suitability of TF approach is predominately evaluated with angiographic assessment of the iliofemoral anatomy during coronary angiography. However, MDCT has shown better characterization of iliofemoral arteries and aortic size, tortuosity, degree of calcifications and plaque burden (Figure 6). Moreover, a detailed vascular anatomy can be clearly visualized with 3D volume rendered and multiplanar reconstructions. For currently available TAVR delivery catheters, a 6-6.5 mm threshold for minimal luminal vessel diameter of the femoral artery is considered to be acceptable.[40]

Traditionally the TA approach is preferred for patients whose peripheral vasculature is not suitable for TF. However, TA is the most invasive technique and it might be contraindicated in patients with certain comorbidities or high frailty indexes (severe pulmonary disease, chest wall deformity, very poor LV function, intracavitary thrombus). Alternatively, TAo has gained popularity due the simplicity of the procedure and superior results compared with the TA access in terms of survival.[41,42] MDCT analysis of the ascending aorta is essential in selecting patients for the TAo TAVR. The anterolateral portion of the ascending aorta 5-7 cm above the aortic annulus, where the cannulation of the aorta takes place (the so called TAo landing zone), should be free of calcium (Figure 6). Bapat *et al.*[43] have shown that the TAo approach is feasible in patients with severe aortic calcifications (porcelain aorta) since the TAo landing zone is frequently spared. Moreover, MDCT permits the evaluation of the spatial relationships between sternum and major vessels in the thorax. This is particularly important in patients with previous coronary artery bypass surgery, where a close proximity of the aforementioned structures or high proximal venous graft anastomoses affect the preferred TAo access route (e.g. opting for mini right thoracotomy instead of mini J sternotomy).[42]

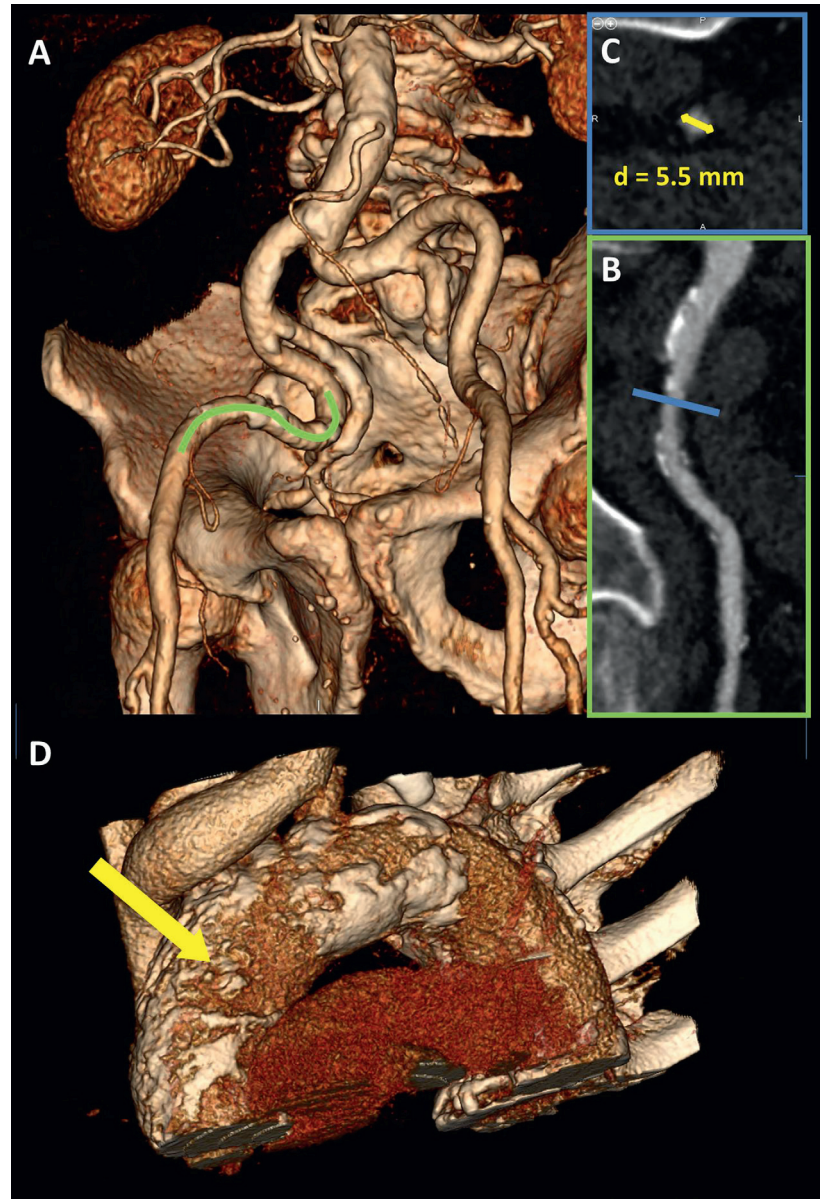

Figure 6: Assessment of TAVR access with multidetector row computed tomography (MDCT). (A) Severely tortuous iliofemoral arteries visualized with 3D volume rendering. **(B)** Segment of the right external iliac artery (green line) was more closely studied in a multiplanar reconstruction plane outlining high atherosclerotic burden with multiple plaques. **(C)** The cross-sectional lumen of the narrowest part of the vessel (blue line) was assessed. The smallest diameter was 5.5 mm (yellow arrow), precluding a safe transfemoral approach for the transcatheter aortic valve replacement (TAVR). **(D)** Severely calcified thoracic aorta – porcelain aorta particularly in the anterolateral portion of the ascendant aorta, corresponding to the landing zone for transaortic approach (yellow arrow).

IMAGING DURING TRANSCATHETER HEART VALVE IMPLANTATION

Procedural guidance during TAVR has been traditionally performed under fluoroscopy and angiography with the support of TEE (Figure 7).[44] This approach is still advocated by the European Association of Cardiovascular Imaging/American Society of Echocardiography (EACVI/ASE) recommendations.[45] However, current generation of TAVR devices with smaller delivery systems have increased the feasibility of TF approach, reduced procedural timings and invasiveness (similar to balloon valvuloplasty) questioning the need of general anesthesia. Indeed some large European TAVR centers have demonstrated excellent feasibility and safety of a simplified TF approach, performed using monitored anesthesia care (defined as cardiovascular and respiratory monitoring of the patient by a qualified anesthesiologist who may or may not be administering concomitant sedation[46]) or local anesthesia only.[47-49]

However, TEE, especially the real time 3D TEE, offers an incremental value over fluoroscopic and angiographic guidance in TAVR: it supports crossing severely calcified native aortic valve, significantly reduces radiation exposure and the use of nephrotoxic iodine contrast[50] and it allows detection of life-threatening complications at an early stage. Aortic annulus rupture, perforation of the myocardium with subsequent pericardial hemorrhage, coronary ostia occlusion resulting in myocardial ischemia, aortic perforation or dissection, prosthesis malpositioning or dislodgement and valvular or paravalvular leaks are the complications that TEE can immediately detect and influence the decision making (Figure 7).

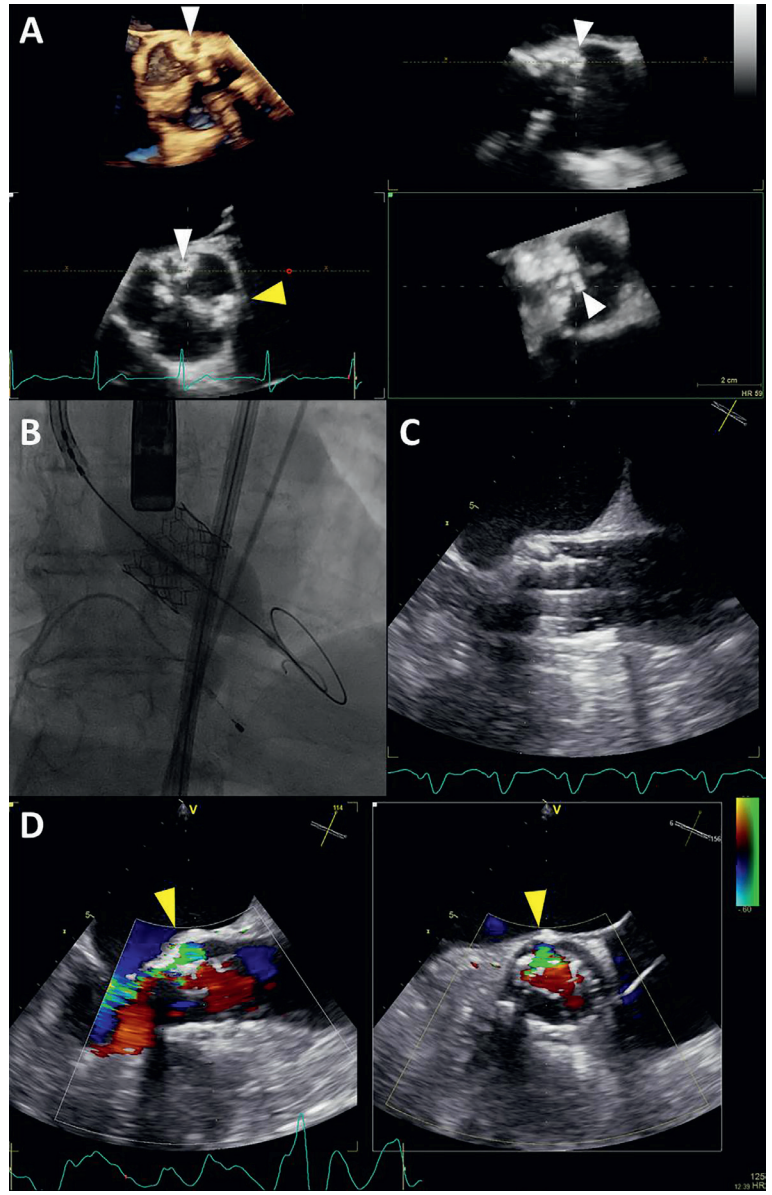

Figure 7: Multimodality imaging during transcatheter aortic valve replacement (TAVR). (A) Periprocedural 3-dimensional transesophageal echocardiography (3D-TEE) revealed severely calcified tricuspid aortic valve (AV). Particularly prominent calcifications were at the level of left- and non-coronary cusps commissure (white arrowheads) and at the level of left- and right-coronary cusps commissure (yellow arrowhead). **(B)** Balloon expandable transcatheter valve deployment, guided by fluoroscopy. **(C)** Concurrent real-time 2D-TEE image of the valve deployment. **(D)** Paravalvular aortic regurgitation (PVAR) visualized with colour Doppler biplane echocardiography (yellow arrowheads). PVAR originates at the level of highest annular calcification burden. The circumference of the PVAR is 20% of the prosthesis frame (short axis view on the right side), suggesting moderate PVAR according to Valve Academic Research Consortium-2 (VARC-2) criteria.[44]

Although currently available prostheses have been associated with lower incidence of significant aortic regurgitation (AR) after TAVR[51,52], this complication remains still of concern since it has been associated with poor prognosis[7,53]. Evaluating the presence and severity of AR should include assessment of both central and paravalvular components, with a combined measurement of "total" AR, reflecting the total volume load imposed on the LV. The methods used in native valve regurgitation (qualitative assessment of the color flow Doppler, vena contracta, pressure half-time on the continuous-wave Doppler recordings) are limited in the setting of paravalvular jets, which are frequently multiple, eccentric and irregular in shape. Moreover, certain portions of the prosthesis ring and LVOT may be difficult to image due to acoustic shadowing. The EACVI/ASE guidelines for evaluation of the prosthetic valves propose the proportion of the circumference of the sewing ring, occupied by the jets, as an alternative semi-quantitative measure of paravalvular aortic regurgitation (PVAR) severity: <10% of the sewing ring suggests mild, 10–20% moderate and >20% suggests severe PVAR.[54] The Valve Academic Research Consortium-2 (VARC-2) has slightly modified these cut-of values in the TAVR setting; mild, moderate, and severe PAVR are defined by <10%, 10 – 29% and ≥30% of the circumference of the prosthesis frame, respectively (Figure 7).[44] Regurgitant volume calculation can be helpful in the TAVR setting as well. The method relies on the comparison of stroke volumes across the AV and another non-regurgitant valve (either mitral or pulmonary). The former can be obtained by subtracting the LV end-systolic volume from the end-diastolic volume or (more commonly) by employing the continuity equation and calculating the stroke volume across the AV. The difference between the stroke volume across AV and the non-regurgitant valve represents the estimate of total AV regurgitant volume. Secondary indices, such as diastolic flow reversal in descending aorta, may provide additional help in assessing the severity of PVAR after TAVR.

Another alternative periprocedural imaging method is the transnasal TEE.[23,45] Smaller transnasal probes allow prolonged monitoring without general anesthesia. However, image quality is lower compared with conventional TEE and transnasal probes do not have 3D capabilities. Some centers have adapted intracardiac echo (ICE) for TAVR guidance.[55] The ICE probe is advanced through the femoral vein into the right atrium, where it brings a close-up view of the aortic root. In addition to obviating the need for general anesthesia, ICE allows uninterrupted monitoring in TAVR (no fluoroscopic interference) and more feasible Doppler-based assessment of pulmonary artery pressures.[55] ICE technology is quickly developing allowing also live 3D imaging (though with a limited 22-90° volume). However, the

need for high expertise, lower image quality in comparison to TEE (especially 3D), possible interference with the pacemaker lead and particularly its high cost limit the widespread use of ICE in TAVR.

LONG-TERM FOLLOW-UP

After TAVR, TTE remains the imaging technique of first choice to evaluate the procedural results, the durability of the prosthesis and changes in LV dimensions and function. Post-discharge clinical, ECG and TTE evaluations at 30 days after TAVR are mandatory.[23,44] Further follow-up recommendations suggest TTE evaluation at 6 months and 1 year following implantation and yearly thereafter.[44] The frequency of follow-up evaluations should be increased if there is any change in clinical status or worsening of echocardiographic findings. However, as the experience with TAVR grows, the frequency of TTE assessment may likely decline towards that of surgical AV replacement with proposed annual check-ups 5 years after valve implantation.[54]

In terms of durability of the implanted prosthesis, valve position, morphology of the prosthetic leaflets and indices of valve stenosis and regurgitation should be evaluated with echocardiography. When calculating the effective orifice area (EOA) or another index of valve opening that employs the ratio of pre- to post-valvular velocities (e.g. Doppler velocity index [DVI]) it is essential to record the pre-valvular velocity (and LVOT CSA) immediately proximal to the stent of the implanted prosthesis. Due to the flow acceleration within the stent, measuring velocities even proximal to the valve cusps results in an overestimation of EOA or AVA.[23,44,45] Clavel *et al.*[56] reported slightly superior hemodynamic performance of transcatheter prostheses compared with the surgical bioprostheses. Fifty patients, who underwent TAVR were matched 1:1 for sex, aortic annulus diameter, LVEF, body surface area, and body mass index with 2 groups of 50 patients that underwent surgical AV replacement with stented or stentless valve prosthesis. Mean transvalvular gradients at 6-12 months after the procedure were significantly lower in the TAVR group (10 ± 4 mm Hg) compared to the surgical AV replacement group with a stented frame prosthesis (13 ± 5 mm Hg) and non-significantly different to the surgical AV replacement group with a stentless valve (9 ± 4 mm Hg).[56] Better hemodynamic results of the transcatheter valves were attributed to the thinner stent frameworks. In addition, the 5-year follow-up results of the PARTNER trial show stable hemodynamic performance of the transcatheter and surgical prostheses without signs of valve degeneration (Figure 8).[7] However, Latib *et al.*[57]

showed in a retrospective analysis of 4266 patients who underwent TAVR in 12 different centers worldwide an incidence of 0.61% of transcatheter valve thrombosis after a median follow-up of 6 years. Of the 26 patients with suspected valve thrombosis, 92% presented with raised mean transvalvular gradients >20 mm Hg and 65% had exertional dyspnoea. Anticoagulation resulted in a significant decrease of transvalvular gradients in all medically treated cases.[57] However, recent studies using 4-dimensional MDCT have suggested that transcatheter valve thrombosis may be more frequent. Leetma *et al.*[58] reported an incidence of 4% in a cohort of 140 patients who underwent MDCT 1-3 months after TAVR. Transcatheter valve thrombosis was defined by the presence of leaflet thickening (low-attenuation masses attached to valve cusps or a diffuse thickening of ≥1 valve cusps) and restriction. Anticoagulation treatment was successful, leading to a complete resolution of thrombi on a control MDCT.[58] Theses MDCT findings may not be accompanied by changes in symptoms or changes in valve hemodynamics as assessed with TTE suggesting that MDCT may detect valve thrombosis at an earlier stage. Makkar *et al.*[8] reported reduced bioprosthesis leaflet motion, detected on 4-dimensional volume-rendered CT scans in 40% (22 of 55 patients) in the Portico Re-sheathable Transcatheter Aortic Valve System US IDE Trial (PORTICO IDE) and in 13% (17 of 132 patients) in two registries of aortic transcatheter and surgical bioprostheses in USA and Denmark. Restoration of leaflet motion was noted in all 11 patients who started warfarin anticoagulation after the CT findings and only in 1 of 10 patients who did not.[8] Of note, again no echocardiographic indices of valve dysfunction were noted. These findings indicated the need for prospective, well-designed, and adequately powered studies that will provide relevant answers about the clinical significance of these findings (both, in terms of neurological outcome and prosthesis durability), the optimal antithrombotic treatment after TAVR as well as the imaging approach in the long-term follow-up.

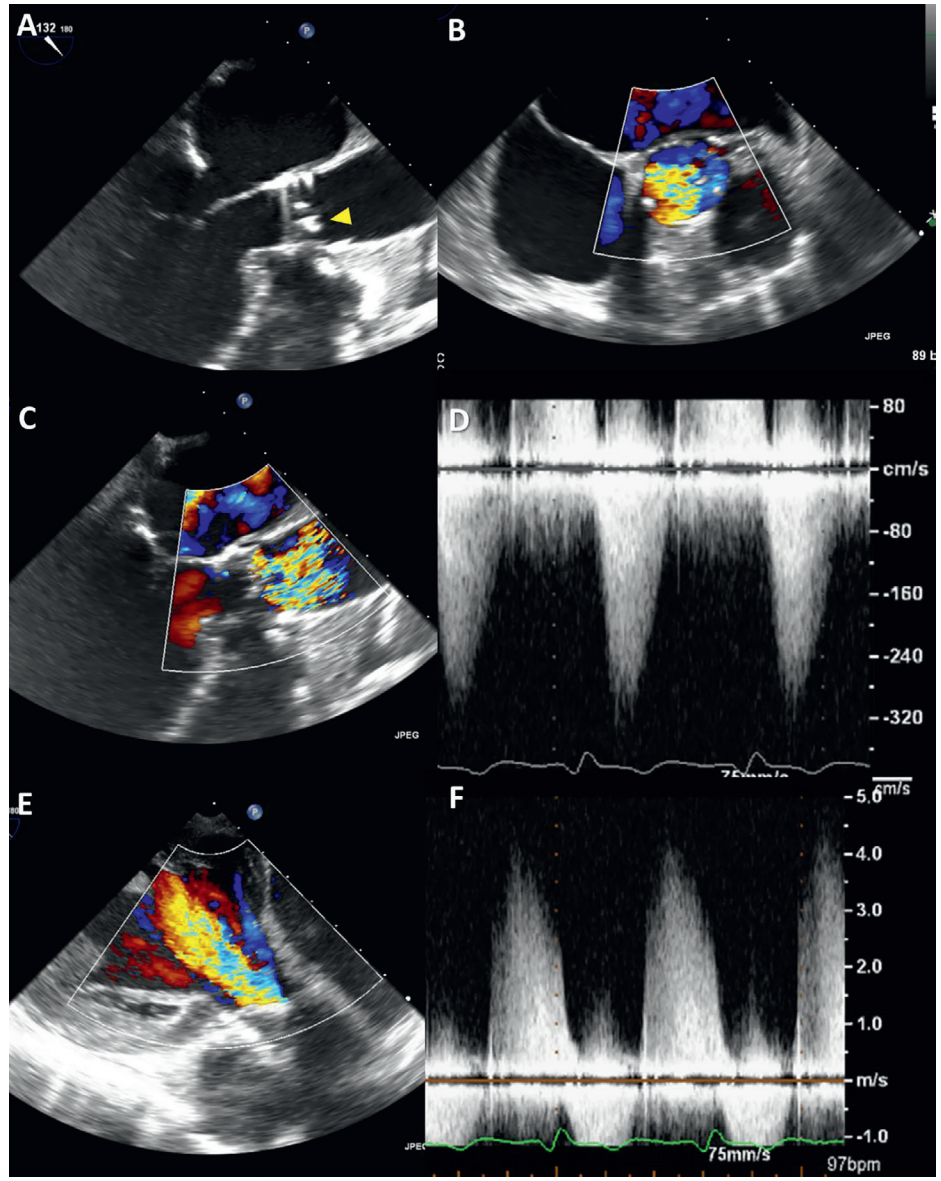

Figure 8: Prosthesis degeneration 4 years after transcatheter valve replacement (TAVR). (A) Transesophageal echocardiography (TEE) shows focally thickened and calcified prosthesis leaflets (yellow arrowhead). **(B)** Color Doppler image in the mid-esophageal short-axis view of the aortic valve reveals turbulent antegrade flow in a limited cross-sectional area. **(C)** Color Doppler of the long-axis view confirms high turbulence downstream the prosthesis, implying severe prosthetic valve stenosis. **(D)** High gradients obtained with continuous wave Doppler confirm significant prosthesis stenosis. **(E)** Color Doppler transgastric view shows severe aortic regurgitation. **(F)** High density and steep downsloping of the continuous wave Doppler recordings of the regurgitant flow confirm severe AR.

Changes in PAVR grade over time should be also evaluated at follow-up. In addition to TTE and TEE, CMR may be employed to assess the severity of PVAR. CMR phase-velocity mapping of the blood flow in ascendant aorta allows independent estimation of the AV regurgitant volume and regurgitant fraction.[59] Sherif *et al*.[60] have shown that quantitative measurements of AR by CMR is superior to semi-quantitative echocardiographic assessment with color flow Doppler imaging and that the latter may underestimate the degree of PVAR after TAVR.

Another adverse outcome after TAVR is infective endocarditis. Results from a large multicenter study report 0.50% incidence of infective endocarditis at 1 year after TAVR.[61] However, the outcome is devastating, with 47% and 66% mortality during the index hospitalization and at 1 year follow up, respectively.[61] TTE and, particularly with prosthetic valves, TEE are the first choice imaging techniques in the diagnostic workup of suspected infective endocarditis, helping to reveal the presence of vegetations, abscesses, pseudoaneurysms, their hemodynamic consequences (usually severe valvular or paravalvular AR), possible involvement of other valves (e.g. extension to anterior mitral leaflet) and to evaluate LV function. Importantly, infective endocarditis should always be suspected in patients with new periprosthetic regurgitation until proven otherwise.[62] Real time 3D TEE is of incremental value for the analysis of vegetation morphology and size and may lead to a better prediction of the embolic risk.[63] MDCT can be used to detect abscesses/pseudoaneurysms with a diagnostic accuracy similar to TEE, and is possibly superior in assessing the extent of perivalvular infective endocarditis extension.[64] In addition, nuclear molecular techniques, particularly radiolabeled white blood cell SPECT/CT and ^{18}F-FDG PET/CT imaging, are evolving as important supplementary methods for patients with suspected infective endocarditis. The main added value of these techniques is the reduction in the rate of misdiagnosed infective endocarditis, classified in the “Possible infective endocarditis” category using the Duke criteria, as well as the detection of peripheral embolic events.[65]

Table 1: Multimodality imaging techniques in TAVR.

Imaging technique	Pre-procedural	Peri-procedural	Follow-up
Echocardiography (TTE/TEE)	• AS severity • AV anatomy and degree of calcification • Aortic annulus size and root anatomy (3D) • Concomitant valvular disease • LV function	• Guiding catheters • Position and deployment of the prosthesis • Valve hemodynamics • Other procedure related complications (pericardial effusion, myocardial ischemia, aortic dissection…)	• Prosthesis deployment and hemodynamics • LV function • Concomitant valvular disease • Valve thrombosis, infective endocarditis (TEE)
Multidetector row Computed Tomography	• Aortic annulus size and root anatomy • AV anatomy and degree of calcification • Thoracic aorta, including calcification burden • Peripheral arteries • LV function • C-arm projections		• Deployment of prosthesis • Valve thrombosis (subclinical) • Infective endocarditis
Cardiac Magnetic Resonance	• Aortic annulus size and root anatomy • AV anatomy • LV function • Thoracic aorta • Peripheral arteries		• Prosthesis deployment and hemodynamics (regurgitation volume) • LV function
Fluoroscopy	• Aortic annulus dimension • Peripheral arteries	• Guiding catheters • Position and deployment of the prosthesis • Valve hemodynamics • Other procedure related complications (aortic annulus rupture, coronary ostia occlusion, aortic dissection…)	
Nuclear Imaging			• SPECT/CT and ^{18}F-FDG PET/CT in assessment of infective endocarditis

3D = 3-dimensional; ^{18}F-FDG PET = ^{18}F-fluorodeoxyglucose positron emission tomography; AS = aortic stenosis; AV = aortic valve; CT = computed tomography; LV = left ventricle; SPECT = single-photon emission computed tomography; TEE = transesophageal echocardiography: TTE = transthoracic echocardiography.

CONCLUSIONS

TAVR is an established therapy for patients with symptomatic severe AS and contraindications or high risk for surgery. To optimize the results of this therapy, accurate selection of patients, planning of the procedure and appropriate surveillance at follow-up are essential. Multimodality imaging plays a central role in these steps. The possibilities are numerous and the strengths and limitations of each imaging technique, the local expertise and availability are important to select the imaging technique to answer the questions arising at each procedural step (Table 1). The learning curve and cumulative evidence show superior accuracy of 3D imaging techniques to size the aortic annulus and select the prosthesis and the refinement in prosthesis design has led to important changes, reducing the invasiveness of the procedure

which is more frequently performed under conscious sedation, fully fluoroscopy guided and using TTE to evaluate the prosthesis function. However, the use of MDCT and CMR at follow-up has provided interesting findings that may have an impact on the management of the patients. Additional studies providing data on durability of the TAVR prostheses will shed light into the incidence of valve thrombosis and infective endocarditis.

REFERENCES

1. Leon MB, Smith CR, Mack M, Miller DC, Moses JW, Svensson LG *et al.* Transcatheter aortic-valve implantation for aortic stenosis in patients who cannot undergo surgery. *New England Journal of Medicine* 2010;363(17):1597-607.
2. Popma JJ, Adams DH, Reardon MJ, Yakubov SJ, Kleiman NS, Heimansohn D *et al.* Transcatheter aortic valve replacement using a self-expanding bioprosthesis in patients with severe aortic stenosis at extreme risk for surgery. *Journal of the American College of Cardiology* 2014;63(19):1972-81.
3. Adams DH, Popma JJ, Reardon MJ, Yakubov SJ, Coselli JS, Deeb GM *et al.* Transcatheter aortic-valve replacement with a self-expanding prosthesis. *New England Journal of Medicine* 2014;370(19):1790-8.
4. Smith CR, Leon MB, Mack MJ, Miller DC, Moses JW, Svensson LG *et al.* Transcatheter versus surgical aortic-valve replacement in high-risk patients. *New England Journal of Medicine* 2011;364(23):2187-98.
5. Holmes DR, Mack MJ. Uncertainty and Possible Subclinical Valve Leaflet Thrombosis. *New England Journal of Medicine* 2015;373(21):2080-2.
6. Kapadia SR, Leon MB, Makkar RR, Tuzcu EM, Svensson LG, Kodali S *et al.* 5-year outcomes of transcatheter aortic valve replacement compared with standard treatment for patients with inoperable aortic stenosis (PARTNER 1): a randomised controlled trial. *Lancet* 2015;385(9986):2485-91.
7. Mack MJ, Leon MB, Smith CR, Miller DC, Moses JW, Tuzcu EM *et al.* 5-year outcomes of transcatheter aortic valve replacement or surgical aortic valve replacement for high surgical risk patients with aortic stenosis (PARTNER 1): a randomised controlled trial. *Lancet* 2015;385(9986):2477-84.
8. Makkar RR, Fontana G, Jilaihawi H, Chakravarty T, Kofoed KF, De Backer O *et al.* Possible Subclinical Leaflet Thrombosis in Bioprosthetic Aortic Valves. *N Engl J Med* 2015;373(21):2015-24.
9. Joint Task Force on the Management of Valvular Heart Disease of the European Society of C, European Association for Cardio-Thoracic S, Vahanian A, Alfieri O, Andreotti F, Antunes MJ *et al.* Guidelines on the management of valvular heart disease (version 2012). *Eur Heart J* 2012;33(19):2451-96.
10. Nishimura RA, Otto CM, Bonow RO, Carabello BA, Erwin JP, 3rd, Guyton RA *et al.* 2014 AHA/ACC guideline for the management of patients with valvular heart disease: a report of the American College of Cardiology/American Heart Association Task Force on Practice Guidelines. *Journal of the American College of Cardiology* 2014;63(22):e57-185.
11. Baumgartner H, Hung J, Bermejo J, Chambers JB, Evangelista A, Griffin BP *et al.* Echocardiographic assessment of valve stenosis: EAE/ASE recommendations for clinical practice. *European Journal of Echocardiography* 2009;10(1):1-25.

12. Fougeres E, Tribouilloy C, Monchi M, Petit-Eisenmann H, Baleynaud S, Pasquet A *et al.* Outcomes of pseudo-severe aortic stenosis under conservative treatment. *European Heart Journal* 2012;33(19):2426-33.
13. Pibarot P, Dumesnil JG. Low-flow, low-gradient aortic stenosis with normal and depressed left ventricular ejection fraction. *Journal of the American College of Cardiology* 2012;60(19):1845-53.
14. Clavel M-A, Messika-Zeitoun D, Pibarot P, Aggarwal SR, Malouf J, Araoz PA *et al.* The complex nature of discordant severe calcified aortic valve disease grading: new insights from combined Doppler echocardiographic and computed tomographic study. *Journal of the American College of Cardiology* 2013;62(24):2329-38.
15. Cueff C, Serfaty JM, Cimadevilla C, Laissy JP, Himbert D, Tubach F *et al.* Measurement of aortic valve calcification using multislice computed tomography: correlation with haemodynamic severity of aortic stenosis and clinical implication for patients with low ejection fraction. *Heart* 2011;97(9):721-6.
16. Clavel M-A, Dumesnil JG, Capoulade R, Mathieu P, Sénéchal M, Pibarot P. Outcome of patients with aortic stenosis, small valve area, and low-flow, low-gradient despite preserved left ventricular ejection fraction. *Journal of the American College of Cardiology* 2012;60(14):1259-67.
17. Jander N, Minners J, Holme I, Gerdts E, Boman K, Brudi P *et al.* Outcome of patients with low-gradient “severe” aortic stenosis and preserved ejection fraction. *Circulation* 2011;123(8):887-95.
18. Poh KK, Levine RA, Solis J, Shen L, Flaherty M, Kang Y-J *et al.* Assessing aortic valve area in aortic stenosis by continuity equation: a novel approach using real-time three-dimensional echocardiography. *European Heart Journal* 2008;29(20):2526-35.
19. Ng AC, Delgado V, van der Kley F, Shanks M, van de Veire NR, Bertini M *et al.* Comparison of aortic root dimensions and geometries before and after transcatheter aortic valve implantation by 2-and 3-dimensional transesophageal echocardiography and multislice computed tomography. *Circulation: Cardiovascular Imaging* 2010;3(1):94-102.
20. Kamperidis V, van Rosendael PJ, Katsanos S, van der Kley F, Regeer M, Al Amri I *et al.* Low gradient severe aortic stenosis with preserved ejection fraction: reclassification of severity by fusion of Doppler and computed tomographic data. *European Heart Journal* 2015;36(31):2087-96.
21. Clavel M-A, Ennezat PV, Maréchaux S, Dumesnil JG, Capoulade R, Hachicha Z *et al.* Stress echocardiography to assess stenosis severity and predict outcome in patients with paradoxical low-flow, low-gradient aortic stenosis and preserved LVEF. *JACC: Cardiovascular Imaging* 2013;6(2):175-83.
22. Bax JJ, Delgado V, Bapat V, Baumgartner H, Collet JP, Erbel R *et al.* Open issues in transcatheter aortic valve implantation. Part 1: patient selection and treatment strategy for transcatheter aortic valve implantation. *European Heart Journal* 2014;35(38):2627-38.

23. Holmes DR, Jr., Mack MJ, Kaul S, Agnihotri A, Alexander KP, Bailey SR *et al.* 2012 ACCF/AATS/SCAI/STS expert consensus document on transcatheter aortic valve replacement. *Journal of the American College of Cardiology* 2012;59(13):1200-54.
24. Altiok E, Koos R, Schroder J, Brehmer K, Hamada S, Becker M *et al.* Comparison of two-dimensional and three-dimensional imaging techniques for measurement of aortic annulus diameters before transcatheter aortic valve implantation. *Heart* 2011;97(19):1578-84.
25. Jilaihawi H, Kashif M, Fontana G, Furugen A, Shiota T, Friede G *et al.* Cross-sectional computed tomographic assessment improves accuracy of aortic annular sizing for transcatheter aortic valve replacement and reduces the incidence of paravalvular aortic regurgitation. *Journal of the American College of Cardiology* 2012;59(14):1275-86.
26. Binder RK, Webb JG, Willson AB, Urena M, Hansson NC, Norgaard BL *et al.* The impact of integration of a multidetector computed tomography annulus area sizing algorithm on outcomes of transcatheter aortic valve replacement: a prospective, multicenter, controlled trial. *Journal of the American College of Cardiology* 2013;62(5):431-8.
27. Jilaihawi H, Doctor N, Kashif M, Chakravarty T, Rafique A, Makar M *et al.* Aortic annular sizing for transcatheter aortic valve replacement using cross-sectional 3-dimensional transesophageal echocardiography. *Journal of the American College of Cardiology* 2013;61(9):908-16.
28. Gurvitch R, Wood DA, Leipsic J, Tay E, Johnson M, Ye J *et al.* Multislice computed tomography for prediction of optimal angiographic deployment projections during transcatheter aortic valve implantation. *JACC: Cardiovascular Interventions* 2010;3(11):1157-65.
29. Kurra V, Kapadia SR, Tuzcu EM, Halliburton SS, Svensson L, Roselli EE *et al.* Pre-procedural imaging of aortic root orientation and dimensions: comparison between X-ray angiographic planar imaging and 3-dimensional multidetector row computed tomography. *JACC: Cardiovascular Interventions* 2010;3(1):105-13.
30. Tamborini G, Fusini L, Gripari P, Muratori M, Cefalù C, Maffessanti F *et al.* Feasibility and accuracy of 3DTEE versus CT for the evaluation of aortic valve annulus to left main ostium distance before transcatheter aortic valve implantation. *JACC: Cardiovascular Imaging* 2012;5(6):579-88.
31. Koos R, Altiok E, Mahnken AH, Neizel M, Dohmen G, Marx N *et al.* Evaluation of aortic root for definition of prosthesis size by magnetic resonance imaging and cardiac computed tomography: implications for transcatheter aortic valve implantation. *International Journal of Cardiology* 2012;158(3):353-8.
32. Smid M, Ferda J, Baxa J, Cech J, Hajek T, Kreuzberg B *et al.* Aortic annulus and ascending aorta: comparison of preoperative and perioperative measurement in patients with aortic stenosis. *European Journal of Radiology* 2010;74(1):152-5.

33. Murphy DT, Blanke P, Alaamri S, Naoum C, Rubinshtein R, Pache G *et al.* Dynamism of the aortic annulus: Effect of diastolic versus systolic CT annular measurements on device selection in transcatheter aortic valve replacement (TAVR). *Journal of cardiovascular computed tomography* 2015.
34. Achenbach S, Delgado V, Hausleiter J, Schoenhagen P, Min JK, Leipsic JA. SCCT expert consensus document on computed tomography imaging before transcatheter aortic valve implantation (TAVI)/transcatheter aortic valve replacement (TAVR). *Journal of cardiovascular computed tomography* 2012;6(6):366-80.
35. Babaliaros VC, Junagadhwalla Z, Lerakis S, Thourani V, Liff D, Chen E *et al.* Use of balloon aortic valvuloplasty to size the aortic annulus before implantation of a balloon-expandable transcatheter heart valve. *JACC: Cardiovascular Interventions* 2010;3(1):114-8.
36. Patsalis PC, Al-Rashid F, Neumann T, Plicht B, Hildebrandt HA, Wendt D *et al.* Preparatory balloon aortic valvuloplasty during transcatheter aortic valve implantation for improved valve sizing. *JACC: Cardiovascular Interventions* 2013;6(9):965-71.
37. Ludman PF, Moat N, de Belder MA, Blackman DJ, Duncan A, Banya W *et al.* Transcatheter aortic valve implantation in the United Kingdom: temporal trends, predictors of outcome, and 6-year follow-up: a report from the UK Transcatheter Aortic Valve Implantation (TAVI) Registry, 2007 to 2012. *Circulation* 2015;131(13):1181-90.
38. Gilard M, Eltchaninoff H, Iung B, Donzeau-Gouge P, Chevreul K, Fajadet J *et al.* Registry of transcatheter aortic-valve implantation in high-risk patients. *New England Journal of Medicine* 2012;366(18):1705-15.
39. Holmes DR, Brennan JM, Rumsfeld JS, Dai D, O'Brien SM, Vemulapalli S *et al.* Clinical outcomes at 1 year following transcatheter aortic valve replacement. *JAMA* 2015;313(10):1019-28.
40. Bax JJ, Delgado V, Bapat V, Baumgartner H, Collet JP, Erbel R *et al.* Open issues in transcatheter aortic valve implantation. Part 2: procedural issues and outcomes after transcatheter aortic valve implantation. *European Heart Journal* 2014;35(38):2639-54.
41. Bapat V, Khawaja MZ, Attia R, Narayana A, Wilson K, Macgillivray K *et al.* Transaortic transcatheter aortic valve implantation using Edwards Sapien valve. *Catheterization and Cardiovascular Interventions* 2012;79(5):733-40.
42. Bruschi G, de Marco F, Botta L, Cannata A, Oreglia J, Colombo P *et al.* Direct aortic access for transcatheter self-expanding aortic bioprosthetic valves implantation. *Annals of Thoracic Surgery* 2012;94(2):497-503.
43. Bapat VN, Attia RQ, Thomas M. Distribution of calcium in the ascending aorta in patients undergoing transcatheter aortic valve implantation and its relevance to the transaortic approach. *JACC: Cardiovascular Interventions* 2012;5(5):470-6.

44. Kappetein AP, Head SJ, Genereux P, Piazza N, van Mieghem NM, Blackstone EH *et al.* Updated standardized endpoint definitions for transcatheter aortic valve implantation: the Valve Academic Research Consortium-2 consensus document. *Journal of the American College of Cardiology* 2012;60(15):1438-54.
45. Zamorano JL, Badano LP, Bruce C, Chan K-L, Gonçalves A, Hahn RT *et al.* EAE/ASE recommendations for the use of echocardiography in new transcatheter interventions for valvular heart disease. *Journal of the American Society of Echocardiography* 2011;24(9):937-65.
46. Fröhlich GM, Lansky AJ, Webb J, Roffi M, Toggweiler S, Reinthaler M *et al.* Local versus general anesthesia for transcatheter aortic valve implantation (TAVR)–systematic review and meta-analysis. *BMC Medicine* 2014;12(1):41.
47. Durand E, Borz B, Godin M, Tron C, Litzler P-Y, Bessou J-P *et al.* Transfemoral aortic valve replacement with the Edwards SAPIEN and Edwards SAPIEN XT prosthesis using exclusively local anesthesia and fluoroscopic guidance: feasibility and 30-day outcomes. *JACC: Cardiovascular Interventions* 2012;5(5):461-7.
48. Greif M, Lange P, Nabauer M, Schwarz F, Becker C, Schmitz C *et al.* Transcutaneous aortic valve replacement with the Edwards SAPIEN XT and Medtronic CoreValve prosthesis under fluoroscopic guidance and local anaesthesia only. *Heart* 2014;100(9):691-5.
49. Kasel AM, Shivaraju A, Schneider S, Krapf S, Oertel F, Burgdorf C *et al.* Standardized methodology for transfemoral transcatheter aortic valve replacement with the Edwards Sapien XT valve under fluoroscopy guidance. *Journal of Invasive Cardiology* 2014;26(9):451-61.
50. Bagur R, Rodés-Cabau J, Doyle D, De Larochellière R, Villeneuve J, Lemieux J *et al.* Usefulness of TEE as the primary imaging technique to guide transcatheter transapical aortic valve implantation. *JACC: Cardiovascular Imaging* 2011;4(2):115-24.
51. Meredith Am IT, Walters DL, Dumonteil N, Worthley SG, Tchetche D, Manoharan G *et al.* Transcatheter aortic valve replacement for severe symptomatic aortic stenosis using a repositionable valve system: 30-day primary endpoint results from the REPRISE II study. *Journal of the American College of Cardiology* 2014;64(13):1339-48.
52. Seiffert M, Fujita B, Avanesov M, Lunau C, Schon G, Conradi L *et al.* Device landing zone calcification and its impact on residual regurgitation after transcatheter aortic valve implantation with different devices. *European Heart Journal Cardiovascular Imaging* 2015.
53. Athappan G, Patvardhan E, Tuzcu EM, Svensson LG, Lemos PA, Fraccaro C *et al.* Incidence, predictors, and outcomes of aortic regurgitation after transcatheter aortic valve replacement: meta-analysis and systematic review of literature. *Journal of the American College of Cardiology* 2013;61(15):1585-95.

54. Zoghbi WA, Chambers JB, Dumesnil JG, Foster E, Gottdiener JS, Grayburn PA *et al.* Recommendations for evaluation of prosthetic valves with echocardiography and doppler ultrasound: a report From the American Society of Echocardiography's Guidelines and Standards Committee and the Task Force on Prosthetic Valves, developed in conjunction with the American College of Cardiology Cardiovascular Imaging Committee, Cardiac Imaging Committee of the American Heart Association, the European Association of Echocardiography, a registered branch of the European Society of Cardiology, the Japanese Society of Echocardiography and the Canadian Society of Echocardiography, endorsed by the American College of Cardiology Foundation, American Heart Association, European Association of Echocardiography, a registered branch of the European Society of Cardiology, the Japanese Society of Echocardiography, and Canadian Society of Echocardiography. *Journal of the American Society of Echocardiography* 2009;22(9):975-1014; quiz 82-4.

55. Bartel T, Edris A, Velik-Salchner C, Muller S. Intracardiac echocardiography for guidance of transcatheter aortic valve implantation under monitored sedation: a solution to a dilemma? *European Heart Journal Cardiovascular Imaging* 2015.

56. Clavel M-A, Webb JG, Pibarot P, Altwegg L, Dumont E, Thompson C *et al.* Comparison of the hemodynamic performance of percutaneous and surgical bioprostheses for the treatment of severe aortic stenosis. *Journal of the American College of Cardiology* 2009;53(20):1883-91.

57. Latib A, Naganuma T, Abdel-Wahab M, Danenberg H, Cota L, Barbanti M *et al.* Treatment and clinical outcomes of transcatheter heart valve thrombosis. *Circulation: Cardiovascular Interventions* 2015;8(4).

58. Leetmaa T, Hansson NC, Leipsic J, Jensen K, Poulsen SH, Andersen HR *et al.* Early aortic transcatheter heart valve thrombosis: diagnostic value of contrast-enhanced multidetector computed tomography. *Circ Cardiovasc Interv* 2015;8(4).

59. Gelfand EV, Hughes S, Hauser TH, Yeon SB, Goepfert L, Kissinger KV *et al.* Severity of mitral and aortic regurgitation as assessed by cardiovascular magnetic resonance: optimizing correlation with Doppler echocardiography. *Journal of Cardiovascular Magnetic Resonance* 2006;8(3):503-7.

60. Sherif MA, Abdel-Wahab M, Beurich HW, Stocker B, Zachow D, Geist V *et al.* Haemodynamic evaluation of aortic regurgitation after transcatheter aortic valve implantation using cardiovascular magnetic resonance. *EuroIntervention* 2011;7(1):57-63.

61. Amat-Santos IJ, Messika-Zeitoun D, Eltchaninoff H, Kapadia S, Lerakis S, Cheema AN *et al.* Infective endocarditis after transcatheter aortic valve implantation: results from a large multicenter registry. *Circulation* 2015;131(18):1566-74.

62. Authors/Task Force M, Habib G, Lancellotti P, Antunes MJ, Bongiorni MG, Casalta JP *et al.* 2015 ESC Guidelines for the management of infective endocarditis: The Task Force for the Management of Infective Endocarditis of the European Society of Cardiology (ESC)Endorsed by: European Association for Cardio-Thoracic Surgery (EACTS), the European Association of Nuclear Medicine (EANM). *European Heart Journal* 2015.

63. Berdejo J, Shibayama K, Harada K, Tanaka J, Mihara H, Gurudevan SV *et al.* Evaluation of vegetation size and its relationship with embolism in infective endocarditis: a real-time 3-dimensional transesophageal echocardiography study. *Circulation: Cardiovascular Imaging* 2014;7(1):149-54.

64. Feuchtner GM, Stolzmann P, Dichtl W, Schertler T, Bonatti J, Scheffel H *et al.* Multislice computed tomography in infective endocarditis: comparison with transesophageal echocardiography and intraoperative findings. *Journal of the American College of Cardiology* 2009;53(5):436-44.

65. Saby L, Laas O, Habib G, Cammilleri S, Mancini J, Tessonnier L *et al.* Positron emission tomography/computed tomography for diagnosis of prosthetic valve endocarditis: increased valvular 18F-fluorodeoxyglucose uptake as a novel major criterion. *Journal of the American College of Cardiology* 2013;61(23):2374-82.

7

Influence of the quantity of aortic valve calcium on the agreement between automated 3-dimensional transesophageal echocardiography and multidetector row computed tomography for aortic annulus sizing

Tomaž Podlesnikar, Edgard A Prihadi, Philippe J van Rosendael, E Mara Vollema, Frank van der Kley, Arend de Weger, Nina Ajmone Marsan, Franjo Naji, Zlatko Fras, Jeroen J Bax, Victoria Delgado

Am J Cardiol. 2018 Jan 1;121(1):86-93

ABSTRACT

Background: Accurate aortic annulus sizing is key for selection of appropriate transcatheter aortic valve implantation (TAVI) prosthesis size. The present study compared novel automated 3-dimensional (3D) transesophageal echocardiography (TEE) software and multidetector row computed tomography (MDCT) for aortic annulus sizing and investigated the influence of the quantity of aortic valve calcium (AVC) on the selection of TAVI prosthesis size.

Methods: A total of 83 patients with severe aortic stenosis undergoing TAVI were evaluated with MDCT and 3D TEE. Maximal and minimal aortic annulus diameter, perimeter and area were measured. AVC was assessed with computed tomography. The low and high AVC burden groups were defined according to the median AVC score.

Results: Overall, 3D TEE measurements slightly underestimated the aortic annulus dimensions as compared to MDCT (mean differences between maximum, minimum diameter, perimeter and area: -1.7 mm, 0.5 mm, -2.7 mm and -13 mm^2, respectively). The agreement between 3D TEE and MDCT on aortic annulus dimensions was superior among patients with low AVC burden (<3025 AU) compared to patients with high AVC burden (≥3025 AU). The inter-observer variability was excellent for both methods. 3D TEE and MDCT lead to same prosthesis size selection in 88%, 95% and 81% of patients in the total population, the low and the high AVC burden group, respectively.

Conclusions: The novel automated 3D TEE imaging software allows accurate and highly reproducible measurements of the aortic annulus dimensions and shows excellent agreement with MDCT to determine the TAVI prosthesis size, particularly in patients with low AVC burden.

INTRODUCTION

Selection of appropriate transcatheter aortic valve implantation (TAVI) prosthesis size, based on accurate measurement of the aortic valve annulus, is crucial to avoid complications.[1] Although the aortic valve annulus is not an anatomical structure, it is defined as the virtual plane bisecting the nadirs of the aortic cusps in their insertion into the aortic wall. Multidetector row computed tomography (MDCT) is currently considered the reference standard to measure the aortic valve annulus. Three-dimensional (3D) transesophageal echocardiography (TEE) permits the acquisition of 3D data along the entire cardiac cycle, allowing for accurate measurements of the aortic annulus without use of nephrotoxic agents and risk of radiation. However, aortic valve calcification (AVC) may impact on the measurement accuracy of 3D TEE. This is an important clinical question, since TAVI is steadily increasing in lower operative risk populations and the most appropriate imaging technique should be chosen considering the accuracy and the potential risks. The present study compared the new automated 3D TEE software with manual MDCT measurements of the aortic annulus dimensions and assessed the agreement between both methods for TAVI prosthesis size selection. In addition, the analysis was stratified based on the AVC burden.

METHODS

Patient population

This retrospective analysis included patients with severe aortic stenosis who underwent clinically indicated TAVI at Leiden University Medical Center, Leiden, The Netherlands, between July 2015 and March 2017. Patients with pre-procedural MDCT data of the aortic valve acquired in systole and 3D TEE data acquired during the procedure with commercially available ultrasound system (E9 or E95 GE-Vingmed, Horten, Norway) were selected. Patients with valve-in-valve procedures were excluded.

Demographic and clinical data were prospectively collected in the departmental electronical clinical files (EPD Vision, Leiden, The Netherlands) and retrospectively analyzed. Baseline transthoracic echocardiographic and procedural TEE data were digitally stored and analyzed off-line with commercially available software (EchoPAC, version 201, GE-Vingmed, Horten, Norway). MDCT data were stored in institutional picture archiving and communication systems, and were analyzed off-line with commercially available software (Vitrea fX 6.7.4, Vital Images, Minnetonka, Minnesota). Aortic valve annulus was defined as the plane bisecting the

lowest insertion points of all 3 aortic valve cusps.[2,3] The agreement between automated 3D TEE software and manual analysis of MDCT data to measure the aortic valve annulus was evaluated within the overall population and divided according to the median value of AVC burden. For this retrospective analysis of clinically acquired data (which were handled anonymously), the institutional review board waived the need for patient's informed consent.

MDCT data acquisition and analysis

Patients underwent pre-procedural MDCT with the volumetric 320-slice MDCT scanner (AquilionOne, Toshiba Medical Systems, Tochigi-ken, Japan) as previously described.[4,5] Aortic valve morphology (tricuspid/bicuspid) was evaluated from double oblique transverse views of the aortic valve. On non-contrast calcium scans, the AVC was quantified according to the Agatston method,[6,7] and the calcium score was expressed in arbitrary units (AU) (Figure 1). The aortic annulus size was measured from the systolic images (30% to 35% of R-R interval) using multiplanar reformation planes (Figure 1). Maximum and minimum diameters, perimeter and planimetered area of the aortic annulus were measured and eccentricity index was calculated.[8]

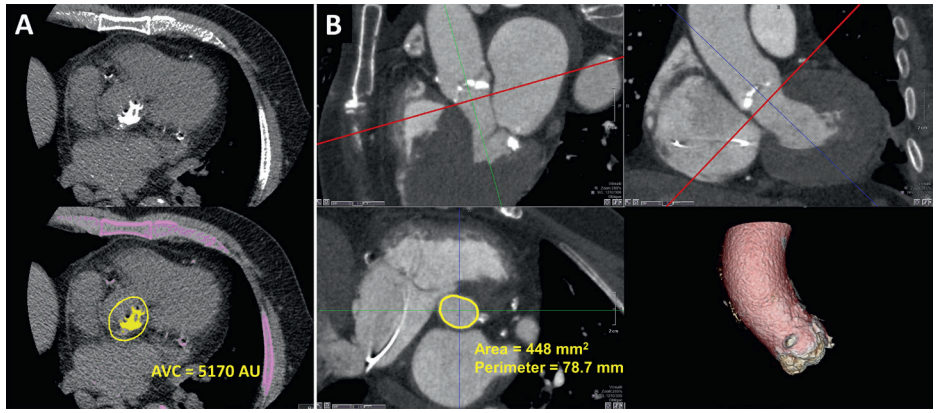

Figure 1: Multidetector row computed tomography of the aortic root. (A) Aortic valve calcium (AVC) burden assessment on non-contrast calcium scan. A series of contiguous transverse slices at the level of the aortic root encompassing the aortic valve were analyzed. The AVC score was determined by delineating the calcium of the aortic valve (yellow line in the bottom image) and expressed in arbitrary units (AU). Calcium in the coronary arteries, the mitral valve annulus and the aortic wall were excluded. **(B)** Multiplanar reconstruction of the aortic valve for measurements of the aortic annulus dimensions. Two orthogonal planes, bisecting the long axis of the left ventricular outflow tract and the ascending aorta, were carefully aligned and a third transverse plane (red line) was moved directly beneath the lowest insertion points of all 3 aortic cusps to obtain the double oblique transverse view of the aortic annulus. Maximum and minimum diameters, perimeter and aortic annulus area were obtained. The right lower image depicts the 3-dimensional volume rendered reconstruction of the aortic root.

3D TEE data acquisition and analysis

Peri-procedural TEE was performed in all patients with commercially available ultrasound systems (E9 or E95, GE-Vingmed, Horten, Norway). In addition to the standard 2-dimensional TEE views,[9] 3D datasets of the aortic valve were acquired from mid-esophageal long-axis or short-axis views of the aortic valve. Real-time single-beat 3D full volume images with at least a frame rate of 12 frames per second were acquired. To avoid shadowing of the anterior part of the aortic annulus caused by bulky calcifications of the aortic valve, out of plane images of the aortic root were acquired if needed (Figure 2). All images were digitally stored and the 3D aortic valve datasets were analyzed offline with 4D Automated Aortic Valve Quantification (4D Auto AVQ) software (EchoPAC, version 201, GE-Vingmed, Horten, Norway). The 4D Auto AVQ allowed automated computation of the mid-systolic dimensions of the aortic annulus (maximum and minimum diameter, perimeter and planimetered area) in 3 steps (Figure 3). In addition, the eccentricity index was calculated.[8]

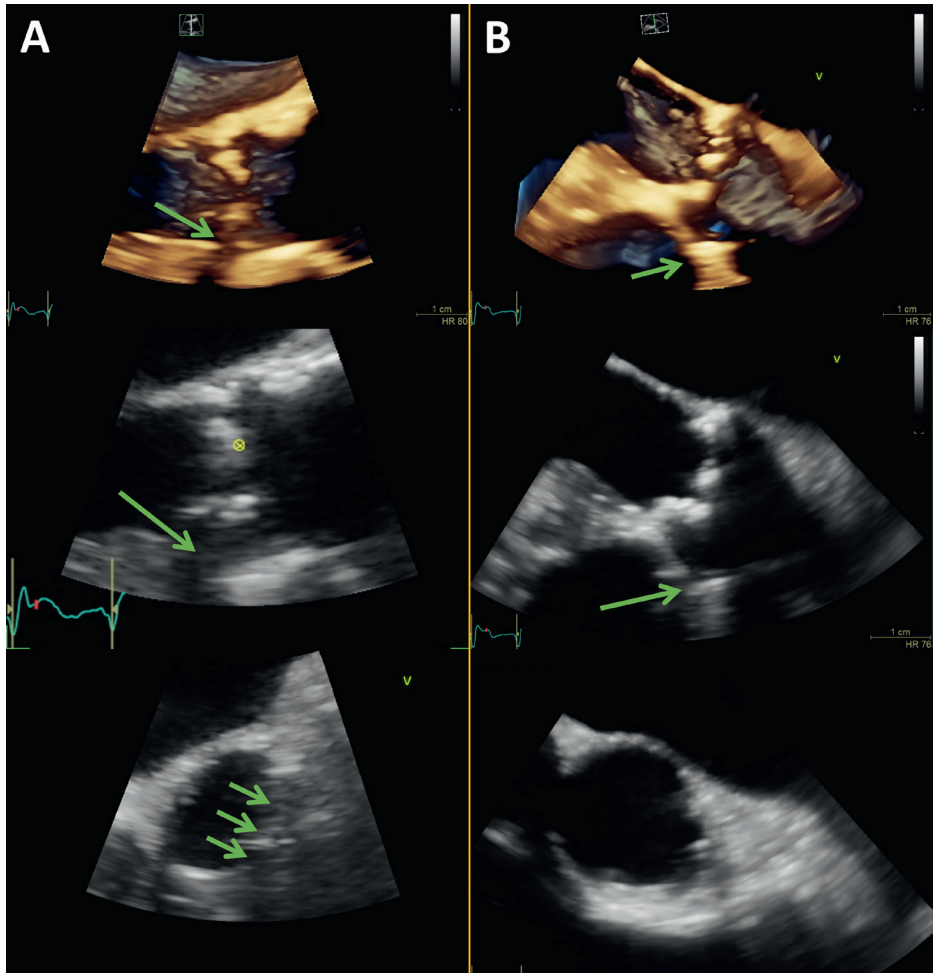

Figure 2: Three-dimensional transesophageal echocardiography acquisition. To avoid shadowing over the aortic annulus caused by calcified aortic cusps, two different 3-dimensional (3D) transesophageal echocardiography datasets of the aortic valve are presented side-to-side with 3D long-axis image on the top, 2-dimensional long-axis multiplanar reconstruction image in the middle and a short-axis multiplanar reconstruction image at the level of aortic annulus in the bottom. **(A)** The aortic valve is parallel to the ultrasound beam and the calcified aortic wall and aortic cusps cause extensive acoustic shadowing over the distal aortic annulus (green arrows), challenging the measurements of the aortic annulus dimensions. **(B)** the 3D aortic valve dataset was acquired with an oblique angle with respect to the ultrasound beam. The acoustic shadowing caused by the calcium is projected over the sinuses of Valsalva (green arrows), leaving the aortic annulus unaffected and enabling us to measure the aortic annulus dimensions accurately.

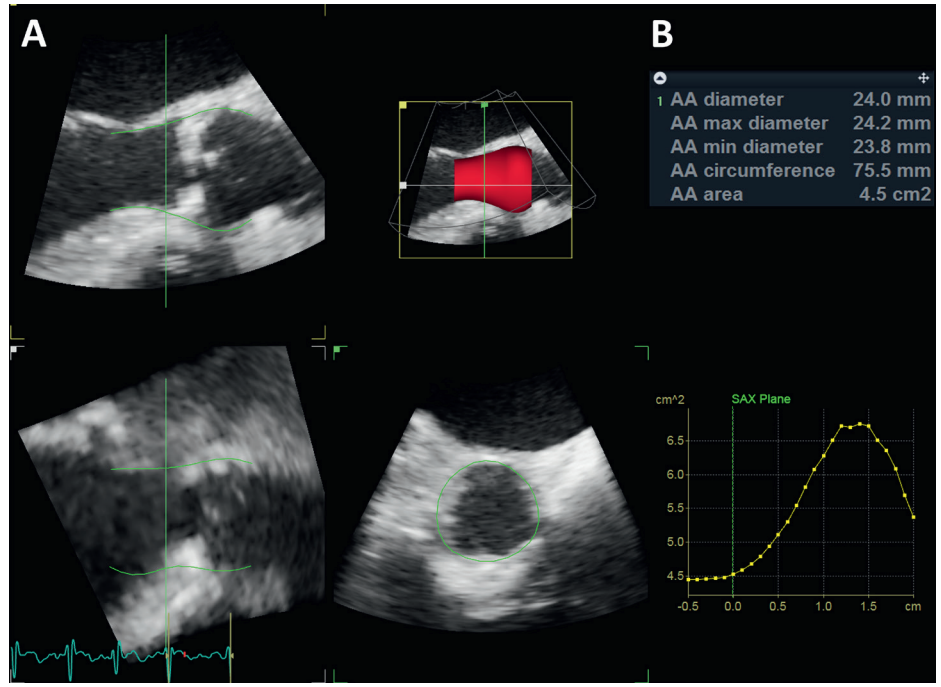

Figure 3: Automated 3-dimensional transesophageal echocardiography analysis of the aortic valve. **(A)** Mid-systolic multiplanar reconstruction of the aortic valve. First, the 2 long-axis orthogonal planes through the aortic valve were aligned and the transverse plane was moved to the hinge points of the aortic valve cusps. Subsequently, the software automatically delineated the left ventricular outflow tract and the aortic root anatomy, allowing for manual adjustments if needed. **(B)** Once the contouring of the aortic root and aortic annulus (AA) had been approved, the 4D Auto AVQ program automatically computed AA dimensions: average diameter (diameter calculated based on the perimeter), maximum and minimum diameter, perimeter and area of the aortic annulus. Graphical presentation of the cross-sectional area along the left ventricular outflow tract and the aortic root is shown below.

Prosthesis size selection

The TAVI prosthesis size was determined according to the sizing charts for the aortic annulus dimensions provided by the manufacturers. Edwards SAPIEN 3 prosthesis size was decided based on the measurements of the aortic annulus area with the following cut-off values: 338-430 mm^2 for a 23-mm, 430-546 mm^2 for a 26-mm, and 540-680 mm^2 for a 29-mm TAVI prosthesis size. Similarly, the Medtronic CoreValve Evolut prosthesis size was decided based on measurements of aortic annulus perimeter: 56.5-62.8 mm for a 23-mm, 62.8-72.3 mm for a 26-mm, and 72.3-81.7 mm for a 29-mm prosthesis size. Paravalvular leak after valve implantation was classified according to the Valve Academic Research Consortium-2 criteria.[10]

Statistical Analysis

Continuous variables are presented as mean ± standard deviation if normally distributed and as median and interquartile range otherwise. Categorical variables are shown as frequencies and percentages. Patients were divided into 2 groups according to the AVC burden: below and above the median value of AVC obtained on MDCT aortic valve calcium scans. Comparisons between the low and high AVC burden groups were performed using independent samples t-test, Mann-Whitney U test, Pearson Chi-Square test or Fischer's exact test, as appropriate. Fischer's exact test was used when the expected value of a categorical variable was <5. The agreement between 3D TEE and MDCT measurements of the aortic annulus dimensions was assessed with Bland and Altman method.[11] A single observer analyzed all data and a second observer, blinded to the results of the first observer, re-measured the first 35 3D TEE and MDCT datasets for assessment of inter-observer variability with intraclass correlation coefficients. Excellent agreement was defined as an intraclass correlation coefficient >0.8. The agreement between 3D TEE and MDCT to determine the TAVI prosthesis size was assessed with Kappa statistics. Excellent agreement was defined by a Kappa >0.8. All statistical analyses were performed using IBM SPSS Statistics 23 (IBM, Armonk, New York) and GraphPad Prism 7 (GraphPad Software, San Diego, California).

RESULTS

Of 85 patients with MDCT and 3D TEE data eligible for the analysis, 2 patients were excluded either due to poor 3D TEE image quality or ECG gating artefacts on MDCT at the level of aortic valve annulus, leaving 83 patients for the final analysis. Demographic, clinical, procedural, echocardiographic and MDCT characteristics are presented in Table 1.

Table 1: Demographic, clinical, procedural, echocardiographic, multidetector row computed tomography and 3-dimensional transesophageal echocardiography characteristics.

	Total population (N=83)	Aortic valve calcium burden		
		Low (N=41)	High (N=42)	P-value
Patient characteristics				
Age (years)	82 [77-86]	80 [75-85]	82 [79-86]	0.092
Men	39 (47%)	12 (29%)	27 (64%)	**0.001**
Body surface area (m^2)	1.84±0.23	1.81±0.20	1.87±0.25	0.274
Body mass index (kg/m^2)	27.0±4.5	27.1±4.5	26.8±4.6	0.805
Bicuspid aortic valve	2 (2%)	1 (2%)	1 (2%)	0.986
Logistic EuroSCORE (%)	13.1 [9.5-20.8]	13.2 [9.4-20.5]	12.6 [9.6-20.9]	0.884
Procedural characteristics				
Transcatheter aortic valve implantation access				0.668
Transfemoral	76 (92%)	37 (90%)	39 (93%)	
Transapical	7 (8%)	4 (10%)	3 (7%)	
Transcatheter aortic valve implantation prosthesis				0.364
Edwards SAPIEN 3	68 (82%)	32 (78%)	36 (86%)	
Medtronic CoreValve Evolut	15 (18%)	9 (22%)	6 (14%)	
More-than-mild paravalvular leak	1 (1%)	0	1 (2%)	1.000
Aortic annulus rupture	1 (1%)	0	1 (2%)	1.000
Echocardiography				
Peak transvalvular gradient (mmHg)	70±24	60±19	79±24	**<0.001**
Mean transvalvular gradient (mmHg)	44±16	38±14	51±16	**<0.001**
Aortic valve area (cm^2)	0.7±0.2	0.8±0.2	0.7±0.2	0.181
Aortic valve area index (cm^2/m^2)	0.40±0.09	0.42±0.10	0.38±0.08	**0.044**
Left ventricular stroke volume index (mL/m^2)	36±10	34±10	38±10	0.140
Left ventricular ejection fraction (%)	60 [42-71]	62 [43-70]	59 [40-72]	0.672
Multidetector row computed tomography				
Aortic valve calcium burden (AU)	3025 [1873-3870]	1873 [1198-2520]	3803 [3512-5176]	
Aortic annulus maximum diameter (mm)	27.3±2.9	26.4±3.0	28.0±2.6	**0.013**
Aortic annulus minimum diameter (mm)	22.1±2.4	21.3±2.0	22.9±2.6	**0.003**
Aortic annulus perimeter (mm)	78.4±8.3	75.6±7.6	81.2±8.0	**0.002**
Aortic annulus area (mm^2)	470±95	441±86	498±97	**0.006**
Eccentricity index	0.19	0.19	0.18	0.620
3-dimensional transesophageal echocardiography				
Aortic annulus maximum diameter (mm)	25.5±2.6	24.9±2.6	26.2±2.5	**0.024**
Aortic annulus minimum diameter (mm)	22.6±2.5	22.0±2.5	23.2±2.5	**0.027**
Aortic annulus perimeter (mm)	75.7±7.7	73.7±7.5	77.7±7.5	**0.019**
Aortic annulus area (mm^2)	458±95	434±90	481±96	**0.023**
Eccentricity index	0.11	0.11	0.11	0.915

Data are presented as mean ± standard deviation, median [interquartile range] or as number (percentage).
AU = arbitrary units.

Comparison of 3D TEE and MDCT measurements of the aortic annulus dimensions

In the overall population, 3D TEE slightly underestimated the aortic annulus maximum diameter, perimeter and area as compared to MDCT (Table 1, Figure 4). In contrast, 3D TEE yielded slightly larger minimum aortic annulus diameter, leading to smaller eccentricity index compared to MDCT (0.11 versus 0.19, P<0.001; respectively). There was a very good agreement between 3D TEE and MDCT for the measurement of the aortic annulus dimensions (Figure 4). Furthermore, excellent inter-observer agreement was observed for each imaging method in the subset of first 35 consecutive patients, with MDCT showing only minimally superior reproducibility than 3D TEE (Table 2).

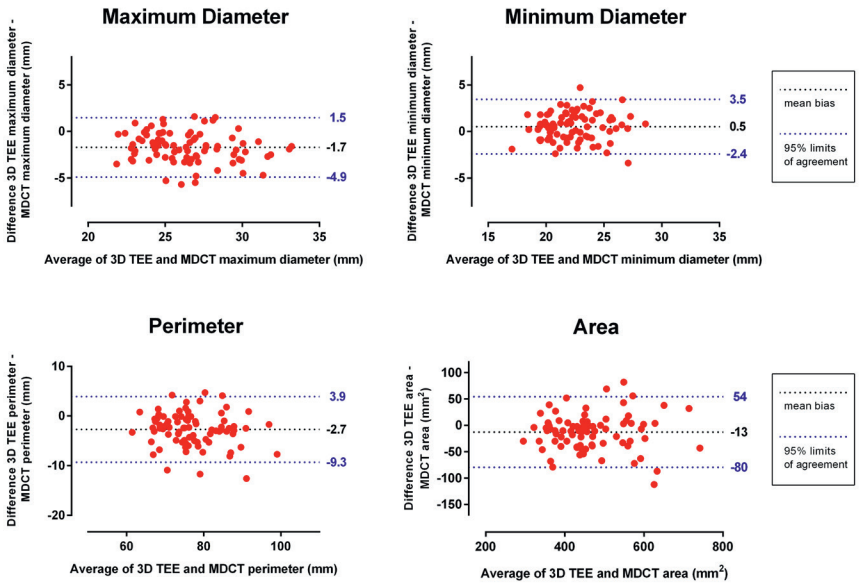

Figure 4: Agreement between automated 3D TEE software and MDCT for the measurement of the aortic annulus dimensions. Bland-Altman plots, showing overall good agreement between 3-dimensional (3D) transesophageal echocardiography (TEE) and multidetector row computed tomography (MDCT) on aortic annulus dimensions measurements.

Table 2: Inter-observer agreement for automated 3-dimensional transesophageal echocardiography analysis and multidetector row computed tomography for the measurement of the aortic annulus dimensions (N = 35 paired measurements).

	3-dimensional transesophageal echocardiography	Multidetector row computed tomography
Maximum diameter	0.912 (0.826-0.956)	0.962 (0.925-0.981)
Minimum diameter	0.925 (0.852-0.962)	0.950 (0.901-0.975)
Perimeter	0.963 (0.927-0.981)	0.984 (0.969-0.992)
Area	0.966 (0.934-0.983)	0.984 (0.943-0.994)

The intraclass correlation coefficients and the 95% confidence intervals are presented.

The effect of AVC burden on 3D TEE and MDCT derived aortic annulus dimensions

The median AVC burden on calcium scans was 3025 AU. Patients were divided into low AVC burden (<3025 AU) and high AVC burden (≥3025 AU). Patients with high AVC burden were more frequently men, had higher transaortic pressure gradients, smaller indexed aortic valve area and larger aortic annulus dimensions compared to patients with low AVC burden (Table 1). The AVC burden was not associated with the incidence of significant paravalvular regurgitation or aortic annulus rupture. The agreement between 3D TEE and MDCT for the measurement of the aortic annulus dimensions was superior among patients with low AVC burden as compared to patients with high AVC burden (Figure 5).

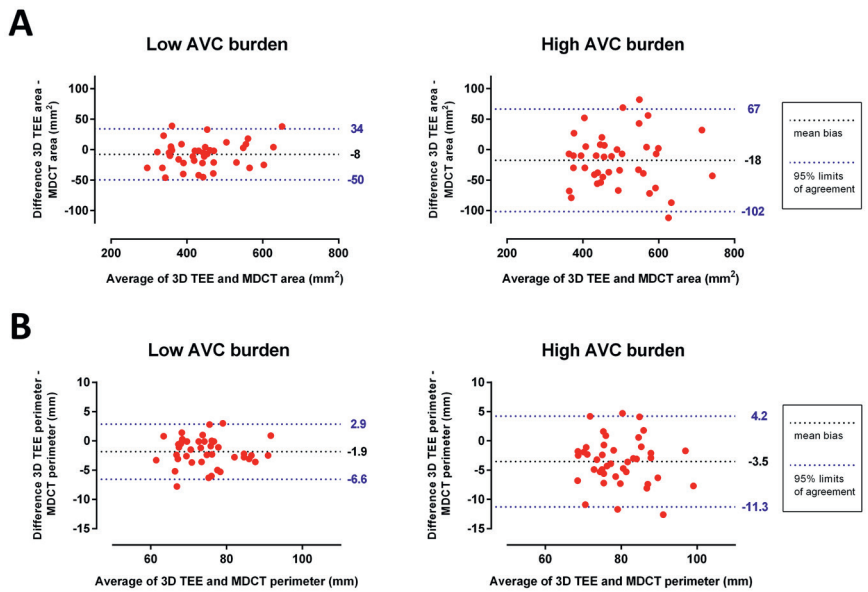

Figure 5: Agreement between automated 3D TEE software and MDCT for the measurement of the aortic annulus dimensions according to the AVC burden. Bland-Altman plots, showing better agreement between automated 3-dimensional (3D) transesophageal echocardiography (TEE) analysis and multidetector row computed tomography (MDCT) on aortic annulus area **(A)** and perimeter **(B)** in patients with low aortic valve calcium (AVC) burden, as compared to the patients with high AVC burden.

Agreement between 3D TEE and MDCT to determine the TAVI prosthesis size

In 73 (88%) patients, 3D TEE and MDCT measurements led to the selection of same TAVI prosthesis size, resulting in excellent agreement in the overall population (Kappa = 0.820) (Table 3). When dividing the population according to the AVC burden, the agreement between 3D TEE and MDCT was superior in the low AVC burden group (the same prosthesis size would have

been selected in 95% of patients, Kappa = 0.926) as compared to the high AVC burden group (agreement in 81% of patients, Kappa = 0.709). The agreement between 3D TEE and MDCT to determine the prosthesis size was not influenced by the eccentricity of the aortic annulus; the eccentricity indexes in 73 patients with concordant and 10 patients with discordant prosthesis sizing were 0.19 versus 0.16 (P=0.336) by MDCT and 0.12 versus 0.10 (P=0.554) by 3D TEE.

Table 3: Agreement between automated 3-dimensional transesophageal echocardiography analysis and multidetector row computed tomography on the selection of transcatheter aortic valve implantation prosthesis size. The agreement is shown for the total population, for the low aortic valve calcium burden group and for the high aortic valve calcium burden group.

TOTAL POPULATION (N=83)				
		Prosthesis size according to MDCT (N)		
		23 mm	**26 mm**	**29 mm**
Prosthesis size according to 3D TEE (N)	**23 mm**	22	7	
	26 mm		24	2
	29 mm		1	27
Inter-rater agreement: **Kappa = 0.820**				
Low aortic valve calcification (N=41)				
		Prosthesis size according to MDCT (N)		
		23 mm	**26 mm**	**29 mm**
Prosthesis size according to 3D TEE (N)	**23 mm**	15	2	
	26 mm		11	
	29 mm			13
Inter-rater agreement: **Kappa = 0.926**				
High aortic valve calcification (N=42)				
		Prosthesis size according to MDCT (N)		
		23 mm	**26 mm**	**29 mm**
Prosthesis size according to 3D TEE (N)	**23 mm**	7	5	
	26 mm		13	2
	29 mm		1	14
Inter-rater agreement: **Kappa = 0.709**				

3D = 3-dimensional; MDCT = multidetector row computed tomography; TEE = transesophageal echocardiography.

DISCUSSION

The present study demonstrates that novel automated 3D TEE imaging software (4D Auto AVQ) allows reliable assessment of aortic annulus dimensions in patients with severe aortic stenosis undergoing TAVI. Compared to MDCT, 3D TEE measurements slightly underestimated the aortic annulus dimensions, particularly in patients with high AVC burden. Importantly, 3D TEE measurements based on 4D Auto AVQ and MDCT led to the same prosthesis size

selection in the majority of the patients. However, the agreement between 3D TEE and MDCT on prosthesis size selection was better among patients with low versus high AVC burden.

Comparison of 3D TEE and MDCT measurements of the aortic annulus dimensions

Several studies have compared the agreement between 3D TEE and MDCT to measure the aortic annulus dimensions.[12-14] Ng *et al*.[12] demonstrated in 53 patients undergoing TAVI that the aortic annulus areas calculated from 3D TEE derived long-axis diameter, as well as measured by 3D TEE planimetry, were smaller compared to MDCT (4.06±0.79 cm^2 versus 4.22±0.77 cm^2 and 4.65±0.82 cm^2, respectively; P<0.001). Vaquerizo *et al*.[13] also showed significant underestimation of 3D TEE derived aortic annulus dimensions compared to MDCT (mean perimeter: 68.6±5.9 mm versus 75.1±5.7 mm, respectively; P<0.001; mean area: 345.6±64.5 mm^2 versus 426.9±68.9 mm^2, respectively; P<0.001). The methodology used to measure the aortic annulus has an important influence on the agreement between MDCT and 3D TEE. Khalique *et al*.[14] showed that when the aortic annulus was measured on 3D TEE data by using an off-label software that permits semiautomated delineation of the aortic annulus in the short-axis view, the underestimation of the aortic annulus size was less than with the manual tracing (435±81 mm^2 for semiautomated 3D TEE post-processing software versus 429±82 mm^2 for manual measurements versus 442±79 mm^2 for MDCT). Moreover, the semiautomated 3D TEE planimetry demonstrated better reproducibility of the aortic annulus measurements compared to manual planimetry. Similarly, we found a slight underestimation of the aortic annulus dimension using novel dedicated automated 3D TEE software as compared to MDCT. In addition, MDCT measurements resulted in larger aortic annulus eccentricity indexes compared to 3D TEE. Automated 3D TEE software algorithm may have accounted for a more circular shape of the aortic annulus; however, larger eccentricity indexes compared to MDCT have also been reported previously with manual 3D TEE measurements.[12,13]

The effect of AVC burden on 3D TEE and MDCT derived aortic annulus dimensions

One of the factors that may influence the accuracy of 3D TEE measurements of the aortic annulus is the AVC burden. Bulky calcification of the aortic valve leaflets and of the aortic root, causing acoustic shadowing over distal aortic annulus, pose a major challenge to accurately delineate the aortic annulus plane on 3D TEE. This may explain the better agreement between 3D TEE and MDCT in patients with low compared to high AVC burden in present study. The

deleterious effect of AVC on the definition of the aortic annulus plane can be reduced with appropriate 3D TEE data acquisition as indicated in Figure 2. However, it needs to be stressed that the terms low and high AVC burden groups identify patients in the upper and lower half of the AVC spectrum observed in our population. In fact, both groups of patients had extensively calcified aortic valves as the median AVC score to divide them into 2 groups, 3025 AU, was well above the suggested cutoff value for severe aortic stenosis proposed by Cueff *et al*.[15] (1651 AU) and by Clavel *et al*.[7] (1274 AU in women and 2065 AU in men). The importance of studying the impact of AVC on the accuracy of aortic annulus measurements should be viewed from the perspective of the anticipated TAVI use in intermediate and eventually low risk patients with severe aortic stenosis and in patients with moderate aortic stenosis with concomitant left ventricular systolic dysfunction, where the AVC burden might be lower than in the classical high risk aortic stenosis population.[16,17] Our results suggest that in these clinical scenarios 3D TEE might represent an attractive alternative to MDCT for preoperative TAVI assessment.

Agreement between 3D TEE and MDCT to determine the TAVI prosthesis size

The agreement between 3D TEE and MDCT to determine the TAVI prosthesis size has been described before.[13,14,18] Vaquerizo *et al*.[13] reported that MDCT and 3D TEE agreed in the prosthesis size in only 44% of patients, if the size was determined by aortic annulus perimeter, and in 38%, if the size was determined by aortic annulus area. On the other hand, Khalique *et al*.[14] observed excellent agreement between 3D TEE and MDCT valve sizing protocols (based on the aortic annulus area); in 94% of patients both imaging techniques would have recommended the same prosthesis size. Husser *et al*.[18] applied the long-axis aortic annulus diameter measurements to determine the TAVI prosthesis size and reported congruent results between 3D TEE and MDCT in 77% of patients (N = 57). Similarly, the present study showed excellent agreement between 3D TEE and MDCT, leading to the same prosthesis size selection in 88% of the patients. When dividing the population according to the AVC burden, the agreement between 3D TEE and MDCT further improved in patients with low AVC burden, as the same prosthesis size was recommended in 95% of patients, whereas high AVC burden had a negative impact, reducing the agreement to 81% of patients. In the majority of patients with high AVC burden and prosthesis-size mismatch, 3D TEE measurements suggested smaller prosthesis size compared to MDCT. Future studies are therefore needed to determine whether these patients require different prosthesis sizing recommendations when assessed with 3D TEE.

Study limitations

The study was conducted retrospectively, in a single center. The impact of this automated post-processing software of 3D TEE data on annulus sizing, prosthesis selection and paravalvular regurgitation rates was not prospectively assessed. No automated MDCT software was used, the measurements were performed manually. However, the observers measuring MDCT data are highly experienced and have reported good inter- and intra-observer reproducibility.[19] In the view of 3D TEE versus MDCT assessment of aortic annulus dimensions, it needs to be emphasized that MDCT allows for simultaneous peripheral arteries anatomy assessment and the planning of the C-arm projections needed for aortic valve prosthesis deployment.

CONCLUSION

Novel automated 3D TEE imaging software (4D Auto AVQ) allows accurate and highly reproducible measurements of aortic annulus dimensions and shows excellent agreement with MDCT to determine the TAVI prosthesis size. 3D TEE performs particularly well in patients with low AVC burden. In case of contraindications for MDCT, 3D TEE is an excellent alternative for preoperative assessment of candidates for TAVI.

REFERENCES

1. Bax JJ, Delgado V, Bapat V, Baumgartner H, Collet JP, Erbel R *et al.* Open issues in transcatheter aortic valve implantation. Part 1: patient selection and treatment strategy for transcatheter aortic valve implantation. *European Heart Journal* 2014;35(38):2627-38.
2. Piazza N, de Jaegere P, Schultz C, Becker AE, Serruys PW, Anderson RH. Anatomy of the aortic valvar complex and its implications for transcatheter implantation of the aortic valve. *Circ Cardiovasc Interv* 2008;1(1):74-81.
3. Kasel AM, Cassese S, Bleiziffer S, Amaki M, Hahn RT, Kastrati A *et al.* Standardized imaging for aortic annular sizing: implications for transcatheter valve selection. *JACC: Cardiovascular Imaging* 2013;6(2):249-62.
4. Delgado V, Ng AC, van de Veire NR, van der Kley F, Schuijf JD, Tops LF *et al.* Transcatheter aortic valve implantation: role of multi-detector row computed tomography to evaluate prosthesis positioning and deployment in relation to valve function. *Eur Heart J* 2010;31(9):1114-23.
5. van Rosendael PJ, Kamperidis V, Kong WK, van Rosendael AR, Marsan NA, Bax JJ *et al.* Comparison of Quantity of Calcific Deposits by Multidetector Computed Tomography in the Aortic Valve and Coronary Arteries. *Am J Cardiol* 2016;118(10):1533-8.
6. Agatston AS, Janowitz WR, Hildner FJ, Zusmer NR, Viamonte M, Jr., Detrano R. Quantification of coronary artery calcium using ultrafast computed tomography. *J Am Coll Cardiol* 1990;15(4):827-32.
7. Clavel M-A, Messika-Zeitoun D, Pibarot P, Aggarwal SR, Malouf J, Araoz PA *et al.* The complex nature of discordant severe calcified aortic valve disease grading: new insights from combined Doppler echocardiographic and computed tomographic study. *Journal of the American College of Cardiology* 2013;62(24):2329-38.
8. Doddamani S, Bello R, Friedman MA, Banerjee A, Bowers JH, Jr., Kim B *et al.* Demonstration of left ventricular outflow tract eccentricity by real time 3D echocardiography: implications for the determination of aortic valve area. *Echocardiography* 2007;24(8):860-6.
9. Hahn RT, Abraham T, Adams MS, Bruce CJ, Glas KE, Lang RM *et al.* Guidelines for performing a comprehensive transesophageal echocardiographic examination: recommendations from the American Society of Echocardiography and the Society of Cardiovascular Anesthesiologists. *J Am Soc Echocardiogr* 2013;26(9):921-64.
10. Kappetein AP, Head SJ, Genereux P, Piazza N, van Mieghem NM, Blackstone EH *et al.* Updated standardized endpoint definitions for transcatheter aortic valve implantation: the Valve Academic Research Consortium-2 consensus document. *Eur Heart J* 2012;33(19):2403-18.

11. Bland JM, Altman DG. Statistical methods for assessing agreement between two methods of clinical measurement. *Lancet* 1986;1(8476):307-10.
12. Ng AC, Delgado V, van der Kley F, Shanks M, van de Veire NR, Bertini M *et al.* Comparison of aortic root dimensions and geometries before and after transcatheter aortic valve implantation by 2-and 3-dimensional transesophageal echocardiography and multislice computed tomography. *Circulation: Cardiovascular Imaging* 2010;3(1):94-102.
13. Vaquerizo B, Spaziano M, Alali J, Mylote D, Theriault-Lauzier P, Alfagih R *et al.* Three-dimensional echocardiography vs. computed tomography for transcatheter aortic valve replacement sizing. *Eur Heart J Cardiovasc Imaging* 2016;17(1):15-23.
14. Khalique OK, Hamid NB, White JM, Bae DJ, Kodali SK, Nazif TM *et al.* Impact of Methodologic Differences in Three-Dimensional Echocardiographic Measurements of the Aortic Annulus Compared with Computed Tomographic Angiography Before Transcatheter Aortic Valve Replacement. *J Am Soc Echocardiogr* 2017;30(4):414-21.
15. Cueff C, Serfaty JM, Cimadevilla C, Laissy JP, Himbert D, Tubach F *et al.* Measurement of aortic valve calcification using multislice computed tomography: correlation with haemodynamic severity of aortic stenosis and clinical implication for patients with low ejection fraction. *Heart* 2011;97(9):721-6.
16. Thyregod HG, Steinbruchel DA, Ihlemann N, Nissen H, Kjeldsen BJ, Petursson P *et al.* Transcatheter Versus Surgical Aortic Valve Replacement in Patients With Severe Aortic Valve Stenosis: 1-Year Results From the All-Comers NOTION Randomized Clinical Trial. *J Am Coll Cardiol* 2015;65(20):2184-94.
17. Spitzer E, Van Mieghem NM, Pibarot P, Hahn RT, Kodali S, Maurer MS *et al.* Rationale and design of the Transcatheter Aortic Valve Replacement to UNload the Left ventricle in patients with ADvanced heart failure (TAVR UNLOAD) trial. *Am Heart J* 2016;182:80-8.
18. Husser O, Holzamer A, Resch M, Endemann DH, Nunez J, Bodi V *et al.* Prosthesis sizing for transcatheter aortic valve implantation--comparison of three dimensional transesophageal echocardiography with multislice computed tomography. *Int J Cardiol* 2013;168(4):3431-8.
19. Delgado V, Ng AC, Schuijf JD, van der Kley F, Shanks M, Tops LF *et al.* Automated assessment of the aortic root dimensions with multidetector row computed tomography. *Ann Thorac Surg* 2011;91(3):716-23.

8

Cardiovascular magnetic resonance imaging to assess myocardial fibrosis in valvular heart disease

Tomaž Podlesnikar, Victoria Delgado, Jeroen J Bax

Int J Cardiovasc Imaging 2018;34(1):97-112

ABSTRACT

The left ventricular (LV) remodeling process associated with significant valvular heart disease (VHD) is characterized by an increase of myocardial interstitial space with deposition of collagen and loss of myofibers. These changes occur before LV systolic function deteriorates or the patient develops symptoms. Cardiovascular magnetic resonance (CMR) permits assessment of reactive fibrosis, with the use of T1 mapping techniques, and replacement fibrosis, with the use of late gadolinium contrast enhancement. In addition, functional consequences of these structural changes can be evaluated with myocardial tagging and feature tracking CMR, which assess the active deformation (strain) of the LV myocardium. Several studies have demonstrated that CMR techniques may be more sensitive than the conventional measures (LV ejection fraction or LV dimensions) to detect these structural and functional changes in patients with severe left-sided VHD and have shown that myocardial fibrosis may not be reversible after valve surgery. More important, the presence of myocardial fibrosis has been associated with lesser improvement in clinical symptoms and recovery of LV systolic function. Whether assessment of myocardial fibrosis may better select the patients with severe left-sided VHD who may benefit from surgery in terms of LV function and clinical symptoms improvement, needs to be demonstrated in prospective studies. The present review article summarizes the current status of CMR techniques to assess myocardial fibrosis and appraises the current evidence on the use of these techniques for risk stratification of patients with severe aortic stenosis or regurgitation and mitral regurgitation.

INTRODUCTION

Valvular heart disease (VHD) is an important public-health problem with an increasing prevalence along with ageing of the population.[1] Moderate and severe VHD on echocardiography affects 2.5% of the population of the United States and increases up to 11.7% in the group of patients aged 75 and older.[2] The decision to operate in patients with severe VHD is frequently complex and relies on an individual risk-benefit analysis. In general, improvement in prognosis compared with natural history of the disease should outweigh the risk of intervention and its potential late consequences, particularly prosthesis-related complications. Current guidelines recommend to intervene in patients with symptomatic severe VHD and in asymptomatic patients with reduced left ventricular (LV) ejection fraction, LV dilatation, pulmonary hypertension, right ventricular dilatation and dysfunction and presence of atrial fibrillation.[1,3] However, most of these adverse consequences of severe VHD are observed in advanced stages of the disease and are partially irreversible after intervention, leading to suboptimal long-term clinical outcomes.[4] Therefore, additional markers that identify early structural and functional consequences of severe VHD before irreversible damage of the myocardium occurs would help to redefine the optimal timing for intervention.

Chronic pressure and volume overload caused by severe left-sided VHD results in LV remodeling. Changes in the extracellular matrix with deposition of collagen I and loss of myofibers at a later stage result in myocardial fibrosis, the hallmark of LV remodeling.[5,6] Cardiovascular magnetic resonance (CMR) imaging techniques permit direct and indirect assessment of myocardial fibrosis. T1 mapping and late gadolinium enhancement (LGE) permit myocardial tissue characterization and provide measures of direct myocardial fibrosis whereas CMR tagging and feature tracking CMR allow for assessment of myocardial deformation (strain), a functional parameter that indirectly reflects myocardial fibrosis. In addition, advances in molecular CMR imaging provide high-specificity tools for detection of myocardial fibrosis. This article provides an overview of current CMR techniques to assess myocardial fibrosis in patients with left-sided VHD.

CMR TECHNIQUES FOR DIRECT ASSESSMENT OF MYOCARDIAL FIBROSIS

LV remodeling in response to chronic pressure and volume overload caused by VHD is characterized by progressive increase of the interstitial space with increased collagen volume

fraction (reactive fibrosis) and eventually apoptosis of myocardial cells which are replaced by firm fibrous tissue (replacement fibrosis or scar). T1 mapping and LGE CMR techniques are currently the most frequently used techniques to directly assess myocardial fibrosis (Table 1).

Table 1: Cardiovascular magnetic resonance techniques to assess myocardial fibrosis valvular heart disease.

CMR technique	Availability	Fibrosis specificity	Advantages	Limitations	Experience in VHD
T1 mapping (native T1 and ECV quantification)	++	+++	Assessment of diffuse fibrosis, early disease changes (preclinical stages). Quantification of the degree of fibrosis.	Multiple methodologies, no standardized reference values, overlap between normal and diseased myocardium.	++
Late gadolinium enhancement	+++	+++	Reference standard for assessment of replacement fibrosis.	Focal fibrosis assessment only.	+++
Molecular imaging	±	++++	Improved visualization of fibrosis, investigation of underlying processes (necrosis, apoptosis, inflammation, scar maturation…).	Experimental technique, animal studies only.	-
CMR tagging	++	+	Current gold standard for myocardial deformation assessment, high reproducibility of the results.	Expertise, additional scan sequences, time consuming post-processing, tag fading through cardiac cycle (only with some techniques), limited in assessment of thin myocardium.	++
Feature tracking CMR	+++	+	Post-processing of SSFP cines (no additional scan sequences), relatively fast post-processing, high feasibility.	Susceptible to through-plane motion artifacts, limited inter-vendor agreement.	+

CMR = cardiovascular magnetic resonance; ECV = extracellular volume; SSFP = steady state free precession; VHD = valvular heart disease.

CMR T1 mapping

The longitudinal magnetization relaxation time of the myocardium, so-called T1 time, is highly sensitive to processes that increase the interstitial space and can be quantified with various techniques.[7] One of the most commonly used in clinical practice is the modified Look-Locker pulse sequence where multiple single-shot images are acquired intermittently in diastole during 9-17 cardiac cycles and the inversion recovery curves are generated (Figure 1, panels A and B). The T1 time can be obtained for any myocardial segment and T1 maps can be generated by determining the T1 time at each pixel location (Figure 1, panel C). Three T1 mapping-derived metrics have been proposed as markers of increased myocardial fibrosis: the native T1 time, the post-contrast T1 time and the myocardial extracellular volume (ECV). With the increase of interstitial fibrosis, the native T1 values (without the use of gadolinium contrast) become longer whereas the post-contrast T1 values become shorter. By combining them, myocardial ECV fraction can be

computed, which quantifies the extracellular matrix space. In the absence of amyloid deposition or edema, collagen I is the main component of the extracellular matrix space and therefore the myocardial ECV fraction is considered a robust marker of myocardial fibrosis.[8-10] The added value of these metrics over LGE is the ability to quantify the degree of fibrosis and, particularly, to detect diffuse interstitial fibrosis, often associated with early stages of the disease.

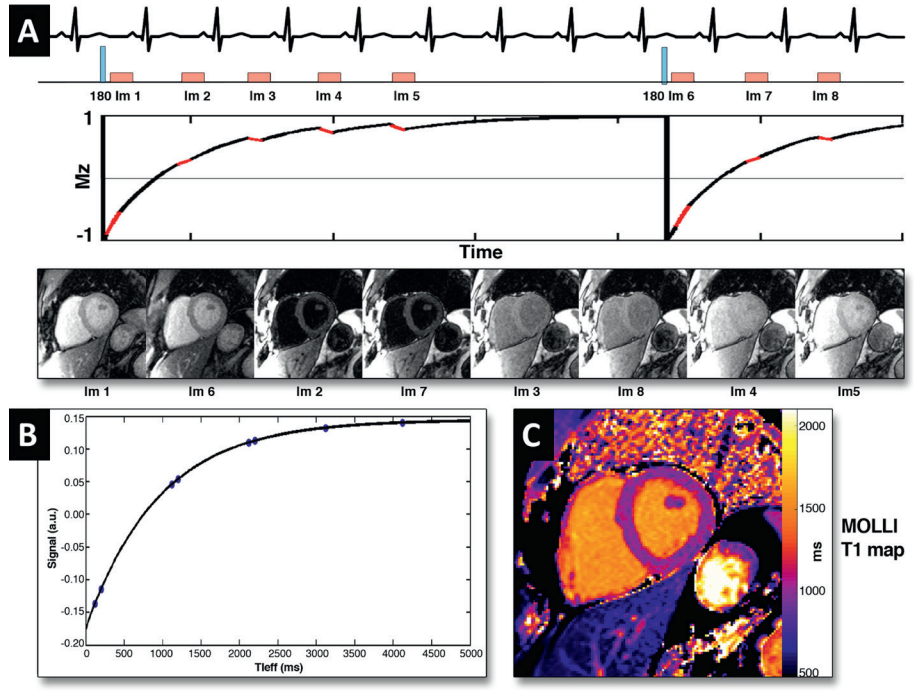

Figure 1: Modified Look-Locker (MOLLI) technique for myocardial T1 mapping. (A) After radiofrequency inversion pulse, myocardial tissue longitudinal magnetization in a stable magnetic field returns to the equilibrium and a series of images are acquired in diastole over several heart beats. The images are sorted in order of increasing T1 times and the T1 recovery curve is obtained by plotting respective signal intensities against T1 time **(B)**. The T1 map is obtained by applying this technique for all pixels in the image **(C)**. Reproduced with permission from Taylor *et al*.[7]

However, it should be noted that the cut-off values of the T1 mapping-derived metrics to define fibrosis cannot be currently established since the values show considerable overlap in normal and diseased myocardium.[11] Moreover, neither of the techniques is entirely specific to myocardial fibrosis; abnormal myocardial ECV fraction can be observed in infiltrative diseases (i.e. amyloidosis) and edema, while native T1 values may also be altered in iron deposition and diffuse fat infiltration.[12] Furthermore, standardization of CMR T1 mapping techniques is necessary to obtain reproducible measurements across different vendors and institutions.

Late gadolinium contrast-enhanced CMR

LGE CMR is considered the reference standard to quantify myocardial replacement fibrosis and scar. The increased extracellular space and decreased capillary density of the fibrous tissue result in increased volume of distribution and prolonged wash-out of gadolinium in comparison to the normal myocardium.[13] Ten to 20 minutes after intravenous administration of gadolinium, inversion recovery images are acquired in mid to late diastole. The inversion time is chosen to null the normal myocardium and provide the best tissue contrast between fibrous tissue, which appears bright, and normal myocardium, which appears black. Distinct patterns of LGE have been described in various cardiac diseases and associated with adverse prognosis (Figure 2).[14-19]

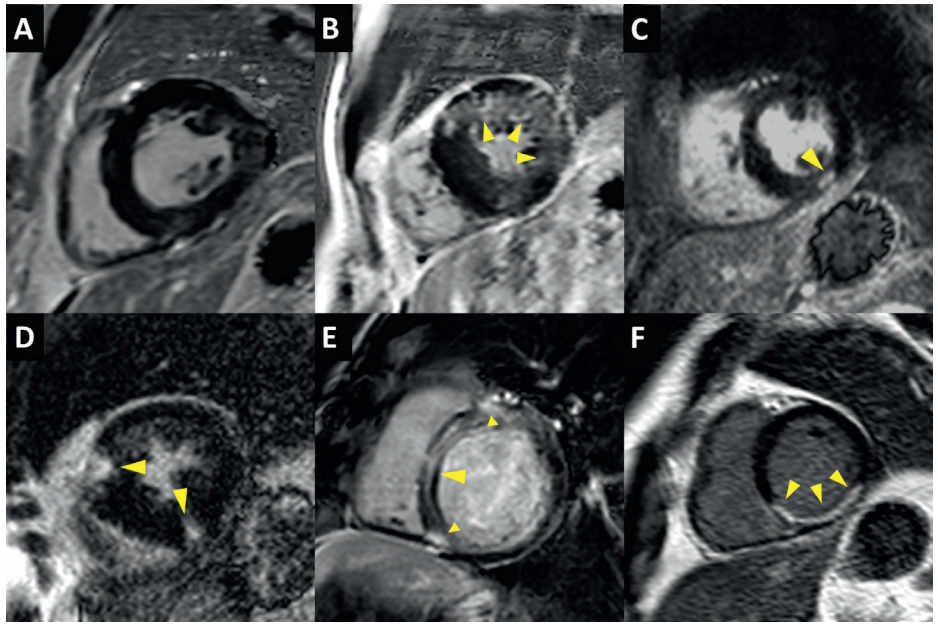

Figure 2: Patterns of late gadolinium enhancement (LGE). (A) No LGE, no focal replacement fibrosis. **(B-E)** Different patterns of non-infarct myocardial fibrosis: **(B)** diffuse patchy LGE of the anterior and lateral wall (arrows); **(C)** focal nodular LGE of the inferior wall (arrow); **(D)** focal LGE of the anterior and inferior right ventricular insertion points (arrow) and **(E)** linear midwall septal LGE with additional foci at the right ventricular insertion points (arrows). **(F)** Typical infarct-type subendocardial LGE distribution is shown (arrows).

Molecular magnetic resonance imaging

Molecular magnetic resonance imaging with the use of collagen-specific contrast agents is a new experimental method for the assessment of myocardial fibrosis. These novel contrast agents have shown to improve visualization of scar and perfusion defects in animal models of

myocardial infarction.[20,21] Furthermore, an elastin/tropoelastin-targeting contrast agent has provided interesting insights into the pathophysiology of remote myocardium extracellular matrix remodeling in a mice model of acute myocardial infarction.[22] Several other molecular probes have been synthesized to study individual processes involved in fibrosis formation, like necrosis, apoptosis, inflammation and scar maturation.[23] Further efficacy and safety studies are needed before clinical implementation. However, the current evidence is promising for future improvements in fibrosis detection and monitoring of molecular processes associated with myocardial remodeling.

CMR TECHNIQUES FOR INDIRECT ASSESSMENT OF MYOCARDIAL FIBROSIS

The functional consequences of myocardial fibrosis such as increased LV stiffness, impaired LV diastolic and systolic function, can be evaluated with CMR tagging and feature tracking CMR (Table 1). These techniques evaluate the active deformation (strain) of the myocardium in 3 orthogonal directions: radial, circumferential and longitudinal. In patients with VHD, the measurement of LV ejection fraction, which merely reflects the change in LV volumes between systole and diastole, may be misleading. For example, in patients with mitral regurgitation, LV ejection fraction may be preserved for long time since the LV is emptying in a low-pressure chamber (left atrium) while myocardial longitudinal strain may be impaired.[24] In patients with severe aortic stenosis, the LV hypertrophy, developed in response to the pressure overload, reduces the wall stress and maintains the LV ejection fraction. However, myocardial longitudinal strain may be impaired.[25] CMR tagging and feature tracking CMR track distinctive features of the myocardium throughout the cardiac cycle and calculate mechanical indices, such as strain, strain-rate, twist and torsion.

CMR tagging

This method is based on alteration of the myocardial tissue magnetization to create trackable markers within the myocardium which are visualized as dark lines in the form of a grid pattern. This allows immediate visual assessment of myocardial deformation, but for a more objective approach and quantification additional post-processing is employed. Recent developments in pulse sequences and image processing have resulted in a plethora of new tagging techniques.[26] The main advantage of CMR tagging over feature tracking CMR is that the imposed tags are more clearly defined and easier tracked than the natural features and are not subject-

ed to through plane displacements, thereby providing more reproducible measurements.[27] The main shortcomings of this technique are the need for additional, elaborate scan sequences with limited accuracy when applied to thin myocardium (such as the remodeled, thinned-wall LV, the right ventricle and the atria) and the time-consuming post-processing.

Feature tracking CMR

Feature tracking CMR is based on post-processing of standard steady state free precession cine images, similar to echocardiographic speckle tracking. Feature tracking CMR algorithms focus on the endo- and epicardial borders and detect the in- and outward motion of the cavity-tissue interface.[27,28] Global and segmental LV longitudinal, circumferential and radial strain, strain-rates, and LV rotational mechanics can be derived from standard long- and short-axis views (Figure 3). Global rather than segmental strain values appear the most reproducible.[29-31] Additional methodology standardization is an important prerequisite for wider dissemination of this technique in clinical practice.

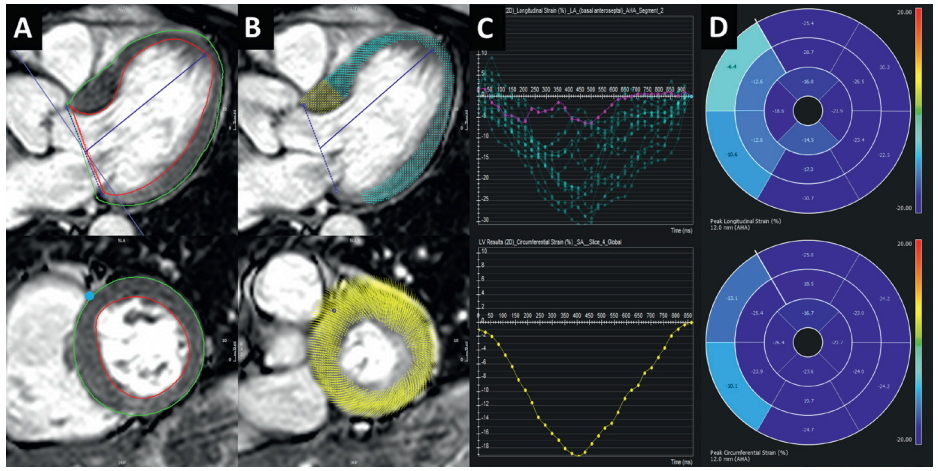

Figure 3: Feature tracking cardiovascular magnetic resonance (CMR) in a patient with severe aortic stenosis. (A) Long-axis (top) and a mid-cavity short-axis (bottom) end-diastolic steady state free precession images. Left ventricular endo- and epicardium are contoured (red and green lines) and the anterior right ventricular insertion point is marked in short-axis (blue dot). **(B)** Fully automated feature tracking analysis is performed by tracking distinctive features along the outlined myocardium borders. **(C)** The derived time-strain curves show a wide variation in segmental longitudinal strain (top) and normal global peak circumferential strain (bottom). The purple-colored curve corresponds to the anteroseptal segment. **(D)** The 16-segment bullseye plots for longitudinal (top) and circumferential (bottom) left ventricular strain, showing impaired myocardial deformation of the basal interventricular septum. (Feature tracking analysis was performed with cvi42 v5.3, Circle Cardiovascular Imaging, Calgary, Canada)

CMR LEFT VENTRICULAR MYOCARDIAL FIBROSIS ASSESSMENT IN VHD: CLINICAL EVIDENCE

Accumulating evidence on the deleterious impact of LV myocardial fibrosis on clinical outcomes after surgical treatment of left-sided VHD has raised interest on tissue characterization and LV strain with CMR techniques.[19,32-36] This evidence is summarized for aortic stenosis (AS) and regurgitation (AR) and for mitral regurgitation (MR) in the following sections.

Aortic stenosis

The pressure overload caused by AS increases LV wall stress and as a consequence the myocardium responds with myocyte hypertrophy to maintain LV systolic function. This myocardial hypertrophy is characterized by an increased muscle fiber diameter with parallel addition of new myofibrils.[37] Furthermore, there is an increase of interstitial fibrosis and myocyte apoptosis, partially as a consequence of oxygen supply-demand mismatch and myocardial ischemia.[37-39] At a late stage in the natural history of severe AS, the LV myocardium is characterized by large areas of myocyte loss and replacement fibrosis causing LV systolic dysfunction and associated with poor prognosis.[38]

The early changes in the interstitial space with increased deposition of collagen I can be assessed with CMR T1 mapping (Table 2).[8,34,40-46] Several studies have validated LV native T1 values and myocardial ECV fraction against histology in patients with AS undergoing aortic valve replacement.[8,34,40,41] In 109 patients with moderate and severe AS, Bull and colleagues[40] showed that LV native T1 values were significantly higher among patients with symptomatic severe AS compared with moderate and asymptomatic severe AS (1014±38 ms vs. 955±30 ms and 972±33 ms, respectively; P<0.05) (Figure 4). A significant correlation was observed between native T1 values and collagen volume fraction assessed on myocardial biopsies (R=0.65, P=0.002). Similarly, Flett and coworkers[8] validated the measurement of myocardial ECV fraction in 18 patients with severe AS. ECV strongly correlated with the histological collagen volume fraction (R^2=0.86; P<0.001). Although still not implemented in routine clinical practice, the measurement of myocardial ECV in patients with AS has important clinical implications.[34,43-46] Increased ECV has been associated with symptoms, worse LV systolic and diastolic function, higher levels of cardiac troponin T and ECG strain.[34,43-46] Recently, Chin *et al*.[34] reported the prognostic implications of myocardial ECV fraction corrected for LV end-diastolic myocardial volume normalized to the

body surface area (iECV) in 166 patients with mild to severe AS. Patients with increased myocardial iECV (≥22.5 ml/m^2) but without LGE (replacement fibrosis) showed significantly higher all-cause mortality and AS-related mortality rates (36 per 1000 patients-year for both) as compared to the patients with normal myocardium (iECV <22.5 ml/m^2, 8 and 0 deaths/1000 patient-years) (Figure 5).

Table 2: CMR studies to detect myocardial fibrosis in valvular heart disease.

Study	No. of patients	Valve Disease	CMR technique	Main findings
Bull *et al.*[40]	109	AS	native T1 mapping	Native T1 values increased along with hemodynamic severity of AS and correlated with the degree of biopsy-quantified fibrosis (R=0.65; P=0.002; N=23).
Lee *et al.*[41]	80	AS	native T1 mapping	Native T1 values at 3T CMR were significantly longer in asymptomatic patients with moderate to severe AS compared to normal controls.
Flett *et al.*[8]	18	AS	ECV	ECV correlated strongly with collagen volume fraction on histology (R^2=0.86; P<0.001).
Dusenbery *et al.*[44]	35	AS	ECV	ECV was significantly higher in patients with congenital AS than in normal subjects.
Flett *et al.*[43]	66	AS	ECV	Patients with severe AS had higher ECV than normal controls.
Chin *et al.*[34]	166	AS	iECV, LGE	Increased iECV was associated with increased all-cause mortality compared to patients with normal iECV (36 vs. 8 deaths/1000 patient-years, respectively).
Chin *et al.*[45]	122	AS	ECV, LGE	ECV and percent of midwall replacement fibrosis (LGE) were associated with increased high-sensitivity cardiac troponin I levels.
Shah *et al.*[46]	102	AS	ECV, LGE	LGE and ECV were associated with ECG strain in patients with mild to severe AS.
Debl *et al.*[47]	22	AS	LGE	LGE was associated with severe LV hypertrophy.
Rudolph *et al.*[48]	21	AS	LGE	LGE was associated with increased LV mass index and LV end-diastolic volume index. LGE was not associated with the severity of AS.
Dweck *et al.*[19]	143	AS	LGE	Midwall fibrosis on LGE CMR was associated with higher mortality than infarct-type LGE (HR: 8.59; 95% CI: 1.97-37.38; P=0.004 and HR: 6.46; 95% CI: 1.39-30.00; P=0.017, respectively).
Barone-Rochette *et al.*[32]	154	AS	LGE	LGE was an independent predictor of all-cause and cardiovascular mortality in patients with severe AS undergoing surgical valve replacement (HR for all-cause mortality: 2.8; 95% CI: 1.3-6.9; P=0.025).
Weidemann *et al.*[49]	58	AS	LGE	The extent of LGE in patients with symptomatic severe AS undergoing aortic valve surgery correlated with biopsy-quantified myocardial fibrosis and remained unchanged at 9 months after surgery.
Azevedo *et al.*[33]	54	AS + AR	LGE	LGE correlated with the extent of fibrosis on histology (r=0.69, P<0.001) and demonstrated significant inverse correlation with the LVEF improvement after surgery (r=-0.47, P=0.02). LGE was associated with worse long-term survival (chi-square=5.85; P=0.02).
Singh *et al.*[50]	174	AS	LGE	Patients with asymptomatic moderate and severe AS who presented with valve related complications during follow-up showed comparable extent of LGE than patients who remained asymptomatic.

Schneeweis *et al.*[51], Singh *et al.*[52]	30, 18	AS	CMR tagging, feature tracking CMR	Reasonable agreement between both techniques, but feature tracking CMR yielded higher strain values than CMR tagging.
Mahmod *et al.*[53]	39	AS	CMR tagging	Patients with AS had impaired LV strain compared to controls.
Al Musa *et al.*[54]	42	AS	CMR tagging, feature tracking CMR	Longitudinal strain rate was impaired in symptomatic vs asymptomatic patients with severe AS and preserved LVEF (−83.4±24.8 %/s and −106.3±43.3 %/s, respectively; P=0.048).
Musa *et al.*[36]	98	AS	CMR tagging	Impaired mid-LV circumferential strain was associated with all-cause mortality after aortic valve replacement (HR: 1.03; 95% CI: 1.01–1.05; P=0.009).
Meyer *et al.*[55]	44	AS	Feature tracking CMR	Peak systolic LV strain of the apical segments was significantly impaired in transapical versus transfemoral transcatheter aortic valve replacement.
Sparrow *et al.*[56]	8	AR	T1 mapping	Post-contrast T1 values in abnormally contracting segments were prolonged compared to controls (532 vs 501 ms, respectively; P=0.002).
de Meester de Ravenstein *et al.*[57]	9	AR	ECV	ECV measured on 3T CMR was strongly correlated with the extent of interstitial fibrosis on histology in patients with severe AR (r=0.79, P=0.011).
Pomerantz *et al.*[58]	14	AR	Myocardial tagging	Global longitudinal and circumferential strain were decreased 2 years after aortic valve replacement, despite an improvement in LVEF and LV size.
Ungacta *et al.*[59]	8	AR	Myocardial tagging	Posterior wall circumferential strain was decreased 6 months after surgery.
Edwards *et al.*[60]	35	MR	ECV, native T1 mapping, LGE	Patients with moderate to severe primary MR had higher ECV compared to controls (0.32±0.07 vs. 0.25±0.02, respectively; P<0.01).
Han *et al.*[61]	25	MR	LGE	LGE of the papillary muscles was present in 63% of patients with MV prolapse.
Chaikriangkrai *et al.*[35]	48	MR	LGE	The presence of LV LGE in chronic severe MR was associated with worse clinical outcomes (HR: 4.8; 95% CI: 1.1 to 20.7; P=0.037).
Maniar *et al.*[62]	15	MR	CMR tagging	Patients with chronic moderate and severe MR and preserved LVEF had impaired septal LV strain values compared to normal controls.
Mankad *et al.*[63]	7	MR	CMR tagging	Patients with severe MR and preserved LVEF had reduced circumferential strain compared to controls (12±6% vs. 21±6%, respectively; p≤0.001).
Ahmed *et al.*[64], Schiros *et al.*[65], Ahmed *et al.*[66]	27, 35, 22	MR	CMR tagging	Global longitudinal and circumferential strain parameters were decreased after MV repair.

AS = aortic stenosis; AR = aortic regurgitation; CMR = cardiovascular magnetic resonance; ECV = extracellular volume; HR = hazard ratio; ICU = intensive care unit; iECV = indexed extracellular volume; LGE = late gadolinium enhancement; LV = left ventricle; LVEF = left ventricular ejection fraction; MR = mitral regurgitation.

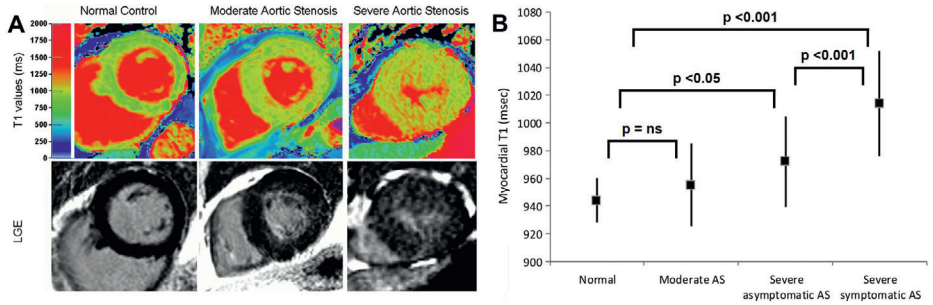

Figure 4: Native T1 mapping in aortic stenosis. (A) Color maps of T1 values of mid-ventricular short-axis slices (top row) and corresponding LGE images (bottom row) of normal controls and patients with moderate and severe AS. The left column shows a normal volunteer (T1=944 ms), the middle column a patient with moderate AS and moderate left ventricular hypertrophy (T1=951 ms) and the right column shows a patient with severe AS with severe left ventricular hypertrophy (T1=1020 ms). **(B)** Whisker-plots of myocardial T1 values of normal controls and of patients with moderate AS, asymptomatic severe AS and symptomatic severe AS. The between-group comparisons with the corresponding P-values are also presented. Adapted with permission from Bull *et al*.[40] AS = aortic stenosis; LGE = late gadolinium enhancement; ns = non-significant.

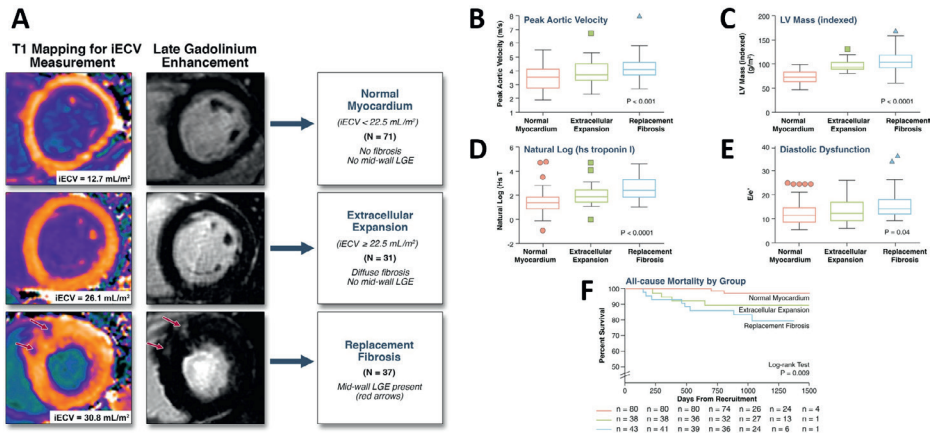

Figure 5: Prognostic implications of interstitial and replacement fibrosis in aortic stenosis. (A) Patients with mild to severe aortic stenosis were categorized into 3 groups based upon cardiovascular magnetic resonance assessments of myocardial fibrosis: normal myocardium (indexed extracellular volume [iECV] <22.5 ml/m^2, no late gadolinium enhancement [LGE]), diffuse myocardial fibrosis (iECV ≥22.5 ml/m^2, no LGE) and replacement fibrosis (presence of midwall LGE). There was a stepwise increase in: **(B)** severity of valve narrowing; **(C)** degree of left ventricular (LV) hypertrophy; **(D)** myocardial injury, assessed by high-sensitivity troponin I concentration (hsTni); **(E)** LV diastolic dysfunction; and **(F)** all-cause-mortality with increased diffuse myocardial fibrosis and replacement fibrosis. Adapted with permission from Chin *et al*.[34]

LGE, myocardial replacement fibrosis, is detected in 19-62% of patients with severe AS.[19,32,47,48] Two forms of LGE can be observed: the ischemic and the non-ischemic pattern. The ischemic pattern is characterized by subendocardial LGE along specific coronary artery territories whereas in the non-ischemic pattern the distribution of LGE can be diffuse, (multi)focal or linear, confined or patchy, and is predominantly located in the midwall myocardial layer and does not correspond to a specific coronary artery territory (Figure 2).[19,32,47,48] The presence and the extent of LGE have been associated with increased LV mass, worse LV ejection fraction, the presence of symptoms, markers of myocardial injury such NT-pro-brain natriuretic peptide and high-sensitivity cardiac troponins and ECG strain (Table 2).[19,32,45,46,48,49] However, LGE was not significantly associated with transaortic gradients or the aortic valve area, common indices of AS severity,[19,32,48] suggesting that there is different individual susceptibility to develop LV hypertrophy and myocardial fibrosis, likely influenced by multiple factors such as advanced age, male sex, obesity and certain genetic variants.[67]

In addition, LGE is an important prognostic marker in patients with AS.[19,32,33] In 143 patients with moderate and severe AS who were followed for 2.0±1.4 years, the presence of LGE was associated with an increase in all-cause and cardiac mortality (every 1% increase in LGE mass was associated with 5% increased risk of all-cause mortality; P=0.005).[19] When dividing the population according to the pattern of LGE, patients with midwall fibrosis (N=54) had higher mortality than patients with infarct-type LGE (N=40) (HR: 8.59; 95% CI: 1.97-37.38; P=0.004 and HR: 6.46; 95% CI: 1.39-30.00; P=0.017, respectively). Furthermore, in 154 patients with severe AS undergoing surgical aortic valve replacement, the presence of LGE was an independent predictor of all-cause and cardiovascular mortality (HR for all-cause mortality: 2.8; 95% CI: 1.3-6.9; P=0.025).[32] Importantly, after aortic valve replacement, LGE does not completely regress and has been associated with incomplete LV functional recovery, worse New York Heart Association functional class and worse survival (Figure 6).[32,33,49] However, detection of LV myocardial fibrosis in patients with asymptomatic moderate and severe AS seems insufficient to identify the patients who will present valve related complications. In the PRIMID AS (PRognostic Importance of MIcrovascular Dysfunction in Aortic Stenosis) study, including 174 patients with asymptomatic moderate to severe AS, the group of patients who presented with cardiovascular death, major adverse cardiovascular events and development of typical AS symptoms, necessitating referral for aortic valve replacement, showed comparable extent of LGE than patients who remained asymptomatic or free of valve related complications during follow-up.[50]

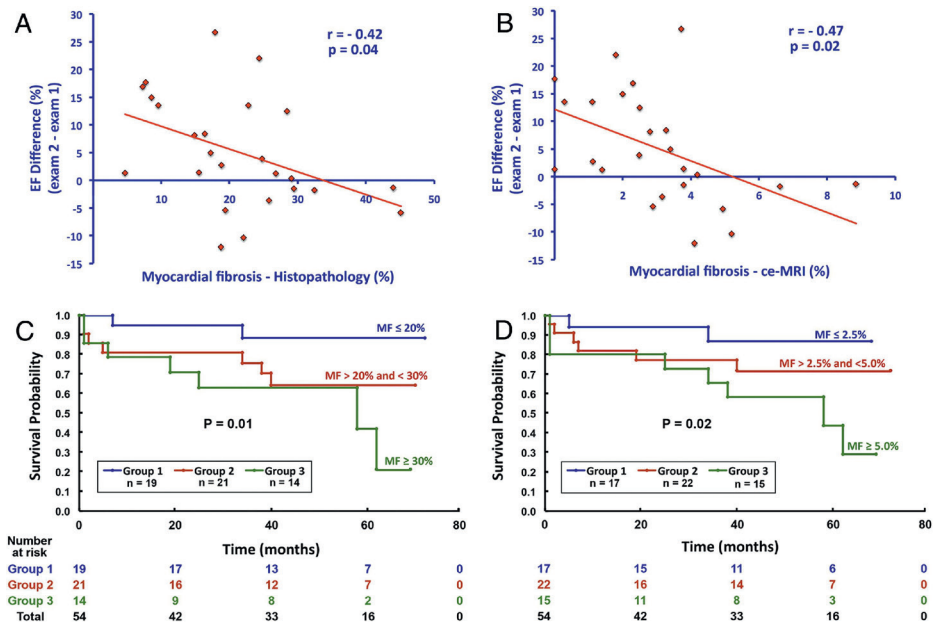

Figure 6: Prognostic implications of late gadolinium enhancement (LGE) cardiovascular magnetic resonance (CMR) in patients with severe aortic stenosis and aortic regurgitation after aortic valve replacement surgery. Linear regression graphs illustrate the inverse relationship between the degree of left ventricular ejection fraction improvement and the amount of myocardial fibrosis by histopathology **(A)** and by LGE CMR **(B)**. The Kaplan-Meier graphs demonstrate significantly worse survival after aortic valve replacement in patients with larger myocardial fibrosis assessed by histopathology **(C)** or LGE **(D)**. Reproduced with permission from Azevedo *et al*.[33] ce-MRI = contrast-enhanced magnetic resonance imaging; EF = ejection fraction; MF = myocardial fibrosis.

Interstitial and replacement myocardial fibrosis lead to impaired LV myocardial deformation which can be detected with strain imaging. Myocardial tagging and feature tracking CMR demonstrated that global as well as regional LV strains were significantly correlated with LGE extent in patients with hypertrophic cardiomyopathy, who exhibit a similar pattern of midwall fibrosis to patients with AS: global and regional LV strain values impair as LGE increases.[68,69] Head-to-head comparisons between tagged and feature tracking CMR in moderate to severe AS have shown reasonable agreement for LV strain measurement, albeit feature tracking provided systematically higher values than CMR tagging.[51,52] The correlation between CMR LV circumferential and longitudinal strain and strain rate and symptomatic status of patients with severe AS and preserved LV ejection fraction was demonstrated by Al Musa *et al*.[54] LV longitudinal strain rate was the most sensitive parameter to discriminate between asymptomatic vs. symptomatic patients (−106.3±43.3 %/s in patients with “no/mild” symptoms vs. −83.4±24.8

%/s in moderate and severely symptomatic patients; P=0.048). The association between LV myocardial strain and outcomes after surgical or transcatheter treatment was demonstrated in two studies.[53] [36] Mahmod and coworkers[53] showed that global LV circumferential, but not longitudinal strain measured on CMR significantly improved at 8 months after aortic valve replacement. Similarly, LV circumferential strain by CMR tagging was significantly associated with all-cause mortality in 98 severe AS patients undergoing surgical and transcatheter aortic valve replacement (HR per each 1% deterioration of circumferential strain: 1.03; 95% CI: 1.01–1.05; P=0.009).[36] Furthermore, the effect of procedural access (transfemoral vs. transapical) on LV mechanics was studied with CMR feature tracking in 44 patients undergoing transcatheter aortic valve replacement.[55] The transapical approach was associated with impaired peak systolic longitudinal strain of the apical segments as compared to the transfemoral approach (-8.9±5.3 vs. -16.9±4.3%, respectively; P<0.001), while there were no differences in LV ejection fraction and peak systolic longitudinal strain of the basal and midventricular segments between both approaches (Figure 7).

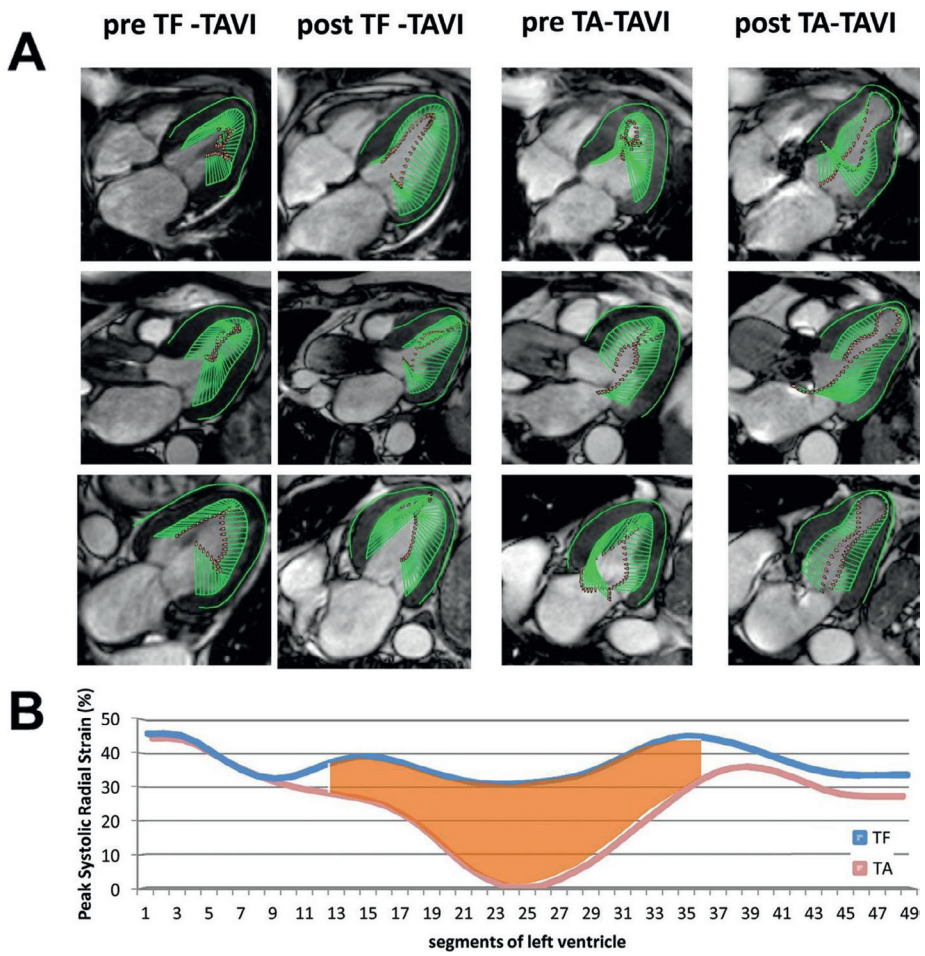

Figure 7: The impact of transcatheter aortic valve implantation on the left ventricular (LV) mechanics, assessed with feature tracking cardiovascular magnetic resonance (CMR). **(A)** Systolic CMR cine frames derived from four- (top row), three- (middle row), and two-chamber (bottom row) LV views of a patient before and after transfemoral (TF) access (left two columns) as well as from a patient before and after transapical (TA) access (right two columns). The green arrows represent velocity vectors illustrating systolic inward motion. The TA transcatheter aortic valve implantation (TAVI) patient shows reduced systolic deformation of the apical LV segments 3 months after the procedure. **(B)** Average peak systolic radial strain values of 49 analyzed segments obtained from all TF-TAVI patients (blue line) and all TA-TAVI patients (red line). The apical segments are displayed in the middle, while the basal segments are displayed on the left and on the right side of the graph. There is a reduction in peak radial strain of the apical segments after TA-TAVI. Adapted with permission from Meyer *et al*.[55]

Aortic regurgitation

In aortic regurgitation (AR), pressure and volume overload induce growth of cardiomyocytes with addition of new sarcomeres in series and interstitial fibrosis, characterized by increased fibronectin and non-collagen components.[70] Several clinical studies have histologically proven pronounced myocardial fibrosis in severe AR at the time of valve surgery.[37,71,72] A few studies have also evaluated myocardial fibrosis with CMR.[33,56,57] Sparrow *et al.*[56] compared myocardial T1 values measured with a modified Look-Locker technique before and after gadolinium contrast in 8 patients with severe AR and 15 normal controls. Patients with AR had significantly prolonged post-contrast T1 values in abnormally contracting segments compared to the controls (532 vs. 501 ms, respectively; P=0.002), suggesting increased interstitial fibrosis. Furthermore, in 9 patients with severe AR who underwent surgical aortic valve replacement, ECV measured on 3T CMR was strongly correlated with the extent of interstitial fibrosis on histology (r=0.79, P=0.011).[57] Replacement fibrosis has been also described in 26 patients with severe AR by Azevedo and colleagues.[33] The authors reported a 69% prevalence of LGE, mostly following a multifocal pattern. The correlation between myocardial replacement fibrosis assessed with LGE and histopathology was good (r=0.70, P<0.001). Moreover, in a combined cohort of 26 patients with severe AR and 28 patients with severe AS, the amount of myocardial fibrosis was inversely correlated with LV functional improvement (r=-0.47; P=0.02) and was associated with worse long-term survival after aortic valve replacement surgery (chi-square = 5.85; P=0.02) (Figure 6).[33] Furthermore, in 14 patients with chronic severe AR, myocardial CMR tagging showed an impairment in global longitudinal and circumferential strain at 2 years after aortic valve replacement (P<0.03 for both), despite an improvement in LV ejection fraction and a decrease in LV size (Figure 8).[58] Similarly, Ungacta *et al*.[59] showed a decrease in posterior wall circumferential strain in patients with AR 6 months after valve replacement. These findings suggest that the presence of LV myocardial fibrosis in patients with AR is a marker of adverse remodeling that may lead to further deterioration in LV strain and poor prognosis after aortic valve surgery.

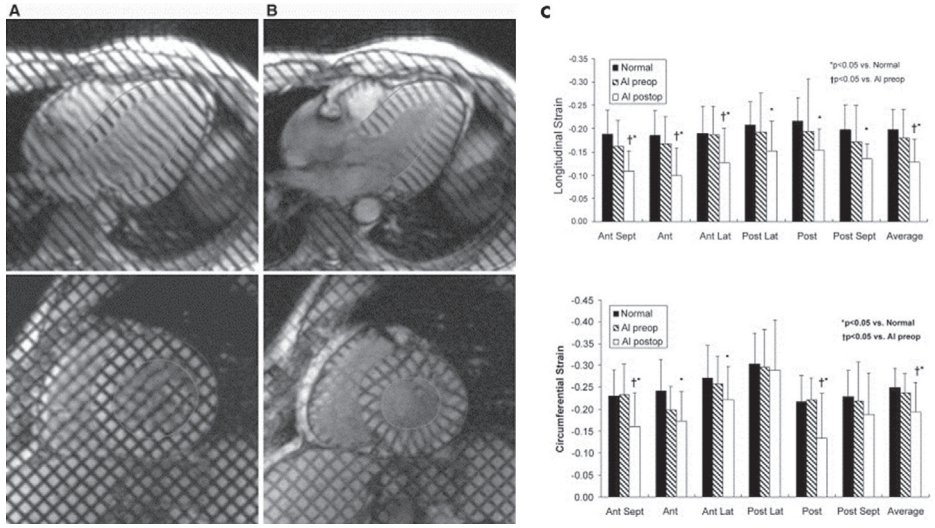

Figure 8: CMR tagging in patients with chronic severe aortic regurgitation. Left ventricular (LV) long-axis (top row) and short-axis (bottom row) cardiovascular magnetic resonance (CMR) tagging images at end-diastole **(A)** and at end-systole **(B)**. A tagging pattern in the form of parallel lines was used for the long-axis cines and a grid pattern for the short-axis cines. Dedicated software was employed for the myocardial deformation analysis. **(C)** At an average of 28±11 months after aortic valve replacement global and regional LV longitudinal and circumferential strain decreased (P<0.05 for both global strain values) despite an improvement in LV ejection fraction and a decrease in LV size, which might imply an ongoing myocardial fibrosis after valve surgery. Adapted with permission from Pomerantz *et al*.[58] AI = aortic insufficiency; Ant = anterior; Lat = lateral; Post = posterior; preop = preoperative; postop = postoperative; Sept = septal.

Mitral regurgitation

Mitral regurgitation (MR) is a heterogeneous disease, broadly classified as organic (primary) or functional (secondary) based on the underlying mechanism. Organic MR is due to intrinsic valvular disease whereas functional MR is caused by regional and/or global LV remodeling without structural abnormalities of the mitral valve.[73] Degenerative mitral valve disease (myxomatous disease and fibroelastic deficiency) is the most frequent etiology of primary MR in developed countries. The indication for mitral valve repair/replacement is determined by the presence of symptoms or LV function deterioration and LV remodeling.[1,3] However, LV remodeling and myocardial fibrosis may occur before the development of symptoms. Chronic LV volume overload associated with MR leads to myocardial hypertrophy and increased interstitial fibrosis.[74] In 35 asymptomatic patients with moderate to severe primary MR, Edwards and colleagues[60] demonstrated higher ECV on CMR as compared to controls (0.32±0.07 vs. 0.25±0.02, P<0.01) (Figure 9). Furthermore, 31% of patients with MR exhibited a non-infarct LGE pattern on CMR. Patients who had non-infarct type LGE presented with higher ECV values compared

to MR patients without LGE (0.35±0.02 vs 0.27±0.03, P<0.01). The ECV values correlated with LV end-systolic volume, measures of systolic and diastolic LV dysfunction as well as with peak oxygen consumption on treadmill testing. The distribution of LGE in patients with MR varies significantly. Han *et al*.[61] demonstrated the presence of LGE of the papillary muscles in 63% of patients with MV prolapse, whereas Chaikriangkrai and coworkers[35] observed LV replacement fibrosis in 40% of patients with chronic severe MR. The presence of LV LGE was associated with worse clinical outcomes in terms of intensive care unit readmission, incidence of permanent pacemaker implantation and rehospitalization (HR: 4.775; 95% CI: 1.100 to 20.729; P=0.037).[35]

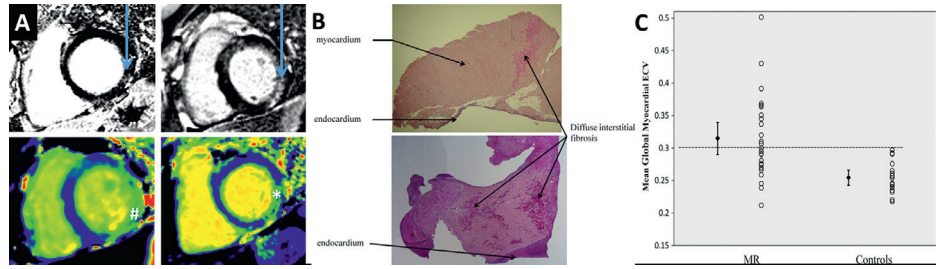

Figure 9: Cardiovascular magnetic resonance (CMR) myocardial fibrosis assessment in primary degenerative mitral regurgitation (MR). (A) Late gadolinium enhanced CMR images (top) and native T1 maps (bottom) in patients with MR. The arrows indicate the presence of midwall replacement fibrosis in the inferolateral wall. The native T1 values were increased in corresponding areas (#=1045 ms and *=1102 ms). **(B)** Left ventricular fibrosis demonstrated on histology: replacement fibrosis can be well-delineated (upper plot) or patchy (lower plot). **(C)** Individual patient data presented in the scatter plot demonstrate a wide overlap of the extracellular volume (ECV) values in patients with MR and controls. However, the mean and the standard error of the mean (error bars) were significantly larger in patients with MR as compared to the controls. Adapted with permission from Edwards *et al*.[60]

These structural changes of the LV myocardium may be associated with subtle functional abnormalities. In 15 patients with chronic moderate and severe MR and preserved LV ejection fraction who underwent CMR with tissue tagging, Maniar *et al*.[62] demonstrated preserved global longitudinal and circumferential strain but abnormal regional strain values: the septal LV segments exhibited impaired strain whereas the lateral segments showed compensatory hyper-contractility. Similarly, Mankad *et al*.[63] showed with CMR tagging abnormal regional strain patterns in patients with severe MR and preserved LV ejection fraction: while radial strain was increased (19±9% vs. 16±6%, P=0.003), circumferential strain was reduced (12±6% vs. 21±6%, p≤0.001) as compared to healthy controls. Several authors have demonstrated a decrease in global longitudinal and circumferential strain parameters on CMR tagging in patients with severe degenerative MR after mitral valve repair, which might imply an ongoing myocardial fibrosis after surgery.[64-66]

FUTURE PERSPECTIVES

Tissue characterization and strain imaging with CMR have provided new insights into the pathophysiology of VHD. Current guidelines recommend valve surgery in severe symptomatic VHD or when LV function decreases.[1,3] However, early detection of LV structural and functional changes may help to identify patients who may benefit from early surgery. It is conceivable that early relief of the pressure or volume overload would result in less damage to the LV and better outcome at follow-up. However, there are currently no prospective data to evaluate whether early surgical valve treatment results in better prognosis in VHD. It may be challenging as well to define the cut-off values of ECV, T1 times, LGE and LV myocardial strains for therapeutic intervention. Standardization in data acquisition and analysis are important issues to be resolved.

The Early Valve Replacement guided by Biomarkers of Left Ventricular Decompensation in Asymptomatic Patients with Advanced Aortic Stenosis (EVOLVED) is the first multicenter randomized controlled clinical trial that will investigate whether the early valve intervention in patients with asymptomatic severe AS and midwall fibrosis on CMR improves patients' clinical outcomes compared to the standard care (NCT03094143). The results of this study may have an impact on future guidelines and recommendations on treatment of VHD.

REFERENCES

1. Joint Task Force on the Management of Valvular Heart Disease of the European Society of C, European Association for Cardio-Thoracic S, Vahanian A, Alfieri O, Andreotti F, Antunes MJ *et al.* Guidelines on the management of valvular heart disease (version 2012). *Eur Heart J* 2012;33(19):2451-96.
2. Nkomo VT, Gardin JM, Skelton TN, Gottdiener JS, Scott CG, Enriquez-Sarano M. Burden of valvular heart diseases: a population-based study. *Lancet* 2006;368(9540):1005-11.
3. Nishimura RA, Otto CM, Bonow RO, Carabello BA, Erwin JP, 3rd, Guyton RA *et al.* 2014 AHA/ACC guideline for the management of patients with valvular heart disease: a report of the American College of Cardiology/American Heart Association Task Force on Practice Guidelines. *J Am Coll Cardiol* 2014;63(22):e57-185.
4. Enriquez-Sarano M, Sundt TM, 3rd. Early surgery is recommended for mitral regurgitation. *Circulation* 2010;121(6):804-11; discussion 12.
5. Villari B, Campbell SE, Hess OM, Mall G, Vassalli G, Weber KT *et al.* Influence of collagen network on left ventricular systolic and diastolic function in aortic valve disease. *J Am Coll Cardiol* 1993;22(5):1477-84.
6. Mewton N, Liu CY, Croisille P, Bluemke D, Lima JA. Assessment of myocardial fibrosis with cardiovascular magnetic resonance. *J Am Coll Cardiol* 2011;57(8):891-903.
7. Taylor AJ, Salerno M, Dharmakumar R, Jerosch-Herold M. T1 Mapping: Basic Techniques and Clinical Applications. *JACC Cardiovasc Imaging* 2016;9(1):67-81.
8. Flett AS, Hayward MP, Ashworth MT, Hansen MS, Taylor AM, Elliott PM *et al.* Equilibrium contrast cardiovascular magnetic resonance for the measurement of diffuse myocardial fibrosis: preliminary validation in humans. *Circulation* 2010;122(2):138-44.
9. Miller CA, Naish JH, Bishop P, Coutts G, Clark D, Zhao S *et al.* Comprehensive validation of cardiovascular magnetic resonance techniques for the assessment of myocardial extracellular volume. *Circ Cardiovasc Imaging* 2013;6(3):373-83.
10. Fontana M, White SK, Banypersad SM, Sado DM, Maestrini V, Flett AS *et al.* Comparison of T1 mapping techniques for ECV quantification. Histological validation and reproducibility of ShMOLLI versus multibreath-hold T1 quantification equilibrium contrast CMR. *J Cardiovasc Magn Reson* 2012;14(1):88.
11. Bulluck H, Maestrini V, Rosmini S, Abdel-Gadir A, Treibel TA, Castelletti S *et al.* Myocardial T1 mapping. *Circ J* 2015;79(3):487-94.
12. Moon JC, Messroghli DR, Kellman P, Piechnik SK, Robson MD, Ugander M *et al.* Myocardial T1 mapping and extracellular volume quantification: a Society for Cardiovascular Magnetic Resonance (SCMR) and CMR Working Group of the European Society of Cardiology consensus statement. *J Cardiovasc Magn Reson* 2013;15:92.

13. Croisille P, Revel D, Saeed M. Contrast agents and cardiac MR imaging of myocardial ischemia: from bench to bedside. *Eur Radiol* 2006;16(9):1951-63.
14. Kim RJ, Wu E, Rafael A, Chen EL, Parker MA, Simonetti O *et al.* The use of contrast-enhanced magnetic resonance imaging to identify reversible myocardial dysfunction. *N Engl J Med* 2000;343(20):1445-53.
15. Wu E, Ortiz JT, Tejedor P, Lee DC, Bucciarelli-Ducci C, Kansal P *et al.* Infarct size by contrast enhanced cardiac magnetic resonance is a stronger predictor of outcomes than left ventricular ejection fraction or end-systolic volume index: prospective cohort study. *Heart* 2008;94(6):730-6.
16. Kwong RY, Chan AK, Brown KA, Chan CW, Reynolds HG, Tsang S *et al.* Impact of unrecognized myocardial scar detected by cardiac magnetic resonance imaging on event-free survival in patients presenting with signs or symptoms of coronary artery disease. *Circulation* 2006;113(23):2733-43.
17. Assomull RG, Prasad SK, Lyne J, Smith G, Burman ED, Khan M *et al.* Cardiovascular magnetic resonance, fibrosis, and prognosis in dilated cardiomyopathy. *J Am Coll Cardiol* 2006;48(10):1977-85.
18. O'Hanlon R, Grasso A, Roughton M, Moon JC, Clark S, Wage R *et al.* Prognostic significance of myocardial fibrosis in hypertrophic cardiomyopathy. *J Am Coll Cardiol* 2010;56(11):867-74.
19. Dweck MR, Joshi S, Murigu T, Alpendurada F, Jabbour A, Melina G *et al.* Midwall fibrosis is an independent predictor of mortality in patients with aortic stenosis. *J Am Coll Cardiol* 2011;58(12):1271-9.
20. Helm PA, Caravan P, French BA, Jacques V, Shen L, Xu Y *et al.* Postinfarction myocardial scarring in mice: molecular MR imaging with use of a collagen-targeting contrast agent. *Radiology* 2008;247(3):788-96.
21. Spuentrup E, Ruhl KM, Botnar RM, Wiethoff AJ, Buhl A, Jacques V *et al.* Molecular magnetic resonance imaging of myocardial perfusion with EP-3600, a collagen-specific contrast agent: initial feasibility study in a swine model. *Circulation* 2009;119(13):1768-75.
22. Protti A, Lavin B, Dong X, Lorrio S, Robinson S, Onthank D *et al.* Assessment of Myocardial Remodeling Using an Elastin/Tropoelastin Specific Agent with High Field Magnetic Resonance Imaging (MRI). *J Am Heart Assoc* 2015;4(8):e001851.
23. Jivraj N, Phinikaridou A, Shah AM, Botnar RM. Molecular imaging of myocardial infarction. *Basic Res Cardiol* 2014;109(1):397.
24. Marciniak A, Claus P, Sutherland GR, Marciniak M, Karu T, Baltabaeva A *et al.* Changes in systolic left ventricular function in isolated mitral regurgitation. A strain rate imaging study. *Eur Heart J* 2007;28(21):2627-36.
25. Delgado V, Tops LF, van Bommel RJ, van der Kley F, Marsan NA, Klautz RJ *et al.* Strain analysis in patients with severe aortic stenosis and preserved left ventricular ejection fraction undergoing surgical valve replacement. *Eur Heart J* 2009;30(24):3037-47.

26. Ibrahim el SH. Myocardial tagging by cardiovascular magnetic resonance: evolution of techniques--pulse sequences, analysis algorithms, and applications. *J Cardiovasc Magn Reson* 2011;13:36.
27. Pedrizzetti G, Claus P, Kilner PJ, Nagel E. Principles of cardiovascular magnetic resonance feature tracking and echocardiographic speckle tracking for informed clinical use. *J Cardiovasc Magn Reson* 2016;18(1):51.
28. Schuster A, Hor KN, Kowallick JT, Beerbaum P, Kutty S. Cardiovascular Magnetic Resonance Myocardial Feature Tracking: Concepts and Clinical Applications. *Circ Cardiovasc Imaging* 2016;9(4):e004077.
29. Padiyath A, Gribben P, Abraham JR, Li L, Rangamani S, Schuster A *et al.* Echocardiography and cardiac magnetic resonance-based feature tracking in the assessment of myocardial mechanics in tetralogy of Fallot: an intermodality comparison. *Echocardiography* 2013;30(2):203-10.
30. Morton G, Schuster A, Jogiya R, Kutty S, Beerbaum P, Nagel E. Inter-study reproducibility of cardiovascular magnetic resonance myocardial feature tracking. *J Cardiovasc Magn Reson* 2012;14:43.
31. Augustine D, Lewandowski AJ, Lazdam M, Rai A, Francis J, Myerson S *et al.* Global and regional left ventricular myocardial deformation measures by magnetic resonance feature tracking in healthy volunteers: comparison with tagging and relevance of gender. *J Cardiovasc Magn Reson* 2013;15:8.
32. Barone-Rochette G, Pierard S, De Meester de Ravenstein C, Seldrum S, Melchior J, Maes F *et al.* Prognostic significance of LGE by CMR in aortic stenosis patients undergoing valve replacement. *J Am Coll Cardiol* 2014;64(2):144-54.
33. Azevedo CF, Nigri M, Higuchi ML, Pomerantzeff PM, Spina GS, Sampaio RO *et al.* Prognostic significance of myocardial fibrosis quantification by histopathology and magnetic resonance imaging in patients with severe aortic valve disease. *J Am Coll Cardiol* 2010;56(4):278-87.
34. Chin CW, Everett RJ, Kwiecinski J, Vesey AT, Yeung E, Esson G *et al.* Myocardial Fibrosis and Cardiac Decompensation in Aortic Stenosis. *JACC Cardiovasc Imaging* 2016.
35. Chaikriangkrai K, Lopez-Mattei JC, Lawrie G, Ibrahim H, Quinones MA, Zoghbi W *et al.* Prognostic value of delayed enhancement cardiac magnetic resonance imaging in mitral valve repair. *Ann Thorac Surg* 2014;98(5):1557-63.
36. Musa TA, Uddin A, Swoboda PP, Fairbairn TA, Dobson LE, Singh A *et al.* Cardiovascular magnetic resonance evaluation of symptomatic severe aortic stenosis: association of circumferential myocardial strain and mortality. *J Cardiovasc Magn Reson* 2017;19(1):13.
37. Krayenbuehl HP, Hess OM, Monrad ES, Schneider J, Mall G, Turina M. Left ventricular myocardial structure in aortic valve disease before, intermediate, and late after aortic valve replacement. *Circulation* 1989;79(4):744-55.

38. Hein S, Arnon E, Kostin S, Schonburg M, Elsasser A, Polyakova V *et al.* Progression from compensated hypertrophy to failure in the pressure-overloaded human heart: structural deterioration and compensatory mechanisms. *Circulation* 2003;107(7):984-91.
39. Rakusan K, Flanagan MF, Geva T, Southern J, Van Praagh R. Morphometry of human coronary capillaries during normal growth and the effect of age in left ventricular pressure-overload hypertrophy. *Circulation* 1992;86(1):38-46.
40. Bull S, White SK, Piechnik SK, Flett AS, Ferreira VM, Loudon M *et al.* Human non-contrast T1 values and correlation with histology in diffuse fibrosis. *Heart* 2013;99(13):932-7.
41. Lee SP, Lee W, Lee JM, Park EA, Kim HK, Kim YJ *et al.* Assessment of diffuse myocardial fibrosis by using MR imaging in asymptomatic patients with aortic stenosis. *Radiology* 2015;274(2):359-69.
42. Chin CW, Semple S, Malley T, White AC, Mirsadraee S, Weale PJ *et al.* Optimization and comparison of myocardial T1 techniques at 3T in patients with aortic stenosis. *Eur Heart J Cardiovasc Imaging* 2014;15(5):556-65.
43. Flett AS, Sado DM, Quarta G, Mirabel M, Pellerin D, Herrey AS *et al.* Diffuse myocardial fibrosis in severe aortic stenosis: an equilibrium contrast cardiovascular magnetic resonance study. *Eur Heart J Cardiovasc Imaging* 2012;13(10):819-26.
44. Dusenbery SM, Jerosch-Herold M, Rickers C, Colan SD, Geva T, Newburger JW *et al.* Myocardial extracellular remodeling is associated with ventricular diastolic dysfunction in children and young adults with congenital aortic stenosis. *J Am Coll Cardiol* 2014;63(17):1778-85.
45. Chin CW, Shah AS, McAllister DA, Joanna Cowell S, Alam S, Langrish JP *et al.* High-sensitivity troponin I concentrations are a marker of an advanced hypertrophic response and adverse outcomes in patients with aortic stenosis. *Eur Heart J* 2014;35(34):2312-21.
46. Shah AS, Chin CW, Vassiliou V, Cowell SJ, Doris M, Kwok TC *et al.* Left ventricular hypertrophy with strain and aortic stenosis. *Circulation* 2014;130(18):1607-16.
47. Debl K, Djavidani B, Buchner S, Lipke C, Nitz W, Feuerbach S *et al.* Delayed hyperenhancement in magnetic resonance imaging of left ventricular hypertrophy caused by aortic stenosis and hypertrophic cardiomyopathy: visualisation of focal fibrosis. *Heart* 2006;92(10):1447-51.
48. Rudolph A, Abdel-Aty H, Bohl S, Boye P, Zagrosek A, Dietz R *et al.* Noninvasive detection of fibrosis applying contrast-enhanced cardiac magnetic resonance in different forms of left ventricular hypertrophy relation to remodeling. *J Am Coll Cardiol* 2009;53(3):284-91.
49. Weidemann F, Herrmann S, Stork S, Niemann M, Frantz S, Lange V *et al.* Impact of myocardial fibrosis in patients with symptomatic severe aortic stenosis. *Circulation* 2009;120(7):577-84.

50. Singh A, Greenwood JP, Berry C, Dawson DK, Hogrefe K, Kelly DJ *et al.* Comparison of exercise testing and CMR measured myocardial perfusion reserve for predicting outcome in asymptomatic aortic stenosis: the PRognostic Importance of MIcrovascular Dysfunction in Aortic Stenosis (PRIMID AS) Study. *Eur Heart J* 2017.
51. Schneeweis C, Lapinskas T, Schnackenburg B, Berger A, Hucko T, Kelle S *et al.* Comparison of myocardial tagging and feature tracking in patients with severe aortic stenosis. *J Heart Valve Dis* 2014;23(4):432-40.
52. Singh A, Steadman CD, Khan JN, Horsfield MA, Bekele S, Nazir SA *et al.* Intertechnique agreement and interstudy reproducibility of strain and diastolic strain rate at 1.5 and 3 Tesla: a comparison of feature-tracking and tagging in patients with aortic stenosis. *J Magn Reson Imaging* 2015;41(4):1129-37.
53. Mahmod M, Bull S, Suttie JJ, Pal N, Holloway C, Dass S *et al.* Myocardial steatosis and left ventricular contractile dysfunction in patients with severe aortic stenosis. *Circ Cardiovasc Imaging* 2013;6(5):808-16.
54. Al Musa T, Uddin A, Swoboda PP, Garg P, Fairbairn TA, Dobson LE *et al.* Myocardial strain and symptom severity in severe aortic stenosis: insights from cardiovascular magnetic resonance. *Quant Imaging Med Surg* 2017;7(1):38-47.
55. Meyer CG, Frick M, Lotfi S, Altiok E, Koos R, Kirschfink A *et al.* Regional left ventricular function after transapical vs. transfemoral transcatheter aortic valve implantation analysed by cardiac magnetic resonance feature tracking. *Eur Heart J Cardiovasc Imaging* 2014;15(10):1168-76.
56. Sparrow P, Messroghli DR, Reid S, Ridgway JP, Bainbridge G, Sivananthan MU. Myocardial T1 mapping for detection of left ventricular myocardial fibrosis in chronic aortic regurgitation: pilot study. *AJR Am J Roentgenol* 2006;187(6):W630-5.
57. de Meester de Ravenstein C, Bouzin C, Lazam S, Boulif J, Amzulescu M, Melchior J *et al.* Histological Validation of measurement of diffuse interstitial myocardial fibrosis by myocardial extravascular volume fraction from Modified Look-Locker imaging (MOLLI) T1 mapping at 3 T. *J Cardiovasc Magn Reson* 2015;17:48.
58. Pomerantz BJ, Wollmuth JR, Krock MD, Cupps BP, Moustakidis P, Kouchoukos NT *et al.* Myocardial systolic strain is decreased after aortic valve replacement in patients with aortic insufficiency. *Ann Thorac Surg* 2005;80(6):2186-92.
59. Ungacta FF, Davila-Roman VG, Moulton MJ, Cupps BP, Moustakidis P, Fishman DS *et al.* MRI-radiofrequency tissue tagging in patients with aortic insufficiency before and after operation. *Ann Thorac Surg* 1998;65(4):943-50.

60. Edwards NC, Moody WE, Yuan M, Weale P, Neal D, Townend JN *et al.* Quantification of left ventricular interstitial fibrosis in asymptomatic chronic primary degenerative mitral regurgitation. *Circ Cardiovasc Imaging* 2014;7(6):946-53.
61. Han Y, Peters DC, Salton CJ, Bzymek D, Nezafat R, Goddu B *et al.* Cardiovascular magnetic resonance characterization of mitral valve prolapse. *JACC Cardiovasc Imaging* 2008;1(3):294-303.
62. Maniar HS, Brady BD, Lee U, Cupps BP, Kar J, Wallace KM *et al.* Early left ventricular regional contractile impairment in chronic mitral regurgitation occurs in a consistent, heterogeneous pattern. *J Thorac Cardiovasc Surg* 2014;148(4):1694-9.
63. Mankad R, McCreery CJ, Rogers WJ, Jr., Weichmann RJ, Savage EB, Reichek N *et al.* Regional myocardial strain before and after mitral valve repair for severe mitral regurgitation. *J Cardiovasc Magn Reson* 2001;3(3):257-66.
64. Ahmed MI, Gladden JD, Litovsky SH, Lloyd SG, Gupta H, Inusah S *et al.* Increased oxidative stress and cardiomyocyte myofibrillar degeneration in patients with chronic isolated mitral regurgitation and ejection fraction >60%. *J Am Coll Cardiol* 2010;55(7):671-9.
65. Schiros CG, Dell'Italia LJ, Gladden JD, Clark D, 3rd, Aban I, Gupta H *et al.* Magnetic resonance imaging with 3-dimensional analysis of left ventricular remodeling in isolated mitral regurgitation: implications beyond dimensions. *Circulation* 2012;125(19):2334-42.
66. Ahmed MI, Guichard JL, Rajasekaran NS, Ahmad S, Mariappan N, Litovsky S *et al.* Disruption of desmin-mitochondrial architecture in patients with regurgitant mitral valves and preserved ventricular function. *J Thorac Cardiovasc Surg* 2016;152(4):1059-70.e2.
67. Dweck MR, Boon NA, Newby DE. Calcific aortic stenosis: a disease of the valve and the myocardium. *J Am Coll Cardiol* 2012;60(19):1854-63.
68. Kim YJ, Choi BW, Hur J, Lee HJ, Seo JS, Kim TH *et al.* Delayed enhancement in hypertrophic cardiomyopathy: comparison with myocardial tagging MRI. *J Magn Reson Imaging* 2008;27(5):1054-60.
69. Bogarapu S, Puchalski MD, Everitt MD, Williams RV, Weng HY, Menon SC. Novel Cardiac Magnetic Resonance Feature Tracking (CMR-FT) Analysis for Detection of Myocardial Fibrosis in Pediatric Hypertrophic Cardiomyopathy. *Pediatr Cardiol* 2016;37(4):663-73.
70. Borer JS, Truter S, Herrold EM, Falcone DJ, Pena M, Carter JN *et al.* Myocardial fibrosis in chronic aortic regurgitation: molecular and cellular responses to volume overload. *Circulation* 2002;105(15):1837-42.
71. Piper C, Schultheiss HP, Akdemir D, Rudolf J, Horstkotte D, Pauschinger M. Remodeling of the cardiac extracellular matrix differs between volume- and pressure-overloaded ventricles and is specific for each heart valve lesion. *J Heart Valve Dis* 2003;12(5):592-600.

72. Mannacio V, Guadagno E, Mannacio L, Cervasio M, Antignano A, Mottola M *et al.* Comparison of Left Ventricular Myocardial Structure and Function in Patients with Aortic Stenosis and Those with Pure Aortic Regurgitation. *Cardiology* 2015;132(2):111-8.
73. Lancellotti P, Moura L, Pierard LA, Agricola E, Popescu BA, Tribouilloy C *et al.* European Association of Echocardiography recommendations for the assessment of valvular regurgitation. Part 2: mitral and tricuspid regurgitation (native valve disease). *Eur J Echocardiogr* 2010;11(4):307-32.
74. Fuster V, Danielson MA, Robb RA, Broadbent JC, Brown AL, Jr., Elveback LR. Quantitation of left ventricular myocardial fiber hypertrophy and interstitial tissue in human hearts with chronically increased volume and pressure overload. *Circulation* 1977;55(3):504-8.

9

Focal replacement and diffuse fibrosis in primary mitral regurgitation: a new piece to the puzzle

Victoria Delgado, Tomaž Podlesnikar

JACC Cardiovasc Imaging 2021;14(6):1161-3

Mitral regurgitation (MR) is one of the most frequent valvular heart diseases. The most common etiology of primary MR is the myxomatous degeneration of the mitral valve, encompassing fibroelastic deficiency and Barlow's disease. In severe chronic primary MR, the presence of symptoms, reduced left ventricular ejection fraction (LVEF ≤60%) or increased left ventricular (LV) end-systolic diameter are indication for mitral valve repair.[1,2] In asymptomatic patients, surgery should be considered if there is high likelihood of durable mitral valve repair, low operative risk and if there is atrial fibrillation, pulmonary hypertension, flail leaflet or dilated left atrium (LA) at sinus rhythm.[1,2] The evidence showing the benefits of early surgery is accumulating. Data from a large cohort of 1512 patients undergoing mitral valve surgery for isolated primary MR revealed that patients who were operated based only on high likelihood of successful mitral valve repair had the best outcome.[3] The rationale for an early intervention is that the longstanding volume overload caused by severe MR may lead to irreversible LV dysfunction. LVEF is considered the parameter of reference to define LV function and to base the decision making. However, LVEF is a late reflector of the structural changes that MR induces, and one fifth of the patients with preoperative LVEF >60% still develops postoperative LV dysfunction.[4] Increased interstitial fibrosis has been confirmed on autopsy in severe primary MR and is considered to play a key role in the development of LV dysfunction.[5]

In the current issue of JACC Cardiovascular Imaging, Kitkungvan and colleges[6] investigated the associates of extracellular volume (ECV) measured with cardiovascular magnetic resonance (CMR) T1 mapping and focal replacement fibrosis on late gadolinium contrast enhanced (LGE) CMR in 424 patients with chronic primary MR and LVEF ≥50%. Patients were divided into two cohorts: patients with mitral valve prolapse (MVP) and patients with primary MR of other etiologies. Patients with MVP were slightly older and were more frequently male than the patients with non-MVP, whereas patients with non-MVP had more frequently history of heart failure and diabetes compared to their counterparts. In terms of CMR findings, patients with MVP had larger LV and right ventricular dimensions, larger LA volumes and more severe MR as compared to patients without MVP. Patients with MVP showed more frequently replacement fibrosis on LGE-CMR and larger ECV values than patients without MVP. The location of LGE was most commonly located in the basal inferolateral and inferior wall in patients with MVP, whereas in patients without MVP the LGE was located in the basal septum. MVP was independently associated with the presence of LGE. In contrast, ECV values increased along the mitral regurgitant fraction and volume

independently of the etiology of the primary MR and the presence of LGE. Elevated ECV was independently associated with symptoms related to MR and clinical events during follow-up. Patients with moderate and severe MR and an ECV ≥30% had higher event rates than their counterparts with similar grade of MR and an ECV <30%.

The use of CMR in the evaluation of patients with primary MR is gaining followers. CMR has an additional value to echocardiography, since it is the reference standard to quantify chamber dimensions and, in multiple and eccentric regurgitant jets, CMR provides better estimation of the MR severity than 2-dimensional echocardiography.[7] However, the most unique feature of CMR is its capability of noninvasive myocardial tissue characterization.

In primary MR due to MVP, Han and coworkers[8] were the first to describe the association between focal LGE in the papillary muscles and the presence of complex ventricular arrythmias. Furthermore, Basso *et al.*[9] proposed a pathophysiological mechanism, in which specific morphological abnormalities of the mitral apparatus (systolic curling and mitral annular disjunction) generate regional myocardial stress that leads to hypertrophy and replacement fibrosis of the papillary muscles and adjacent myocardium providing a substrate for the development of malignant ventricular arrhythmia. The present results demonstrate that focal LV fibrosis in the inferior and inferolateral LV wall is a unique feature of MVP and is not observed in primary MR of other etiologies.[6] However, the present study does not provide data on the association between LGE and ventricular arrhythmias.

When evaluating diffuse structural changes of the extracellular matrix, Edwards *et al*.[10] described for the first time increased ECV (suggestive of diffuse interstitial fibrosis) in 35 patients with asymptomatic moderate and severe primary MR compared to the healthy individuals. In the current study,[6] ECV was larger in patients with MVP than in patients with primary MR of other etiologies and the main determinants of larger ECV were age, male sex and larger mitral regurgitant fraction. However, it is important to note the significant overlap of the ECV values across individuals with various grades of MR.

The present study provides new knowledge in primary MR: while focal replacement fibrosis is related to the etiology of primary MR, diffuse myocardial fibrosis is associated with the severity of MR. How do we use this information in clinical practice?

The measurement of ECV may help in the timing of intervention; increased ECV has been associated with reduced exercise capacity as well as with greater perceived level of exertion in patients with primary MR.[10] In addition, among asymptomatic patients with primary MR, increased ECV has been associated with adverse outcome.[6,11] In contrast, the

presence of LGE may help to identify the patients with primary MR that are at risk of ventricular arrhythmias and who could benefit from an implantable cardioverter defibrillator. The majority of the patients with MVP who present with ventricular arrhythmias or sudden cardiac death do not present with severe MR to operate on.[12] The ongoing "Mitral FINDER" trial[13] will provide important answers to define the role of CMR in the management of patients with primary MR.

REFERENCES

1. Nishimura RA, Otto CM, Bonow RO, Carabello BA, Erwin JP, 3rd, Fleisher LA *et al.* 2017 AHA/ACC Focused Update of the 2014 AHA/ACC Guideline for the Management of Patients With Valvular Heart Disease: A Report of the American College of Cardiology/American Heart Association Task Force on Clinical Practice Guidelines. *J Am Coll Cardiol* 2017;70(2):252-89.
2. Baumgartner H, Falk V, Bax JJ, De Bonis M, Hamm C, Holm PJ *et al.* 2017 ESC/EACTS Guidelines for the management of valvular heart disease. *Eur Heart J* 2017;38(36):2739-91.
3. Enriquez-Sarano M, Suri RM, Clavel MA, Mantovani F, Michelena HI, Pislaru S *et al.* Is there an outcome penalty linked to guideline-based indications for valvular surgery? Early and long-term analysis of patients with organic mitral regurgitation. *J Thorac Cardiovasc Surg* 2015;150(1):50-8.
4. Quintana E, Suri RM, Thalji NM, Daly RC, Dearani JA, Burkhart HM *et al.* Left ventricular dysfunction after mitral valve repair--the fallacy of "normal" preoperative myocardial function. *J Thorac Cardiovasc Surg* 2014;148(6):2752-60.
5. Fuster V, Danielson MA, Robb RA, Broadbent JC, Brown AL, Jr., Elveback LR. Quantitation of left ventricular myocardial fiber hypertrophy and interstitial tissue in human hearts with chronically increased volume and pressure overload. *Circulation* 1977;55(3):504-8.
6. Kitkungvan D, Yang EY, El Tallawi KC, Nagueh SF, Nabi F, Khan MA *et al.* Extracellular Volume in Primary Mitral Regurgitation. *JACC Cardiovasc Imaging* 2021;14(6):1146-60.
7. Zoghbi WA, Adams D, Bonow RO, Enriquez-Sarano M, Foster E, Grayburn PA *et al.* Recommendations for Noninvasive Evaluation of Native Valvular Regurgitation: A Report from the American Society of Echocardiography Developed in Collaboration with the Society for Cardiovascular Magnetic Resonance. *J Am Soc Echocardiogr* 2017;30(4):303-71.
8. Han Y, Peters DC, Salton CJ, Bzymek D, Nezafat R, Goddu B *et al.* Cardiovascular magnetic resonance characterization of mitral valve prolapse. *JACC Cardiovasc Imaging* 2008;1(3):294-303.
9. Basso C, Iliceto S, Thiene G, Perazzolo Marra M. Mitral Valve Prolapse, Ventricular Arrhythmias, and Sudden Death. *Circulation* 2019;140(11):952-64.
10. Edwards NC, Moody WE, Yuan M, Weale P, Neal D, Townend JN *et al.* Quantification of left ventricular interstitial fibrosis in asymptomatic chronic primary degenerative mitral regurgitation. *Circ Cardiovasc Imaging* 2014;7(6):946-53.
11. Kitkungvan D, Yang EY, El Tallawi KC, Nagueh SF, Nabi F, Khan MA *et al.* Prognostic Implications of Diffuse Interstitial Fibrosis in Asymptomatic Primary Mitral Regurgitation. *Circulation* 2019;140(25):2122-4.

12. Hourdain J, Clavel MA, Deharo JC, Asirvatham S, Avierinos JF, Habib G *et al.* Common Phenotype in Patients With Mitral Valve Prolapse Who Experienced Sudden Cardiac Death. *Circulation* 2018;138(10):1067-9.
13. Liu B, Edwards NC, Neal DAH, Weston C, Nash G, Nikolaidis N *et al.* A prospective study examining the role of myocardial Fibrosis in outcome following mitral valve repair IN DEgenerative mitral Regurgitation: rationale and design of the mitral FINDER study. *BMC Cardiovasc Disord* 2017;17(1):282.

10

Summary, conclusions and future perspectives

Samenvatting, conclusies en toekomstperspectieven

SUMMARY

SUMMARY Part I: Cardiovascular magnetic resonance-derived left ventricular strain after acute myocardial infarction

In **Part I** the role of left ventricular (LV) strain with feature-tracking cardiovascular magnetic resonance (CMR) to evaluate myocardial injury and cardioprotective effects of early intravenous metoprolol were explored in the Effect of Metoprolol in Cardioprotection During an Acute Myocardial Infarction (METOCARD-CNIC) clinical trial. In **Chapter 2** an overall improvement of global circumferential (GCS) and longitudinal (GLS) strain between 1-week and 6-month follow-up after the acute anterior ST-segment elevation myocardial infarction (STEMI) treated with primary percutaneous coronary intervention (PCI) was demonstrated (change in GCS and GLS 3.2%, P<0.001 for both). This was paralleled by an increase in left ventricular ejection fraction (LVEF) and a reduction in late gadolinium enhancement (LGE)-assessed infarct size over 6 months after STEMI, and is in line with previous findings from speckle-tracking echocardiography.[1] Moreover, early administration of intravenous metoprolol was associated with more preserved LV GCS and GLS at 1 week after myocardial infarction (GCS: -13.9±3.8% versus -12.6±3.9%, respectively; P=0.013; GLS: -11.9±2.8% versus -10.9±3.2%, respectively; P=0.032). On the other hand, the differences in global LV strain indices at 6 months after STEMI did not reach the level of statistical significance. However, when dividing the overall cohort of patients in quartiles of GCS and GLS, there were significantly lower number of patients receiving early intravenous metoprolol in the first GCS and GLS quartile (i.e., the worst LV systolic function), both at 1 week and at 6 months after STEMI. These results strengthen the evidence to support the use of early intravenous metoprolol in STEMI patients without contraindications to beta-blockers undergoing primary PCI.

In **Chapter 3** the evolution of the LV circumferential strain has been studied separately for the infarct and the remote zone myocardium. Since the METOCARD-CNIC trial included a homogeneous population of anterior STEMI patients with a culprit lesion in the left anterior descending coronary artery (LAD), the infarct zone was defined as the LAD perfusion territory while the rest of the LV myocardium was defined as the remote zone.[2-4] In the overall population the infarct zone strain significantly improved from 1 week to 6 months after STEMI (from -8.6% to -14.5%; P<0.001), while no significant changes in the remote zone strain were observed (from -19.5% to -19.2%; P=0.466). Similar results were observed among different subgroups of patients – the infarct zone strain improved in patients who did and did not receive

early intravenous metoprolol in addition to the standard STEMI therapy, in patients with and without microvascular obstruction (MVO), intramyocardial hemorrhage (IMH), and in patients who developed adverse LV remodeling at 6 months after STEMI (defined as ≥20% increase in LV end-diastolic volume). This demonstrates a preserved healing capacity of the infarcted myocardium even in the presence of adverse CMR findings (e.g., MVO or IMH). On the other hand, no significant dynamics in the remote zone circumferential strain were observed among the analyzed subgroups, apart from patients who developed adverse LV remodeling. Among them the remote zone strain worsened between 1 week and 6 months after STEMI (P=0.036), indicating that possible maladaptive processes like excessive inflammation/fibrosis of the remote myocardium[5] may become manifest as an impaired circumferential strain. Moreover, regional strain analysis demonstrated that patients receiving early intravenous metoprolol had more preserved infarct zone circumferential strain compared to the control group, both at 1 week and at 6 months after STEMI (P=0.038 and P=0.033; respectively). This is a very important finding, especially in the view that the differences in global strain between both treatment arms at 6 months were nonsignificant,[6] underscoring the long-lasting cardioprotective effects of early intravenous metoprolol. Interestingly, no significant differences in the remote zone circumferential strain were found between both groups of patients, implying that the beneficial cardioprotective effects were largely confined to the infarct zone myocardium.

Chapter 4 focuses on the long-term 5-year follow-up data of patients included in the METOCARD-CNIC trial. In contrast to the previously published results,[7] a significant reduction in major adverse cardiac events (MACE; a prespecified clinical endpoint, comprised of death, rehospitalization for heart failure, reinfarction and malignant ventricular arrhythmias) among patients receiving early intravenous metoprolol was demonstrated (HR: 0.500, 95% CI: 0.277-0.903; P=0.022). Impaired LV GCS and GLS strain were significantly associated with increased occurrence of MACE (GCS: HR:1.208, 95%CI:1.076-1.356, P=0.001; GLS: HR:1.362, 95%CI:1.180-1.573, P<0.001). On multivariable analysis, LV GLS provided incremental prognostic value over LGE and LVEF for the occurrence of MACE (LGE+LVEF chi-square=12.865, LGE+LVEF+GLS chi-square=18.459; P=0.012). Patients with more impaired GLS (above median value ≥-11.5%) who received early intravenous metoprolol were 64% less likely to experience MACE than their counterparts with same degree of GLS impairment (HR:0.356, 95%CI:0.129-0.979; P=0.045). These results show that early intravenous metoprolol had a long-term beneficial clinical effect, particularly in patients who were at a greater risk for the adverse events due to severely impaired LV systolic function.

SUMMARY Part II: Multimodality cardiac imaging in valvular heart disease

Multimodality cardiac imaging plays a central role in the management of patients with valvular heart disease (VHD). In **Chapter 5** the role of imaging to assess patients with VHD and coexisting heart failure was explored. Two common scenarios were discussed, i.e. secondary mitral regurgitation (MR) and low-flow low-gradient severe aortic stenosis (AS) with reduced LVEF. The challenges to determine the severity of secondary MR and to decide upon the optimal treatment option (medical therapy versus surgical or percutaneous intervention) with standard transthoracic echocardiography derive from the fact that the evaluation of MR severity is heavily influenced by the LV loading conditions, systemic blood pressure, the non-circular shape of regurgitant jet orifice and by temporal variation of MR during cardiac cycle. 3-dimensional (3D) echocardiography with direct planimetric measurement of vena contracta and regurgitant volume estimation with phase-contrast CMR may overcome some of these difficulties. Among patients with AS, reduced LVEF and contractile reserve, dobutamine stress echocardiography is the primary diagnostic method to differentiate between true severe and pseudo-severe AS. On the other hand, among patients with discrepant measures of AS severity and no contractile reserve, the assessment of aortic valve calcification burden with cardiac computed tomography (CT) may help to estimate the severity of AS. Furthermore, the role of multimodality imaging to select the optimal intervention in patients with secondary MR (surgical repair, replacement or percutaneous edge-to-edge repair) and AS (surgical versus transcatheter aortic valve replacement) were discussed.

In **Chapter 6** the advantages and limitations of different cardiac imaging techniques for patient selection, procedural planning and follow-up after transcatheter aortic valve replacement (TAVR) were explored. Compared to 2-dimensional methods 3D techniques like 3D transesophageal echocardiography (TEE), multidetector row computed tomography (MDCT) and CMR have proven to more accurately determine the aortic annulus size, the most important parameter for the choice of TAVR prosthesis size. The use of 3D methods has translated into lower incidence of significant paravalvular regurgitation after TAVR. The detailed vascular anatomy assessment (vessel size, tortuosity, degree of calcification and plaque burden) of the thoracoabdominal aorta and iliofemoral arteries using MDCT allows planning of the optimal TAVR access route (transfemoral, transaortic or transapical). While most of the centers currently perform TAVR under fluoroscopic guidance, periprocedural TEE as well as transthoracic echocardiography can be of an added value for early assessment of procedural complications (e.g., paravalvular and valvular regurgitation, aortic an-

nulus rupture, coronary ostium occlusion, prosthesis malpositioning or dislodgement), reduced radiation exposure and lower use of nephrotoxic contrast. After TAVR, transthoracic echocardiography remains the first-choice imaging technique to evaluate the procedural results, the durability of the prosthesis, and the changes in LV dimensions and function. However, recent studies using MDCT, which showed an increased incidence of hypo-attenuated leaflet thickening with reduced leaflet motion of TAVR prostheses (an early marker of prosthetic valve thrombosis), raised a question whether MDCT should be systematically included in the surveillance of TAVR patients.[8-10]

In **Chapter 7** novel automated 3D TEE imaging software was shown to allow reliable assessment of the aortic annulus dimensions in patients with severe AS undergoing TAVR. Compared to MDCT, 3D TEE measurements slightly underestimated the aortic annulus dimensions, which is in line with previously published literature.[11-13] The agreement between 3D TEE and MDCT for the measurement of the aortic annulus dimensions was superior among patients with low aortic valve calcification burden compared to the patients with high calcification burden. Importantly, 3D TEE measurements based on automatic software analysis and MDCT led to the same prosthesis size selection in the majority (88%) of the patients. However, the agreement between 3D TEE and MDCT on the prosthesis size selection was better among patients with low versus high aortic valve calcification burden (agreement in 95% versus 81% of patients; respectively) and in the majority of patients the 3D TEE measurements suggested smaller prosthesis size compared to MDCT. 3D TEE thus represents a valuable alternative to MDCT in patients with AS undergoing TAVR when the latter is contraindicated (impaired renal function) and might be particularly attractive in patients with less calcified aortic valves.

Chapter 8 focuses on the role of CMR to assess myocardial fibrosis in severe VHD. In patients with AS the presence of LGE, a marker of focal replacement fibrosis, and increased values of native T1 or extracellular volume (ECV), markers of diffuse interstitial myocardial fibrosis, have been associated with worse symptoms, worse LV systolic and diastolic function and higher levels of serum cardiac biomarkers. The presence of LGE was associated with an increase in all-cause mortality among patients with high grade AS, which has been recently confirmed in a large multi-center observational study.[14] Furthermore, all-cause mortality rates rose progressively across patients with normal indexed ECV without LGE (no myocardial fibrosis), patients with increased indexed ECV without LGE (diffuse interstitial myocardial fibrosis) and patients with LGE (focal replacement myocardial fibrosis), implying adverse

outcome with more advanced stages of myocardial fibrosis assessed with CMR. Similarly, LV circumferential strain with CMR tagging was significantly associated with all-cause mortality in severe AS patients undergoing surgical and transcatheter aortic valve replacement. The data on myocardial fibrosis in aortic regurgitation and MR is less extensive, however studies have shown an inverse correlation between the amount of myocardial fibrosis and measures of systolic and diastolic function, functional capacity and long-term survival after valve surgery.

In **Chapter 9** the role of myocardial fibrosis was further discussed with the emerging data on patients with mitral valve prolapse (MVP). Focal replacement fibrosis of the papillary muscles and of the inferolateral LV wall, detected with LGE, has been characterized as a unique feature of MVP, that has neither been observed in primary MR of other etiologies nor has been associated with the severity of MR. On the other hand, the diffuse interstitial fibrosis detected with ECV was shown to be a marker of the severity of MR unrelated to the mechanism. Focal replacement fibrosis has been proposed as a substrate for the electrical instability of the adjacent myocardium and represents a hallmark of the so-called arrhythmogenic MVP, which describes patients with MVP who have an increased risk for malignant ventricular arrythmias and sudden cardiac death.[15]

CONCLUSIONS AND FUTURE PERSPECTIVES

The assessment of LV strain as a functional surrogate of myocardial injury in acute myocardial infarction with feature-tracking CMR is feasible, both as a global and regional functional parameter. LV strain can provide important insights into the healing processes in the myocardium. In particular, LV GLS assessed early after PCI can provide important prognostic information above conventional CMR parameters like LVEF and LGE in the risk stratification of STEMI patients. Paralleled with the advances of the primary PCI and long-term medical therapy after STEMI, novel therapies aiming at reducing the acute ischemia-reperfusion injury are pursued. Early intravenous beta blockade was the first cardioprotective medical therapy that showed prognostic benefit in a randomized clinical trial and was adopted by the current European Society of Cardiology guidelines as a class IIa recommendation for hemodynamically stable STEMI patients undergoing primary PCI.[16] However, large-number data from observational studies and patient registries are required to confirm the same findings in the real-life situation. Importantly, LV strain

assessment with feature-tracking CMR can serve as a powerful complementary tool to evaluate the benefits of novel cardioprotective therapies.

Multimodality cardiac imaging plays a central role in the management of patients with VHD (Figure 1). Transthoracic echocardiography, TEE, cardiac CT and CMR help in the assessment of the etiology of VHD, valve anatomy, mechanism and severity of dysfunction and co-existing VHD. 3D techniques provide important advantages over standard 2-dimensional imaging. Furthermore, imaging provides crucial insights into ventricular remodeling and dysfunction, the most important adverse consequences of VHD. Parameters like chamber volumes and ejection fraction are the key to decide the eligibility and optimal timing for valve intervention, as recommended by the current guidelines.[17,18] However, novel risk markers, such as myocardial fibrosis with CMR and strain imaging with echocardiography and CMR may redefine our future treatment strategies. Clinical trials comparing early valve intervention versus standard care in patients with asymptomatic severe AS and primary MR, who do not meet current guidelines criteria for surgery but present with LV myocardial fibrosis, are recruiting patients.[19,20] Advanced imaging helps in discovering high-risk features of adverse outcome, e.g. increased risk of life-threatening ventricular arrhythmias in MVP patients with papillary muscles or lateral LV wall fibrosis, detected with LGE-CMR. Future clinical trials need to investigate whether implantable cardioverter defibrillator in these patients would lead to favorable outcomes. Wide implementation of TAVR established multimodality imaging, in particular cardiac CT, a key for procedural planning. With emerging transcatheter mitral and tricuspid valve therapies, CT and other 3D imaging techniques will have even greater impact on procedural planning. 3D TEE is fundamental to guide percutaneous edge-to-edge mitral valve repair and novel transcatheter therapies. Fusion imaging, i.e., side-by-side registration of data rendered by more than 1 non-invasive imaging modality (CT or CMR with real-time fluoroscopy and TEE) may increase the smoothness of structural interventions by combining anatomic, morphological, and functional information. Finally, cardiac imaging is essential to evaluate the long-term results of valve interventions to detect possible complications and to compare the efficacy of novel therapies with the gold standards in order to improve patients outcome.

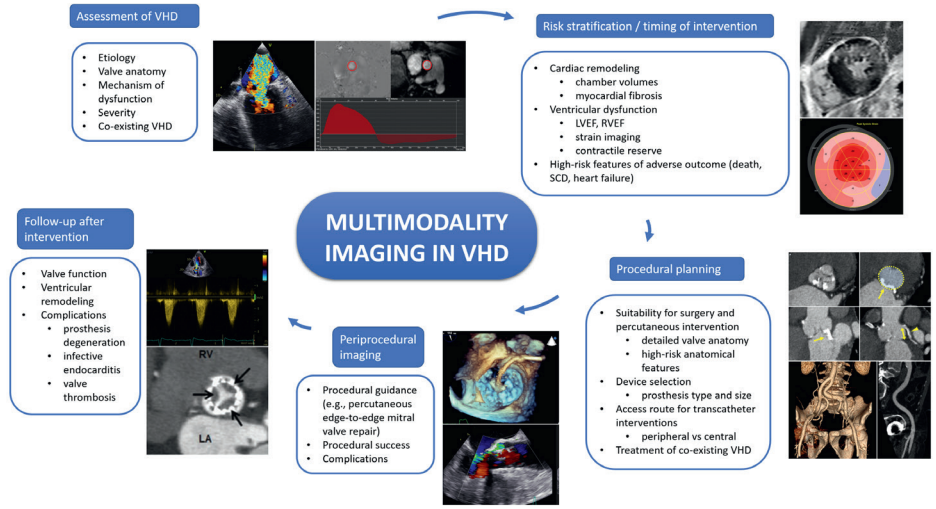

Figure 1: Multimodality cardiac imaging in valvular heart disease. LVEF = left ventricular ejection fraction; RVEF = right ventricular ejection fraction; SCD = sudden cardiac death; VHD = valvular heart disease.

REFERENCES

1. Antoni ML, Mollema SA, Atary JZ, Borleffs CJ, Boersma E, van de Veire NR *et al.* Time course of global left ventricular strain after acute myocardial infarction. *Eur Heart J* 2010;31(16):2006-13.
2. Lang RM, Badano LP, Mor-Avi V, Afilalo J, Armstrong A, Ernande L *et al.* Recommendations for cardiac chamber quantification by echocardiography in adults: an update from the American Society of Echocardiography and the European Association of Cardiovascular Imaging. *Eur Heart J Cardiovasc Imaging* 2015;16(3):233-70.
3. Ortiz-Perez JT, Rodriguez J, Meyers SN, Lee DC, Davidson C, Wu E. Correspondence between the 17-segment model and coronary arterial anatomy using contrast-enhanced cardiac magnetic resonance imaging. *JACC Cardiovasc Imaging* 2008;1(3):282-93.
4. Cerci RJ, Arbab-Zadeh A, George RT, Miller JM, Vavere AL, Mehra V *et al.* Aligning coronary anatomy and myocardial perfusion territories: an algorithm for the CORE320 multicenter study. *Circ Cardiovasc Imaging* 2012;5(5):587-95.
5. Bulluck H, Rosmini S, Abdel-Gadir A, White SK, Bhuva AN, Treibel TA *et al.* Automated Extracellular Volume Fraction Mapping Provides Insights Into the Pathophysiology of Left Ventricular Remodeling Post-Reperfused ST-Elevation Myocardial Infarction. *J Am Heart Assoc* 2016;5(7).
6. Podlesnikar T, Pizarro G, Fernandez-Jimenez R, Montero-Cabezas JM, Sanchez-Gonzalez J, Bucciarelli-Ducci C *et al.* Effect of Early Metoprolol During ST-Segment Elevation Myocardial Infarction on Left Ventricular Strain: Feature-Tracking Cardiovascular Magnetic Resonance Substudy From the METOCARD-CNIC Trial. *JACC Cardiovasc Imaging* 2019;12(7 Pt 1):1188-98.
7. Pizarro G, Fernandez-Friera L, Fuster V, Fernandez-Jimenez R, Garcia-Ruiz JM, Garcia-Alvarez A *et al.* Long-term benefit of early pre-reperfusion metoprolol administration in patients with acute myocardial infarction: results from the METOCARD-CNIC trial (Effect of Metoprolol in Cardioprotection During an Acute Myocardial Infarction). *J Am Coll Cardiol* 2014;63(22):2356-62.
8. Leetmaa T, Hansson NC, Leipsic J, Jensen K, Poulsen SH, Andersen HR *et al.* Early aortic transcatheter heart valve thrombosis: diagnostic value of contrast-enhanced multidetector computed tomography. *Circ Cardiovasc Interv* 2015;8(4).
9. Makkar RR, Fontana G, Jilaihawi H, Chakravarty T, Kofoed KF, De Backer O *et al.* Possible Subclinical Leaflet Thrombosis in Bioprosthetic Aortic Valves. *N Engl J Med* 2015;373(21):2015-24.
10. Vollema EM, Kong WKF, Katsanos S, Kamperidis V, van Rosendael PJ, van der Kley F *et al.* Transcatheter aortic valve thrombosis: the relation between hypo-attenuated leaflet thickening, abnormal valve haemodynamics, and stroke. *Eur Heart J* 2017;38(16):1207-17.

11. Ng AC, Delgado V, van der Kley F, Shanks M, van de Veire NR, Bertini M *et al.* Comparison of aortic root dimensions and geometries before and after transcatheter aortic valve implantation by 2- and 3-dimensional transesophageal echocardiography and multislice computed tomography. *Circ Cardiovasc Imaging* 2010;3(1):94-102.
12. Khalique OK, Hamid NB, White JM, Bae DJ, Kodali SK, Nazif TM *et al.* Impact of Methodologic Differences in Three-Dimensional Echocardiographic Measurements of the Aortic Annulus Compared with Computed Tomographic Angiography Before Transcatheter Aortic Valve Replacement. *J Am Soc Echocardiogr* 2017;30(4):414-21.
13. Vaquerizo B, Spaziano M, Alali J, Mylote D, Theriault-Lauzier P, Alfagih R *et al.* Three-dimensional echocardiography vs. computed tomography for transcatheter aortic valve replacement sizing. *Eur Heart J Cardiovasc Imaging* 2016;17(1):15-23.
14. Musa TA, Treibel TA, Vassiliou VS, Captur G, Singh A, Chin C *et al.* Myocardial Scar and Mortality in Severe Aortic Stenosis: Data from the BSCMR Valve Consortium. *Circulation* 2018.
15. Basso C, Iliceto S, Thiene G, Perazzolo Marra M. Mitral Valve Prolapse, Ventricular Arrhythmias, and Sudden Death. *Circulation* 2019;140(11):952-64.
16. Ibanez B, James S, Agewall S, Antunes MJ, Bucciarelli-Ducci C, Bueno H *et al.* 2017 ESC Guidelines for the management of acute myocardial infarction in patients presenting with ST-segment elevation: The Task Force for the management of acute myocardial infarction in patients presenting with ST-segment elevation of the European Society of Cardiology (ESC). *Eur Heart J* 2018;39(2):119-77.
17. Baumgartner H, Falk V, Bax JJ, De Bonis M, Hamm C, Holm PJ *et al.* 2017 ESC/EACTS Guidelines for the management of valvular heart disease. *Eur Heart J* 2017;38(36):2739-91.
18. Otto CM, Nishimura RA, Bonow RO, Carabello BA, Erwin JP, 3rd, Gentile F *et al.* 2020 ACC/AHA Guideline for the Management of Patients With Valvular Heart Disease: A Report of the American College of Cardiology/American Heart Association Joint Committee on Clinical Practice Guidelines. *Circulation* 2021;143(5):e72-e227.
19. Bing R, Everett RJ, Tuck C, Semple S, Lewis S, Harkess R *et al.* Rationale and design of the randomized, controlled Early Valve Replacement Guided by Biomarkers of Left Ventricular Decompensation in Asymptomatic Patients with Severe Aortic Stenosis (EVOLVED) trial. *Am Heart J* 2019;212:91-100.
20. Liu B, Edwards NC, Neal DAH, Weston C, Nash G, Nikolaidis N *et al.* A prospective study examining the role of myocardial Fibrosis in outcome following mitral valve repair IN DEgenerative mitral Regurgitation: rationale and design of the mitral FINDER study. *BMC Cardiovasc Disord* 2017;17(1):282.

SAMENVATTING

SAMENVATTING Deel I: De rol van magnetische resonantie imaging voor het bepalen van de linkerventrikel strain functie na een acuut myocardinfarct

In **Deel I** is onderzocht op wat voor manier het met magnetische resonantie imaging (MRI) analyseren van de linkerventrikel (LV) strain functie nieuwe inzichten kan geven in patiënten met een recent myocardinfarct. Met strain imaging wordt de mate en snelheid van het cyclisch (gedurende systole en diastole) deformeren van het myocardweefsel onderzocht en hierdoor weergeeft LV strain beter de intrinsieke cardiale functie dan bijvoorbeeld het bepalen van de ejectiefractie waarbij enkel wordt gekeken naar de ratio tussen het eind-diastolische en eind-systolische LV volume. Het met MRI beoordelen van de LV strain werd toegepast in de studie patiënten van de ”Metoprolol in Cardioprotection During an Acute Myocardial Infarction (METOCARD-CNIC)” studie. Er werd onderzocht of het intraveneus (IV) toedienen van metoprolol een cardioprotectief effect oplevert. **Hoofdstuk 2** toonde een verbetering van zowel de globale als de circumferentiële myocardiale contractiliteit tussen de eerste week, en 6 maanden na het gedotterde acute ST-elevatie infarct: de globaal longitudinale (GLS) en circumferentiële (GCS) strain verbeterde met 3.2%, P<0.001. MRI toonde ook een verbetering van LV functie aan als deze werd beoordeeld o.b.v. de ejectiefractie; hiernaast was er afname in de grootte van het litteken, gemeten o.b.v. de grootte van late gadolinium enhancement (LGE). Huidige verbetering van LV strain 6 maanden post-infarct, hier met MRI gemeten, komt overeen met eerdere echocardiografische studies waarin LV strain werd bepaald o.b.v. speckle-tracking echocardiografie.[1] Het IV toedienen van metoprolol resulteerde in een betere globale longitudinale en in een circumferentiële LV strain 1 week na het infarct t.o.v. de patiënten die geen IV metoprolol kregen (GCS: -13.9±3.8% vs.12.6±3.9%; P=0.013; GLS: -11.9±2.8% vs. -10.9±3.2%. P=0.032). Na 6 maanden was er echter geen verschil in myocardiale functie tussen de 2 groepen. Bij het o.b.v. GCS en GLS in kwartielen categoriseren van de patiënten bleek wel dat er in de groep patiënten met de laagste contractiliteit ook het minst aantal patiënten was wat met IV metoprolol was behandeld. Deze resultaten onderbouwen de ratio voor het toedienen van IV metoprolol als cardioprotectieve maatregel in ST-elevatie infarct patiënten die een acute dotterbehandeling ondergaan (indien niet gecontra-indiceerd).

In **Hoofdstuk 3** werd specifiek gekeken naar de verschillen in circumferentiële LV strain tussen geinfarceerd weefsel vs. “remote” weefsel. Aangezien in de METOCARD-CNIC trial enkel patienten met een acuut ST-elevatie infarct van de voorwand o.b.v. een culprit in de linker anteri-

eure descenderende coronair (LAD) geïncludeerd werden, werd het stroomgebied van de LAD gedefinieerd als infarctgebied, en de overige LV wanden als "remote".[2-4] In de gehele populatie verbeterde de circumferentiële strain in de infarct zone significant tussen 1 week en 6 maanden post infarct (van -8.6% tot -14.5%; P<0.001), terwijl in de remote zone de strain al direct 1 week na het infarct weer hersteld was (-19.5% tot -19.2%; P=0.466). Eenzelfde verbetering in circumferentiële strain van het infarct gebied werden gevonden in verschillende subgroepen: in de patiënten met of zonder IV metoprolol, in de patiënten met en zonder microvasculaire obstructies, intramyocardiale bloeding en in de patiënten wiens myocard negatieve remodeling toonde 6 maanden na het infarct (≥20% stijging van het LV eind-diastolische volume). De verbetering in circumferentiële strain van het infarct gebied toont de genezende capaciteit van het myocard aan, zelfs als er al aanwijzingen zijn voor vergevorderde schade zoals microvasculaire obstructies of bloedingen. In de patiënten met negatieve remodeling was te zien dat juist de circumferentiële strain van het "remote" myocard na 6 maanden was verslechterd t.o.v. week 1 post-infarct (P=0.036). Dit zou kunnen duiden op mogelijke excessieve inflammatie / fibrose van het "remote" myocard.[5] Het met circumferentiële strain analyseren van de contractiliteit van het geinfarceerde myocard toonde een betere contractiliteit aan, zowel 1 week, als 6 maanden post-infarct in de patiënten die IV metoprolol hadden gekregen. (P=0.038 en P=0.033). Dit verschil in circumferentiële strain in het infarct gebied is een belangrijke bevinding omdat als de hartfunctie o.b.v. de globale strain wordt beoordeeld er tussen beide groepen geen verschil te zien was na 6 maanden.[6] Op de circumferentiële strain van "remote" myocard had het toedienen van IV metoprolol geen significant effect.

In **Hoofdstuk 4** worden de 5-jaars data van de METOCARD-CNIC studie beschreven. In tegenstelling tot eerdere studies,[7] was er een significante vermindering in het aantal majeure negatieve events in de patiënten die IV metoprolol na hun infarct hadden gekregen. De gebruikte uitkomstmaat omvatte het aantal doden, de rehospitalisaties voor hartfalen, re-infarcten en maligne hartritmestoornissen: (IV metoprolol vs. geen IV metoprolol = HR: 0.500, 95% CI: 0.277-0.903; P=0.022). Zowel een verminderde circumferentiële strain als globaal longitudinale strain waren geassocieerd met het ontstaan van majeure negatieve events. (GCS: HR:1.208, 95% CI:1.076-1.356, P=0.001; GLS: HR:1.362, 95% CI:1.180-1.573, P<0.001). In de multivariate analyse bleek GLS van additief prognostische waarde t.o.v. LGE en de LV ejectiefractie voor het ontstaan van majeure negatieve events. (LGE+LVEF chi-square=12.865, LGE+LVEF+GLS chi-square=18.459; P=0.012). In de patiënten met een verminderde GLS (o.b.v. de mediane waarde van -11.5%) resulteerde het toedienen van IV metoprolol in een 64% lagere kans op

majeure negatieve events. Deze resultaten tonen dat het toedienen van IV metoprolol na een recent hartinfarct gunstige effecten kan hebben op de lange termijn, met name in de patiënten met het hoogste risico vanwege ernstige LV dysfunctie.

SAMENVATTING Deel 2: Multimodality imaging voor kleplijden

Het met meerdere imaging modaliteiten onderzoeken van patiënten met kleplijden kan helpen in het bepalen van de juiste behandeling voor deze patiënten. In **Hoofdstuk 5** werd onderzocht hoe imaging kan helpen in patiënten met én kleplijden én hartfalen. Het hoofdstuk richtte zich op patiënten met secundaire mitralisklep insufficiëntie waarbij de insufficiënte mitralisklep het gevolg is van een gedilateerde of dysfunctionerende LV en naar patiënten met een verminderde LV ejectiefractie en ernstige low-flow-low-gradiënt aortaklepstenose. Het met standaard echocardiografie accuraat beoordelen van de ernst van de mitralisklep insufficiëntie wordt bemoeilijkt doordat de ernst van de lekkage voor een groot deel bepaald wordt doordat volumestatus en bloeddruk weer de vorm en grootte van het sluitingsdefect beïnvloeden. Met 2-dimensionale (2D) echocardiografie wordt het sluitingsdefect van de mitralisklep als circulair beschouwd, terwijl dit in de praktijk juist een door de hartcyclus heen wisselende, elliptische configuratie heeft. Door gebruik te maken van 3D echocardiografie kan de vorm en grootte van het sluitingsdefect direct worden beoordeeld in en-face views waardoor er geen geometrische assumpties nodig zijn. Hiernaast kan ook MRI data gebruikt worden voor de kwantificatie van de ernst van de mitralisklep insufficiëntie. Voor patiënten met een aortaklepstenose en verminderde LV ejectiefractie is het de vraag of de aortaklep niet goed opent vanwege een te laag slagvolume of dat de aortaklep daadwerkelijk ernstig aangetast is en daardoor niet goed opent. Ter differentiatie hiervoor is dobutamine stress echocardiografie de eerste aangewezen stap. Bij een intrinsieke aortaklepziekte zal met dobutamine de gradiënt hierover toenemen, terwijl de gradiënt niet veel toeneemt in het geval de aortaklep ook beter gaat openen door een door de dobutamine gestimuleerde hogere LV flow. Voor patiënten wiens voorwaarts LV volume niet veel door dobutamine kan verbeteren (klein slagvolume, of onvoldoende contractiele reserve) kan ook computer tomografie (CT) gebruikt worden voor het kwantificeren van de ernst van de aortaklepstenose door de hoeveelheid calcium te meten. Hiernaast werd in dit hoofdstuk nog de rol van multimodality imaging besproken om de optimale manier van interventie te bepalen: voor de mitralisklep een chirurgische reparatie of vervanging of een transcatheter edge-to-edge reparatie, en voor de aortaklep een chirurgische vs. transcatheter vervanging.

In **Hoofdstuk 6** werden de voor- en nadelen besproken van de verschillende imaging technieken voor het bepalen van de juiste patiënt selectie criteria, de manier van preprocedurele planning en voor de follow-up van patiënten die een transcatheter aortaklep implantatie (TAVI) ondergaan. Vergeleken met 2D beeldvormingstechnieken is het bewezen dat 3D technieken zoals 3D slokdarmechocardiografie, CT en MRI accurater metingen van de aorta annulus geven, en de gemeten dimensies bepaalt de grootte van de te implanteren prothese. Het gebruik van 3D technieken vertaalde zich in een lagere incidentie van paravalvulaire lekkage na TAVI. Hiernaast weergeeft CT de gehele aorta en wordt een goed beeld verkregen van de vasculaire anatomie: grootte, tortuositeit, mate van calcificatie waardoor bepaald kan worden of een transfemorale toegang mogelijk is, of dat er toch voor een transapicale benadering gekozen dient te worden. Hoewel veel centra TAVI tegenwoordig verrichten met behulp van enkel fluoroscopie, kan echocardiografie (slokdarm en transthoracaal) van toegevoegde waarde zijn voor het vroegtijdig diagnosticeren van complicaties zoals paravalvulaire lekkage, het ruptureren van de annulus, malappositie en coronaire occlusie. Hiernaast daalt de blootstelling aan ioniserende straling en aan nefrotoxisch contrast. Na TAVI is transthoracale echocardiografie de eerste modaliteit voor het bepalen van de hemodynamische resultaten, de durabiliteit van de prothese en de mate van LV remodeling. Nieuwere studies toonden dat juist CT gebruikt kan worden voor het vroegtijdig opsporen van “hypo-attennuated leaflet thickening” (HALT), een fenomeen waarbij de klepbladen van de prothese in beweging belemmerd worden door vroege kleptrombose. Dit resulteerde in de vraag of CT niet als standaard imaging techniek gebruikt dient te worden in de post-procedurele evaluatie van TAVI patiënten.[8-10]

In **Hoofdstuk 7** werd aangetoond dat post-processing software voor 3D echocardiografie beelden gebruikt kan worden voor het automatisch meten van de annulus dimensies. Vergeleken met CT waren de 3D echo metingen licht onderschat, en dit is vergelijkbaar met eerdere studies.[11-13] De correlatie tussen 3D echo en CT voor het meten van de aorta annulus dimensies was beter in de patiënten met een lagere mate van aortaklepcalcificatie. Vanuit een klinisch oogpunt is het van belang dat in 88% van de patiënten de prothese maat hetzelfde zou zijn o.b.v. de 3D echo en o.b.v de CT metingen. In de patiënten met een lage calcificatie burden was dit zelfs 95%, vs. in 81% van de patiënten met een hoge calcificatie burden. In de gevallen waarin 3D echo en CT verschilden, gaf 3D echo vaak een kleinere prothese maat aan. Het meten van de annulus dimensies voor het sizen van de prothese middels 3D TEE kan dus een goed alternatief zijn voor CT in patiënten met een (relatieve) contra-indicatie voor CT, met name in patiënten met een minder gecalcificeerde aortaklep.

Hoofdstuk 8 richt zich op het met MRI onderzoeken van het ontstaan van myocardiale fibrose in patiënten met ernstig kleplijden. Met MRI kan middels LGE focale verlittekening (replacement fibrosis) worden aangetoond en middels de T1 techniek kan de mate van extracellulair volume worden beoordeeld. Een toename van T1 waarden betekent een toegenomen aanwezigheid van extracellulair volume en dit is een marker voor diffuse (i.t.t. focale) fibrose. Zowel de aanwezigheid van LGE als toegenomen T1 waarden zijn geassocieerd met meer symptomen, meer systolische en diastolische LV dysfunctie en verhoogde cardiale enzymen. De aanwezigheid van LGE is geassocieerd met een hogere mortaliteit in patiënten met een significante aortaklepstenose.[14] De mortaliteitscijfers nemen parallel toe aan de mate van fibrosering, met de beste prognose in de patiënten zonder fibrose (normale T1 waarden, geen LGE), een hogere mortaliteit in de patiënten met verhoogde T1 waarden maar zonder LGE, en de hoogste mortaliteit in de patiënten met en verhoogde T1 waarden en de aanwezigheid van LGE. Met MRI kan dus een risico-inschatting worden gemaakt voor patiënten met een significante aortaklepstenose. Hiernaast bleek ook de met MRI bepaalde circumferentiële strain van de LV geassocieerd te zijn met de mortaliteit in patiënten die een chirurgische of transcatheter aortaklepvervanging ondergaan. Voor aorta- en mitralisklep insufficiëntie is de prognostische waarde van het met MRI beoordelen van de mate van myocardiale fibrose minder robuust onderbouwd in studies, al zijn er wel studies die een omgekeerd evenredige relatie laten zien tussen de mate van fibrosering en de systolische en diastolische LV functie, functionele capaciteit en lange-termijn uitkomsten na klepchirurgie.

In **Hoofstuk 9** werd bediscussieerd wat de rol van myocardiale fibrose is in patiënten met een mitralisklep prolaps. Het ontstaan van focale verlittekening (gedetecteerd met LGE) rondom de papillairspieren van de inferolaterale LV wand is een karakteristieke entiteit van een mitralisklep prolaps wat niet wordt gezien in andere oorzaken van mitralisklep insufficiëntie, en ook niet gerelateerd is aan de ernst. Daarentegen bleek de mate van diffuse fibrose (gedetecteerd met verhoogde T1 waarden) wel geassocieerd te zijn met de ernst van de mitralisklep insufficiëntie (ongeacht het mechanisme). Focale verlittekening is wel in verband gebracht met het ontstaan van ventriculaire ritmestoornissen en is hierdoor vermoedelijk een belangrijke factor in het zogenoemde aritmogene mitralisklep prolaps syndroom waarmee patiënten worden beschreven die en een mitralis prolaps hebben en zich presenteren met ventriculaire ritmestoornissen en hiermee een verhoogde kans op plotse hartdood hebben.[15]

CONCLUSIES EN TOEKOMSTPERSPECTIEVEN

Het met MRI beoordelen van de LV strain in patiënten met een acuut hartinfarct geeft vernieuwde inzichten in de mate van schade en de kans op herstel van de hartspier op langere termijn. De GLS gemeten enkele dagen na de dotterbehandeling voor een acuut hartinfarct blijkt de prognose beter te kunnen voorspellen dan LV ejectiefractie of de mate van verlittekening zoals bepaald met LGE. De acute dotterbehandeling en huidige medicamenteuze therapie hebben de prognose voor een acuut ST-elevatie infarct enorm verbeterd. Er is echter wel een discussie gaande of juist het ontstaan van reperfusie schade een deel van de gunstige effecten van een dotterbehandeling weer teniet doet en vanuit dit oogpunt worden er strategieën bedacht om de mate van reperfusie schade te beperken. Het IV toedienen van bètablokkers was de eerste therapie die cardioprotectieve effecten bleek te hebben in een gerandomiseerde studie en heeft een klasse IIa aanbeveling in de Europese richtlijn van het ST-elevatie infarct voor hemodynamisch stabiele patiënten die een acute dotterbehandeling ondergaan.[16] Desondanks zijn resultaten uit grotere observationele studies en registries nodig om deze bevindingen ook in de dagelijkse praktijk bevestigd te zien worden. Dit proefschrift heeft laten zien dat het bepalen van de LV strain met MRI een geschikte imaging modaliteit kan zijn om te beoordelen of nieuwe therapieën cardioprotectieve effecten opleveren.

Het met meerdere imaging modaliteiten beoordelen van patiënten met klepziekten speelt een belangrijke rol in het bepalen van de meest geschikte behandelstrategie (Figuur 1). Transthoracale en slokdarm echocardiografie, CT en MRI kunnen helpen met het bepalen van de oorzaak, mechanismen en ernst van het klepvitium, en met het beoordelen van de anatomie in het kader van eventuele chirurgische of percutane interventie. 3D technieken geven een geïntegreerder beeld van het probleem dan dat er met 2D imaging verkregen kan worden. Hiernaast wordt gekeken naar wat de impact van het klepvitium is op de ventriculaire geometrische remodeling en eventuele dysfunctie. Vooralsnog zijn parameters als LV en rechter ventrikel dimensies en ejectiefractie doorslaggevend voor het bepalen van de indicatie en timing voor interventie.[17,18] Aanvullende markers zoals het bepalen van de intrinsieke LV functie o.b.v. strain (echocardiografisch of met MRI) of de mate van myocardiale fibrose zoals wordt bepaald met MRI kunnen de besluitvorming voor patiënten met klepziekten verder verfijnen en helpen met het re-definiëren van de optimale behandel strategie. Er zijn klinische studies gaande waarin voor asymptomatische patiënten met een ernstige aortaklepstenose of structurele mitralisklep insufficiëntie (die volgens huidige richtlijnen geen indicatie voor interventie hebben) wordt bekeken of vroegtijdige interventie beter is dan de standaard therapie als er wel aanwijzingen zijn voor myocardiale fibrosering.[19,20] Geavanceerde beeldvorming helpt in het identificeren van factoren die geassocieerd zijn met een negatieve uitkomst. Een voorbeeld hiervan is het aantonen van focale verlittekening rondom de papillairspieren in patiënten met een mitralisklep prolaps want dit is geassocieerd met het ontstaan van ventriculaire ritmestoornissen. Toekomstige studies moeten aantonen of het implanteren van een interne defibrillator voor deze patiënten gunstig is voor de prognose. Voor transcatheter vervanging van de aortaklep is duidelijk aangetoond dat implementatie van multimodality imaging leidt tot betere resultaten. Voor transcatheter interventies voor de mitralis- en tricuspidalisklep zijn CT en 3D echocardiografie zelfs nog belangrijker omdat de geometrie van de mitralis- en tricuspidalisklep nog een stuk complexer is dan van de aortaklep. 3D slokdarmechocardiografie is dé beeldvormingstechniek voor het tijdens de procedure begeleiden van de transcatheter mitralisklep- en tricuspidalisklep reparatie. De implementatie van fusion imaging, het simultaan gebruiken van meerdere technieken tijdens de procedure, bijvoorbeeld CT met real-time fluoroscopie en slokdarmechocardiografie zal de effectiviteit van deze procedures verder kunnen verbeteren. Ten slotte is beeldvorming essentieel in het beoordelen van de lange termijn resultaten en voor het diagnosticeren van mogelijke complicaties en op deze manier kunnen de nieuwe technieken ook beter worden vergeleken met de huidige therapie.

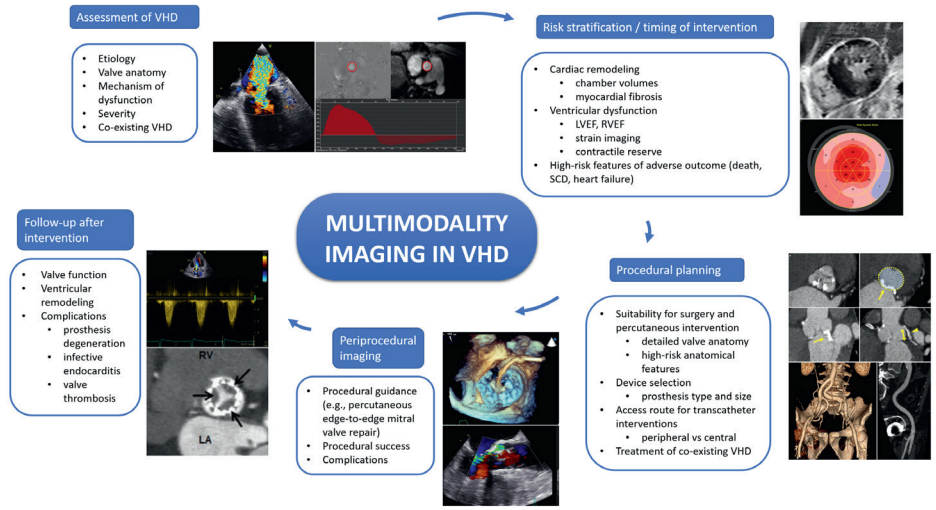

Figure 1: Multimodality cardiac imaging in valvular heart disease. LVEF = left ventricular ejection fraction; RVEF = right ventricular ejection fraction; SCD = sudden cardiac death; VHD = valvular heart disease.

REFERENCES

1. Antoni ML, Mollema SA, Atary JZ, Borleffs CJ, Boersma E, van de Veire NR *et al.* Time course of global left ventricular strain after acute myocardial infarction. *Eur Heart J* 2010;31(16):2006-13.
2. Lang RM, Badano LP, Mor-Avi V, Afilalo J, Armstrong A, Ernande L *et al.* Recommendations for cardiac chamber quantification by echocardiography in adults: an update from the American Society of Echocardiography and the European Association of Cardiovascular Imaging. *Eur Heart J Cardiovasc Imaging* 2015;16(3):233-70.
3. Ortiz-Perez JT, Rodriguez J, Meyers SN, Lee DC, Davidson C, Wu E. Correspondence between the 17-segment model and coronary arterial anatomy using contrast-enhanced cardiac magnetic resonance imaging. *JACC Cardiovasc Imaging* 2008;1(3):282-93.
4. Cerci RJ, Arbab-Zadeh A, George RT, Miller JM, Vavere AL, Mehra V *et al.* Aligning coronary anatomy and myocardial perfusion territories: an algorithm for the CORE320 multicenter study. *Circ Cardiovasc Imaging* 2012;5(5):587-95.
5. Bulluck H, Rosmini S, Abdel-Gadir A, White SK, Bhuva AN, Treibel TA *et al.* Automated Extracellular Volume Fraction Mapping Provides Insights Into the Pathophysiology of Left Ventricular Remodeling Post-Reperfused ST-Elevation Myocardial Infarction. *J Am Heart Assoc* 2016;5(7).
6. Podlesnikar T, Pizarro G, Fernandez-Jimenez R, Montero-Cabezas JM, Sanchez-Gonzalez J, Bucciarelli-Ducci C *et al.* Effect of Early Metoprolol During ST-Segment Elevation Myocardial Infarction on Left Ventricular Strain: Feature-Tracking Cardiovascular Magnetic Resonance Substudy From the METOCARD-CNIC Trial. *JACC Cardiovasc Imaging* 2019;12(7 Pt 1):1188-98.
7. Pizarro G, Fernandez-Friera L, Fuster V, Fernandez-Jimenez R, Garcia-Ruiz JM, Garcia-Alvarez A *et al.* Long-term benefit of early pre-reperfusion metoprolol administration in patients with acute myocardial infarction: results from the METOCARD-CNIC trial (Effect of Metoprolol in Cardioprotection During an Acute Myocardial Infarction). *J Am Coll Cardiol* 2014;63(22):2356-62.
8. Leetmaa T, Hansson NC, Leipsic J, Jensen K, Poulsen SH, Andersen HR *et al.* Early aortic transcatheter heart valve thrombosis: diagnostic value of contrast-enhanced multidetector computed tomography. *Circ Cardiovasc Interv* 2015;8(4).
9. Makkar RR, Fontana G, Jilaihawi H, Chakravarty T, Kofoed KF, De Backer O *et al.* Possible Subclinical Leaflet Thrombosis in Bioprosthetic Aortic Valves. *N Engl J Med* 2015;373(21):2015-24.
10. Vollema EM, Kong WKF, Katsanos S, Kamperidis V, van Rosendael PJ, van der Kley F *et al.* Transcatheter aortic valve thrombosis: the relation between hypo-attenuated leaflet thickening, abnormal valve haemodynamics, and stroke. *Eur Heart J* 2017;38(16):1207-17.

11. Ng AC, Delgado V, van der Kley F, Shanks M, van de Veire NR, Bertini M *et al.* Comparison of aortic root dimensions and geometries before and after transcatheter aortic valve implantation by 2- and 3-dimensional transesophageal echocardiography and multislice computed tomography. *Circ Cardiovasc Imaging* 2010;3(1):94-102.
12. Khalique OK, Hamid NB, White JM, Bae DJ, Kodali SK, Nazif TM *et al.* Impact of Methodologic Differences in Three-Dimensional Echocardiographic Measurements of the Aortic Annulus Compared with Computed Tomographic Angiography Before Transcatheter Aortic Valve Replacement. *J Am Soc Echocardiogr* 2017;30(4):414-21.
13. Vaquerizo B, Spaziano M, Alali J, Mylote D, Theriault-Lauzier P, Alfagih R *et al.* Three-dimensional echocardiography vs. computed tomography for transcatheter aortic valve replacement sizing. *Eur Heart J Cardiovasc Imaging* 2016;17(1):15-23.
14. Musa TA, Treibel TA, Vassiliou VS, Captur G, Singh A, Chin C *et al.* Myocardial Scar and Mortality in Severe Aortic Stenosis: Data from the BSCMR Valve Consortium. *Circulation* 2018.
15. Basso C, Iliceto S, Thiene G, Perazzolo Marra M. Mitral Valve Prolapse, Ventricular Arrhythmias, and Sudden Death. *Circulation* 2019;140(11):952-64.
16. Ibanez B, James S, Agewall S, Antunes MJ, Bucciarelli-Ducci C, Bueno H *et al.* 2017 ESC Guidelines for the management of acute myocardial infarction in patients presenting with ST-segment elevation: The Task Force for the management of acute myocardial infarction in patients presenting with ST-segment elevation of the European Society of Cardiology (ESC). *Eur Heart J* 2018;39(2):119-77.
17. Baumgartner H, Falk V, Bax JJ, De Bonis M, Hamm C, Holm PJ *et al.* 2017 ESC/EACTS Guidelines for the management of valvular heart disease. *Eur Heart J* 2017;38(36):2739-91.
18. Otto CM, Nishimura RA, Bonow RO, Carabello BA, Erwin JP, 3rd, Gentile F *et al.* 2020 ACC/AHA Guideline for the Management of Patients With Valvular Heart Disease: A Report of the American College of Cardiology/American Heart Association Joint Committee on Clinical Practice Guidelines. *Circulation* 2021;143(5):e72-e227.
19. Bing R, Everett RJ, Tuck C, Semple S, Lewis S, Harkess R *et al.* Rationale and design of the randomized, controlled Early Valve Replacement Guided by Biomarkers of Left Ventricular Decompensation in Asymptomatic Patients with Severe Aortic Stenosis (EVOLVED) trial. *Am Heart J* 2019;212:91-100.
20. Liu B, Edwards NC, Neal DAH, Weston C, Nash G, Nikolaidis N *et al.* A prospective study examining the role of myocardial Fibrosis in outcome following mitral valve repair IN DEgenerative mitral Regurgitation: rationale and design of the mitral FINDER study. *BMC Cardiovasc Disord* 2017;17(1):282.

APPENDIX

LIST OF PUBLICATIONS

1. **Podlesnikar T**, Delgado V. Update: Cardiac Imaging (II). Transcatheter Aortic Valve Replacement: Advantages and Limitations of Different Cardiac Imaging Techniques. *Rev Esp Cardiol (Engl Ed)* 2016;69(3):310-21.
2. Abou R, Leung M, Tonsbeek AM, **Podlesnikar T**, Maan AC, Schalij MJ, Ajmone Marsan N, Delgado V, Bax JJ. Effect of Aging on Left Atrial Compliance and Electromechanical Properties in Subjects Without Structural Heart Disease. *Am J Cardiol* 2017;120(1):140-7.
3. Yoon SH, Whisenant BK, Bleiziffer S, Delgado V, Schofer N, Eschenbach L, Fujita B, Sharma R, Ancona M, Yzeiraj E, Cannata S, Barker C, Davies JE, Frangieh AH, Deuschl F, **Podlesnikar T**, Asami M, Dhoble A, Chyou A, Masson JB, Wijeysundera HC, Blackman DJ, Rampat R, Taramasso M, Gutierrez-Ibanes E, Chakravarty T, Attizzani GF, Kaneko T, Wong SC, Sievert H, Nietlispach F, Hildick-Smith D, Nombela-Franco L, Conradi L, Hengstenberg C, Reardon MJ, Kasel AM, Redwood S, Colombo A, Kar S, Maisano F, Windecker S, Pilgrim T, Ensminger SM, Prendergast BD, Schofer J, Schaefer U, Bax JJ, Latib A, Makkar RR. Transcatheter Mitral Valve Replacement for Degenerated Bioprosthetic Valves and Failed Annuloplasty Rings. *J Am Coll Cardiol* 2017;70(9):1121-31.
4. Hensen LCR, Goossens K, **Podlesnikar T**, Rotmans JI, Jukema JW, Delgado V, Bax JJ. Left Ventricular Mechanical Dispersion and Global Longitudinal Strain and Ventricular Arrhythmias in Predialysis and Dialysis Patients. *J Am Soc Echocardiogr* 2018;31(7):777-83.
5. Leung M, Abou R, van Rosendael PJ, van der Bijl P, van Wijngaarden SE, Regeer MV, **Podlesnikar T**, Ajmone Marsan N, Leung DY, Delgado V, Bax JJ. Relation of Echocardiographic Markers of Left Atrial Fibrosis to Atrial Fibrillation Burden. *Am J Cardiol* 2018;122(4):584-91.
6. **Podlesnikar T**, Delgado V, Bax JJ. Cardiovascular magnetic resonance imaging to assess myocardial fibrosis in valvular heart disease. *Int J Cardiovasc Imaging* 2018;34(1):97-112.
7. **Podlesnikar T**, Delgado V, Bax JJ. Imaging of Valvular Heart Disease in Heart Failure. *Card Fail Rev* 2018;4(2):78-86.
8. **Podlesnikar T**, Prihadi EA, van Rosendael PJ, Vollema EM, van der Kley F, de Weger A, Ajmone Marsan N, Naji F, Fras Z, Bax JJ, Delgado V. Influence of the Quantity of Aortic Valve Calcium on the Agreement Between Automated 3-Dimensional Transesophageal Echocardiography and Multidetector Row Computed Tomography for Aortic Annulus Sizing. *Am J Cardiol* 2018;121(1):86-93.

9. van der Bijl P, **Podlesnikar T**, Bax JJ, Delgado V. Sudden Cardiac Death Risk Prediction: The Role of Cardiac Magnetic Resonance Imaging. *Rev Esp Cardiol (Engl Ed)* 2018;71(11):961-70.
10. Cameli M, Marsan NA, D'Andrea A, Dweck MR, Fontes-Carvalho R, Manka R, Michalski B, **Podlesnikar T**, Sitges M, Popescu BA, Edvardsen T, Fox KF, Haugaa KH. EACVI survey on multimodality training in ESC countries. *Eur Heart J Cardiovasc Imaging* 2019;20(12):1332-6.
11. Haugaa KH, Marsan NA, Cameli M, D'Andrea A, Dweck MR, Carvalho RF, Holte E, Manka R, Michalski B, **Podlesnikar T**, Popescu BA, Schulz-Menger J, Sitges M, Stankovic I, Maurer G, Edvardsen T. Criteria for surveys: from the European Association of Cardiovascular Imaging Scientific Initiatives Committee. *Eur Heart J Cardiovasc Imaging* 2019;20(9):963-6.
12. **Podlesnikar T**, Lapinskas T. Cardiac Involvement in Connective Tissue Disorders. *JACC: Case Reports* 2019;1(2):243-5.
13. **Podlesnikar T**, Pizarro G, Fernandez-Jimenez R, Montero-Cabezas JM, Sanchez-Gonzalez J, Bucciarelli-Ducci C, Ajmone Marsan N, Fras Z, Bax JJ, Fuster V, Ibanez B, Delgado V. Effect of Early Metoprolol During ST-Segment Elevation Myocardial Infarction on Left Ventricular Strain: Feature-Tracking Cardiovascular Magnetic Resonance Substudy From the METOCARD-CNIC Trial. *JACC Cardiovasc Imaging* 2019;12(7 Pt 1):1188-98.
14. Ajmone Marsan N, Michalski B, Cameli M, **Podlesnikar T**, Manka R, Sitges M, Dweck MR, Haugaa KH. EACVI survey on standardization of cardiac chambers quantification by transthoracic echocardiography. *Eur Heart J Cardiovasc Imaging* 2020;21(2):119-23.
15. Bunc M, Cercek M, **Podlesnikar T**, Terseglav S, Steblovnik K. Valve-in-valve transcatheter aortic valve implantation with fracturing of a failed small surgical aortic bioprosthesis: a case report. *Eur Heart J Case Rep* 2020;4(6):1-5.
16. Michalski B, Dweck MR, Marsan NA, Cameli M, D'Andrea A, Carvalho RF, Holte E, **Podlesnikar T**, Manka R, Haugaa KH. The evaluation of aortic stenosis, how the new guidelines are implemented across Europe: a survey by EACVI. *Eur Heart J Cardiovasc Imaging* 2020;21(4):357-62.
17. Pezel T, Coisne A, Mahmoud-Elsayed H, Mandoli GE, Elgamal SM, **Podlesnikar T**, Cameli M, Grapsa J, Lafitte S, Edvardsen T, Donal E, Dreyfus J. EACVI communication paper: first international young dedicated multimodal cardiovascular imaging simulation education event organized by the ESC. *Eur Heart J Cardiovasc Imaging* 2020;21(2):124-6.

18. **Podlesnikar T**, Pizarro G, Fernández-Jiménez R, Montero-Cabezas JM, Greif N, Sánchez-González J, Bucciarelli-Ducci C, Marsan NA, Fras Z, Bax JJ, Fuster V, Ibáñez B, Delgado V. Left ventricular functional recovery of infarcted and remote myocardium after ST-segment elevation myocardial infarction (METOCARD-CNIC randomized clinical trial substudy). *J Cardiovasc Magn Reson* 2020;22(1):44.
19. **Podlesnikar T**, Pizarro G, Fernández-Jiménez R, Montero-Cabezas JM, Sánchez-González J, Bucciarelli-Ducci C, Ajmone Marsan N, Fras Z, Bax JJ, Fuster V, Ibáñez B, Delgado V. Five-Year Outcomes and Prognostic Value of Feature-Tracking Cardiovascular Magnetic Resonance in Patients Receiving Early Prereperfusion Metoprolol in Acute Myocardial Infarction. *Am J Cardiol* 2020;133:39-47.
20. Delgado V, **Podlesnikar T.** Focal Replacement and Diffuse Fibrosis in Primary Mitral Regurgitation: A New Piece to the Puzzle. *JACC Cardiovasc Imaging* 2021;14(6):1161-3.
21. Bularga A, Saraste A, Fontes-Carvalho R, Holte E, Cameli M, Michalski B, Williams MC, **Podlesnikar T**, D'Andrea A, Stankovic I, Mills NL, Manka R, Newby DE, Schultz-Menger J, Haugaa KH, Dweck MR. EACVI survey on investigations and imaging modalities in chronic coronary syndromes. *Eur Heart J Cardiovasc Imaging* 2021;22(1):1-7.
22. Sitges M, Ajmone Marsan N, Cameli M, D'Andrea A, Carvalho RF, Holte E, Michalski B, **Podlesnikar T**, Popescu BA, Schulz-Menger J, Stankovic I, Haugaa KH, Dweck MR. EACVI survey on the evaluation of left ventricular diastolic function. *Eur Heart J Cardiovasc Imaging* 2021;22(10):1098-1105.
23. **Podlesnikar T**, Cardim N, Ajmone Marsan N, D'Andrea A, Cameli M, Popescu BA, Schulz-Menger J, Stankovic I, Toplisek J, Maurer G, Haugaa KH, Dweck MR. EACVI survey on hypertrophic cardiomyopathy. *Eur Heart J Cardiovasc Imaging* 2022;23(5):590-597.
24. **Podlesnikar T**, Berlot B, Dolenc J, Goricar K, Marinko T. Radiotherapy-induced cardiotoxicity: the role of multimodality cardiovascular imaging. *Front Cardiovasc Med* 2022 (in press).

ACKNOWLEDGEMENTS

The articles in this thesis were written at the Cardiology department at Leiden University Medical Center, where I have spent two years of PhD research fellowship. I would like to express my deepest gratitude to:

Professor Jeroen J Bax, for the opportunity to do my research fellowship in Leiden, where I've experienced how cardiology practice and scientific research is conducted at the highest level and I've witnessed a tremendous growth in my professional career. Thank you for all your faith in me, patience, critical appraisal of my research work and motivation.

Victoria Delgado, for her unfailing guidance and support in my research work and the training in multimodality imaging. Dear Victoria, thank you for always being there for me, be it a comma in the manuscript or advice for life, your endless passion, energy, work attitude, your wisdom and humor will always echo in my mind and in my heart.

Nina Ajmone Marsan, for her support in my research work and training, in particular for the amazing tips and tricks in transesophageal echocardiography during structural heart interventions.

Borja Ibanez and his team in "Centro Nacional de Investigaciones Cardiovasculares" in Madrid, Spain, for giving me the opportunity to start a collaborative project on the METOCARD-CNIC clinical trial, which encompasses a major part of my PhD thesis. I am extremely grateful for your support and critical appraisal of my abstracts and manuscripts.

Chiara Bucciarelli-Ducci, for opening the doors into the world of cardiovascular magnetic resonance for me. Without the amazing training and sharing of your expertise at the Bristol Heart Institute, Bristol, United Kingdom, prior to my coming to Leiden, much of my PhD thesis could not come true.

Professor Zlatko Fras, for having trust in me and providing me the excellent opportunity to start the research fellowship at the LUMC, as well as for solving many obstacles related to the cardiology training in Slovenia. I am deeply grateful for your long-lasting support in my professional career.

Professor Martin J Schalij for the opportunity to work at the Cardiology department at the LUMC for two years and for supporting the presentations my research work at several international forums. Many thanks to you, Frank van der Kley and other personnel in the cathlab, where I got my first experience with the structural heart interventions that were not available in my country.

The European Society of Cardiology (ESC) for awarding me a Training Grant.

Philippe van Rosendael for helping me with the Dutch translation of parts of the thesis.

International fellows – Edgard, Pieter, Melissa, William, Tea, Giulia and Francesca for helping me with the research work, for excellent discussions in the journal clubs, for creating a truly inspiring working atmosphere and enjoyable free time. I feel we've become friends for life!

Dutch fellows from the imaging team – Rachid, Farnaz, Laurien, Mara, Philippe, Jeff, Mohammed, Alexander, Mai, Suzanne, Mand, Yasmine, Liselotte, Marlieke – as well as other research fellows in the Cardiology Department for creating an inspiring and friendly working environment, for helping me getting around in and out of LUMC and creating a lot of extracurricular fun. Your hospitality made me feel at home in the Netherlands!

Mum and dad, for your love and support on my educational path since childhood. You've always listened to my aspirations, believed in me, encouraged me in difficult times and celebrated my successes. By instilling the values of hard work and lifelong learning you've encouraged me to pursue my dreams.

Dearest Blanka, for your unconditional love, support, faith in me and for all the sacrifices that you've made for me during my career. Living together with you and our newborn sun Tibor made my fellowship in Leiden one the most beautiful times of my life.

Dearest Tibor, for being my sunshine, my pride, my fountain of motivation, my infinite love.

CURRICULUM VITAE

Tomaž Podlesnikar was born on 26th October 1981 in Maribor, Slovenia. He graduated at the II. Gimnazija Maribor high school with the Diploma of the International Baccalaureate and the award of Slovenian Minister of Education and Sport in 2000. He obtained his medical degree at the Faculty of Medicine, University of Ljubljana, with dean's special award for excellent study success in 2007. In 2014 he became internal medicine specialist, magna cum laude, and pursued training in cardiology and vascular medicine. He was awarded the European Association of Cardiovascular Imaging (EACVI) Training Grant in 2015 and spent 6 months of training in cardiovascular magnetic resonance (CMR) at Bristol Heart Institute, University Hospitals Bristol NHS Foundation Trust, Bristol (United Kingdom) under supervision of Dr Chiara Bucciarelli-Ducci. Moreover, he was awarded the European Society of Cardiology (ESC) Training Grant in 2016 and spent 2 years of clinical training and research in multimodality cardiovascular imaging at the Department of Cardiology, Leiden University Medical Center, Leiden (The Netherlands) under supervision of Prof Jeroen J Bax and Dr Victoria Delgado. In 2018 he became cardiology and vascular medicine specialist, magna cum laude. He currently holds the position of cardiologist at the Department of Cardiac Surgery, University Medical Centre Maribor, Slovenia, and the Department of Cardiology, University Medical Centre Ljubljana, Slovenia. His main expertise is multimodality cardiovascular imaging, in particular echocardiography and CMR. He holds the EACVI Level 2 Certification in CMR and EACVI certification in adult transthoracic echocardiography. He also works as a sports cardiologist at the Institute of Sports Medicine, Faculty of Medicine, University of Maribor. He is an assistant at the Faculty of Medicine, University of Maribor, Slovenia. He has been an active member of several EACVI committees and National Ambassador of Slovenia among the EACVI young community (Heart Imagers of Tomorrow – HIT). He has also been an active member of the Working Group for Cardiovascular Imaging in the Slovenian Society of Cardiology. He has been a director and a member of the organizing and scientific committees of several international medical conferences organized by the Slovenian Society of Cardiology. He has published several peer reviewed journal articles, presented his research at major international cardiology conferences and has given scientific lectures at international cardiovascular imaging congresses. He has been a principal investigator in the University Medical Centre Ljubljana for international multicentric clinical trials and registries. He is an emerging editorial consultant for Journal of the American College of Cardiology (JACC) Cardiovascular Imaging and an editorial consultant for JACC: Case Reports.